

Investigation and optimization of biosynthetic pathways from entomopathogenic bacteria

Dissertation
zur Erlangung des Doktorgrades
der Naturwissenschaften

vorgelegt beim Fachbereich 15
der Johann Wolfgang Goethe-Universität
in Frankfurt am Main

von
Siyar Kavakli

Frankfurt am Main 2023

D30

vom Fachbereich für Biowissenschaften (15) der
Johann Wolfgang Goethe-Universität als Dissertation angenommen.

Dekan:
Prof. Dr. Sven Klimpel

Gutachter:
Prof. Dr. Helge B. Bode
Prof. Dr. Martin Grininger

Datum der Disputation: 21.04.2023

Table of Contents

Abbreviations	I
Zusammenfassung	IV
Summary	IX
1 Introduction	1
1.1 <i>Photorhabdus</i> and the mutualistic symbiosis with <i>Heterorhabditis</i>	3
1.2 Features of specialized metabolites in <i>Photorhabdus</i>	4
1.3 PKS and FAS	8
1.3.1 Acyltransferases (AT)	10
1.3.2 Acyl Carrier Protein (ACP) or thiolation domain.....	10
1.3.3 Ketoacyl Synthases (KS).....	11
1.3.4 Modifying domains.....	12
1.3.5 Termination and release	13
1.3.6 PKS architecture.....	14
1.3.7 PKS type I.....	14
1.3.8 PKS type II.....	15
1.3.9 PKS type III.....	17
1.3.10 FAS I	17
1.3.11 FAS II	18
1.3.12 N-acetylcysteamine thioesters (SNAC)	20
1.4 Identification and activation of natural products	21
1.5 Elucidation of SM structure and their biosynthetic pathways	23
1.6 Biosynthesis of stilbenes	24
1.7 Aim of this work.....	29
2 Material and Methods.....	30

2.1	Topic A: Biosynthesis characterization of stilbene related pathways	30
2.1.1	Cultivation of strains	30
2.1.2	Microorganisms	30
2.1.3	Plasmids	31
2.1.4	Oligonucleotides	32
2.1.5	DNA and plasmid extraction	40
2.1.6	Plasmid construction and transformation for <i>in vitro</i> assays and heterologous production	41
2.1.7	Cultivation of bacteria and heterologous expression	41
2.1.8	Protein production and purification	41
2.1.9	In vitro assays.....	42
2.1.10	Feeding experiment with SNAC- and CA-derivatives	43
2.1.11	Purification of CA-SNAC product.....	43
2.1.12	HPLC-HR-MS.....	44
2.2	Topic B: Optimization of production titers of stilbene derivatives	45
2.2.1	Cultivation of strains	45
2.2.2	Microorganisms	46
2.2.3	Plasmids	47
2.2.4	Oligonucleotides and double stranded DNA-fragments.....	48
2.2.5	DNA and plasmid extraction	58
2.2.6	Gene deletions via homologous recombination	59
2.2.7	Deletion and promoter exchange via CRISPR/Cas12	59
2.2.8	Overproduction of stilbenes	60
2.2.9	Production and purification of IPS	61
2.2.10	Purification of IPS.....	61

2.3	Topic C: Epoxide derivatives and reactions	62
2.3.1	Microorganisms	62
2.3.2	Plasmids	62
2.3.3	Feeding and inversed feeding experiments	62
2.3.4	Purification of EPS	63
2.3.5	Solid-phase peptide synthesis	63
2.3.6	Reaction of amino acids, peptides and proteins with epoxides	66
3	Results	67
3.1	Topic A: Biosynthesis characterization of stilbene related pathways	67
3.1.1	<i>In vitro</i> production of 5-phenyl-2,4-pentadienoyl-StIE	67
3.1.2	Heterologous production of stilbenes	68
3.1.3	Quantification of IPS titers	70
3.1.4	Substrate specificity of stilbene related enzymes	72
3.1.5	SNAC-feeding and formation of hydrazines	74
3.1.6	Biosynthesis of benzylideneacetone (BZA)	79
3.2	Topic B: Optimization of production titers of stilbene derivatives	81
3.2.1	Increase of starting building blocks	82
3.2.2	Influence of pathway deletions	82
3.2.3	Cultivation in insect media and its influence on epoxide formation	83
3.2.4	Promoter exchanges in front of stilbene related enzymes and phenylalanine upregulation	85
3.2.5	Cultivation with XAD	86
3.2.6	Dependence of StIB	87
3.2.7	Assessment of different media and combination of all approaches	88
3.2.8	Overproduction of EPS	90

3.2.9	Overview of stilbene yields	91
3.3	Topic C: Stilbene epoxides and epoxidation of peptides and proteins	93
3.3.1	Analysis of EPS related derivatives	93
3.3.2	<i>In vitro</i> reactions of epoxides with amino acids, peptides and proteins	98
4	Discussion and outlook	105
4.1	Topic A Biosynthetic characterization of stilbene related pathways	105
4.1.1	Biosynthesis of stilbenes	105
4.1.2	Hydrazines - N-N bond formation	113
4.1.3	Biosynthesis of benzylideneacetone.....	117
4.2	Optimization of production titers of stilbenes.....	122
4.2.1	Increase of substrate building blocks.....	122
4.2.2	Promoter exchanges and impact of XAD.....	125
4.2.3	Assessment of different cultivation media.....	126
4.2.4	Outlook on further optimization.....	127
4.3	Topic C EPS related derivatives and reactions	129
4.3.1	<i>In vivo</i> production of EPS and its derivatives.....	129
4.3.2	Purification of EPS.....	131
4.3.3	<i>In vitro</i> reactions of epoxides with amino acids, peptides and proteins ...	132
4.3.4	Observation of further stilbene derivatives.....	135
5	Literature.....	137
6	Supplementary information	144
7	Attachment.....	159
8	Erklärung.....	179
9	Versicherung.....	179

Abbreviations

AasS	acyl-acyl-carrier protein synthetase
ACC	Acetyl-CoA carboxylase
ACN	Acetonitrile
ACP	Acyl carrier protein
antiSMASH	Antibiotics and secondary metabolite analysis shell
AHL	Acyl-homoserine lactone
AQ	Anthraquinone
ara	L-arabinose
AT	Acytransferase
ATP	Adenosine triphosphate
BGC	Biosynthetic gene cluster
BKD	Branched- chain keto acid dehydrogenase
BM	<i>Bombxy mori</i> medium
boc	<i>tert.</i> -butoxycarbonyl
bp	base pairs
BPC	Base peak chromatogram
BZA	Benzylideneacetone
CA	Cinnamic acid
CA-CoA	Cinnamoyl-CoA
CHS	Chalcone synthase
CLF	chain length factor
Cm	Chloramphenicol
CRISPR	Clustered regularly interspaced short palindromic repeats
DAR	Dialkylresorcinols
DCM	Dichlormethan
DEBS	6-deoxyerythronolide synthase
DH	Dehydratase
DIPEA	N,N-Diisopropylethylamine
DMF	Dimethylformamide
EIC	Extracted Ion Chromatogram

EPS	2-isopropyl-5-(3-phenyl-oxiranyl)-benzene-1,3-diol
ER	Enoylreductase
ESI	Electrospray-ionisation
FA	Formic acid
FAD	Flavine-adenine dinucleotide
FAS	Fatty acid synthase
FMN	Flavinmononucleotide
GFP	Green fluorescent protein
Gm	Gentamycin
HAL	Histidine ammonium lyase
HCTU	2-(6-Chloro-1H-benzotriazole-1-yl)-1,1,3,3-tetramethylammonium hexafluorophosphate
HF	<i>Hermetia illucens</i> fat medium
HFIP	Hexafluoroisopropanol
HPLC	High performance liquid chromatography
HR	High resolution
IJ	infective juvenile
IPS	3,5-dihydroxy-4-isopropyl- <i>trans</i> -stilbene
Km	Kanamycin
KR	Ketoreductase
KS	Ketosynthase
LB	Lysogeny broth
M-form	Mutualistic form
MCoA	Malonyl-CoA
MAT	Malonyl/acetyltransferase
MCAT	Malonyl-CoA acyltransferase
MeOH	Methanol
MPT	Malonyl/palmitoyltransferase
MS	Mass spectrometry
<i>m/z</i>	mass to charge ratio
NAD(P)H	Nicotinamide adenine dinucleotide (phosphate)

NMP	N-Methyl-2-pyrrolidone
NMR	Nuclear magnetic resonance
NP	Natural product
NRPS	Non-ribosomal peptide synthetase
OD	Optical density
OSMAC	One Strain Many Compounds
P-form	Pathogenic form
PAL	Phenylalanine ammonium lyase
PK	Polyketide
PKS	Polyketide synthase
PO	Phenoloxidase
Ppant	Phosphopantetheinyl
PPTase	Phosphopantetheinyl transferase
SM	Specialized metabolites
Sm	Spectinomycin
SNAC	N-acetylcysteamine thioester
SPPS	Solid phase peptide synthesis
STS	Stilbene synthase
t-Bu	<i>tert.</i> -butyl
TE	Thioesterase
TFA	Trifluoroacetic acid
TOF	time of flight
TPP	Thiaminepyrophosphate
VA	Vanillic acid
WT	Wild type
Xyl	Xylose

Zusammenfassung

Bakterien der Gattung *Photorhabdus* leben in mutualistischer Symbiose mit Nematoden der Gattung *Heterorhabditis*. Es handelt sich um Gram-negative Bakterien, die eine Vielzahl unterschiedlicher Sekundärmetabolite produzieren von denen einige für die Symbiose mit dem Wirt wichtig sind. Eine wichtige Klasse jener Sekundärmetabolite, die auch pharmakologische Relevanz besitzen sind Polyketide, die durch sogenannte Polyketidsynthasen (PKS) synthetisiert werden. PKS katalysierte Reaktionen besitzen chemisch eine große Ähnlichkeit zu Reaktionen, die von Enzymen der Fettsäurebiosynthese, den Fettsäuresynthasen (FAS) katalysiert werden.

Beide Systeme nutzen Malonyl-Einheiten als Bausteine, die von sogenannten Ketosynthase-Domänen (KS) mittels Claisen-Kondensation unter Bildung einer C-C-Brücke miteinander verknüpft werden. Die für die Verknüpfung benötigten Substrate werden hierfür von sogenannten Acyl-Carrier-Proteinen (ACPs) sowohl zu den KS als auch zu den weiteren beteiligten Enzymen transportiert, die für die weitere Prozessierung und Vielfalt wichtig sind. Für den Transport müssen die ACPs zunächst über sogenannte Phosphopantetheinyl Transferasen aktiviert werden, indem unter Abspaltung von Adenosindiphosphat der Phosphopantethein-Arm (Ppant-arm) eines Coenzym A-(CoA) Moleküls auf einen konservierten Serin-Rest der zweiten α -Helix des ACPs übertragen wird. Anders als bei PKS-Systemen, werden Moleküle in der Fettsäurebiosynthese meist vollständig reduziert bzw. gesättigt. Daher bieten FAS-Systeme weniger Vielfalt als PKS abgeleitete Strukturen, die nach einer Claisen-Kondensation, aber auch nach einer Reduktion durch Ketoreduktasen (KRs), Dehydrierung durch Dehydratasen (DHs) oder auch wie bei der FAS nach einer Reduzierung durch Enoylreduktasen (ERs) einen Modifikationszyklus abschließen. Die Vielfalt von PKS-Systemen wird zusätzlich von weiteren Enzymen wie Zykласen, Aromatasen, Methyltransferasen oder auch Glykosyltransferasen erhöht.

PKS und FAS können in verschiedene Typen unterteilt werden. Typ I Systeme sind kovalent miteinander verbunden als Teil eines Proteins und reichen von einem Modul (iterative Typ I PKS) zu multimodularen Komplexen. Typ I FAS kommen meist in Eukaryoten und Pilzen vor, während PKS-Systeme dieses Typs vor allem in Prokaryoten

anzutreffen sind und typischerweise lineare oder zyklische Produkte erzeugen. Domänen von Typ-II FAS und PKS kommen im Gegensatz dazu als einzelständige Proteine vor, die über intermolekulare Wechselwirkungen miteinander interagieren. Während PKS II ausschließlich in Bakterien vorkommen, findet man FAS II sowohl in Bakterien, als auch in den Plastiden und Mitochondrien von Pflanzen und Eukaryoten. PKS II produzieren meistens aromatische Polyketide und besitzen oft einen sogenannten *chain-length factor* (CLF), der jedoch auch durch eine zweite KS-Domäne ersetzt werden kann. Diese Domänen schirmen das reaktive Polyketid-Rückgrat während der Verlängerung ab und vermeiden somit Nebenreaktionen. Pflanzen und Bakterien besitzen zusätzlich PKS III-Systeme, die ausschließlich CoA-gebundene Verlängerungseinheiten verwenden und nicht auf ACPs angewiesen sind. Sie bestehen aus monofunktionalen Proteinen, die durch wiederholte Claisen-Kondensationen das Produkt verlängern und typischerweise aromatische Substrate als Starteinheiten verwenden.

Der Schwerpunkt dieser Arbeit befasste sich dem Typ II PKS-System bakterieller Stilbene. 3,5-Dihydroxy-4-isopropyl-*trans*-stilben auch bekannt als Isopropylstilben (IPS), ist der prominenteste Vertreter dieser Gruppe von Produkten, das ausschließlich in Bakterien der Gattung *Photorhabdus* vorkommt und daher als Organismus-spezifischer Biomarker betrachtet werden kann. Es wirkt als Virulenzfaktor auf das Immunsystem von Insekten, indem es deren Phenoloxidase inhibiert und somit dem Symbionten von *Photorhabdus* einen Vorteil bei der Jagd nach Beute verschafft. Pharmakologisch hemmt IPS zudem die lösliche Epoxidhydrolase und hat daher Einfluss auf Entzündungsreaktionen. Es erhielt im Sommer 2022 die Zulassung als Medikament gegen Psoriasis und ist der erste klinisch zugelassene Wirkstoff aus der *Photorhabdus* Gattung. Abseits von *Photorhabdus* werden jegliche Stilbene von pflanzenbasierten PKS III Systemen synthetisiert, in denen eine Vielzahl von Derivaten produziert werden. Durch *in vitro* Assays mit gereinigten Proteinen konnte der vollständige Biosyntheseweg von Stilbenen aufgeklärt werden. Die Biosynthese von IPS ist, im Gegensatz zu ähnlichen Produkten aus Pflanzen, deutlich komplizierter, da die bakterielle Produktion eine größere Anzahl von Enzymen und Intermediaten umfasst. Der Biosyntheseweg besteht aus zwei Ästen, die zur Produktion von zwei an der Zyklisierung beteiligten Intermediaten benötigt werden. Es handelt sich dabei um Isovaleryl- β -ketoacyl-ACP und 5-Phenyl-2,4-

pentadienoyl-ACP, wobei die beteiligten Enzyme für die Synthese von letzterem bisher unbekannt waren. Die Zyklisierungsreaktion wird durch die KS/Zyklase StID katalysiert, indem eine hierfür wichtige Michael-Addition durchgeführt wird. Im Rahmen dieser Arbeit konnte gezeigt werden, dass es sich bei den ausstehenden Enzymen um die KS-, KR- und DH-Domänen der Fettsäurebiosynthese handelte. Obwohl diese Isoenzyme mit Sequenzidentitäten von über 73 % auch in *E. coli* vorliegen, war es nicht möglich, sie während heterologer Produktionen zu komplementieren. Es stellte sich heraus, dass die KS FabH eine Art *Gatekeeper*-Enzym darstellte, da es im Gegensatz zum Isoenzym aus *E. coli* auch aromatische Strukturen wie Zimtsäure-CoA anstatt des üblichen Acetyl-CoA akzeptierte. Mithilfe von Fütterungsexperimenten wurde zudem gezeigt, dass *Photorhabdus* auch *meta*-substituierte Zimtsäuren verwerten kann, um somit halogenierte IPS-Derivate herzustellen. Dabei entstanden auch die an der *meta* Position halogenierten 5-Phenyl-2,4-pentadiensäuren. Es konnte somit gezeigt werden, dass es sich bei der Biosynthese bakterieller Stilbene um ein ungewöhnliches Typ II FAS/PKS-Hybrid-System handelt.

Bei der Durchführung von Komplementierungsstudien mit Zimtsäure-N-acetylcysteamin, einem synthetischen Zimtsäure-Analogon wurde die Bildung von Hydrazin-Derivativen in *Photorhabdus* und *Xenorhabdus* entdeckt, indem das Produkt aufgereinigt und mittels HPLC-MS verifiziert wurde. Hydrazine besitzen charakteristische N-N-Bindungen und kommen selten als Naturstoffe vor. Gemäß anderen Publikationen wurden im Anschluss fünf Gene mittels CRISPR/Cas deletiert, welche sich jedoch nicht als Ursprung für die Bildung besagter Strukturen bestätigen ließen.

Bei einem weiteren in dieser Arbeit untersuchten Sekundärmetabolit handelt es sich um Benzylidenaceton (BZA). BZA wird sowohl von *Photorhabdus*- und *Xenorhabdus*-Stämmen produziert und findet verschiedenste Anwendungen in der Natur und der Industrie. Industriell wird BZA als Glanzmittel in der Galvanik, aber auch für die chemische Synthese des Antikoagulans Warfarin verwendet. Es wirkt als Antibiotikum gegen Gram-negative Bakterien und hemmt zudem die Phospholipase A₂, die essentiell für die Signalkaskade in Immunreaktionen ist. Aufgrund seiner strukturellen Ähnlichkeit zur Zimtsäure und des β -ketoacyl-Produkts aus der IPS-Biosynthese wurde eine

Hypothese für die Biosynthese von BZA abgeleitet. Mithilfe von *in vitro* Assays war es möglich die an der Biosynthese beteiligten Proteine zu ermitteln und BZA heterolog in *E. coli* zu produzieren. Die Zugabe von Zimtsäure und Produktion der CoA-Ligase StlB, des ACP StlE und der KS FabH, ermöglichte die Produktion von 1.8 mg/l, das einer Vervielfachung des Produktionstiters um den Faktor 150 gegenüber *Photorhabdus*- und *Xenorhabdus*-Wildtypen entsprach.

Ein weiterer Aspekt dieser Arbeit befasste sich mit der Generierung von *Photorhabdus*-Stämmen, die höhere IPS-Produktionstiters erzielten als der Wildtyp und sich besonders gut für die Reinigung von IPS einigten. Hierfür wurden unter Anwendung von CRISPR/Cas Deletionen und Promoteraustausche im Genom durchgeführt. Somit war es möglich, konkurrierender Biosynthesewege zu deletieren und zeitgleich für spätere Aufreinigungen von IPS keinerlei störende Hintergrundsignale durch weitere Sekundärmetabolite wie Antrachinone, GameXPepptide, Phurealipide oder Epoxystilbene zu erhalten. In weiteren Schritten wurden starke induzierbare Promoter vor Genen der IPS-Biosynthese erfolgreich eingesetzt. Dies wurde mit Plasmid-basierter Expressionen von Genen zur Steigerung der Phenylalanin-Produktion kombiniert, die resistent gegen die sogenannte *Feedback*-Inhibition waren. Bei Phenylalanin handelt es sich um den Vorläufer der Zimtsäure, dem zentralen Substrat für die Biosynthese von IPS. Durch diese Faktoren war es möglich den Titer um den Faktor sieben von ca. 23 mg/l auf knapp 160 mg/l zu erhöhen.

Parallel wurden unterschiedliche Medien zur Optimierung der Kultivierungsbedingungen angepasst und getestet. Hierbei wurden fett- und peptid-reiche Medien wie das PP3M oder auf Insekten und Insektenfett-basierende Medien verwendet, um die natürliche Umgebung von *Photorhabdus* nachzuahmen. Da IPS das Immunsystem von Insekten inhibiert, wurde vermutet, dass die Kultivierung in Präsenz von Insekten die Stilben-Produktion positiv beeinflussen könnte. Als optimale Bedingung wurden 5 % Zugabe von Larven des Seidenspinners *Bombxy mori* zu Wasser oder XPP-Medium ermittelt, das zur erhöhten Produktion von IPS und dessen epoxidiertem Derivat (EPS) führte. In einem Epoxidase-defizienten Wildtyp-Stamm wurde die Produktion von IPS in dem Medium ebenfalls um den Faktor sieben, ähnlich wie bei dem weiter oben erwähnten Stamm,

verbessert. Die Produktion von Sekundärmetaboliten lässt sich zudem häufig durch die Zugabe von Styren-Divinylbenze-Polymer basierter XAD-Harze erhöhen, die Metabolite binden und somit akkumulieren können. Kultivierung mit diesem Harz erhöhte die Produktion im Wildtypen um das Dreifache und eignete sich besonders, um die Reinigung von Naturstoffen zu erleichtern, da es bereits eine Extraktion vorwegnimmt. Die Kombination des XAD mit dem Insektenmedium und der Stammoptimierung führte zu einer Produktion von mehr als 860 mg/l IPS.

Der letzte Abschnitt dieser Arbeit widmete sich dem EPS und dessen Derivaten. Die erzeugten Stämme eigneten sich besonders, das andernfalls unter Laborbedingungen lediglich sehr gering produzierte EPS zu analysieren. Mithilfe von Fütterungs- und inversen Fütterungs-Experimenten konnte gezeigt werden, dass der Epoxidring mit Aminosäuren und Peptiden unter der Bildung von β -Amino-Alkoholen umgesetzt wird. Dies führte zur Hypothese von Epoxidierungen als eine mögliche posttranslationale Modifikation in *Photorhabdus*. Da sich sowohl die chemische Synthese als auch die Reinigung von EPS aufgrund dessen Instabilität als nicht erfolgreich erwies, wurden mit Styrenoxid und Stilbenoxid zwei strukturell ähnliche Epoxide verwendet, um *in vitro* Assays mit Aminosäuren, per Festphasensynthese hergestellter Peptide und mit einem gereinigten Protein durchgeführt. Dabei konnte die Epoxidierung für alle genannten Strukturen als Machbarkeitsstudie erfolgreich dargestellt werden.

Der Ansatz zur Reinigung von EPS in einem optimierten Produktionsstamm lieferte 17 UV-aktive Fraktionen, von denen die meisten mit Stilben-Derivaten assoziiert werden konnten. Obwohl es sich dabei mit großer Wahrscheinlichkeit hauptsächlich um unterschiedliche Peptide handelte, die den Epoxidring öffneten, wurden auch dimerisierte Stilben-Strukturen entdeckt, zu denen Strukturvorschläge anhand ihrer MS-Fragmentierungen gemacht wurden. Zusätzlich konnte auch das *cis*-Isomer des IPS und ein weiteres Derivat detektiert werden, das vermutlich eine Amino-Gruppe im Resveratrolring, ähnlich dem bereits bekannten Lumiquinon A, trägt.

Summary

This work addresses the investigation of the biosynthesis mechanisms of type II polyketide synthase (PKS) and fatty acid synthase (FAS) derived specialized metabolites (SMs) from *Photorhabdus laumondii*.

The elucidation of the biosynthetic pathway of the bacterial 3,5-dihydroxy-4-isopropyl-trans-stilbene (IPS) was one of the major topics of this thesis. IPS exhibits several bioactive characteristics as it inhibits the phenoloxidase of insects, acts antibacterial, but also influences the soluble epoxide hydrolase which is involved in inflammatory reactions. It was recently approved as a treatment against psoriasis by the FDA and is the first *Photorhabdus* derived drug.

The stilbene generation in *Photorhabdus* requires the formation of the two acyl-carrier-protein (ACP) bound 5-phenyl-2,4-pentadienoyl- and isovaleryl- β -ketoacyl-moieties. The ketosynthase (KS)/cyclase StID catalyzes a ring formation via a Michael-addition between the two intermediates which is then further processed by an aromatase. The formation of 5-phenyl-2,4-pentadienoyl-ACP was shown via *in vitro* assays with purified proteins by proving the influence of the KS FabH, ketoreductase FabG and dehydratase FabA or FabZ of the fatty acid metabolism. While *E. coli* was able to complement most of these enzymes in attempts to produce IPS in the heterologous host, the *Photorhabdus* derived FabH was not replaceable despite 73 % sequence identity with the *E. coli* based isoenzyme, acting as a gatekeeper enzyme for cinnamic acid (CA) moieties. Furthermore, the ability to incorporate *meta*-substituted halogenated CA-derivatives was shown in order to produce 3-chloro- and 3-bromo-IPS. While studying the stilbene biosynthesis, the ability of *Photorhabdus* and *Xenorhabdus* to produce hydrazines was also discovered.

The second investigated biosynthesis was the formation of benzylideneacetone (BZA). BZA is produced by *Photorhabdus* and *Xenorhabdus* strains acting as a suppressor for the immune cascade of insects and has also antibiotic activities towards Gram-negative bacteria. Due to its structural similarity towards CA and the intermediates during the stilbene formation, a shared mechanism for *Photorhabdus* and *Xenorhabdus budapestensis* was proposed due to their ability to produce CA. The production of BZA was also dependent on the stilbene related CoA-ligase, the ACP and FabH. It was verified

in vitro and *in vivo* in *E. coli* yielding a 150-fold increase of the BZA production compared to the *Photorhabdus* and *Xenorhabdus* wildtype (WT) strains.

The second part of this work deals with the optimization of *P. laumondii* strains regarding the production titers of IPS. Therefore, several deletions of other SM related genes as well as promoter exchanges in front of stilbene related genes were carried out. These approaches were combined with the upregulation of the phenylalanine by heterologous plasmid expression, since it is the precursor of CA. Another approach applied in parallel was the optimization of the cultivation conditions with different media and supplementation with XAD-resins. It was proved that media rich on fatty acids or peptides led to higher optical densities of the cultures and thus to higher titers of stilbenes. Since IPS is inhibiting the phenoloxidase, an enzyme important for the insect immunity, it was hypothesized that cultivation in media containing insects might enhance the output of this SM. Starting from 23 mg/l of IPS in the *P. laumondii* WT strain, it was possible to increase the production levels to more than 860 mg/l by utilizing the mentioned approaches.

The last topic of this thesis focuses on the production of epoxidated IPS (EPS) and its derivatives. Under laboratory conditions, only a low titer of EPS was observed for the wildtype strain. However, the optimized IPS strains and IPS-production conditions could also be applied for EPS which led to higher productions and also to the detection of many new derivatives. Most of the EPS derivatives were amino acid or peptide derived acting as nucleophiles to open the epoxide ring and yielding β -amino-alcohols. However, purification and chemical synthesis attempts to obtain EPS failed due to its poor stability. Epoxides were utilized in *in vitro* assays with amino acids, peptides and proteins to get insights whether epoxidations might act as posttranslational modification in *Photorhabdus*. The reactions were performed with styrene oxide and stilbene oxide replacing EPS based on their structural similarity. The modifications were executed successfully although proteomics approaches with *in vivo* data are required to confirm these findings. During the purification attempts of EPS, further derivatives were detected. The structures of dimerized stilbenes, a *cis*-isomer of IPS and another derivative that might incorporate an amino-group in the resveratrol ring were proposed on the basis of the HPLC-MS data.

1 Introduction

The term natural products (NPs) describes a wide range of metabolites produced by all living organisms. Compounds derived from bacteria, fungi and plants have been used by humans for treatment of disease for centuries¹. Due to millions of years of evolution, microorganisms offer a huge array of NPs exhibiting a plethora of different characteristics which can be used for medical applications, in the agrochemical sector for crop protection as well as in the cosmetic and the food industry²⁻⁴. These molecules can be distinguished into primary metabolites and secondary metabolites also called specialized metabolites (SM)⁵.

Primary metabolites can be found in all living organisms and can be assigned to lipids, amino acids or oligonucleotides and are not rich sources for medical treatments⁵. They are essential for the viability and the growth of the organism. SM however are only found in certain groups of organisms and were developed for evolutionary advantages over the time⁶. Their exact role in nature is often not known, but SM range from compounds important for the development of the organism to toxic compounds for protecting the producer or also for pathogenicity and for communication with the same or other species⁷. SM are generally not essential for the growth of microorganisms and therefore the SM encoding genes can be deleted. However, their absence might impair their survival in their natural ecological niche due to the missing evolutionary advantages. Deterrents and toxic compounds are molecules of interest due to their potential utilization in the medical field as antibiotic agents. These compounds can often be found in areas with various organisms competing for the same ecological niche. The most prominent discovery in this research area is the work of Dr. Alexander Fleming who found and isolated the first known antibiotic penicillin in 1928, obtaining the Nobel Prize for his findings in 1944⁸. Regarded as one of the historic milestones not only in his research area, but also in general for humanity saving millions of lives in the following decades, his findings ignited a great interest in SM research heralding what was later called the golden era of antibiotics between the 1950s and 1960s¹. However, with the broader use of these new drugs many bacteria attained resistance against the mode of action of antibiotics leading to the antimicrobial resistance crisis⁹. The surge of resistant bacteria is accompanied with a

decline of new medications and thus leads to one of humanities greatest challenges for the upcoming decades together with the man-made climate change and accessing new energy supplies^{1,10,11}. Studies even showed an acceleration in the acquisition of new antibiotic resistances due to rising temperatures^{12,13}.

Besides antibiotics, SM offer also other various characteristics for medical applications as immunosuppressive anticancer agents or pancreatic lipase inhibitors, as antifungals in the agrochemical sector or as biofilm-inhibitors for applications in hospitals (Figure 1 for a selection of chemical structures of some SM)^{14,15}. They consist of various classes of metabolites with great chemical diversity, which are synthesized by polyketide synthases (PKS), non-ribosomal peptide synthetases (NRPS), ribosomally synthesized and post-translationally modified peptides (RiPPs), terpenes and saccharides¹⁶.

Declining genome sequencing costs and increasing computing powers offered a great opportunity to approach the field of NP research within the last decade since it was possible to analyse and compare many of the mentioned metabolite classes. Although the number of sequenced genomes and entries in genome databases is rising, which allows genome mining approaches for the identification of new biosynthetic gene clusters (BGCs) some major challenges still remain. Only already known BGCs can be identified and prediction of biological activities is not possible with this strategy¹⁷. However, organisms often cannot be cultivated under laboratory conditions or yield poor production levels. To overcome this issue, it is often crucial to understand the biosynthetic mechanism to increase the production titers or transfer the relevant genes into a heterologous host¹⁸.

There are also cases that biosynthetic genes are not encoded within one cluster, thus hampering approaches to heterologously produce SM from not cultivatable organisms¹⁶. This is also a challenge for scientists working with metagenomes since the heterologous host might not encode all *trans*-genes or might not be able to produce all encoded enzymes necessary for the biosynthesis¹⁹.

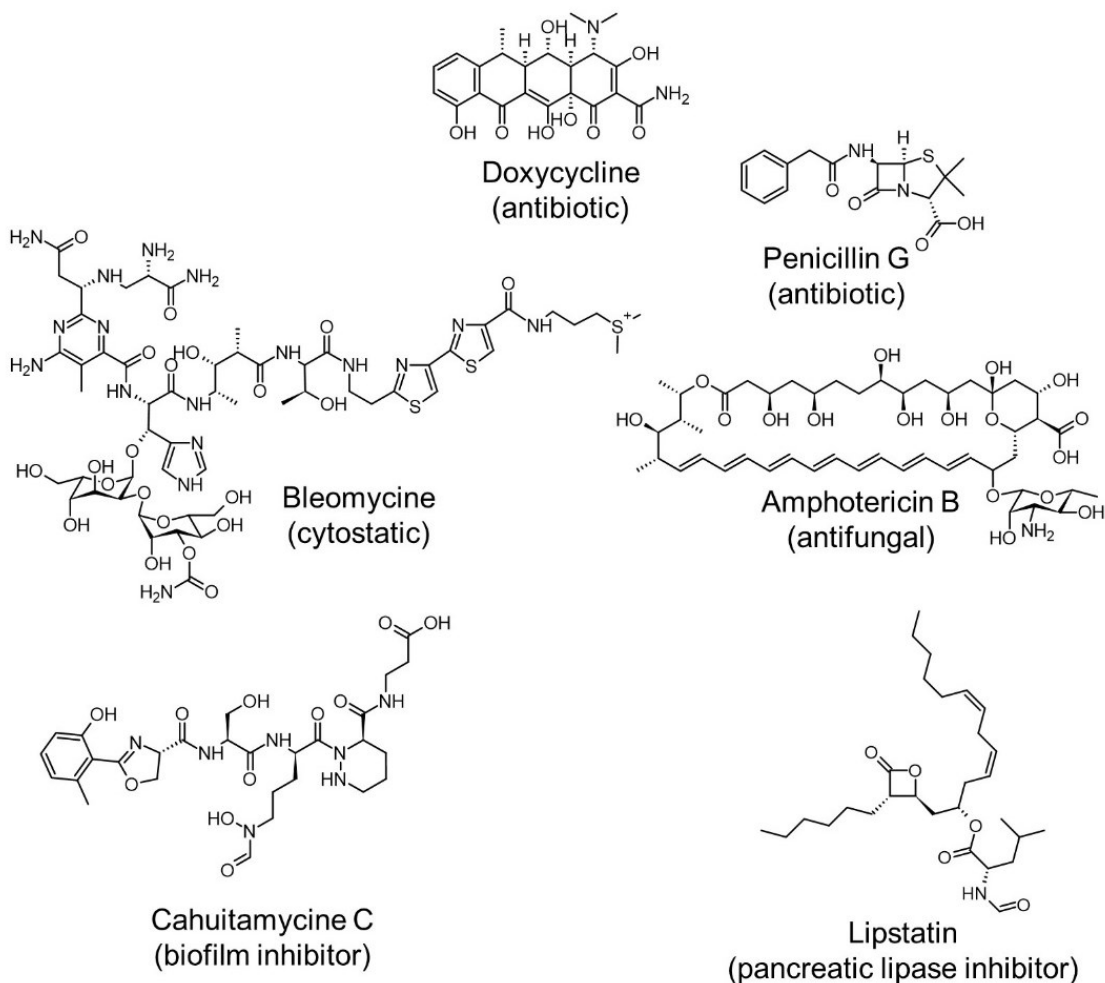


Figure 1. Structures of selected bioactive SMs with different applications^{8,20-24}.

1.1 *Photorhabdus* and the mutualistic symbiosis with *Heterorhabditis*

Photorhabdus laumondii TT01 is a mesophilic Gram-negative, facultative anaerobic, motile, rod shaped bacterium which was originally isolated from the nematode *Heterorhabditis bacteriophora* (*H. bacteriophora*) in Trinidad and Tobago²⁵⁻²⁷. Both organisms live in close mutualistic symbiosis with *P. laumondii* living in the gut of *H. bacteriophora*. The infective juveniles (IJs) of latter nematodes live in the soil and search for insect larvae. After the nematode enters the insect via natural openings, the bacteria are released into the haemolymph where they sense the different habitat and undergo a switch from the mutualistic form (M-form) to a so-called pathogenic form (P-form) and start to produce toxic SM to kill the insect (Figure 2). The switch between forms

is accompanied by a change in phenotype (loss of pigments) and production of many different SM^{28,29}. The nematode and the bacteria utilize the nutrients of the insect cadaver for reproduction and growth. After two to three life cycles from larval to adult stage, a new generation of IJs colonized by *P. laumondii* leaves the insect and finds new prey. The bacteria and nematodes can colonize and kill a variety of different insects which is also a reason why *Heterorhabditis* is used in agricultural pest control³⁰. *Xenorhabdus* bacteria conduct a similar life-cycle as *Photorhabdus*, but live in symbiosis with their nematode host from the genus of *Steinernema*³¹.

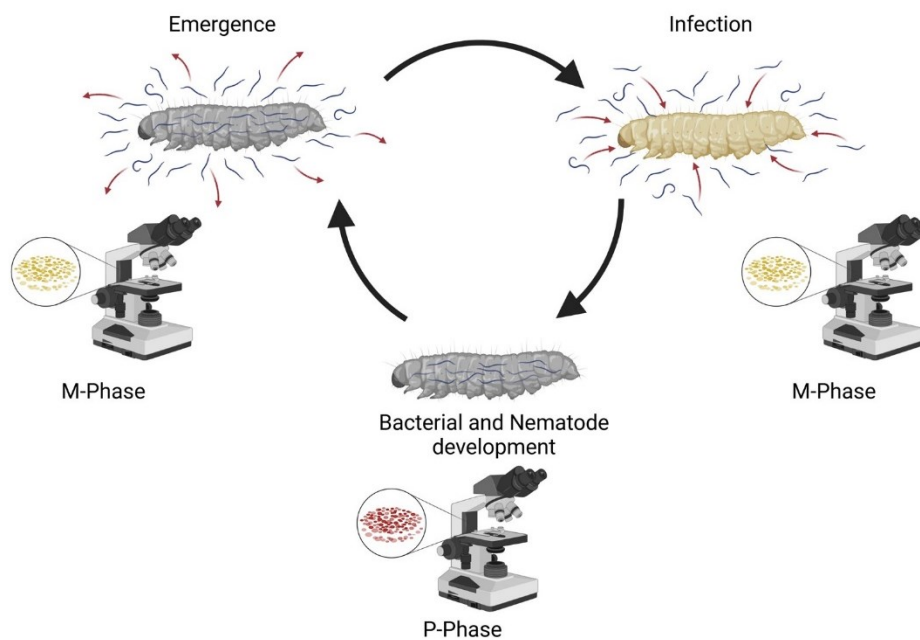


Figure 2. Life cycle of the entomopathogenic *Photorhabdus*-*Heterorhabditis*- complex. *H. bacteriphora* IJs transport *P. laumondii* in its gut and infects insect larvae. Upon infection the bacteria are released into the hemocoel, replicate and convert from M- to P-form (indicated by the change of phenotype from yellow to red in the magnification) to kill the insect. The nematodes develop until the nutrients are deprived. A new generation of IJs ingest *P. laumondii* and emerge from the cadaver to repeat the cycle with a new prey. Figure adapted and modified according to Shi and Bode, 2018⁷. Created with BioRender.com

1.2 Features of specialized metabolites in *Photorhabdus*

Photorhabdus and the closely related *Xenorhabdus* strains encode up to 6.5 % of their respective genome to the production of NPs. Due to its cultivability in the lab without its

host and its characteristics to produce a lot of SM, *P. laumondii* thus became one of the model organisms for production and analysis of NPs from Gram-negative bacteria³².

Photorhabdus strains harbor a diverse array of BGCs. These are responsible for the production of antibiotic metabolites (darobactin and odilorhabdin), for quorum sensing and thus responsible for cell communication (photopyrones and dialkylresorcinols (DARs)), development of nematodes (isopropylstilbene, IPS), insect virulence factors (rhabduscin, rhabdopeptides and benzylideneacetone (BZA)) and proteasome inhibitors (glidobactins) as shown in Figure 3^{7,33,34}. However, many of the produced SMs harbour more than one bioactivity like DARs which have also antimicrobial, fungicidal or nematicidal activities^{35,36}.

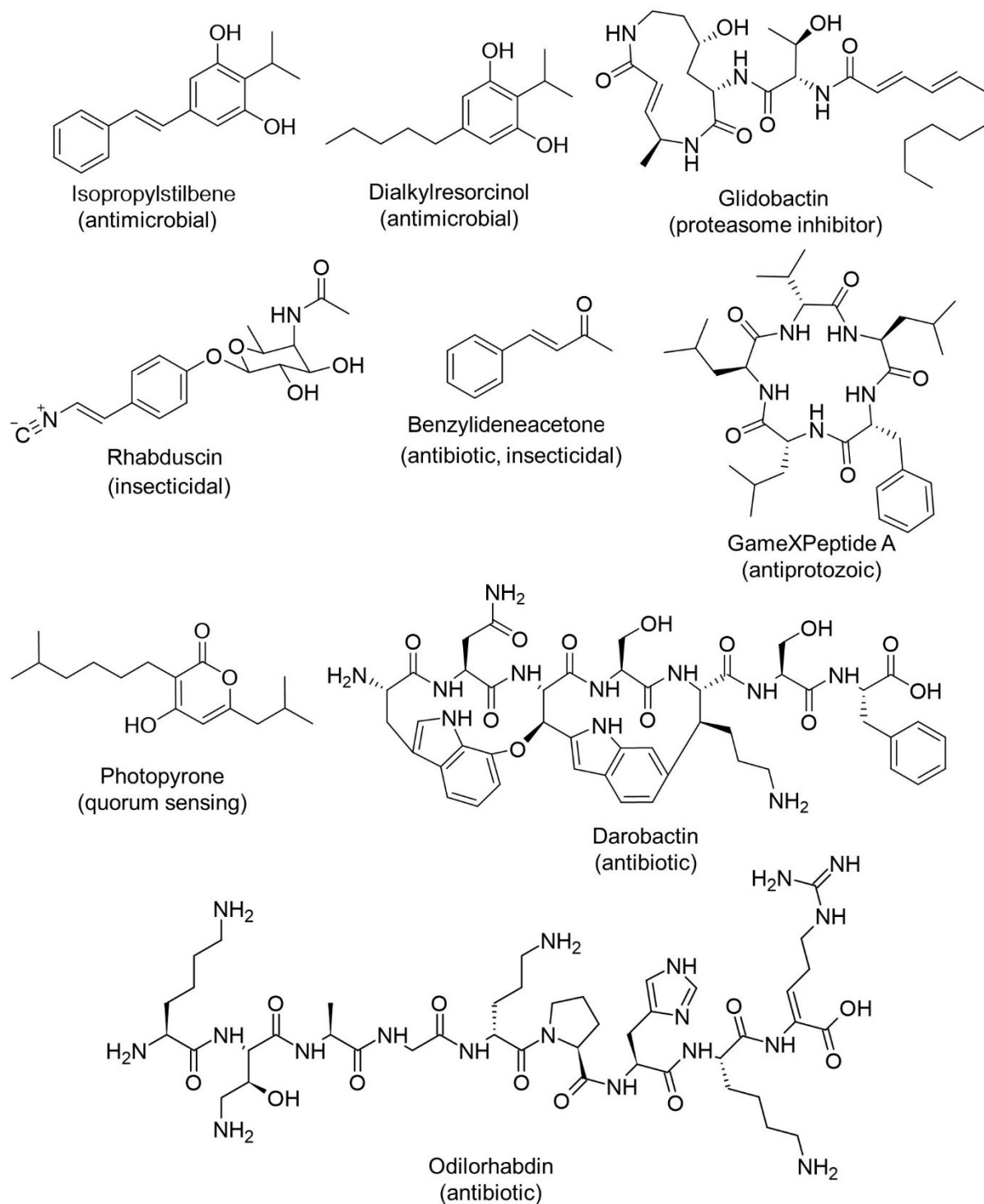


Figure 3. Structures of selected SMs isolated from *Photorhabdus* and *Xenorhabdus* strains with associated bioactivities^{7,33,34,37}.

While the mode of action of most of the *Photorhabdus* and *Xenorhabdus* derived antibiotic or antimicrobial compounds remain unclear, odilorhabdin targets the small ribosomal

subunit at a novel binding site and darobactin targets the outer membrane of Gram-negative bacteria^{33,34}.

Photopyrones and DARs depict two classes of quorum sensing molecules besides the well-known acyl-homoserine lactones (AHLs)³⁸⁻⁴⁰. They are sensed by the LuxR-like receptors PluR and PauR and activate the *Photorhabdus* clumping factor (PCF) which is encoded by the *pcfABCDE*F operon and activates cell clumping and also shows insect pathogenicity³⁹.

Photorhabdus and *Xenorhabdus* induced insect pathogenicity is caused by impacting several checkpoints in the immune system. Insects utilize a phenoloxidase (PO) to induce melanogenesis which protects the insect against pathogens⁴¹. For suppression of the insect's immune response, metabolites like rhabduscin and rhabdopeptides target the PO signal cascade. Rhabduscin is a tyrosine based SM which contains a rare terminal isonitrile group and an amidoglycosyl moiety and inhibits the PO at a nanomolar scale⁴². Rhabdopeptides are NRPS derived linear peptides (two to eight amino acids) containing a C-terminal amine and different degrees of N-methylations^{43,44}. This large class of peptides (comprising more than 60 known peptides) inhibit the serine proteases P1 and P2 which are also important for the PO cascade⁴⁴.

Phospholipase A₂ catalyzes the formation of arachidonic acid which is further processed to eicosanoids like prostaglandins which act among signaling molecules for the immune system⁴⁵. Phospholipase A₂ is inhibited by several SMs produced by *Photorhabdus* and *Xenorhabdus* such as BZA, *cis*-cyclo-proline-tyrosine or p-hydroxyphenyl propionic acid^{45,46}. While BZA is the most potent and also the most produced inhibitor its biosynthesis remains still unclear⁴⁶. Besides Phospholipase A₂, these molecules also inhibit the activity of PO and also hemocyte nodulation and can also be applied to protect plants against Gram-negative bacterial pathogens^{46,47}. The latter is related to the production of eicosanoids and also part of the cellular immune response of insects. When insects are attacked by microorganisms, aggregation of hemocytes is induced to trap the intruders⁴⁸.

Some *Photorhabdus* strains are able to produce eukaryotic proteasome inhibitors like glidobactins. Glidobactins target the 20S proteasome which is important for the protein

quality machinery and are hence a promising class of molecules against diseases like cancer since cancer cells tend to have increased levels of proteasome activity^{49,50}.

1.3 PKS and FAS

The SMs in this work are produced by PKS and fatty acid synthases (FAS) of *P. laumondii* TT01. Therefore this chapter will introduce the involved domains and mechanisms in the biosynthesis of PKS and FAS. Polyketides and fatty acids use similar building blocks (acetyl- and malonyl-CoA, (MCoA)) and share similar machineries although they differ from a structural point of view. Both products are produced by a machinery of enzymes which transport covalently bound intermediates from one active site to another⁵¹.

The reaction mechanism of PKS and FAS can be distinguished into three steps which include the initiation, the elongation and the procession or modification of the substrates⁵². They share a similar mechanism which is initiated with the loading of the so-called acyl-carrier proteins (ACPs) by Acyltransferases (AT). ACPs transport the respective substrates to the catalytic domains where elongation and modification steps take place. ACPs are proteins with a conserved serine residue which can be post-translationally modified with a CoA derived phosphopantetheine (Ppant) moiety converting the ACP from the *apo*- to the *holo*-state catalyzed by a phosphopantetheinyl transferase PPTase (Figure 4a)⁵³. PKS and FAS use decarboxylative Claisen thioester condensations of CoA-moieties for the elongation of the respective polyketide or fatty acid chain catalyzed by ketoacyl synthases (KS) as shown in Figure 4b⁵². The procession or modification reactions are catalyzed by ketoreductase (KR), dehydratase (DH) and enoylreductase (ER) domains (Figure 4). While PKS can vary in their ability to incorporate a broader substrate specificity, their respective chain length and in their degree of reduction, FAS typically carry out a full cycle of reduction to achieve a saturated acyl chain⁵². Both enzyme complexes share their repeated cycles of elongation and reduction reactions until a desired chain length is achieved and the product is released from the protein machinery. The release of the product from the ACP is typically achieved by hydrolysis or macrocyclization catalyzed by a thioesterase (TE). The hydrophobic character of the substrate channel of a TE favors the macrolactone formation over hydrolysis reactions for compounds like erythromycin⁵⁴. The structural diversity of polyketides over fatty acids

is achieved by various factors. These comprise from utilization of broader range of building blocks, to varying degrees of reduction and cyclization reactions and formation of so-called shunt products which are formed by spontaneous intramolecular cyclization. Another important factor are tailoring reactions. These reactions are carried out by tailoring enzymes and include various glycosylation (N-, C- and O-glycosylation), alkylation, acyl transfer, and hydroxylation, but also epoxidation, halogenation, transamination, nitrile and alkyne formation⁵¹.

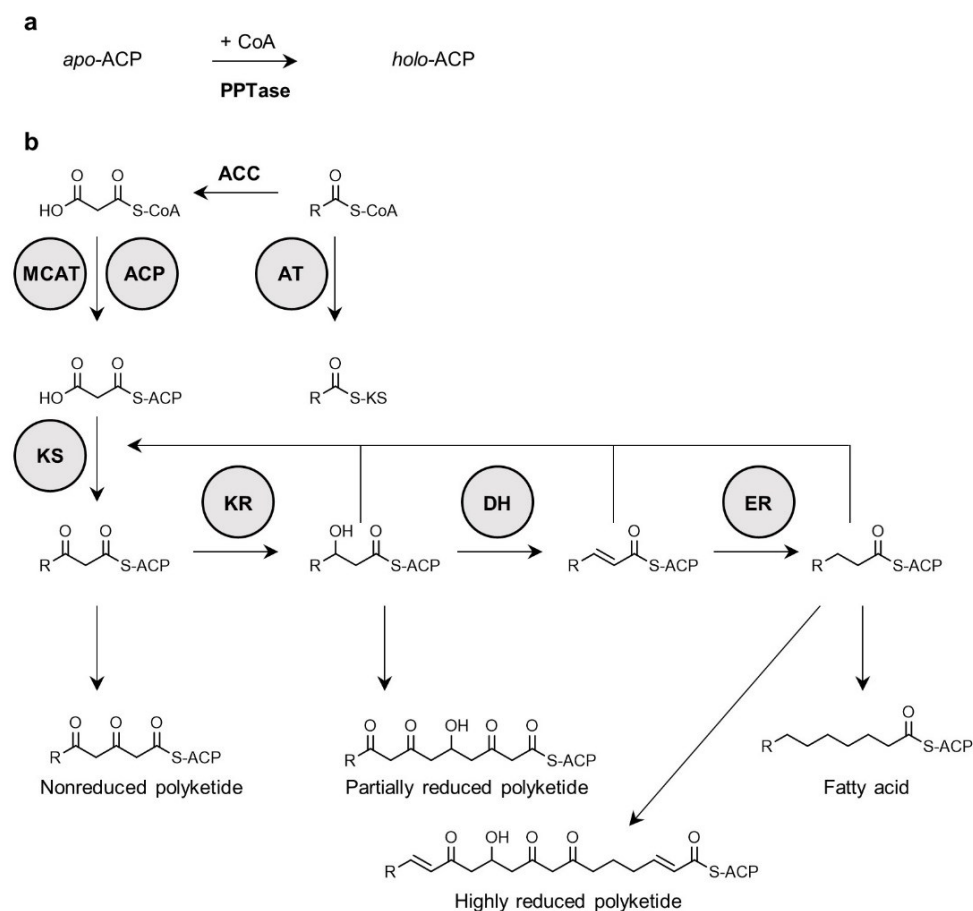


Figure 4. Mechanism of polyketide and fatty acid biosynthesis. Transfer of the CoA based Ppant arm to shift the ACP from *apo*- to *holo*-form catalyzed by a PPTase (phosphopantetheinyl transferase) (a). Malonyl-CoA and acetyl- or acyl-CoA (represented with R) from primary metabolism are utilized by a ketosynthase (KS) in a decarboxylative Claisen-condensation reaction forming a β-ketoacyl ACP. The product is processed by a ketoreductase (KR), a dehydratase (DH) and an enoylreductase (ER) resulting in a fully saturated acyl chain during fatty acid biosynthesis. In the polyketide biosynthesis, the processing reactions can be skipped yielding a non-reduced polyketide or utilized for the generation of a partially or highly reduced polyketide. ACC = acetyl-CoA carboxylase, MCAT = Malonyl-CoA Acetyltransferase.

1.3.1 Acyltransferases (AT)

ATs transfer acyl units onto the Ppant arm of an ACP domain. That reaction consists of a two-step mechanism. In the first step, the AT domain recognizes an acyl-CoA and binds the acyl moiety. The second step comprises the transfer to the Ppant arm of the ACP. Due to their substrate specificity, ATs often act as gate keepers for the respective PKS or FAS system⁵⁵. Substrates can vary, especially for PKS systems and include malonyl- and methylmalonyl-CoA, but also rarer substrates like allyl-malonyl-CoA in the biosynthesis of the immunosuppressive drug FK-506^{55,56}.

1.3.2 Acyl Carrier Protein (ACP) or thiolation domain

ACPs which are also referred to as thiolation or T-domains interact with all catalytic domains of PKS and FAS systems. They represent the smallest domain with about 10 kDa molecular weight and consist of four helices. In contrast to the other domains of PKS and FAS, ACPs do not show any catalytic activity. They are activated by posttranslational modification catalyzed by PPTases like AcpT, AcpS or Sfp which transfer the Ppant moiety from CoA onto a conserved serine residue at the start of the second α -helix of the ACP⁵⁷. The shift from the inactive *apo*- to the active *holo*-form provides a Ppant arm with a terminal thiol residue which enables the binding of substrate building blocks for synthesis of polyketides and fatty acids. The second helix is also important for interactions between the ACP and other protein domains and is also named "recognition helix"⁵⁸. ACPs consist of many polar and negatively charged amino acids which grant a certain flexibility required for the interaction with the various active sites of PKS or FAS systems⁵⁹. In type II systems it was shown that the helices II and III build a hydrophobic pocket which is used for sequestering the elongating product chain to protect it from side reactions which is not necessary in type I systems due to their close proximity to the next catalytic domains⁶⁰. However, there is a second form where the ACP presents the bound substrate to the active center of the catalytic domain. This switch between these two positions is also known as chain flipping mechanism⁶⁰.

1.3.3 Ketoacyl Synthases (KS)

KS belong to the proteins of the thiolase superfamily⁶¹. Built as homodimers, KS enzymes initiate the formation of C-C bonds by decarboxylative Claisen condensation which is carried out by the catalytic triad consisting of cysteine, histidine and asparagine or histidine⁵². The mechanism is also known as ping pong mechanism which includes the transacylation of the KS by an ACP and the condensation reaction where the C-C bond is generated (Figure 5a)⁶². Similar to cysteine and serine proteases an oxyanion hole for stabilization of the tetrahedral reaction intermediates is used which is also stabilized by a gating mechanism of a conserved phenylalanine residue (Figure 5b)⁶³. The cysteine in the catalytic triad binds the CoA or ACP bound starter moiety. Afterwards an ACP bound malonyl moiety which was also transported to the catalytic center of the KS is decarboxylated and the resulting carbanion stabilized by the other two residues of the catalytic triad. The nucleophilic carbanion can then attack the starter substrate resulting in the formation of β -ketoacyl product which is then transferred onto an ACP⁶⁴.

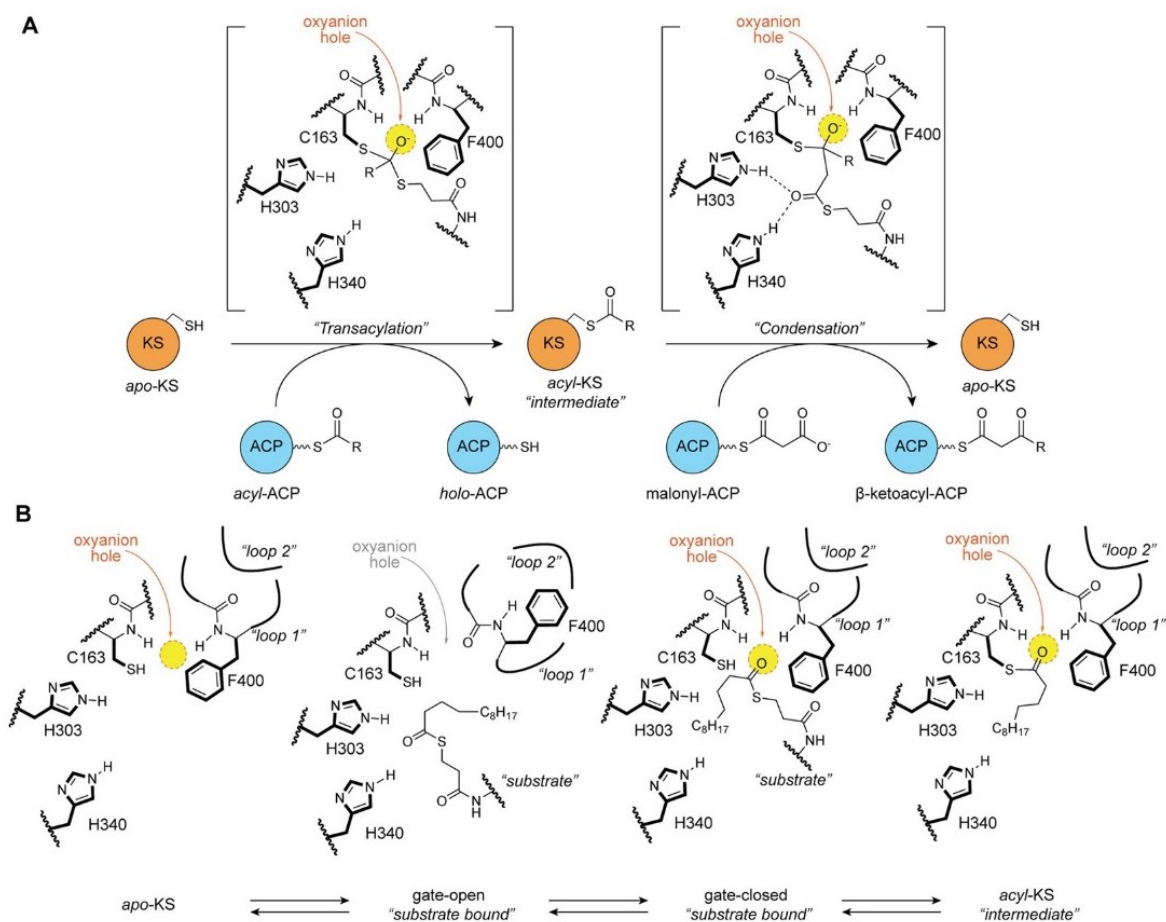


Figure 5. KS ping-pong reaction and gating mechanism overview. (A) Schematic illustration of the active site and oxyanion hole (in yellow) of the ketosynthase ping-pong mechanism. The tetrahedral intermediates generated during transacylation and condensation are stabilized by the oxyanion hole and the conserved phenylalanine. (B) Gating mechanism coordinated by loops 1 and 2 and the Phe400 gating residue. Each active site displays an advancing step during the transacylation half-reaction starting with the *apo*-KS active site and ending with the acyl-KS intermediate. Figure taken from Mindrebo *et al.*, 2021⁶³.

1.3.4 Modifying domains

Besides AT, ACP and KS, PKS and FAS also include KR, DH and ER domains. KRs consist of two subdomains, each similar to a short-chain dehydrogenase/reductase (SDR) monomer and utilize NADPH as a cofactor⁶⁵. While one subdomain exhibits a Rossmann fold and provides a structural role by stabilizing the other subdomain, the latter catalyzes the reduction from β -ketoacyl- to β -hydroxyacyl with the catalytic tyrosine and serine⁶⁵. KR domains can be distinguished in A and B types which determines the stereo chemistry

of the synthesized product. While type A KR's generate the S-isomer due to the substrate entering the active center of the enzyme from the left side (guided by a tryptophane residue), type B KR's lead to the formation of the R-isomer since their substrates enter from the right site (guided by a leucine residue from an LDD-motif)⁶⁶. The hydroxyl group can be further reduced by DH domains which incorporate a C-C double bond through the removal of water in either *cis*- or *trans*-position. DHs can be recognized due to a specific structural element containing a conserved "Hotdog" fold which contains of a α -helix wrapped by β -sheets which is also common in TEs⁶⁷. The last step of the modifying or processing enzymes is carried out by an ER. ER domains are NADPH dependent domains and reduce C-C double bonds to single bonds. They can be distinguished in short, medium and long chain dehydrogenase/reductase (SDR, MDR or LDR) superfamily depending on their respective substrate specificity, while most of them are part of the SDR family⁶⁸.

1.3.5 Termination and release

PKS and FAS systems both use TE domains to terminate the biosynthesis cycle and release the respective products. TE domains have similar to KS domains a binding channel which plays a crucial role regarding the chain length of the nascent polyketide or fatty acid⁶². They also show a growing affinity for hydrophobic tails which also plays a role in the regulation of the chain length⁶².

TE domains belong to the α/β -hydrolase superfamily, which also includes proteases, lipases and esterases⁶⁹. Members of this superfamily share a conserved catalytic triad consisting of serine, histidine and asparagine. TE domains can release the linear polyketide via hydrolysis as well as catalyze the formation of macrocyclic products via intramolecular nucleophile attack of a hydroxyl or amino group⁶⁹. Intramolecular cyclization reactions catalyzed by TE domains are common for PKS systems. Another release mechanism which has been discovered is the TE mediated catalysis of Dieckmann condensation, an intramolecular Claisen Condensation, which forms a tetrameric acid ring in the formation of HSAF, an antifungal compound from *Lysobacter enzymogenes*⁷⁰.

Another domain for the termination of the synthesis are reductase domains⁶⁹. These domains belong to the NADPH dependent SDRs and are more known for a reductive release forming aldehydes or alcohols⁶⁹. There are also other domains which can release products from FAS and PKS. The AT domain in the synthesis of lovastatin was described to be able to release the polyketide from the PKS machinery⁷¹. Other domains to release polyketides from PKS are Baeyer-Villiger-monooxygenases and lactamases⁶⁹.

1.3.6 PKS architecture

PKS can be divided in three different types which differ in their use of building blocks, architecture and occurrence in organisms.

PKS type I are large, linear arranged protein complexes with covalently linked enzyme domains which use various ACP-bound substrates and are predominantly common in bacteria and fungi⁵¹. Type II PKS however are dissociable complexes of proteins, acting iteratively and monofunctionally and utilize ACP bound malonyl units for extension⁵¹. Type II PKS are exclusive for bacteria. PKS type III are mainly found in plants, some bacteria and fungi and use MCoA instead of malonyl-ACP as extender units. They act in an iterative mechanism⁵¹. Besides these types of PKS there are also PKS-NRPS hybrids which can be found in bacteria and fungi and which accept ACP bound malonyl-units and amino acids for the elongation cycles.

1.3.7 PKS type I

Type I PKS can be divided into non-iterative and iterative systems⁷². Non-iterative ones are mainly present in prokaryotes and are known to form multimodular megasynthases up to several megadaltons⁷². Domains of an AT, ACP, KS build one module which can also carry further processing domains as a KR, DH and an ER. Non-iterative type I PKS systems harboring an AT are also called *cis*-AT PKS systems. Depending on the number of modules it is possible to determine the amount of extension cycles. The association of the chemical structure of the product with the number of modules of the PKS is called collinearity⁵¹. This principle can be utilized for the construction of new engineered PKS systems or to grasp which PKS might be involved in the biosynthesis of a compound. However, there are also cases of module skipping or the use of ATs which are encoded

somewhere else in the genome and thus are called *trans*-AT PKS. This might result in a structure which seems not fitting, at first sight, for the PKS of interest⁵¹.

A well-studied model representing non-iterative PKS type I systems is the 6-deoxyerythronolide synthase (DEBS) involved in the biosynthesis of erythromycin which is a *cis*-AT PKS (Figure 6)⁷³.

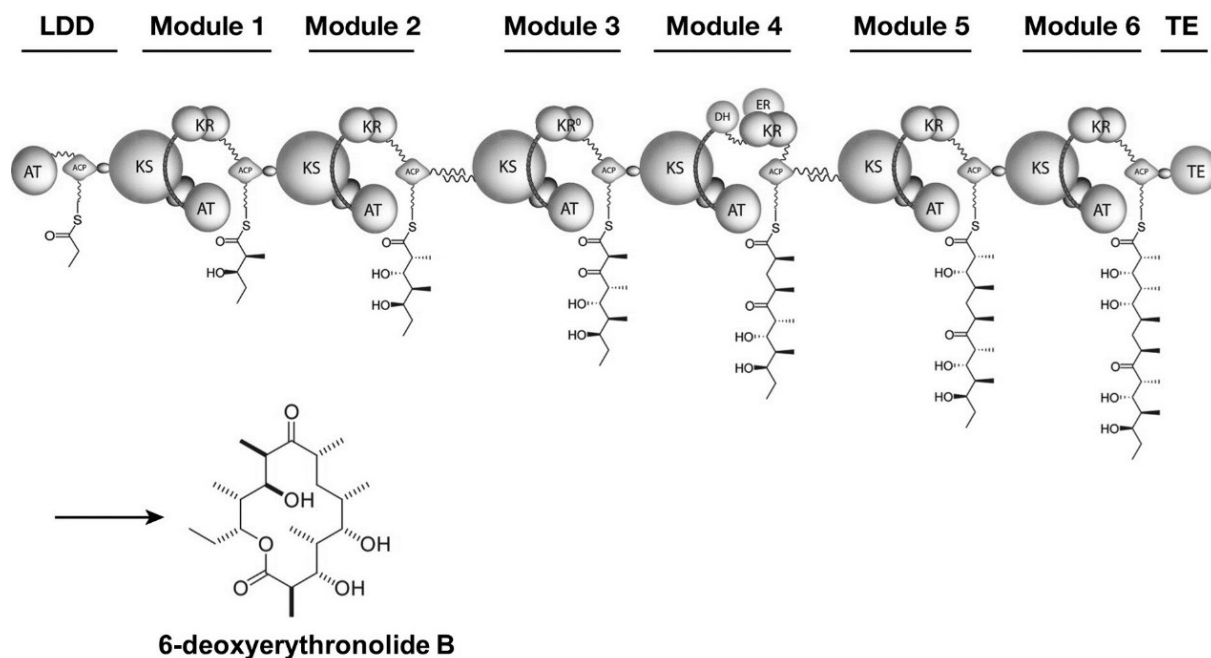


Figure 6. Example of a type I *cis*-AT PKS assembly line of a DEBS enzyme. The assembly line consists of a loading didomain (LDD), six extension modules and a TE domain for the termination of the reaction. The LDD incorporates a propionyl moiety as starter unit, while each elongation step utilizes a methyl malonyl- unit. The terminal thioesterase releases the cyclic heptaketide. Taken and adapted from Khosla *et al.*, 2007⁷³.

Iterative type I PKS are mainly present in fungi and also in some bacteria⁵¹. They do not exhibit the principle of collinearity as the non-iterative type and can thus use a domain or even a module several times. This type of PKS can be further classified as nonreducing, partially reducing or highly reducing depending on the presence of the optional processing domains (KR, DH and ER)⁵¹.

1.3.8 PKS type II

Type II PKS are common for prokaryotes and act iteratively since they consist of monofunctional and free-standing enzymes. This type of PKS is known for so called

minimal PKS which only consist of an ACP and two KS which build a heterodimer (KS_{α} and KS_{β})⁷⁴. KS_{β} is also known as chain length factor (CLF) and does not exhibit the catalytic active cysteine residue for the initiation of the Claisen condensation. Type II PKS typically produce aromatic products and thus also use KRs, cyclases and aromatases although several polyenes were discovered within the last years^{75,76}. PKS of this type are common for Gram-positive bacteria as *Streptomyces* while for Gram-negative bacteria only a few examples are known. The latter are involved in the biosynthesis of anthraquinones (AQs) and IPS in *Photorhabdus* strains^{77,78}. A typical elongation cycle involves MCoA which is loaded onto a *holo*-ACP by a malonyl-CoA acyltransferase (MCAT). The malonate moiety is transferred from the ACP to a cysteine residue of the KS where it is used for the reaction with another acyl unit. This results in the formation of a β -ketoacyl product which can be processed by repetitive cycles until it reaches its final length determined often by the CLF. Typical chain lengths for type II PKS vary from C₁₆ (actinorhodin) to C₂₀ (tetracenomycin) and C₂₄ (pradimicin) as shown in Figure 7⁷⁴.

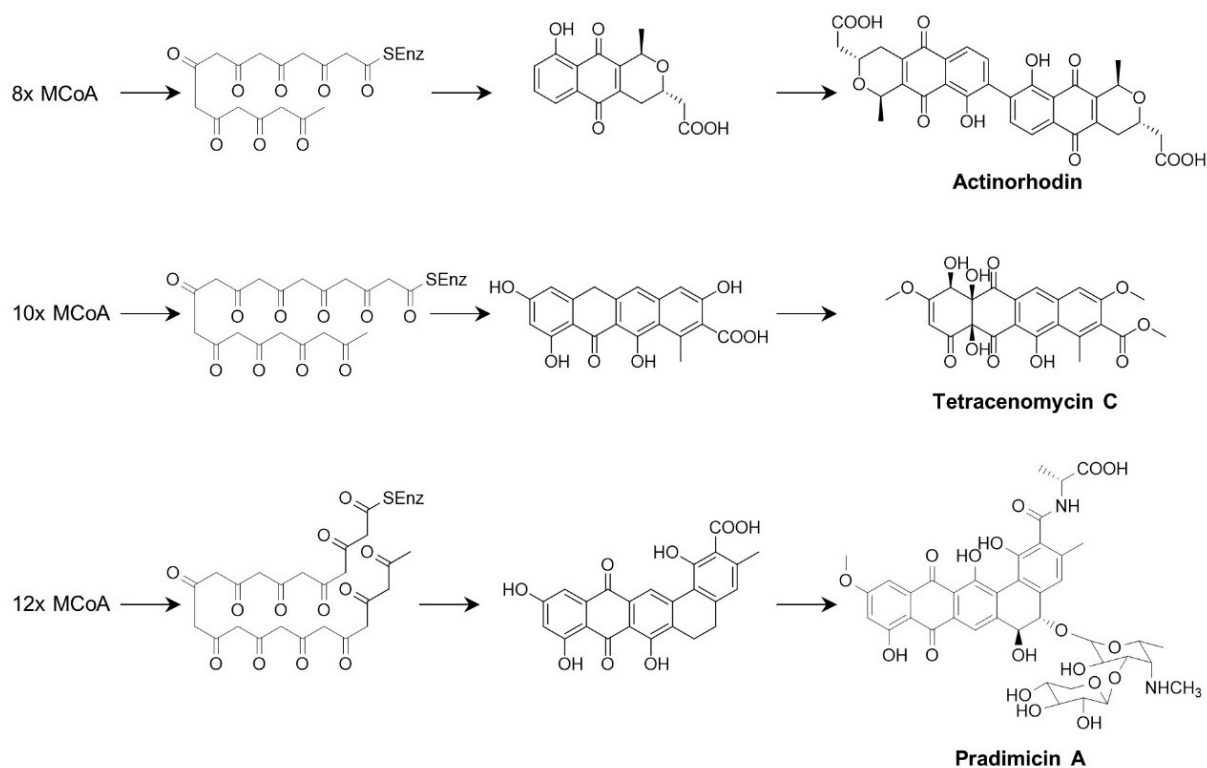


Figure 7. Example of three different PKS II derived polyketides with varying chain lengths⁷⁹⁻⁸¹.

1.3.9 PKS type III

The plant associated type III PKS systems are well known for the synthesis of polyphenols and for the utilization of CoA-moieties instead of ACP bound molecules. Models representing this type of PKS are the chalcone (CHS) and stilbene synthases (STS) (Figure 8)⁸². Typical type III PKS starter units for these examples are *p*-coumaroyl- and cinnamoyl-CoA which are derived from tyrosine and phenylalanine and are processed with repeated elongation cycles with MCoA forming a linear polyketide chain which afterwards cyclizes to naringenin or resveratrol by intramolecular aldol reactions⁸².

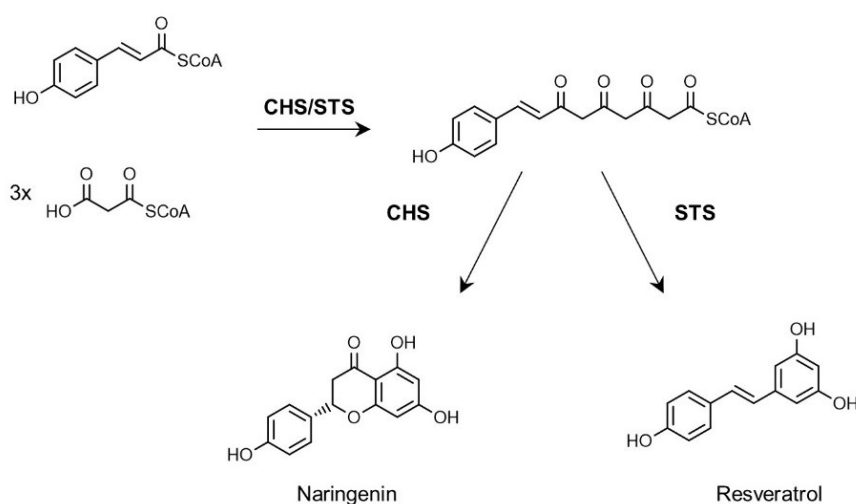


Figure 8. Biosynthesis of the *p*-Coumaroyl-CoA derived Naringenin and Pinosylvin after three elongation steps with MCoA catalyzed by the PKS III systems CHS or STS in plants. Figure adapted and modified according to Yu *et al.*, 2012⁸².

1.3.10 FAS I

FAS can be differentiated between type I and type II systems. FAS I are similar to PKS I and form huge megaenzyme complexes containing several catalytic domains and acting in an iterative manner⁵². Type I FAS are ubiquitous for mammals, fungi and some bacteria (corynebacteria, mycobacteria and nocardia) and generate saturated fatty acids with chain lengths usually ranging from C₁₄ to C₁₆⁵². They use acetyl-CoA for the priming and MCoA for the elongation reaction. The loading of the CoA moieties onto the ACPs is carried out by the malonyl/acetyltransferase (MAT) or the malonyl/palmitoyltransferase (MPT, only in fungi)⁶². The condensation is catalyzed by a KS and further processed by

KR, DH and ER domains similar to type I PKS systems. The termination of the synthesis is conducted by a TE or MAT/MPT domain.

1.3.11 FAS II

FAS II can be found in bacteria, plants and archaea. This type of FAS is similar to type II PKS systems and utilizes monofunctional enzymes. They are able to synthesize various chain lengths which can also vary from unsaturated, hydroxy and also (ante-) iso-branched fatty acids⁸³.

The type II FAS contains various monofunctional enzymes. The biosynthesis of fatty acids involves three different KS which build homodimers and are called FabH, FabB and FabF.

FabH is involved in the first elongation step in the biosynthesis. It has a substrate specificity for acetyl-CoA and binds the substrate covalently onto a conserved cysteine residue⁸³. FabH catalyzes the Claisen condensation of the acetyl-CoA starter unit with a malonyl-ACP forming the β -ketoacyl product⁸³. The malonyl-ACP necessary for the reaction is provided by the MCAT (FabD) which covalently binds the malonyl-moiety from MCoA onto a serine residue and transfers it afterwards onto a *holo*-ACP. MCoA is generated from acetyl-CoA catalyzed by the biotin dependent acetyl-CoA carboxylase (ACC), a biotin ligase providing the cofactor for the reaction. FabB and FabF are responsible for the subsequent elongation cycles of longer ACP bound acyl-groups. Both enzymes share their substrate specificity. However, FabB is necessary in *E. coli* for the elongation of the 10 carbon unsaturated *cis*-3-decenoyl-ACP intermediate while FabF is essential for the elongation of C16:1 to C18:1 fatty acid⁸⁴. There are also organisms producing only FabF which in turn can replace the functions of FabB⁸⁵.

After the elongation step, a ketoreduction step is carried out by the KR FabG. FabG is a NADPH-dependent tetrameric protein which forms a characteristic Rossmann fold to bind its cofactor⁸⁶. The DHs FabA and FabZ conduct the dehydration step in the FAS systems. The two DHs differ in their oligomerisation and hence in the number of ACPs they are able to bind. While FabA is dimeric and can bind two ACPs, the hexameric FabZ is able to bind up to three ACPs. Due to a differently shaped active tunnel FabA bears also an isomerase activity besides its function as DH and can thus perform the conversion from

trans-2-decenoyl-ACP to its *cis*-form. Both DHs show a broad specificity regarding the chain lengths of the substrates whereas FabZ shows a higher activity towards shorter chains which starts decreasing from C₆ while FabA showed a stronger activity for medium chain acyl-ACPs (C₈-C₁₂)⁸⁷. The last step of an elongation/procession cycle is the NADH-dependent reduction of the chain by the ER FabI or FabK. For unsaturated fatty acid chains, the reduction by the tetrameric ER is skipped.

Although most PKS systems utilize MCoA for the generation of the SMs there are polyketides built by non-acetate moiety starter units. The *bkd* operon which is encoding the proteins of the branched-chain keto acid dehydrogenase (BKD) complex is necessary for the biosynthesis of branched-chain carboxylic acids which are used for branched-chain fatty acids, but also utilized for the synthesis of SMs like avermectin or pristinamycin^{88,89}. Those carboxylic acids are built from the branched-chain amino acids valine, leucine and isoleucine which are processed to the corresponding 2-oxo carboxylic acid by a transaminase and then decarboxylated to isobutyryl-, isovaleryl- and 2-methylbutyryl-CoA (Figure 9). The BKD complex shares a high similarity with the pyruvate dehydrogenase complex and consists of three enzymes which build the multienzyme complex. E1 which is the first of the three subunits is a thiamine pyrophosphate (TPP) dependent dehydrogenase that decarboxylates the 2-oxo carboxylic acid to a TPP bound intermediate. The carboxylic acid is then transferred to a lipoic acid moiety bound to E2, the second subunit of the BKD complex⁸⁸. After this step, the carboxylic acid is transferred onto a free CoA generating the CoA thioester⁸⁸. The E3 enzyme uses FAD as cofactor to regenerate the reduced lipoic acid while FAD can be regenerated with NAD⁺⁸⁸.

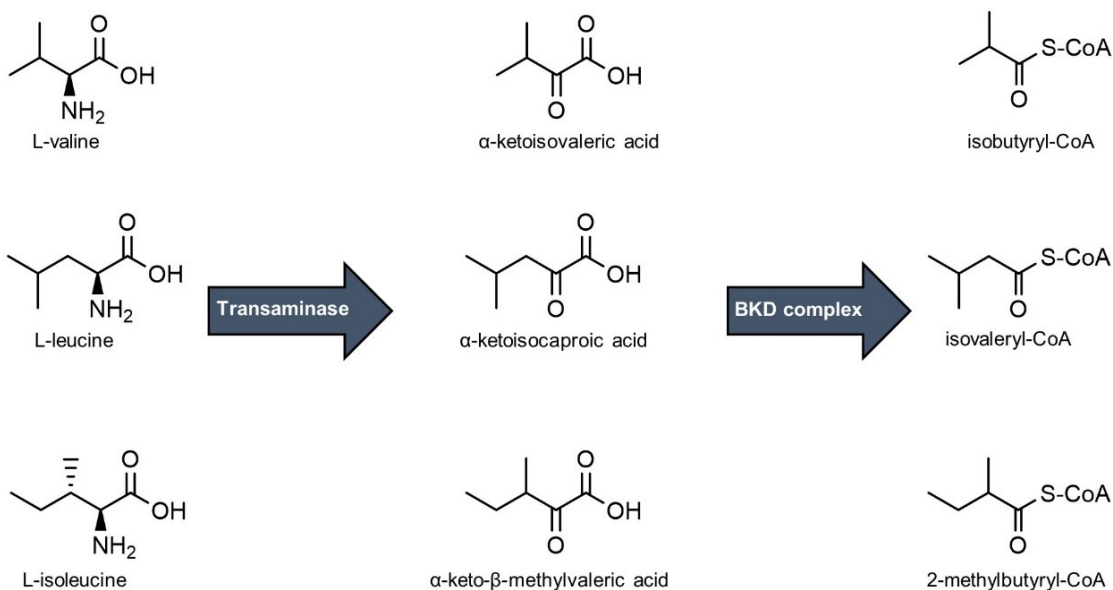


Figure 9. Conversion of iso-branched amino acids to α -keto acids and further to their correspondent CoA thioesters. Figure adapted according to Brachmann *et al.*, 2012⁸⁸.

The resulting CoA thioesters can afterwards be used by β -ketoacyl-acyl-carrier-protein synthase III enzymes like FabH or other specific KS to catalyze the condensation reaction. Although most organisms only possess one FabH for the elongation of acetyl-CoA with MCoA, some bacteria possess two isozymes with altering substrate specificities in order to utilize branched CoA moieties. The second FabH of *Bacillus subtilis* for example is able to use isobutyryl-, isovaleryl- and 2-methylbutyryl-CoA for the priming reaction⁸³.

1.3.12 N-acetylcysteamine thioesters (SNAC)

N-acetylcysteamine thioesters (SNACs) are biomimetic substructures of CoA and are used as a chemical tool to study biosynthetic pathways *in vitro* and *in vivo*⁹⁰. They exhibit only a truncated part of the Ppant arm without the nucleotide and pantothenic acid residue of CoA (Figure 10). Advantages of SNACs compared to CoA are the lower cost for synthesis, a higher stability and fewer potential side reactions⁹⁰. SNACs are also membrane permeable and can hence enter bacterial cells in contrast to CoA-derivatives⁹⁰. SNACs can be used in cases where CoA or carrier protein-bound thioesters are required and thus are especially useful for FAS, PKS and NRPS related reactions.

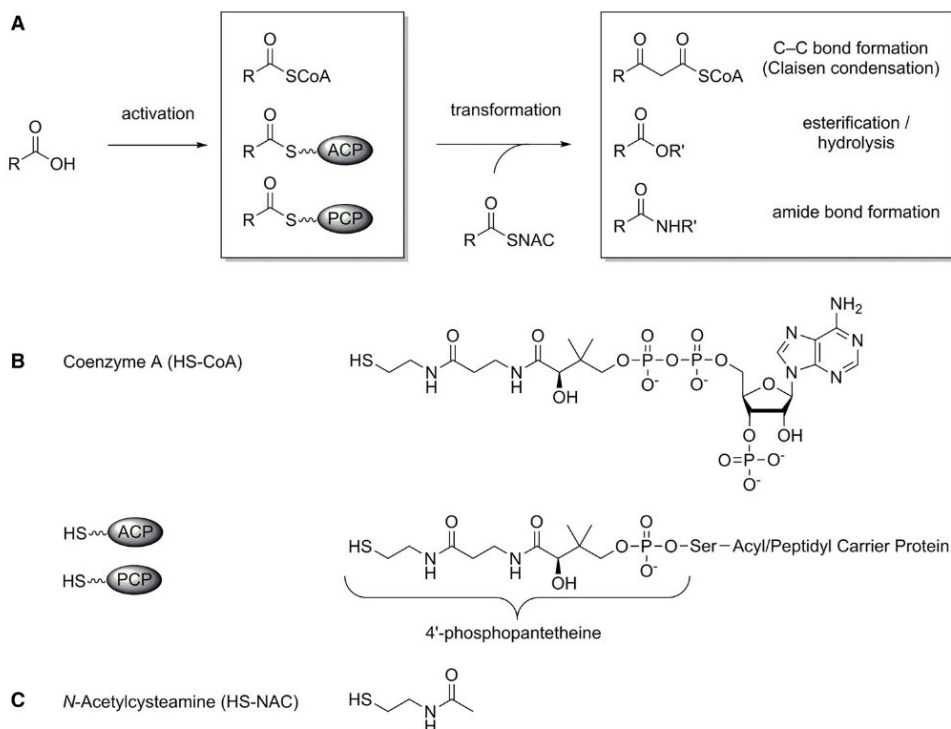


Figure 10. Activation of carboxylic acids as thioesters and carrier protein bound. Synthetic NAC thioesters can be used as substrate mimics *in vivo* and *in vitro* for new C-C bond formation, esterification, hydrolysis and amide bond formation (A). Chemical structures of CoA and *holo*-ACP or PCP with the structure of the Ppant arm (B) and the chemical structure of SNAC (C). Taken from Franke & Hertweck, 2016⁹⁰.

1.4 Identification and activation of natural products

For the identification and isolation of SMs, strains are cultivated followed by purification of the compounds and screening regarding their bioactivity. Since conditions in laboratories are artificial and challenging to mimic the natural habitat of some bacteria, it is often difficult to produce and isolate every potential compound that an organism has encoded in their respective BGC. A considerable number of BGCs which are not expressed under standard laboratory conditions are called silent gene clusters.

An approach to overcome this issue and also the high expenses of high throughput screenings is the so called *One Strain MAny Compounds* (OSMAC) principle⁹¹. Hereby, potent strains harboring several BGCs are cultivated with altering cultivation conditions e.g. different media, antibiotic stress, varying oxygen levels, pH, temperature or supplementation of precursors which can be used for biotransformation⁹¹. OSMAC is not only useful to find new SM, but is also an option to improve production conditions for

higher outputs of certain compounds. This principle is similar to one of the strategies for the optimization of fermentations. However, the latter is a research area for itself which developed from classical medium optimization methods where only one parameter was varied at a time while keeping other variables constant to more complex and statistic driven approaches yielding better results⁹². Often the use of rich media containing high amounts of carbon, nitrogen or phosphate sources helps to enhance production titers. From an economical view it is necessary to find a good ratio between cost and benefit for bigger fermentations. Regarding the cultivation of *Photorhabdus* strains which focus on insects as prey and grow optimal in their carcasses, it might be useful to use the latter for developing cultivation media (Figure 11). Within the last years ideas emerged of so called insect farming to recycle expired food and apply them as animal feed since insects are significantly more efficient with nutrients⁹³. They also require less land and emit less greenhouse gases than livestock⁹³.

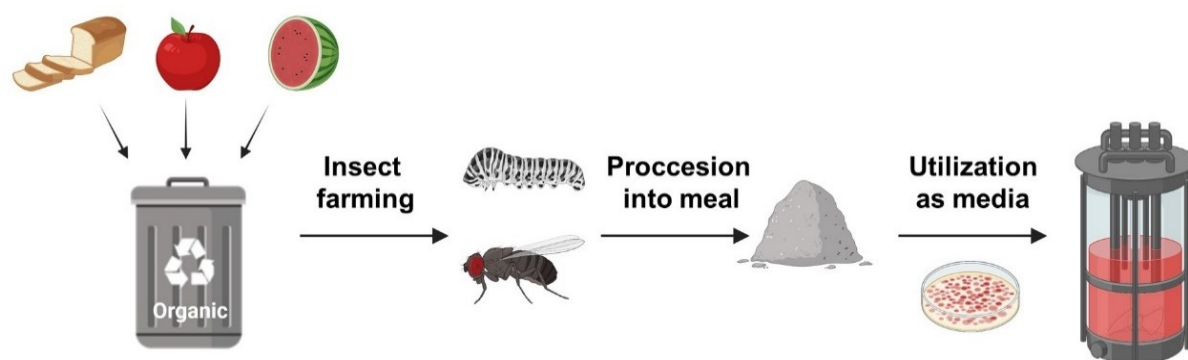


Figure 11. From organic waste to rich media for biotechnological applications. Organic wastes are used to grow insects which are then processed to enriched protein and fat containing insect meal. The latter can be utilized for cultivation of bacteria like *Photorhabdus* and *Xenorhabdus* in a bioreactor. Created with BioRender.com

Another approach to activate silent clusters is the co-cultivation or mixed fermentation of organisms which might interact in nature⁹⁴. This approach tries to mimic the ecological niche based on signaling molecules and interspecies communication⁹⁴.

Within the last decade approaches were developed to exploit the occurrence of NP related genes in clustered organization. The rise of bioinformatics and the shrinking cost of genome sequencing opened the field of genome-driven NP discovery. The genes of

the BGCs could be linked to biosynthetic pathways of SMs and also used to create natural product databases like antiSMASH (antibiotics and secondary metabolite analysis shell) which were used to analyze BGCs and to find similar clusters in other organisms⁹⁵. The predictions rely on similarity in conserved domains of characteristic enzymes and are based on Hidden Markov Models⁹⁶. The insights gained through bioinformatics led to more specific advances to solve the issue regarding silent genes clusters⁹⁷. These include deletion or expression of pathway specific transcription factors, refactoring of a BGC by insertion of a constitutive promoter or heterologous expression⁹⁷. The blue pigment indigoidine from *P. laumondii* which is also encoded by a silent or cryptic gene cluster was successfully activated via heterologous expression in *E. coli* and exchange of its natural promoter by Brachmann *et al.* in 2012⁹⁸. The method for the promoter exchange in *P. laumondii* includes the conjugation of an integrative plasmid with an *E. coli* donor strain and is well established in the Bode lab. The plasmid carries an inducible promoter in front of a heterologous region corresponding to the beginning of the first gene in the BGC of interest. Due to homologous recombination, the inducible promoter is inserted into the genome. In combination with the deletion of *hfq* which abolishes the production of most SMs in proteobacteria, this approach is referred to as “easy Promoter Activated Compound Identification” (easyPACId)⁹⁹. Nowadays a more advanced method for a marker- and scar less editing was developed by editing the genome with CRISPR/CAS12 (unpublished, by Alexander Rill)¹⁰⁰. This enables a less time consuming and efficient approach to edit several loci in the genome since no antibiotic resistance remains which makes this method even more valuable for compounds which need more than one promoter exchange for its activation. The exchange with a strong promoter and deletions of biosynthetic pathways can also help to overcome another common issue with metabolites which are produced only in a low yield and hence enable to approach otherwise challenging purifications due to higher NP-titers and reduced backgrounds.

1.5 Elucidation of SM structure and their biosynthetic pathways

In order to elucidate the structure of a NP, an array of different methods can be utilized. After extraction and separation with various potential methods depending on the chemical and physical properties of the compound, the purified NP can be analyzed via nuclear

magnetic resonance (NMR) spectroscopy for structure determination¹⁰¹. NMR spectroscopy is the most powerful tool for the identification of chemical structures and offers many advantages such as a non destructive analysis, high reproducibility and simple sample preparations. However, often the isolated SM lack the purity or yield for NMR analysis. One alternative method is the high resolution mass spectrometry (HR-MS) which is also sufficient to predict chemical sum formulas without application of time and resource consuming large scale cultures and purifications¹⁰². HR-MS based approaches can also be combined with supplementation and complementation experiments with isotope labelled chemicals to determine the number of certain atoms in a compound and to find derivatives and precursor metabolites¹⁰³. Such supplementation or feeding experiments have been conducted for more than 80 years in life sciences to study metabolism and can for instance be used to predict the configuration of an amino acid in a compound¹⁰⁴. A similar approach is the so-called inverse feeding of cultures. Instead of supplementing the cultures with isotope labeled substrates, the cultivation is carried out in media containing ¹³C or ¹⁵N. This leads to a shift in the MS-analysis depending on the number of C- and N-atoms occurring in the structure of the respective compound. After detection of the molecule with its shifted mass, non-labelled building blocks like amino acids which might be involved in the synthesis of the NP can be added to the culture. Incorporation of the lower mass building blocks will lead to a mass shift and thus help to draw conclusions regarding the chemical sum formula and structure of the molecule of interest¹⁰⁵. Other MS based structure elucidation methods include MS² fragmentation patterns and coupling with a liquid chromatography (LC) prior to the MS to see shifts in hydrophobicity between two similar compounds¹⁰⁶. Both methods are especially useful in combination with a chemical standard. HR-MS is also a valuable tool in combination with *in vitro* assays to comprehend reactions from biosynthetic pathways and engineering approaches based on determining and altering substrate specificities of enzymes¹⁰⁷.

1.6 Biosynthesis of stilbenes

Stilbenes are a typical plant derived SM and are a result of stilbene synthases, a type III PKS system. So far, the exclusive non-plant derived stilbene product is IPS (also known as tapinarof) and its derivatives that are produced by all *Photorhabdus* strains (Figure 12).

Therefore, IPS is regarded as a strain specific biomarker³⁷. IPS exhibits a number of biological activities. It is essential for the development of the *Heterorhabditis* nematodes which live in mutualistic symbiosis with the *Photorhabdus* strains, but has also antimicrobial and antifungal activity which might be a potential protective agent against food competitors¹⁰⁸. IPS is also a virulence factor and inhibits the phenoloxidase and the juvenile hormone epoxide hydrolase of insects¹⁰⁹⁻¹¹¹. It has also an inhibitory effect on the soluble epoxide hydrolase which is an interesting pharmaceutical target for inflammatory diseases due to its influence on the signal cascade of arachidonic acid¹⁰⁹. Derivatives of IPS were also successfully synthesized and applied against protozoa like *Trypanosoma cruzi*, the causative of Chagas disease, and against *Leishmania donovani* which causes Leishmaniose¹¹². IPS was also subject of clinical studies as a treatment against psoriasis and was approved by the FDA by summer 2022 and is today marketed as Vtama®¹¹³⁻¹¹⁵. So far it is the only approved drug from *Photorhabdus* and *Xenorhabdus*.

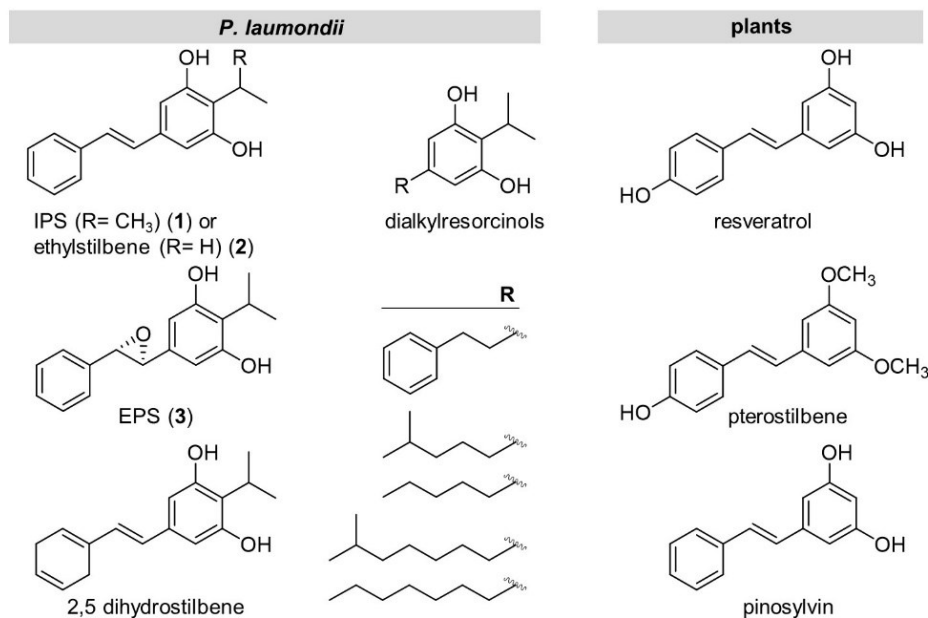


Figure 12. Chemical structures of stilbenes derived from *Photorhabdus* and plants. Figure adapted from Kavakli et al., 2022¹¹⁶.

The synthesis of stilbenes in *Photorhabdus* differs from the mechanism in plants. *Photorhabdus* strains are the only known microorganisms producing stilbenes. While plants make use of a PKS III system applying repetitive cycles of condensation reactions

until the polyketone is cyclized, *Photorhabdus* generates two reaction intermediates which then perform the addition and cyclization by a PKS II system which is rather uncommon for Gram-negative bacteria making this biosynthesis even more special^{78,117}. Instead of being comprised in one BGC location, the genes encoding the proteins for the biosynthesis are spread within the genome (*stlA*, *stlB*, *stlCDE* and *bkdABC*, Figure 13a)⁷⁸.

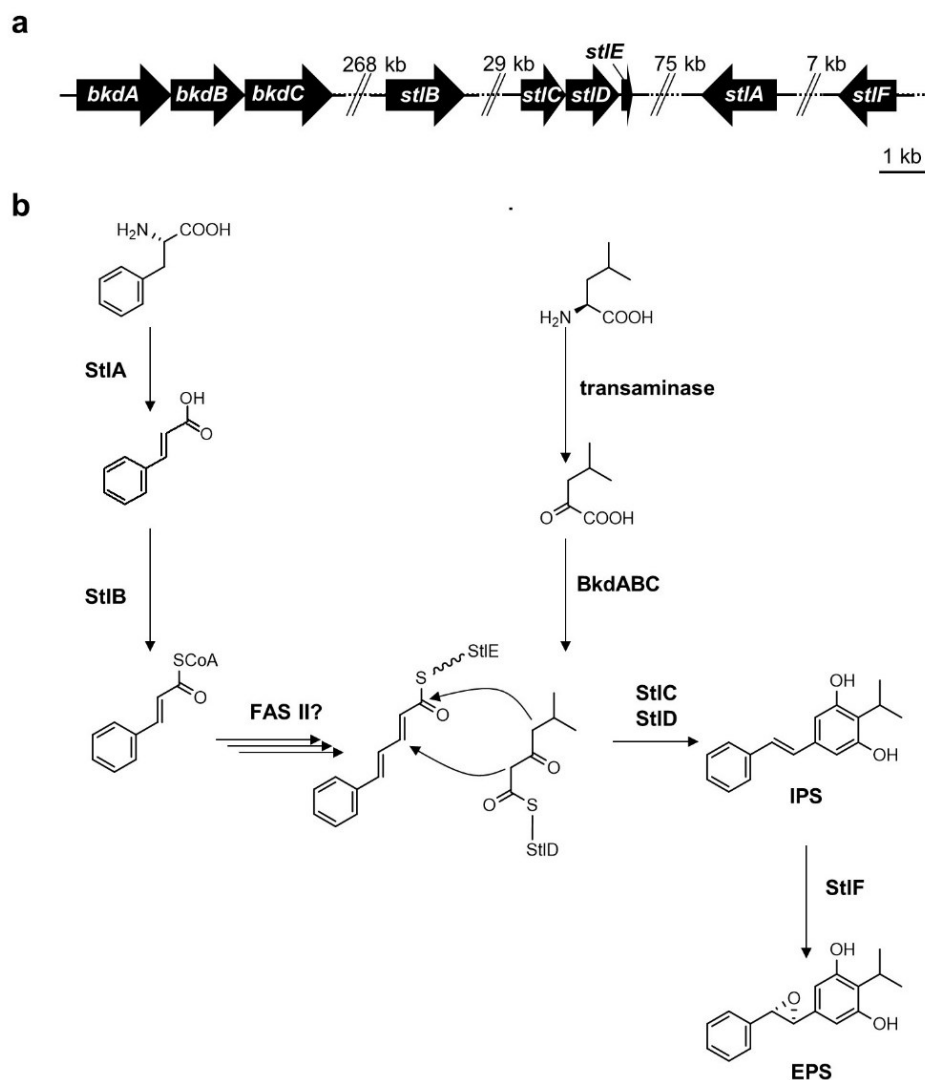


Figure 13. Genes involved in IPS production (a) and suggested IPS biosynthesis (b) in *P. laumondii* TT01. BkdABC = branched-chain- α -keto acid dehydrogenase with ketosynthase (*plu1883-1885*), StlB = CoA ligase (*plu2134*), StlC = aromatase (*plu2163*), StlD = ketosynthase/cyclase (*plu2164*), StlE = acyl-carrier protein (*plu2165*), StlA = phenylalanine ammonium lyase (*plu2234*), StlF = epoxidase (*plu2236*), FAS II = fatty acid synthase type II. Figure adapted from Joyce *et al.*, 2008 and Mori *et al.*, 2016^{78,117}.

The biosynthesis of IPS and its derivatives in *Photorhabdus* starts with a phenylalanine ammonium lyase (PAL, StIA) which is required for the formation of cinnamic acid (CA) from phenylalanine (Figure 13b)⁷⁸. Afterwards the CA is proposed to be transferred onto a CoA by StIB resulting in the formation of cinnamoyl-CoA (CA-CoA)⁷⁸. In this reaction StIB acts as a CoA ligase which utilizes ATP and generates an AMP bound acid intermediate which is then loaded onto the CoA moiety. For shuttling between the reaction sides, StIE is utilized, an ACP that is encoded in the *stlCDE* operon. The next steps of the synthesis require the formation of the α,β -unsaturated carbonyl compound 5-phenyl-2,4-pentadienoyl-ACP which needs one elongation, reduction and dehydration step as it has been suggested by Fuchs *et al.* for the formation of cyclohexanediones (CHDs) and DARs¹¹⁸. Data from my master thesis suggest that enzymes from the FAS II might be involved in the synthesis of the mentioned intermediate¹¹⁹.

In order to obtain the second intermediate crucial for the cyclization reaction, leucine is deaminated by a transaminase obtaining 4-methyl-2-oxovaleric acid. The latter is then converted to isovaleryl-CoA by the BkdA/BkdB-dehydrogenase complex. The KS BkdC catalyzes the reaction for the formation of the isovaleryl- β -ketoacyl intermediate, the second important compound for the cyclization reaction⁸⁸.

The 5-phenyl-2,4-pentadienoyl-moiety acts as a Michael acceptor and the cyclization and aromatization with the isovaleryl- β -ketoacyl intermediate is carried out by the KS StID and the aromatase StIC. Biochemical characterization of StID carried out by the Abe group showed the presence of two acyl-binding pockets although StID presents the homodimeric thiolase-like fold typical for KS¹¹⁷. A cavity for the elongation and cyclization was revealed between those two binding pockets. Moreover, StID has a broad substrate specificity for longer acyl chains which can be bound due to a large hydrophobic pocket and which explains the biosynthesis of various 1,3-cyclohexanediones with alternating acyl chain lengths¹¹⁸. The cyclization reaction yields a carboxy cyclohexanedione intermediate which is accepted by StIC for the aromatization yielding IPS. *In vitro* assays have shown the necessity of the carboxylic acid group for the binding of StIC¹¹⁷. IPS can be stereo-selectively epoxidized by a FAD dependent monooxygenase or epoxidase which is named StIF in this work^{120,121}. Data from the Crawford group showed that epoxy-

isopropylstilbene (EPS) shows less bacterial host cytotoxicity than IPS, while the virulence of IPS against insects, its antifungal and antimicrobial activity remain similar for EPS¹²¹. They were also able to find proline conjugated derivatives in insect models which resulted in the opening of the epoxide ring, but did not show any antifungal or antimicrobial activities anymore¹²¹. Two years ago, IPS dimers (also named duotaps, shown in Figure 14) were discovered which were produced by *P. laumondii* exposed to the oxidative agent Paraquat (1,1'-dimethyl-4,4'-bipyridinium dichloride). The resulting stilbene dimers yielded an up to ten-fold increase in its antimicrobial activity against the Gram-positive vancomycin-resistant *Enterococcus faecalis* (VRE) and methicillin-resistant *Staphylococcus aureus* (MRSA)¹²². The mode of action remains still unclear, but initial data suggest that these compounds target the cell wall of Gram-positive bacteria¹²³.

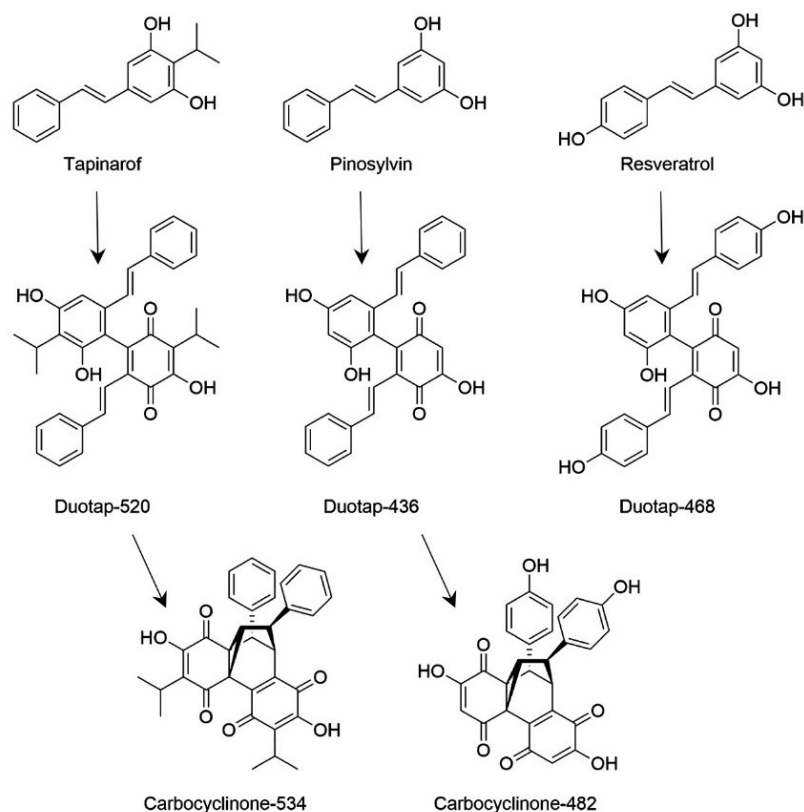


Figure 14. Structures of *Photorhabdus* and plant derived stilbene monomers, dimers (duotap) and carbocyclinone derivatives. The dimerization was catalyzed by a cupin enzyme from *P. laumondii* encoded by the gene *plu1886*. The carbocyclinones are produced by spontaneous reactions and build racemic mixtures. Taken and adapted from Goddard *et al.*, 2020¹²³.

1.7 Aim of this work

This work aims at the elucidation of the remaining unresolved steps of the biosynthesis of the PKS II associated IPS which was already started within my master thesis. Although the biosynthesis had been studied in the past extensively by the Bode and the Abe groups, the enzymes involved in the biosynthesis of the 5-phenyl-2,4-pentadienoyl-moiety acting as a Michael-acceptor for the already described cyclization reaction to generate the resveratrol ring remained unclear as well as the transfer into another host for a heterologous production. The role of IPS as a subject within clinical trials during the start of this work and now as the first FDA approved drug originating from the genus of *Photorhabdus* raises the relevance of this work. The objective was to transfer the insights gained by *in vitro* characterizations of the respective enzyme catalyzed reactions to the heterologous production in *E. coli* as another bacterial host.

BZA is another *Photorhabdus* as well as *Xenorhabdus* derived antibiotic molecule whose biosynthesis remained unclear and should be resolved with similar approaches as the production of IPS since it also could not be assigned to a BGC with antiSMASH.

A further topic in this work deals with the generation of a *P. laumondii* strain suited to produce high titers of IPS. By applying CRISPR/Cas as a tool to delete pathways or enhance the production or turnover of certain substrates, an optimized strain solely for the production of stilbene derivatives should be achieved. Additionally, different cultivation media were assessed in order to determine the optimal production conditions for the generated strain.

The last chapter of this work focuses on stilbene derivatives produced after production of a stilbene monooxygenase also known as epoxidase. Feeding experiments combined with LC-MS and also large cultures and purifications were carried out in order to detect novel stilbene derivatives and to purify EPS. Moreover, *in vitro* assays with epoxides, synthesized peptides and purified proteins are carried out to give insights into new modification reactions.

2 Material and Methods

2.1 Topic A: Biosynthesis characterization of stilbene related pathways

In the following sections all materials and methods used for the conducted experiments for topic A shown in chapter 2.1 are described. Many of the herein described methods are part of the publication “*Biosynthesis of the Multifunctional Isopropylstilbene in Photorhabdus laumondii Involves Cross-Talk between Specialized and Primary Metabolism*” by Siyar Kavakli[#], Gina L. C. Grammbitter[#] and Helge B. Bode* ([#] shared first author, *corresponding author). The publication is attached in chapter 7.

2.1.1 Cultivation of strains

All *E. coli* strains used were grown in Lysogeny Broth (LB) medium (10 g/l tryptone, 5 g/l yeast extract and 5 g/l NaCl, pH 7.5) at 37°C and 180°rpm. *Photorhabdus* strains were cultivated at 30°C. Solid media contained also 1.5% (w/v) agar. For selection kanamycin (Km), spectinomycin (Sm, each 50 µg/ml final concentration), chloramphenicol (Cm, 34 µg/ml final concentration) and gentamycin (Gm, 20 µg/ml final concentration) were used.

2.1.2 Microorganisms

All microorganisms, which were used in topic A, their genotype and the references, are listed in Table 1.

Table 1. List of strains, their genotype and their source used in topic A of this thesis.

Strain	Genotype	Reference
<i>E. coli</i> DH10B	F ⁻ <i>araDJ39</i> Δ(<i>ara</i> , <i>leu</i>)7697 Δ <i>lacX74 galU galK rpsL deoR</i> ϕ8O <i>dlacZ</i> ΔM15 <i>endA1 nupG recA1 mcrA</i> Δ(<i>mrr hsdRMS mcrBC</i>)	Invitrogen
<i>E. coli</i> BL21 (DE3) Gold	F ⁻ , <i>ompT</i> , <i>gal</i> , <i>dcm</i> , <i>hsdSB</i> (<i>r_B</i> ⁻ <i>m_B</i> ⁻), <i>lon</i> , λ(<i>DE3</i> [<i>lacI</i> , <i>lacUV5-T7</i> , <i>gene1</i> , <i>ind1</i> , <i>sam7</i> , <i>nin5</i>])	Invitrogen
<i>P. laumondii</i> TT01	wild type, Rif ^r (spontaneous)	124
<i>P. laumondii</i> TT01 Δ <i>antJ</i> Δ <i>gxpS</i>	wild type, Rif ^R , markerless deletion of <i>plu4185</i> and <i>plu3263</i>	this work

<i>P. laumondii</i> TT01 $\Delta antJ$ $\Delta gxpS$ $\Delta stlA$	wild type, Rif ^R , markerless deletion of <i>plu4185</i> , <i>plu3263</i> and <i>plu2234</i>	this work
ARs77 (<i>P. laumondii</i> TT01)	wild type, Rif ^R , markerless deletion of <i>plu3263</i> , <i>plu2234</i> , <i>plu2076</i> , <i>plu2670</i> , <i>plu4186–plu4194</i> , <i>plu1877-1881</i> , <i>plu3532-3539</i> and <i>plu0897-0899</i>	Alexander Rill
<i>X. doucetiae</i> DSM 17909	wild type, amp ^r	DSMZ

2.1.3 Plasmids

In the following (Table 2) an overview of the used plasmids for topic A is provided.

Table 2. Overview of the plasmids used in topic A, their description and the source.

Plasmid	Genotype	Reference
pACYC Duet-1	P15A ori, T7lac promoter, Cm ^r	Novagen
pCDF Duet-1	CDF ori, T7lac promoter, Sm ^r	Novagen
pCOLA Duet-1	ColA ori, T7lac promoter, Km ^r	Novagen
pSUMO_sfp	ColE1 ori, T7lac promoter, <i>sumo</i> , <i>sfp</i> , Km ^r	Dr. Carsten Kegler
pCDF_stlB_Strep	CDF ori, T7lac promoter, <i>plu2134 (stlB)</i> , Sm ^r	this work
pCOLA_stlE_strep	ColA ori, T7lac promoter, <i>plu2165 (stlE)</i> , Km ^r	this work
pACYC_stlC_Strep	P15A ori, T7lac promoter, <i>plu2163 (stlC)</i> , Cm ^r	this work
pCDF_stlE_Strep	CDF ori, T7lac promoter, <i>plu2165 (stlE)</i> , Sm ^r	this work
pCDF_fabH_Strep	CDF ori, T7lac promoter, <i>plu2835</i> , Sm ^r	this work
pCDF_fabB_Strep	CDF ori, T7lac promoter, <i>plu3184</i> , Sm ^r	this work
pCDF_fabF_Strep	CDF ori, T7lac promoter, <i>plu2831</i> , Sm ^r	this work
pACYC_fabG_Strep	P15A ori, T7lac promoter, <i>plu2833</i> , Cm ^r	this work
pCOLA_fabA_Strep	ColA ori, T7lac promoter, <i>plu1772</i> , Km ^r	this work
pCOLA_fabZ_Strep	ColA ori, T7lac promoter, <i>plu0683</i> , Km ^r	this work
pACYC_fabH_Strep	P15A ori, T7lac promoter, <i>plu2835</i> , Cm ^r	this work
pCOLA_bkdABC_Strep	ColA ori, T7lac promoter, <i>plu1883-1885</i> , Km ^r	this work
pCDF_stlB_Strep_stlCDE	CDF ori, T7lac promoter, <i>plu2134 (stlB)</i> , <i>plu2163-2165 (stlCDE)</i> , Sm ^r	this work
pCDF_stlB_Strep_stlE	CDF ori, T7lac promoter, <i>plu2134 (stlB)</i> , <i>plu2165 (stlCDE)</i> , Sm ^r	this work

pACYC_fabH_Strep_fabG	P15A ori, T7lac promoter, <i>plu2835 (fabH)</i> , <i>plu2833 (fabG)</i> Cm ^r	this work
pSEVA221	RK2 ori, Km ^r	125
pSEVA631	pBBR1 ori, Gm ^r	125
pSEVA221_ara	RK2 ori, ara promoter, Km ^r	Alexander Rill
pSEVA631_ara	pBBR1 ori, ara promoter, Gm ^r	Alexander Rill
pSEVA221_fabH_bkdABC_fabG	RK2 ori, ara promoter, <i>plu2835 (fabH)</i> , <i>plu1883- 1885 (bkdABC)</i> , <i>plu2833 (fabG)</i> , Km ^r	this work
pSEVA631_stlBCDE	pBBR1 ori, ara promoter, <i>plu2134 (stlB)</i> , <i>plu2163-2165 (stlCDE)</i> , Gm ^r	this work
pAR20	pBBR1 ori, <i>sacB</i> , <i>araC</i> , <i>araBAD</i> , <i>tetR</i> , crRNA framework, Km ^r	Alexander Rill
pAR20_ΔCupin1	pBBR1 ori, <i>sacB</i> , <i>araC</i> , <i>araBAD</i> , <i>tetR</i> , crRNA framework, Km ^r , containing 500 bp up- and downstream of <i>plu0952</i>	this work
pAR20_ΔCupin2	pBBR1 ori, <i>sacB</i> , <i>araC</i> , <i>araBAD</i> , <i>tetR</i> , crRNA framework, Km ^r , containing 500 bp up- and downstream of <i>plu0999</i>	this work
pAR20_ΔCupin3	pBBR1 ori, <i>sacB</i> , <i>araC</i> , <i>araBAD</i> , <i>tetR</i> , crRNA framework, Km ^r , containing 500 bp up- and downstream of <i>plu1323</i>	this work
pAR20_ΔCupin4	pBBR1 ori, <i>sacB</i> , <i>araC</i> , <i>araBAD</i> , <i>tetR</i> , crRNA framework, Km ^r , containing 500 bp up- and downstream of <i>plu1886</i>	this work
pAR20_ΔCupin5	pBBR1 ori, <i>sacB</i> , <i>araC</i> , <i>araBAD</i> , <i>tetR</i> , crRNA framework, Km ^r , containing 500 bp up- and downstream of <i>plu2325</i>	this work

2.1.4 Oligonucleotides

All oligonucleotides for the generation of the plasmids are listed in Table 3 and Table 4.

Table 3. Overview of the used oligonucleotides for the generation of the plasmids and the utilized templates. The overhangs of the oligonucleotides were underlined.

Plasmid	Oligonucleotide 5' to 3'		Template
pACYC_fabH_ Strep	SK18	<u>GAGAACCTATACTTCCAGGGATAT</u> ACAAAAATTTTAGGTACAGGTAGT TATC	<i>P. laumondii</i> TT01
	SK22	<u>GATTACTTTCTGTTCTGACTTAAGC</u> <u>ATTATTA</u> AAAACGTATCAGTGCCG	
	GG68	<u>TCCCTGGAAGTATAGGTTCTCTTT</u> <u>TTCGAACTGCGGGTGGCTCCACA</u> <u>IGGTATATCTCCTTATTAAGTTAA</u> AC	pACYC Duet-1
	SW1	TTAACCTAGGCTGCTG	
pCOLA_bkdABC _Strep	SK23	<u>GAGAACCTATACTTCCAGGGAATA</u> GACGTACAGATCAATGAAGTACC	<i>P. laumondii</i> TT01
	SK24	<u>GATTACTTTCTGTTCTGACTTAAGC</u> <u>ATTACT</u> GTTTTGCAACCACG	
	GG68	<u>TCCCTGGAAGTATAGGTTCTCTTT</u> <u>TTCGAACTGCGGGTGGCTCCACA</u> <u>IGGTATATCTCCTTATTAAGTTAA</u> AC	pCOLA Duet-1
	SW1	TTAACCTAGGCTGCTG	
pCDF_stlB_ Strep	SK25	<u>GAGAACCTATACTTCCAGGGAGA</u> GAAAGTCTGGCTAAAACATTATC	<i>P. laumondii</i> TT01
	SK26	<u>GATTACTTTCTGTTCTGACTTAAGC</u> <u>ATTACTATGCTACATTCCTGACCTT</u> TTC	
	GG68	<u>TCCCTGGAAGTATAGGTTCTCTTT</u> <u>TTCGAACTGCGGGTGGCTCCACA</u> <u>IGGTATATCTCCTTATTAAGTTAA</u> AC	pCDF Duet-1
	SW1	TTAACCTAGGCTGCTG	
pCDF_stlB_ _StlCDE	SK27	<u>GTTAAGTATAAGAAGGAGATATAC</u> <u>ATATGAAACGTGTTCTTGTAGTGT</u> CG	<i>P. laumondii</i> TT01
	SK28	<u>GTGGCAGCAGCCTAGGTTAATTAG</u> TTAGCGGATTCCAACCTTG	
	GG108	CATATGTATATCTCCTTCTTATACT TAAC	pCDF_stlB_ Strep
	GG109	TAATTAACCTAGGCTGCTGCCAC	

Materials and Methods

pACYC_fabH_ Strep_fabG	SK29	<u>GTTAAGTATAAGAAGGAGATATAC</u> <u>ATATGAGATTAGATGGAAAGATTG</u> CATTAG	<i>P. laumondii</i> TT01
	SK30	<u>GTGGCAGCAGCCTAGGTTAATTAG</u> TTCATATACATGCCGCC	
	GG108	CATATGTATATCTCCTTCTTATACT TAAC	pACYC_fabH_ Strep
	GG109	TAATTAACCTAGGCTGCTGCCAC	
pCDF_fabH_ Strep	SK18	<u>GAGAACCTATACTTCCAGGGATAT</u> ACAAAAATTTTAGGTACAGGTAGT TATC	<i>P. laumondii</i> TT01
	SK19	<u>AGCGGTGGCAGCAGCCTAGGTTA</u> <u>ATTAAAAACGTATCAGTGCCG</u>	
	GG68	<u>TCCCTGGAAGTATAGGTTCTCTTT</u> <u>TTCGAACTGCGGGTGGCTCCACA</u> <u>IGGTATATCTCCTTATTAAGTTAA</u> AC	pCDF Duet-1
	SW1	TTAACCTAGGCTGCTG	
pCDF_fabB_ Strep	SK1	<u>GAGAACCTATACTTCCAGGGAAG</u> GTATTTAATGAAGCGCGTAG	<i>P. laumondii</i> TT01
	SK2	<u>AGCGGTGGCAGCAGCCTAGGTTA</u> <u>ATTAAGCTGAATACTTGCTCATCA</u> C	
	GG68	<u>TCCCTGGAAGTATAGGTTCTCTTT</u> <u>TTCGAACTGCGGGTGGCTCCACA</u> <u>IGGTATATCTCCTTATTAAGTTAA</u> AC	pCDF Duet-1
	SW1	TTAACCTAGGCTGCTG	
pCDF_fabF_ Strep	SK3	<u>GAGAACCTATACTTCCAGGGATCT</u> AAGCGTCGAGTAGTTG	<i>P. laumondii</i> TT01
	Sk4	<u>AGCGGTGGCAGCAGCCTAGGTTA</u> <u>ATTAATCAGGTTAATCTTACGG</u>	
	GG68	<u>TCCCTGGAAGTATAGGTTCTCTTT</u> <u>TTCGAACTGCGGGTGGCTCCACA</u> <u>IGGTATATCTCCTTATTAAGTTAA</u> AC	pCDF Duet-1
	SW1	TTAACCTAGGCTGCTG	
pACYC_fabG_ Strep	SK5	<u>GAGAACCTATACTTCCAGGGAAGA</u> TTAGATGGAAAGATTGCATTAG	<i>P. laumondii</i> TT01

Materials and Methods

	SK6	<u>AGCGGTGGCAGCAGCCTAGGTTA</u> <u>ATTAGTTCATATACATGCCGC</u>	pACYC Duet-1
	GG68	<u>TCCCTGGAAGTATAGGTTCTCTTT</u> <u>TTCGAACTGCGGGTGGCTCCACA</u> <u>IGGTATATCTCCTTATTAAGTTAA</u> AC	
	SW1	TTAACCTAGGCTGCTG	
pCOLA_fabA_ Strep	SK7	<u>GAGAACCTATACTTCCAGGGAGTT</u> GATAAACTTAAATCCTACACAAAA G	<i>P. laumondii</i> TT01
	SK8	<u>AGCGGTGGCAGCAGCCTAGGTTA</u> <u>ATTAGAAAGCGCTGGTATCTTTAA</u> AC	
	GG68	<u>TCCCTGGAAGTATAGGTTCTCTTT</u> <u>TTCGAACTGCGGGTGGCTCCACA</u> <u>IGGTATATCTCCTTATTAAGTTAA</u> AC	pCOLA Duet-1
	SW1	TTAACCTAGGCTGCTG	
pCOLA_fabZ_ Strep	SK9	<u>GAGAACCTATACTTCCAGGGAAGT</u> GATAATCATACTCTGCACATTG	<i>P. laumondii</i> TT01
	SK10	<u>AGCGGTGGCAGCAGCCTAGGTTA</u> <u>ACTAAACCTCACGACGGC</u>	
	GG68	<u>TCCCTGGAAGTATAGGTTCTCTTT</u> <u>TTCGAACTGCGGGTGGCTCCACA</u> <u>IGGTATATCTCCTTATTAAGTTAA</u> AC	pCOLA Duet-1
	SW1	TTAACCTAGGCTGCTG	
pSEVA221-ara	AR585	GTCGTGACTGGGAAAACC	pSEVA221 + araC Pbad fragment
	AR586	TCCTGTGTGAAATTGTTATCC	
pSEVA631-ara	AR585	GTCGTGACTGGGAAAACC	pSEVA631 + araC Pbad fragment
	AR586	TCCTGTGTGAAATTGTTATCC	
pSEVA221-fabH- bkdABC-fabG	SK188	<u>AGAAAGAGGGGAAATACTAGATGT</u> ATACAAAAATTTTAGGTACAG	pSEVA221-ara
	SK189	<u>TTAATGCTTGTTAAAAACGTATCAG</u> TGCC	
	SK190	<u>ACGTTTTTAACAAGCATTAAAGCGC</u> AATAAC	

	SK192	<u>AAGCTGTGTCTTACTGTTTTGCAA</u> CCAC	
	SK193	<u>AAACAGTAAGACACAGCTTCACT</u> ATAAC	
	SK194	<u>AGGGTTTTCCCAGTCACGACTTAG</u> TTCATATACATGCCG	
	AR585	GTCGTGACTGGGAAAACC	
	AR587	CTAGTATTTCCCCTCTTTCTC	
pSEVA631- stlBCDE	SK184	<u>AGAAAGAGGGGAAATACTAGTTG</u> GAGAAAGTCTGGCTAAAAC	pSEVA631-ara
	SK185	<u>ATCGGCACCTCTATGCTACATTCC</u> TGACC	
	SK186	<u>TGTAGCATAGAGGTGCCGATGAAT</u> GGCTC	
	SK187	<u>AGGGTTTTCCCAGTCACGACTTAG</u> TTAGCGGATTCCAACCTTTGAAC	
	AR585	GTCGTGACTGGGAAAACC	
	AR587	CTAGTATTTCCCCTCTTTCTC	

Table 4. Utilized oligonucleotides for the assembly of the CRISPR/Cas9 and pSEVA-plasmids.

pAR20_ΔCupin1	
HA-L	AGAGCTTGTCTCTGGTGTCTCAAATTTATGACACCATTTCC CACTGAGTCGTATGGTGGTCGGTGTACCACAAGATCTCAGT AAACGTACTIONACTATGGTCGCCCGCAAGAGCAAGACTACCT GCTCGACTTCAACTTAGATGCGAAGACATTACAGCGTCATA TCCGGGCAGGATATCGTCATCCTGGAGCGCACTTCTTCCTC CCCGATGGTACCAAGGTGGTTGTTTTGTCTGCAATAGTGCC CCATGGCGTAGATATAGGCGTCCCTAATTTGCCTGGATGTA TTGTTCAAACCGCGTCAGGCATTTTCATTGCGACGGCTGAT GAGTGGCTGCAATACTCACAGTTGAAGTGAATGGTGTCTGA GAGTCCCGCCGTGCCTAATACTATACCCGAGATTTTCAGAC TGGCCCGTCAGATGACTATCAGAGATGAAATAGCGTCCAAT ACACAAGACCAAATGGCTTGTGTTACCGATTTCTAGCGAGA GAGATGATG
HA-R	TTTGCTGCATTCACCTACTTCACACCCATTCTTAAAGATATT ACGGGTTACAGTGATCGGGCAGTAGCGAGTTTATTGTTTAT CTATGGGGCCGCTACTGTGATCGGCAATGACAGGTTTGAC GAAAGGACTGGCGCGTGATCTTGGCGGAAAGGGTGTCTCAG GTGAACCAGATTTCTCCAGGCCCTATTGATACGGACATGAA

	<p>CCCTGTCAATGGTTCTAATGCTGATTTCTGGCGCAGACTTA CTGTCCCTGGCTGGTATGGCTCAACAACCTGATATTGCAGCC GTCGTGAGCTTTTTGGCAAGTAAGGAGGCTGATTTTGTAC TGGTGCGGATATTGCGGTGGATGGTGAACAAATATTTGAT TTCTGGATTGGAATCATAGTACCACCTGTTCAATTTAGGCG GCTATGGGCGTGAATAGCTTATATACCCTATGGATTTCAA GATGGATCGCGACGGCAAGGGAGCGAACCCCGGGA</p>
<p>pAR20_ΔCupin2</p>	
HA-L	<p>ACGTAATGAAAAATTAAGTCATGGAAGGTATTGAGGTTAATA AGGCTAATTTTCCAGATACCTGAGTTGTAGTGATGGGACAT AAAGGTGTTCTATCAGGTAGAGGTAACACAATTCTGTTTTG GTTATATTGCTGACAATGGACATATTTTTTTGTTAGCTTCTTTC AGCGGCAATGTTGTTATTTCAACAGATATTATTTTTTCACTA CACGATGATTATCCTAATTGCTGAAATATCATCAGGGGCCT GTTTGTATCCATAGGAAATGATGATAGCGATTACATAACGC CATTCCACAGTCAAATCTGGTGGAGTATGGGGGAAGTAT TTACGCTGTTTTCTCCGAGTAGCTATTTTGCTTTCCTTAT TTGCTGAAAAGCAAAGGATGTATTGTCAATAATGCGCCTGT GTCGGGACTAGGCGCTGATTGGGAAGGCCTACACTATTCC CCAGTCATATAGTTATCTATGCTCCCGGGGATTCTCTCCCT TG</p>
HA-R	<p>TTGGTTAATGAACCTTCAATGGGCTAAAGAAGGCACCCGAA GGGTGCCCTCCAAAATTTATATCTGTAACCAGATATATGAAC AAGAAATTAATAATTTTTCTGGGAAACACATGGAATTATG TTGGGCTTTCTTCAGAAGTTGAAAATTTTGGTGACTATATAC AAACATTTGTGGGAAATATTCCTGTCATTTTAATCCGTGATA GAAAAGGAATATTGCGCGTATTTGTAAACCGTTGTCCCAT AGAGGAGCAAAGATCTGCCATAACCCTCAGGGTAATACTAA GTTACTTGTATGTCCTTATCATGAGTGGGCATTTAGTTTAGA GGGTAACCTAGCTGGGATGCCTTTTAGAAAAGGGATTAATG GAAAAGGTGGAATGTCTGAATTTTTTTCATCCTGAAGAACAT GGTTTGCAAGCTCTTAATGTGACTGAGAGACATGGTGTTGT ATTTGCGAGTTTTTTCATATGATATTGAACCATTTGAAACAT</p>
<p>pAR20_ΔCupin3</p>	
HA-L	<p>TTATTGGGGTTTGGTGTAGCACATTAAGAAAAGCGCGCTT GTGGAAAGTGTATATACCCAATGGATTTCAAGATGCATCGC GACGGCAAGGGAGTGAATCCCCGGGAGCATAGCTAACTAT GTGACCGGGGTGAGTGAATGCCAACAAGAGGCAGTT TGAAAGATGACGGGTATAGATAACGATGTGACCGGGGTGA GCGAGTGTAGCCAACAAGAGGCAACTTGAAAGATAACGG</p>

	<p>ATATAGAACGATAATATAGTTCAACCACCACTGTTATTACGT AGAATGATGCAGTTAATATTATAAAAAAACTTATCGGTAATT TTGATGGCACTTTTTGTGCGTTTGTGTCAGAAATTACCAGCATA TGACATGGTATTGCTAGGATAATTAGATAAGATAGGCCGAA ATGGTAACTAAGATAAAATATGTTGAGTATTATTTCAAGATG GTTAAAAAATACAACTTTACAATGAACTACAATATTAGAGG TAATTATA</p>
HA-R	<p>TAAGTAAGTGTAGGTTTTATAGATTGTATTTAAAAACAGATA ATGTTTTACCCGGGATAGATGTTATTAGCAATATCCCGGTG GTATATATATATTAATTTTCATCTCAATTATTGAATTTTTTATT AGTTAACTTTGATCATTAAATGATTCTCTATAATAGAAAAAC AAATCACAATTGGTAGTTTATTTTTTAAATATTATCATTGGT AAATAATTTTATATCTATTTTAGTTAGAAAGTATTTGTATTAAT CGATCTGTTTTCTAGTATTTTCTTATAGTGTTAATCTTTCGTT TTTGTATTATTTCTATTTTATATCAATGAGGTGTATAACTTC TATCTCGTTATTTTTAATGTGTTCTCTGTCATGTTTTACAAA AAATCCTTTTTTCACTATTGATAATTTGTGGTGCGAAAAATA ATCTTTATAGATGTCGATTAGATGATTTTAATTTCTTTCTTA ATGTAATGTTTTTATTTTGTAATC</p>
pAR20_ΔCupin4	
HA-L	<p>TGCTTCTTTGTTGGCTGCACTCACTCACCCCGGTCACATAG CTATCTATGCTCCCGGGGATTCGCTCCCTTGCCGTCGCGAT GCATCTTGAAATCCATAGGGTATATATATCTTTGAAATAATT ATTTTTAGTGAGGGTTAAGATCAAGCTTAATTAACGCCATTA TTGTCCTAATTTAATAATATAATTAACCTGACTTTTTTCTGAT ATTATTTTCAACTCGGATTATATTCTACAAAGAAATTTAAAT AAGCGTTTTACAGTGATTGTTATCACAGAGTGAGCTTTTGTA AAATACTACTATGGAATTATATATTTCTATTTGATATATTGTT AATAACTAGTTGGTTTCTTATCGATATGAGTTTGTGATGAT TGAGGTTTTACTGTGAAATATCATTTTATTTGATAGAGAGAT AATGTTAATTCAATTAACCAAGAGAAATGATAGTCACTTTAA AATAAAATTTTATTTGTAGAGATAAAAGGAAG</p>
HA-R	<p>CTTGGGATAAATTAATATGTGCTAGTGCTTGATGGGTTGC GAGAATGCCATGATATTCATGAAGGTAATTATAAATCAGGAT AAGTCATTGGAGTGATAAAAGGATGATATGAGCATCTCATG AAGGGGATCAGGTACTAGCCTATGGAATATTAATTTACTG AAAATAAAATGGAGAAATATATTAGAGATAATATGCTATTGT AATGATAAAGGTGGAATAACGATTGAAATTATTTAATCTA ATATTTAAATTGGAAAATAATTTCAATGAGTGGCGGTAATGA GTTTTCGGATGGAATTAACCTTATACCCTATGGATTTCAAGA</p>

	TGGATCGCGACGGCAAGGGAGAGAGTCCCTGGGAGCATA GCAAACCTATGTGACCGGGGTGAGCGAGTGCAGCCAACAAA GAGGCAATTTGAAGGATAACGGGTATAAATAACCTGAGTTC TGGTTAAGCCGTTACTAACATATCCATTTCTAAGCAGGAAAT ATTCA
pAR20_ΔCupin5	
HA-L	TCATCGCCCTATTCCCGGCTGTAACCGCTTCGGGGATACC GAAAAAACCTCTTTACAGGCAATTTACGTTATGAAGGTG AACCACGCCGGCTTTATAGTGGTTGTGTCATGTTATTAGAT AGCTCAGGTAAACTGGATGCTGCGCTGGTATTACGTTCTCT CTATCAGCATCAAGGTCGCTGTTGGCTCCAGGCTGGCGCA GGATTGGTCAGAGATTCAAAACCAGAAAGAGAGTGGCAGG AACTTGTGAAAACTTGACTGCATTATGAAATACGTTCCGCC CTTGCTCTGGTAAAAAGAGTAAATGAAGTAATAACTTTTCC GGGAAAACCAGAGTTGTCTCTGGTTTTCCCTAGACGACTAA TTTTCTACTATGCTTAATCAGTCACCTCTAATTTTTCTTCCG TGACAACCAGTAACTTAAAAAATCAAACAATAGATATCAG CTTGCAACTATTCTTGCTGGTACCCATTTAATTGGAGGCAA TAAAT
HA-R	GGTGTATTGAATCTATATGACCTTGTATATCAAAAATAGCCT CGTTTACACGGGGCTTTATTAGTAAAAAACGTTCAATGAAA ATTATTTATTAGGTGAGTTTTTTATTAACAAGGATCGAAAATT GCCTATTTCTGCCATACGCAATGATTATCTTACATTTACAT AACCCGCCATGACTATATTAATAATTTTTGTTAACATAAAAT TATCCTATTCTTAAAGTCCGTATTGGTTCAATTTATTTTTAGT GTCCTCTGTTTTTATTTAACTCATTTCATTATTTATTTAACTAA TATTAACCTAATGATTTAAATGAAAAAAAATCAACGAGAAAT GGAAAAGAAAAGCTTGCTAATAATTCTTGCGTAAGTTAATT TTACATTGAAATTAACGCTTAAAAAGCCAGGGAAAACCTCTAT ATTTAAAGTTGAAATTTATATTAGTAGCGACAAATTGCGGAG TTTTCTGCCAGAAATTTTCAT
Promoter sequences	
araC-Pbad	AAGCGGATAACAATTTACACAGGATCATGACAACCTTGACG GCTACATCATTCACTTTTTCTTCAAACCGGCACGGAACCTC GCTCGGGCTGGCCCCGGTGCATTTTTTAAATACCCGCGAG AAATAGAGTTGATCGTCAAACCAACATTGCGACCGACGGT GGCGATAGGCATCCGGGTGGTGTCAAAGCAGCTTCGCC TGGCTGATACGTTGGTCTCGCGCCAGCTTAAGACGCTAAT CCCTAACTGCTGGCGGAAAAGATGTGACAGACGCGACGGC GACAAGCAAACATGCTGTGCGACGCTGGCGATATCAAATT

	<p>GCTGTCTGCCAGGTGATCGCTGATGTACTGACAAGCCTCG CGTACCCGATTATCCATCGGTGGATGGAGCGATCCGTTAAT CGCTAGCATGCGCCGAGTAACAATTGCTCAAGCAGATTTA TCGCCAGCAGCTCCGAATAGCGCCCTTCCCCTTGCCCGGC GTTAATGATTTGCCCAAAAAGTCGCTGAAATGCGGCTGGT GCGCTTCATCCGGGCGAAAGAACCCCGTATTGGCAAATATT GACGGCCAGTTAAGCCATTCATGCCAGTAGGCGCGCGGAC GAAAGTAAACCCACTGGTGATACCATTGCGGAGCCTCCGG ATGACGACCGTAGTGATGAATCTCTCCTGGCGGGAACAGC AAAATATCACCCGGTCGGCAAACAAATTCTCGTCCCTGATT TTTACCACCCCCTGACCGCGAATGGTGAGATTGAGAATAT AACCTTTCATTCCCAGCGGTTCGGTCGATAAAAAAATCGAGA TAACCGTTGGCCTCAATCGGCGTTAAACCCGCCACCAGAT GGGCATTAACGAGTATCCCGGCAGCAGGGGATCATTTTG CGCTTCAGCCATATTCACCACCCTGAATTGACTCTCTTCCG GGCGCTATCATGCCATACCGCGAAAGGTTTTGCACCATTGCG ATGGCGCGCCGCCATTGGACCAAACGAAAAAAGGCCCCC CTTTCGGGAGGCCTCTTTTCTGGAATTTGGTACCGAGGCTT AACGATCGTTGGCTGAGAAACCAATTGTCCATATTGCATCA GACATTGCCGTCACTGCGTCTTTTACTGGCTCTTCTCGCTA ACCAAACCGGTAACCCCGCTTATTAAGCATTCTGTAACA AAGCGGGACCAAAGCCATGACAAAAACGCGTAACAAAAGT GTCTATAATCACGGCAGAAAAGTCCACATTGATTATTTGCAC GGCGTCACACTTTGCTATGCCATAGCATTATTTATCCATAAGA TTAGCGGATCCTACCTGACGCTTTTTATCGCAACTCTCTACT GTTTCTCCATACCCGAGCTGTCACCGGATGTGCTTTCCGGT CTGATGAGTCCGTGAGGACGAAACAGCCTCTACAAATAATT TTGTTTAATACTAGAGAAAGAGGGGAAATACTAG</p>
--	--

2.1.5 DNA and plasmid extraction

The NEB Monarch Genomic DNA Purification Kit was used for the extraction of genomic DNA (gDNA) following the protocol provided by the manufacturer. The extraction of plasmids was carried out by use of the Monarch Plasmid Miniprep Kit according to the manufacturer instructions.

2.1.6 Plasmid construction and transformation for *in vitro* assays and heterologous production

The genes of interest were amplified by PCR (Phusion or Q5 polymerase) and fused with the plasmid backbones via HotFusion or Golden Gate assembly^{126,127}. The plasmids were used to transform *E. coli* BL21(DE3) Gold and *E. coli* DH10B cells by electroporation (1250 V, 25 μ F and 200 Ω). The respective plasmids were verified via Colony PCR, digestion or sequencing.

2.1.7 Cultivation of bacteria and heterologous expression

E. coli BL21 (DE3) Gold and *E. coli* DH10B were transformed with pCDF_stlBCDE, pACYC_fabH and pCOLA_bkdABC or pSEVA221_fabH-bkdABC-fabG and pSEVA631_stlBCDE. The strains were cultivated for 3 days, supplemented with the respective antibiotic (34 μ g/ml Cm, 50 μ g/ml Km, 50 μ g/ml Sm and 20 μ g/ml Gm), 1 mM cinnamic acid (CA) and induced with 1 mM IPTG and 2% Amberlite® XAD-16 (Sigma-Aldrich) resin. The cultures were discarded and the compounds isolated from the resin with methanol (MeOH) or ethylacetate. The ethylacetate extracts were dried and resolved in MeOH and measured with *high performance liquid chromatography high resolution mass spectrometry* (HPLC-HR-MS).

2.1.8 Protein production and purification

E. coli BL21 (DE3) was transformed with protein production plasmids (Table 3). Protein production was achieved using an auto-induction protocol. Therefore 1 l LB-medium was supplemented with 20 ml 50 x 5052 (25% glycerol, 2.5% glucose, and 10% α -lactose monohydrate), 50 ml 20 x NPS (1 M Na₂HPO₄, 1 M KH₂PO₄, and 0.5 M (NH₄)₂SO₄), 1 ml 1 M MgSO₄ the respective antibiotics (34 μ g/ml Cm, 50 μ g/ml Km and 50 μ g/ml Sm). This auto-induction medium was inoculated with the overnight culture and incubated at 37°C and 180 rpm to an optical density (OD) between 0.4-0.8. Afterwards the culture was cooled down for 15-45 min at 4°C and incubated overnight at 25°C and 180 rpm.

2.1.8.1 Purification of Strep-tagged StIB, StIE, FabB, pIFabF, pIFabH, pIFabG, pIFabA, pIFabZ

Cells were harvested via centrifugation at 17,000 g for 10 min and resuspended in Strep-tag binding buffer (400 mM NaCl, 50 mM Tris, pH 8, pH 8.5 StIB, pH 7.4 StIC). One tablet of cOmplete Protease Inhibitor Cocktail (Roche) and lysozyme were added to the buffer and incubated for 20-30 min at 4°C. After cell lysis by sonication, cell debris was removed by ultra-centrifugation (20-30 min, 48,000 g, 4°C) and the protein was purified over a 5 ml StrepTrap HP column (GE Healthcare) by an ÄKTApurifier system (GE Healthcare). Proteins were eluted with Strep-tag elution buffer (400 mM NaCl, 50 mM Tris, 2.5 mM d-desthiobiotin, pH 8, pH 8.5 StIB, pH 7.4 StIC). All proteins were concentrated to 2-10 mg/ml utilizing Amicon concentration devices (Merck, 3,000 or 10,000 Da cut-off filter) and stored with addition of 25% (v/v) glycerol buffer (20 mM in aliquots at -80 °C until needed).

2.1.8.2 Purification of His6-tagged Sfp-SUMO

Cells were harvested and resuspended in His-tag binding buffer (300 mM NaCl, 20 mM Tris, 20 mM imidazol, pH 8.5) and with addition of one tablet cOmplete Protease Inhibitor Cocktail (Roche) and lysozyme incubated for 30 min at 4°C. After cell lysis by sonication, cell debris was removed by centrifugation (35 min, 48,000 g, 4°C) and the supernatant was transferred to a 5 ml HisTrap FF column (GE Healthcare) by an ÄKTApurifier system (GE Healthcare). The protein was eluted with His-tag elution buffer (300 mM NaCl, 20 mM Tris, 500 mM imidazol, pH 8.5) and buffer exchanged in storage buffer (20 mM HEPES, 1 mM DTT, 25% (v/v) glycerol, pH 8.5) using a PD-10 desalting column (Amersham Biosciences). It was further concentrated to 2-10 mg/ml using Amicon concentration devices (Merck, 30,000 Da cut-off filter) and stored in aliquots at -80 °C.

2.1.9 In vitro assays

2.1.9.1 Preparation of malonyl-StIE (elongation-ACP)

The ACP StIE was buffer exchanged in reaction buffer (10 mM Tris, 1 mM DTT, pH 8.5) with PD SpinTrap G-25 columns (Amersham Biosciences). Reactions were performed

using 50 μ M StIE, 1 mM malonyl-CoA, 0.5 μ M Sfp-SUMO (in storage buffer) and incubated for 1 h at 30°C. The reaction was analyzed by HPLC-HR-MS.

2.1.9.2 Chain elongation, ketoreduction and dehydration with FAS II enzymes

CA-CoA or CA-SNAC (Cinnamoyl-N-Acetylcysteamine, synthesized and provided by Dr. Isam Elamri, Bode group) and malonyl-StIE assay were mixed 1:2 and chain elongation reaction was performed by addition of 10 μ M FabH or FabB or FabF and further incubated for 1 h at 30°C, prior to adding 10 μ M FabG and 1 mM NADPH for ketoreduction reaction and 10 μ M FabA or FabZ for dehydration reaction.

All StIE-bound *in vitro* reactions were analyzed using HPLC-HR-MS. MS¹ and MS². BPC and TIC spectra were summarized according to the retention time of modified ACP. If the retention time of two StIE species differed more than 0.4 min, the separately summarized spectra were overlaid. Theoretical average masses of modified ACPs were predicted using IsotopePattern (Bruker).

2.1.10 Feeding experiment with SNAC- and CA-derivatives

10 ml overnight cultures of *E. coli* DH10B, TT01 strains (WT and $\Delta antJ\Delta gxpS$, $\Delta antJ\Delta gxpS\Delta stlA$ and ARs77) and *X. doucetiae* were inoculated and on the next day used to inoculate 5-10 ml production cultures which were fed with 0.5 – 1 mM SNAC derivatives (CA, 4-Cl-CA, C₇- and C₁₁ alkynes, all synthesized and provided by Dr. Isam Elamri, Bode group) or CA-derivatives (3-chloro-, 3-bromo-, 3-hydroxy-, 3-nitro-, 2-nitro, 4-chloro-CA). The cultures were cultivated for 3 days at 180 rpm and 30 °C and extracted with MeOH.

1 l LB-medium was inoculated as a production culture and fed with 20 mg CA-SNAC and isolated via Interchim flash (chapter 2.1.11) after cultivation for 3 days at 30 °C.

2.1.11 Purification of CA-SNAC product

The culture was discarded and the XAD resin harvested with a filter. Afterwards the XAD beads were washed three times with each 400 ml ethylacetate (with 0.1% FA) for half an hour. The ethylacetate was combined with C18 silica gel (Sigma Aldrich) and dried in a round bottom flask by rotary evaporation. The dried powder was then applied onto a C18 flash column (PF-15C18AQ-F0120 by Interchim) and purified with an ACN/water gradient

ranging from 35 to 70 % ACN and a flow rate of 46 min at the puriFlash 5.050 by Interchim. Fractions with a UV-absorption of 290 nm were collected and dried by rotary evaporation. The purified peak was analyzed by HPLC-HR-MS and NMR.

2.1.12 HPLC-HR-MS

XAD extracts of *E. coli* and *P. laumondii* cultures as well as *in vitro*-assays of StIE-bound reactions were analyzed via HPLC-HR-ESI-UV MS using a Dionex Ultimate 3000 LC system (Thermo Fisher) equipped with a DAD (Impact II) or (microTOF II)-3000 RS UV-detector (Thermo Fisher) and coupled to an Impact II or microTOF II electrospray ionization mass spectrometer (Bruker).

The separation of XAD extracts was achieved via a C18 column (ACQUITY UPLC BEH, 50 mm x 2.1 mm x 1.7 μ m, Waters) using H₂O and ACN containing 0.1% (v/v) formic acid (FA) as mobile phases. HPLC was performed at a flow rate of 0.4 ml/min with 5% ACN equilibration (0-2 min) followed by a gradient from 5-95% ACN (2-14 min, 14-15 min 95% ACN) ending with a re-equilibration step of 5% ACN (15-16 min). For internal mass calibration, 10 mM sodium formate was injected within the first two min. The HPLC-MS analysis was set to positive mode with a mass range of m/z 100-1200 and an UV at 190-800 nm.

Analysis of ACP derivatives was performed with a C3 column (Zorbax 300SB-C3 300Å, 150 mm x 3.0 mm x 3.5 μ m, Agilent). ACN and H₂O containing 0.1% (v/v) FA were used as mobile phases at a flow rate of 0.6 ml/min. HPLC was performed with 30% ACN equilibration (0-1.5 min), followed by a gradient from 30-65% ACN (1.5-27 min) and a further elution step with 95% ACN (27-30 min). The internal mass calibration was utilized with the injection of an ESI-L Mix (Agilent).

For data analysis of UV-MS-chromatograms, Compass DataAnalysis 4.3 (Bruker) was used. The theoretical average masses of StIE and its modifications was calculated using Compass IsotopePattern 3.0 (Bruker).

2.2 Topic B: Optimization of production titers of stilbene derivatives

In the following sections all materials and methods used for the conducted experiments for topic B shown in chapter 2.2 are described.

2.2.1 Cultivation of strains

E. coli ST18 strains used were grown in LB medium (Table 5) and aminolevulinic acid (Ala, 50 µg/ml final concentration) at 37°C and 180°rpm. *P. laumondii* strains were cultivated at 30°C. Solid media contained also 1.5% (w/v) agar. For selection Km (50 µg/ml final concentration for *E. coli* and 25 µg/ml final concentration for *P. laumondii*) and Cm (34 µg/ml final concentration for *E. coli* and 17 µg/ml for *P. laumondii*) were used.

Table 5. Overview of the used media in Topic B of this thesis.

Medium	Composition
LB	10 g/l tryptone 5 g/l yeast extract 5 g/l NaCl
XPPM ⁹⁹	10 g/l glycerol 20 ml/l salt A (M9) 20 ml/l salt B (M9) 2g/l amino acid mix 1g/l sodium pyruvate ad dd H ₂ O, after autoclaving 2 ml/l vitamin solution 1 ml/l trace element solution
PP3M	10 g glycerol 20 ml/l salt A (M9) 20 ml/l salt B (M9) 20 g/l proteose peptone no. 3 1g/l sodium pyruvate ad dd H ₂ O, after autoclaving 2 ml/l vitamin solution 1 ml/l trace element solution
1% HF	10 g/l tryptone 1 % <i>Hermetia illucens</i> fat
BM	5 % <i>Bombxy mori</i> (powdered) ad XPPM

2.2.2 Microorganisms

All microorganisms, which were used in topic B, their genotype and the references, are listed in Table 6.

Table 6. List of strains, their genotype and their source used in topic B of this thesis.

Strain	Genotype/description	Reference
<i>E. coli</i> ST18- λ pir	Tp ^r Sm ^r , <i>recA thi hsdR</i> ⁺ RP4-2-Tc::Mu-Km::Tn7, λ pir phage lysogen, Δ <i>hemA</i>	128
<i>P. laumondii</i> TT01	wild type, Rif ^r (spontaneous)	129
<i>P. laumondii</i> TT01 Δ <i>stlF</i>	wild type, Rif ^r , markerless deletion of <i>plu2236</i>	this work
<i>P. laumondii</i> TT01 pex <i>stlCDE</i> (<i>ara</i>)	wild type, Rif ^r , promoter exchange <i>plu2163</i> with L-ara promoter	this work
<i>P. laumondii</i> TT01 Δ <i>antJ</i>	wild type, Rif ^r , markerless deletion of <i>plu4185</i>	AK Bode
<i>P. laumondii</i> TT01 Δ <i>antJ</i> Δ <i>gxpS</i>	wild type, Rif ^r , markerless deletion of <i>plu4185</i> and <i>plu3263</i>	this work
<i>P. laumondii</i> TT01 Δ <i>antJ</i> Δ <i>gxpS</i> Δ <i>stlF</i> pex <i>stlA</i> (<i>xyl</i>)	wild type, Rif ^r , markerless deletion of <i>plu4185</i> , <i>plu3263</i> , <i>plu4844</i> , <i>plu2236</i> and markerless promoter exchange in front of <i>plu2234</i> with xylose promoter	this work
<i>P. laumondii</i> TT01 Δ <i>antJ</i> Δ <i>gxpS</i> pex <i>stlA</i> (<i>xyl</i>)	wild type, Rif ^r , markerless deletion of <i>plu4185</i> , <i>plu3263</i> , <i>plu4844</i> and markerless promoter exchange in front of <i>plu2234</i> with xylose promoter	this work
<i>P. laumondii</i> TT01 Δ <i>antJ</i> Δ <i>gxpS</i> Δ <i>stlF</i> pex <i>stlA</i> (<i>xyl</i>)	wild type, Rif ^r , markerless deletion of <i>plu4185</i> , <i>plu3263</i> , <i>plu4844</i> , <i>plu2236</i> and markerless promoter exchange in front of <i>plu2234</i> with xylose promoter	this work
<i>P. laumondii</i> TT01 Δ <i>antJ</i> Δ <i>gxpS</i> pex <i>stlA</i> (<i>xyl</i>) <i>stlCDE</i> (<i>van</i>)	wild type, Rif ^r , markerless deletion of <i>plu4185</i> , <i>plu3263</i> , <i>plu4844</i> , markerless promoter exchange in front of <i>plu2234</i> with xylose and <i>plu2163</i> with vanillic acid promoter	this work
<i>P. laumondii</i> TT01 Δ <i>antJ</i> Δ <i>gxpS</i> Δ <i>stlF</i> pex <i>stlA</i> (<i>xyl</i>) <i>stlCDE</i> (<i>tac</i>)	wild type, Rif ^r , markerless deletion of <i>plu4185</i> , <i>plu3263</i> , <i>plu4844</i> , <i>plu2236</i> , markerless promoter exchange in	this work

	front of <i>plu2234</i> with xylose and <i>plu2163</i> with tac promoter	
<i>P. laumondii</i> TT01 $\Delta antJ$ $\Delta gxpS$ $\Delta pliA$ pex <i>stIA</i> (xyl) <i>stICDE</i> (van)	wild type, Rif ^r , markerless deletion of <i>plu4185</i> , <i>plu3263</i> , <i>plu4844</i> , <i>plu2076</i> markerless promoter exchange in front of <i>plu2234</i> with xylose and <i>plu2163</i> with vanillic acid promoter	this work
<i>P. laumondii</i> TT01 $\Delta antJ$ $\Delta gxpS$ $\Delta stIF$ $\Delta pliA$ pex <i>stIA</i> (xyl) <i>stICDE</i> (tac)	wild type, Rif ^r , markerless deletion of <i>plu4185</i> , <i>plu3263</i> , <i>plu4844</i> , <i>plu2236</i> , <i>plu2076</i> , markerless promoter exchange in front of <i>plu2234</i> with xylose and <i>plu2163</i> with tac promoter	this work

2.2.3 Plasmids

An overview of all plasmids utilized in Topic B is provided in Table 7.

Table 7. Overview of the plasmids used in topic B, their description and the source.

Plasmid	Genotype/description	Reference
pAR20	pBBR1 ori, <i>sacB</i> , <i>araC</i> , <i>araBAD</i> , <i>tetR</i> , crRNA framework, Km ^r	Alexander Rill
pEB17_Km	R6K γ ori, oriT, <i>araC</i> , <i>araBAD</i> , Km ^r	99
pAR20_ $\Delta stIF$	pBBR1 ori, <i>sacB</i> , <i>araC</i> , <i>araBAD</i> , <i>tetR</i> , crRNA framework, Km ^r , containing 500 bp up- and downstream of <i>plu2236</i>	this work
pEB17_ $\Delta gxpS$	R6K γ ori, oriT, <i>araC</i> , <i>araBAD</i> , Km ^r , containing 757 bps up- and 707 bp downstream of <i>plu3263</i>	this work
pAR20_pex- <i>stIA</i> (xyl)	pBBR1 ori, <i>sacB</i> , <i>araC</i> , <i>araBAD</i> , <i>tetR</i> , crRNA framework, Km ^r , containing 500 bps upstream and at the start of <i>plu2076</i> and xylose promoter	this work
pAR20_pex- <i>stICDE</i> (tac)	pBBR1 ori, <i>sacB</i> , <i>araC</i> , <i>araBAD</i> , <i>tetR</i> , crRNA framework, Km ^r , containing 500 bps upstream and at the start of <i>plu2163</i> and tac promoter	this work
pAR20_pex- <i>stICDE</i> (van)	pBBR1 ori, <i>sacB</i> , <i>araC</i> , <i>araBAD</i> , <i>tetR</i> , crRNA framework, Km ^r , containing 500	this work

	bps upstream and at the start of <i>plu2163</i> and van promoter	
pAR20_Δ <i>pliA</i>	pBBR1 ori, <i>sacB</i> , <i>araC</i> , <i>araBAD</i> , <i>tetR</i> , crRNA framework, Km ^r , containing 500 bps up- and downstream of <i>plu2076</i>	Alexander Rill
pAR20_Δ <i>bkdABC</i>	pBBR1 ori, <i>sacB</i> , <i>araC</i> , <i>araBAD</i> , <i>tetR</i> , crRNA framework, Km ^r , containing 500 bps up- and downstream of <i>plu1883</i>	this work
pAR20_ <i>pex-plu2236</i> (<i>xyl</i>)	pBBR1 ori, <i>sacB</i> , <i>araC</i> , <i>araBAD</i> , <i>tetR</i> , crRNA framework, Km ^r , containing 500 bps upstream and at the start of <i>plu2236</i> and <i>xyl</i> promoter	this work
pAR20_ <i>pex-plu2236</i> (<i>hcaE</i>)	pBBR1 ori, <i>sacB</i> , <i>araC</i> , <i>araBAD</i> , <i>tetR</i> , crRNA framework, Km ^r , containing 500 bps upstream and at the start of <i>plu2236</i> and <i>hcaE</i> promoter	this work
pS3	pBBR1 ori, PLacUV5, Cm ^r	130
pY3	p15A ori, PLacUV5, Amp ^r	130
pY3-KN	p15A ori, PLacUV5, Km ^r , contains the backbone of pY3 and replaced the ampicillin resistance gene with kanamycine resistance	this work
pF3	p15A ori, PLacUV5, KN ^r , containing the backbone of pY3-KN and replaced <i>tyrA</i> with <i>pheA</i> G309C	this work
pACYC_ <i>aratacl</i>	P15A ori, <i>araC</i> , <i>araBAD</i> , <i>tacl</i> , Cm ^r	131
pACYC_ <i>aratacl_stIF</i>	P15A ori, <i>araC</i> , <i>araBAD</i> , <i>tacl</i> , Cm ^r , containing <i>plu2236</i>	this work
pACYC_ <i>aratacl-accABCD-birA</i>	P15A ori, <i>araC</i> , <i>araBAD</i> , <i>tacl</i> , Cm ^r , containing <i>plu0688</i> , <i>plu4074</i> , <i>plu4075</i> , <i>plu3171</i> and <i>plu4732</i>	this work

2.2.4 Oligonucleotides and double stranded DNA-fragments

An overview of all oligonucleotides for the generation of the plasmids and their corresponding templates are listed in Table 8.

Table 8. List of oligonucleotides, the plasmids they were used for and the templates used in topic B of this thesis.

Plasmid	Oligonucleotide 5' to 3'		Template
pEB17_ΔgxpS	SK40	CAATTTGTGGAATTCCTCCGGGAGAG CTCCCACGGCACAACAGGTAAAATA TTTAG	<i>P. laumondii</i> TT01
	SK41	GTCGGTGACGACATATCTGTTCAGA AAGCAATGAATTGTGAAGCGGA	
	SK42	CTCCGCTTCACAATTCATTGCTTTC TGAACAGATATGTCGTCACC	
	SK43	ATATGTGATGGGTAAAAAGGATCG ATCCTGCGGATAGGTCCATTTTTCA	
	GG23	GAGCTCTCCCGGGAATTCC	pEB17
	GG138	AGGATCGATCCTTTTTAACCCATC	
pACYC_aratacl_ΔstfF	SK161	GCTAACAGGAGGAATTCATGCAT GTCGGCATTATTGGG	<i>P. laumondii</i> TT01
	SK162	TGTCAACAGCTCCTGCAGTTAACGT CGGTGTTGATGACT	
	SK137	CTGCAGGAGCTGTTGACAATTA	pACYC_aratacl
	SK138	GGAATTCCTCCTGTTAGCCCAA	
pACYC_aratacl-accABCD-birA	SK145	GGCTACGGTCTCCATTCATGAGTCT GAATTTTCTTGAATTTG	pACYC_aratacl
	SK146	GGCTACGGTCTCTCCGTACTCTTCT GTTTCATTCAGCAATAACCATATTG C	
	SK147	GGCTACGGTCTCTACGGAATCACA CTCATGG	
	SK148	GGCTACGGTCTCATCCGTCTGAATC TGGCTTATTAAGTTTCCTGTAACCC C	
	SK149	GGCTACGGTCTCACGGAAAGATCA TTCAATGAG	
	SK150	GGCTACGGTCTCCATCTTCTTTATT GGTACTTATTTG	
	SK151	GGCTACGGTCTCCAGATGCCTGAA GGCGAAATTGATGCTGTG	
	SK152	GGCTACGGTCTCGTGTCTTAACAAC CTCTTAAAGAAATCTCC	
	SK137	CTGCAGGAGCTGTTGACAATTA	<i>P. laumondii</i> TT01
	SK138	GGAATTCCTCCTGTTAGCCCAA	

pY3-KN	SK109	CCTATCGATGCATAATGTGCCTGTC CACATTTCCCCGAAAAG	pY3
	SK110	GCAGAAACGTCTAGAAAGATGCCA CTGTCAGACCAAGTTTACGAG	
	AR111	TGGCATCTTCTAGGACGTTTC	pCOLA-DUET
	AR112	GACAGGCACATTATGCATCGAT	
pF3	SK111	ATGGCTGGAAACACAATTG	pY3-KN
	SK112	TTACATCACCGCAGCAAAC	

All double stranded DNA fragments that were purchased for the assembly of plasmids are listed in Table 9.

Table 9. List of oligonucleotides which were purchased for the construction of CRISPR/Cas12 plasmids and the construction of the pF3-plasmid.

pAR20_ΔstIF	
HA-L	GCGAGGGAAGGGCTTGGTTGTGAGTTAATCACGGAAAAAATAG ATATGACACCATTCTACTTCAAGGGTGTAAATGTTGAACCGGTT GATCCCATTCATCCCGATACAGGGAGTGATTACCCTGTCTGGG ATGCAAATAGGGCATATAAGGCCGGCGATAGAGTGAGTTGGAA CAATCAAATTGGGAAGCTAAATGGTGGAAATAGAGGCACCGAG CCAGATGGTGCAGGAACATCTGATGCTTATCCTTGGGTAAAAA TTGCATAATTAATTAAGCCAAGCCACCAGTATGATATATCTACT GGTGGCGTTTATAATATATCCGTCATCTTTCAAGTTGCCTCTTT GTTGGCTGCACTCCCTCACCCCGGTCACATCGTTATCTATGCT CCCGGGGATTCGCTCCCTTGCCGTCGCGATCCATCTTGAAATC TATTGGGTATAAGTGTATCTAGAGTAATGATATGGAATTCGTTC CGGTATGACAATTTACTCGGAATA
HA-R	GTATTTCTCCTGTTGTAGATACGAGCGATTCTGGCTAAATCGTG GTGATTATATCTATTTGATATTATCTAATTACAGCCATGACTTTT TTGTAGTATTTAAAATAAAAATACTGTACATAGAAATAGAGCA AGAAAGCTTGGAGTTTTATCGCTAAAAATAGTTGGCAAAAAAAT TATGTCTCTGTTTATTAAGCAATATTTAATTAATAAATGATCGC TTAAATTGTCAAAGTGAATTTTTAATGTTTAAGTTTTATAATTTTC CATAAAATTAACACTTTATAGTGATATGAGTGTTAATATAGCTTT ATGTCTATTTACGTATTCAAGACCACATGACAGTAAATGATGTT TGTGTGAATAAATTAATTCATCTTGTTTCGATCTTCAACTATT TAAGATGTTTATTAATGTGATTATTAATAACTCCACTGCTCTCTA ATTTCTATTCCAATTGAATTTAAGATATTTTTCTCCAATTATGAA ATATTT

pAR20_Δ<i>pliA</i>	
HA-L	<p>AACCGGCGTATTAAGTTGGGCTACGGTCTCGAGATATTATGAT AATTATCGCCGATTTTTTCATGTCGTCTAAGAACTTTAAATAATTT CTACTGTTGTAGATGAGAAGTCATTTAATAAGGCCACTGGCTCA CCTTCGGGTGGGCCTTTCTGCGCAATTGTTAGGCCAATTACCA ACTTGGTATTGTTGCAGGTAGTTAGTTGGAATGCGTTTTTCAAT ATATATTTTGCCGGAGGGTGTGAATTTAAATTTAATTTAATCAC TCATTAATAGAAATTAAGAATAATTTTAAATACATAAAATAATG CATTTGGTTTTCGGTGGTAACAATGCCATTACTTTGTTTGGCAAG GTAAC TTGATTCCACTTAATACAAAATGGGCTATCAGTATAAAG CGTATAGTTTAATTTTTATGAAAGAAAAATAACAATTTGGAGGTG AAGAAAATGATTATATTAGGGATCAGTGGCCTTCCTAATGCTCA ACGTTTTCTGCGAGAGAATAATCCAGAGGTGAGTAAATTAGAT GAACGTATTTGCCAGGGAGTCGATAGTGCAGCCTGTGTGATTA TTGATGGAAAATTGTTGCAGCGGCGGCGGAAGAGCGTTTTAC GGGAGAGAAAGGAACAGGGCGGTTTTCTGCTAATGCCATTAAT TATTGTTTGGCGGAAGCAGGGTATCTGCGCTCCACTAGAGACC GTAGCC</p>
HA-R	<p>CACCACAGGTCTCGCACTGGTATCTGCGCTCCACTAAAGCCTG AACGTGCTTTTAACGCAACTTTTTGGCGATTATTGAAAGAGGTA CAGAAGATAACCGGTTATGGTTGTCTGGTGAATACTTCATTCAA CGTTAGAGGACAGCCGCTTATTATGTCACCGGAGATTGCAATA GAGACGTTTTTGAAAAC T TCACTGGACAAACTTTATATTGAGGG ATTTGTCGTATGGAAAGAATAATCCTGATGGCGTCCTGATAAAA ATGTCAGTTAATTGATTTTGGGATAACATGTGTTTCTTTGTCATC TTAGAAAAATGTTTGGAGATAAATTTGATGATATGGAAACACA TTCTTTCTATTTGCAAAACAGAGATTGTTTGCCGGGCGGCATAA CGTTATCATCGATCAGCAAAGGTAATATAAAAATATGATATACC CAATGGATTTCAAGATGGATCGCGACGGCAAGGGAGTGATGG GGATTTGGTAACGTATATCAATATGCTATCATGATATAGAGTTG ATAGGATCCCACACCGCATATGCTGGATCCTTGACAGCTAGCT CAGTCCTAGGTATAATACTAGTTTCGAGATTTTCAGGAGCTAAGG AAGCTAAAGTCTAAGAACTTTAAATAATTTCTACTGTTGTAGATG ATGAGGATTGCGACACTATTTTTGAGACACGTCTCGAGACCGT AGCCCTTCCAAGAATCCGTCTAGT</p>
pAR20_Δ<i>bkdABC</i>	
HA-L	<p>TATATTGTATTGTAATCATGGAAATGCCGGCGCTTGTTGGTCCT ACTCTTAACGAATGGCTGTTGTTTCATCGGTTGGAGTTTTTTAAA</p>

	<p>TGGTGTACATTATGTTTCAGGACAATGCTAAAAATTTAGGGAAT ACCATGACAGCCGAAACCATTTATGGTTATGGAGATAATTTTTC CCCCATGTTAGATGTATATACCCTATGGATTTCAAGATGCATC GCGACGGCAAGGGAGCGAACCCAGGAGCATAGATAACTATG TGGCCGGGGTGAGTGAGTGCAGCCAACAAAGAGGCAACTTGA AAGATGACGGGTATAAACGTAATTAATAAATTGTGGCCGTATATC TCTATCTTTTGAATTCGTGTAGGTAATAACCCTACATTCCTTC TTTATCGGGATCTATAGTCTCTCAAGTAATCATGAACGGGACTA CCCC GTGTTTCGCTTTTTTATCAAGCATTAAAGCGCAATAACGACA ACTACCACGTAACTATTT</p>
<p>HA-R</p>	<p>GCAGTGAAGCGGGATAGGAAAACCAGAAAGCATGGTGGAGAT CCCACAATTTTCGTAAGAGGTTGTGGGGTTTCTTTGAGGCACAA TTTATGCTGTTCCACCCTTGTGATAAAGATGAAATATCAGATCTAT ACCCGTCATCTTTCAAGTTGCTTCTTTGTTGGCTGCACTCACTC ACCCCGGTCACATAGCTATCTATGCTCCCGGGGATTTCGCTCCC TTGCCGTCGCGATGCATCTTGAAATCCATAGGGTATATATATCT TTGAAATAATTATTTTTAGTGAGGGTTAAGATCAAGCTTAATTAA CGCCATTATTGTCCTAATTTAATAATATAATTAACCTGACTTTTTT CTGATATTATTTTCAACTCGGATTATATTCTACAAAGAAATTTAA AATAAGCGTTTTACAGTGATTGTTATCACAGAGTGAGCTTTTGT AAAATACTACTATGGAATTATATATTTCTATTTGATATATTGTTAA TAACTAGTTGGTT</p>
<p>pAR20_pex-stlA</p>	
<p>HA-L</p>	<p>GGCTACGGTCTCTAGATACAAATTTAATTGAGGAGGTAATTGTA ACAATGTCTAAGAACTTTAATAATTTCTACTGTTGTAGATGAGA AGTCATTTAATAAGGCCACTGGCTCACCTTCGGGTGGGCCTTT CTGCGCAATTGTTAGGCCAATTACCAACTTGGTCTAATATTCCA CAGAAACCAATAACTAATTTATCATAAGCAAAGGATTATCTAAA AGGTGCTGTAATCTATTCCTCTACCTCGACGAATGGGATCTTG ATTTCTTGTAATCGACCGTCATATTGCGACCAATCTGTATAAT AACCAAAAACCTTTAGGTTTTATTTTCGTGTGTCATATTTATTATAGA CTGGTAATGCGATTCTTCCCGATGTGTA ACTGAAATTTATTGTT TCAGTTGATGGATTGAAATTATCTATCTGATAAGACTGTTCACTA AAAGAATCTGTCTGGATTATTTTTGACATAAATCACCTCGACTA GATATCAGTTTATTTTTCGATGAACACTCCAATTGCTTTATTTAC GTGGTAACATAATTACATTCTAGTTTGTATTCTTAGGAAAACAAA TAATTGTTATTTGTTTGATTGTTAATGATCAACTAAAATTTATGTC AACGGGATTTATATTACCGACCTTACTATCAGATTTCAAACA CTAGAGACCGTAGCC</p>

<p>HA-R</p>	<p>GGCTACGGTCTCATCCAATGAAAGCTAAAGATGTTTCAGCCAAC CATTATTATTAATAAAAAATGGCCTTATCTCTTTGGAAGATATCTA TGACATTGCGATAAAACAAAAAAGTAGAAATATCAACGGAGA TCACTGAACTTTTGACGCATGGTCGTGAAAAATTAGAGGAAAA TTAAATTCAGGAGAGGTTATATATGGAATCAATACAGGATTTGG AGGGAATGCCAATTTAGTTGTGCCATTTGAGAAAATCGCAGAG CATCAGCAAATCTGTAACTTTTCTTTCTGCTGGTACTGGGGA CTATATGTCCAAACCTTGTATTAAGCGTCACAATTTACTATGTT ACTTTCTGTTTGCAAAGGTTGGTCTGCAACCAGACCAATTGTCG CTCAAGCAATTGTTGATCATATTAATCATGACATTGTTCTCTG GTTCTCTGCTATGGCTCAGTGGGTGCAAGCGGTGATTTAATTC CTTTATCTTATATTGCACGAGCATTATGTGGTATCGGGGATCCC ACACCGCATATGCTGGATCCTTGACAGCTAGCTCAGTCCTAGG TATAACTAGTTTCGAGATTTTCAGGAGCTAAGGAAGCTAAAGT CTAAGAACTTTAATAATTTCTACTGTTGTAGATTATCTATACTA ATTTGTATCCTTAGGGAGTTGTCTTGAGACCGTAGCC</p>
<p>pAR20_pex-st/CDE</p>	
<p>HA-L</p>	<p>CTGAAAACACCCGCACCGACCATAGAGCTGAGTACCAGAGCA GTAAGCGCTGTGAGACCTAGTTTCTTTTCCAAAAATATGTTCT AATATGACATAAACTGCATTATTAACCAGTTCATTATCCTGATCA TAAAGATGAACTGGGTATCGGGTTTTATCGCTTCCAAGCTGTA CAGAACGGAGAAACAGACTGATTGAACCTAGAAATAGGGGGG GATTCTACGAAGGGTATGAGCTGGATGCAATGGTTTTCTATGC AAATAACTATAAAATTTATGCATTGTTTGATGGTGAGTTTGGGT GTGGTGAGATGCAATTTATTTTTATAAGCTGATATGCGTTATTTT TATAATGCTGTTTATTGTAAGTAAGTAAGTAAGTAAGTAAGTAAG AATTACTATGGTGTTATTACTAATTAAGTAATTTTTATTTAATTT TTTCGATCGATCTCAAATTTAATAAAATAGTTGTGAAAAATAAA GTTTTACCTCTAATTTTCATTT</p>
<p>HA-R</p>	<p>AAACGTGTTCTTGTAGTGTGCTATTCCCAAAGCGGCCAATTGAT CGAGGTGGTAAAAAGCTTAATTTACCCCTGCAAGAGTCTGAC GAGATATACATCCGTGAAGTTATTCTGAAACCGATTCTGAATT TGAATTTCCCTGGAAGTTTTCTAAATTTGTTGATGTTTTCCAGA AACAGTGCAGTTACATCCGCCTGAGCTAGCGCCTTTGAATCTG GAAGACGAAGAACCTTTTGATTTGGTCATATTAGGCTACCAAGT TTGGTATTTATCACCGGCTCCTCCGATAGTGGCATTCTTAAGA GTGAAGAAGGAAAGCGTTTACTTAATGGCCGACCAGTGGTGAC AGTTATTGCTTGCCGAAACATGTGGTTGATAGCTCAAGAACTG TCAAAGATTGTTGCATGAAAGTGGAGCGTATTTGCGTGATAAC</p>

	GTGGTCTTTGTTGATAAAGCAAACCTTTTTTGGCAGAGTATTCAC AACCCCGATATGGCTA
pAR20_pex-plu2236	
HA-L	GGCTACGGTCTCGAGATTCGCTAAAAATAGTTGGCAAAAAAATT ATGTGTCTAAGAACTTTAAATAATTTCTACTGTTGTAGATGAGAA GTCATTTAATAAGGCCACTGGCTCACCTTCGGGTGGGCCTTTC TGCGCAATTGTTAGGCCAATTACCAACTTGGTCATATTCTCCTA TCGCGTTGTATAGCCAAATAAGCGCTATCCCCTCTTCATTTAAT GAACGTGAAGCGGCTAAAAAACCTCTTGTGGAAATTCCATAT GATGGATAACACCGGTAGAAACAACAACATCAAATTGATTATCT CGTGTTAGCTTCTCAATCGTATTATTTTCTAGCGTGACGTTATC CAACTGATGATAAGATATCAACTTATCTGCCACCTCTAACGCTT TATCCGTCATATCAATACCCACAAATTGGGTATCGGGATACATA CTTGCCAGCCCTAACAAACGATGCCCGTTCCACAGCCTAAAT CAAGCACATATTTTCCCGTTAAATAATCCGGCTTAAATATAAGC CTTATCACCGTAGCCATATCATAAATAAGATTGTCTCCAATAGC AGAAGTAGGATATGGATATCGGTTATACATCGCTTTGACGTCCT GATTACTCATATTTATTTCTCCGAACAAAATGACAAATCAGTAGT ACTAGCACTAGAGACCGTAGCC
HA-R	GGCTACGGTCTCATCCAATGCATGTCGGCATTATTGGGGCGGG GATTGGTGGTACATGTTTAGCCCATGGATTACGTAACATGGAA TAAAAGTGACGATATATGAACGAAACTCTGCCGCATCATCCATA CTTCCGGGTTATGGAATTCATATAAATTCATTCGGTAAGCAAGC ACTGCAAGAATGCCTCCCGGCTGAAAACCTGGCTAGCCTTTGAG GAGGCATCAAGATATATTGGCGGACAATCCCGGTTTTATAATG AACGTATGCGTCTTCTCGCCGTTTCATGGCGGTATTTCTCCAATG GCAGGGAAAATTATTTCCGAACAACGTTTGTCAATTAGCAGAAC TGAAGTGAAGAAATACTCAACAAGGGGCTTGCAAATACCATTC AATGGAACAAAACATTCGTCCGTTATGAACATATTGAAAACGGT GGTATTAATAATTTCTTTGCCGATGGCAGTCACGAAAATGTGCA TGTCCTTGTGCGGTGCAGACGGTAGCAATTCAAAAGTACGGGAT CCCACACCGCATATGCTGGATCCTTGACAGCTAGCTCAGTCCT AGGTATAATACTAGTTCGAGATTTTCAGGAGCTAAGGAAGCTAA AGTCTAAGAAGCTTTAAATAATTTCTACTGTTGTAGATGCCAGAAT CGCTCGTATCTACAACAGGAGAAGTCTAGAGACCGTAGCC
pAR20_pex-bkdABC	
HA-L	ATCAAAATAATTTAGCAAAGTAATGAATTATTCCTATGTCTTATC ATTGCAGGGCTCAAAGATATAGGTAAGAACCTGTTTTTTAATTG TATTGTGATTATTCGTATTGTGATTATATTGTATTGTAATCATGG AAATGCCGGCGCTTGTTGGTCTACTCTTAACGAATGGCTGTT

	<p>G TTCATCGGTTGGAGTTTTTTAAATGGTGTACATTATGTTTCAG GACAATGCTAAAAATTTAGGGAATACCATGACAGCCGAAACCA TTTATGGTTATGGAGATAATTTTTCCCCCATGTTAGATGTATAT ACCCTATGGATTTCAAGATGCATCGCGACGGCAAGGGAGCGA ACCCCAGGAGCATAGATAACTATGTGGCCGGGGTGAGTGAGT GCAGCCAACAAAGAGGCAACTTGAAAGATGACGGGTATAAACG TAATTA AAAATTGTGGCCGTATATCTCTATCTTTTGCAATTCGTG TAGGTAATAACCCTACATTC</p>
<p>HA-R</p>	<p>G TGAGGAAAAAGAGAGTGATAGACGTACAGATCAATGAAGTAC CTCTTAAGGAACACAGCCCTTCAATTAATGATTGTTTGGATGAG CAAAAGTTACTTTATGACATGCTGCTGTCACGGGAATTTGATAA TCGTAGTGCGATAGTCACACGACAAGGCCGAGCTTGGTTTCAT GTGTCGGCTGCTGGACATGAAGGGTTGGCTGTGTTGCCTCAG CTTATGGAAAAAATGATGTACTGGTTCCTTACTATCGTGATCG GGCGTTAGTATTAGCGCGTGGTATGTCTATTGTTGAAATGACAA GGGA ACTTATGGGTAAGGCCACTTCTCACTCGGCCGGCCGAA CCATGTCGAATCATTCTGCTCCAAGAGCATAATATCTTCTCG GTAGTCAGCTTGACCGGAACCAATGTATCCCGCGGCTGGC GCTGCTTGGGCAAGCGTGTGGACAATAAAAATGGGCTTGTG TGTGTGGTGTGCGCGATGCGGCAACT</p>
<p style="text-align: center;">Promoter sequences</p>	
<p>Tac</p>	<p>A ACCGGCGTATTAAGTTGGGCTACGGTCTCACACTGCACCTTT TTGTTATCAATAAAAAAGGCCCCCGATTTGGGAGGCCTTTTTA GTTAGAGGATCCTTATCACTGCCCGCTTTCAGTCGGGAAACC TGTCGTGCCAGCTGCATTAATGAATCGGCCAACGCGCGGGGA GAGGCGGTTTGCATTTGGGCGCCAGGGTGGTTTTTCTTTTCA CCAGTGAGACTGGCAACAGCTGATTGCCCTTCACCGCCTGGC CCTGAGAGAGTTGCAGCAAGCGGTCCACGCTGGTTTGCCCA GCAGGCGAAAATCCTGTTTGATGGTGGTTAACGGCGGGATATA ACATGAGCTATCTTCGGTATCGTCGTATCCCACTACCGAGATAT CCGCACCAACGCGCAGCCCGGACTCGGTAATGGCGCGCATTG CGCCAGCGCCATCTGATCGTTGGCAACCAGCATCGCAGTGG GAACGATGCCCTCATTGAGCATTGTCATGGTTTGTGAAAACCG GACATGGCACTCCAGTCGCCTTCCCGTTCCGCTATCGGCTGAA TTTGATTGCGAGTGAGATATTTATGCCAGCCAGCCAGACGCAG ACGCGCCGAGACAGAACTTAATGGGCCCGCTAACAGCGCGAT TTGCTGGTGACCAATGCGACCAGATGCTCCACGCCAGTCG CGTACCGTCCATGGGAGTAATAACTGTTGATGGGTGTC TGGTCAGAGACATCAAGAAATAACGCCGGAACATTAGTGCAGG CAGCTTCCACAGCAATGGCATCCTGGTCATCCAGCGGATAGTT</p>

	<p>AATGATCAGCCCACTGACGCGTTGCGCGAGAAGATTGTGCACC GCCGCTTTACAGGCTTCGACGCCGCTTCGTTCTACCATCGACA CCACCACGCTGGCACCCAGTTGATCGGCGCGAGATTTAATCGC CGCGACAATTTGCGACGGCGCGTGCAGGGCCAGACTGGAGGT GGCAACGCCAATCAGCAACGACTGTTTGCCCGCCAGTTGTTGT GCCACGCGGTTGGGAATGTAATTCAGCTCCACCATCGCCGCTT CCACTTTTTCCCGCGTTTTTCGCAGAAACGTGGCTGGCCTGGTT CACCACGCGGGAAACGGTCATATAAGAGACACCGGCATACTCT GCGACATCGTATAACGTTACTGGTTTCATATTCACCACCCTGAA TTGACTCTCTTCCGCTAGCACTGTACCTAGGACTGAGCTAGCC GTCAACATTGGACCAAACGAAAAAAGGCCCCCTTTTCGGGAG GCCTCTTTTCTGGAATTTGGTACCGAGGCTTAACGATCGTTGG CTGTGTTGACAATTAATCATCGGCTCGTATAATGTGTGGAATTG TGAGCGCTCACAATTAGCTGTCACCGGATGTGCTTTCCGGTCT GATGAGTCCGTGAGGACGAAACAGCCTCTACAAATAATTTTGT TAAAATAATTTTGTTTAACTTTTCGAGACCGTAGCCCTTCCAAGA ATCCGTCTAGT</p>
<p>Van</p>	<p>AACCGGCGTATTAAGTTGGGCTACGGTCTCACACTGCACCTTT TTGTTATCAATAAAAAAGGCCCCCGATTTGGGAGGCCTTTTTTA GTTAGAGGATCCTTATCAATCTGCACGAATTGACCATGCTGCAC CCAGCGGTGCGCCTGCGCTTGCTGCTGCTTCAAAAACCTTTTGC ATTACGAATTGCTGCCAGTGATGATCACGCATAATACGTTCTG CACCTTCGGCATCACACAGCTAACTGCATCCAGAACTGCCTG ATGCTGACGATGTGCTGCCAGCAGATGTTTCATATTCGGCAGAC AGGTCCATCAGATCCAGGGCCAGTGCACCGGCTGCTGCAAAC GGTTCAAACCATACGTGCCAGTGCCTTTCAACTGCACCATT ACCTGCTGCGCTAACCAGGGTATCATGAAATGCCTGATTATAT GCGGCATAACGATCCAGATCTTCACCATTAGGCGACCGGCTG CAAACAGTGCTTCACCTTCTGCAATCAGTACAACAAAACGTGCA TGGGTTTCTGCGGTCATAACCAGTTCTGCCAGACGACGTGCTG CAAACCTTCCAGAACACCACGAACCTTCAATTGCATCACGAATC TGATCGCTGCTAACACCACGGGCTGCATAACCACGTGCACCCA GACGAACAACCAGACCTTCTTGTTCCAGTGAACGCAGTGCGAT ACGAACCGGCATACGGCTAACACCCAGTGCTGCTGCGGTTCGG AATTTCTGCAATACGTTCCACCACTTTTGATTTACCGCTTGCAAT CATTTTACGCAGTGCCATCATAACACGCTGACCCGGTTTAATAC GAGGCATGTCCATTATTCACCCCTGAATTGACTCTCTTCCGC TAGCACTGTACCTAGGACTGAGCTAGCCGTCAACATTGGACCA AAACGAAAAAAGGCCCCCTTTTCGGGAGGCCTCTTTTCTGGAA TTTGGTACCGAGGCTTAACGATCGTTGGCTGATTGGATCCAATT</p>

	<p>GACAGCTAGCTCAGTCCTAGGTACCATTGGATCCAATAGCTGT CACCGGATGTGCTTTCCGGTCTGATGAGTCCGTGAGGACGAAA CAGCCTCTACAAATAATTTTGTAAAATAATTTTGTAACTTTC GAGACCGTAGCCCTTCCAAGAATCCGTCTAGT</p>
<p>Xyl</p>	<p>AACCGGCGTATTAAGTTGGGCTACGGTCTCACACTGCACCTTT TTGTTATCAATAAAAAAGGCCCCCGATTTGGGAGGCCTTTTAA GTTAGAGGATCCTTACTACAACATGACCTCGCTATTTACATCGC GATACTCTTTTGGCGTCGTGTCATATGCTTTTTTAAAAACAGAG TAGAAATATTGCAGCGATGGATAACCGCACATTTGCGATATCTC ATTGATCGACAAGGTGGTTGAAATCAGCAGACTGCGCGCTTTC TCCAGCTTCTCGGCATGAATCATGGCATGGATGGTTTCACCCA CCTCTTCTTAAAACGCTTCTCAAGATTGGAGCGCGAGATCCC GACCGCATCCAGTACCTGATCCACTTTAATCCCTTTACAGGCGT GATTACGAATGTAATGCATGGCCTGAATAACGGCGGGATCGGT CAGCGAGCGATAATCTGTTGAGCGCCGTTCAATGACGCGAACT GGTGGGACCAAATTCGCTGTAGCGGCATTTCTTCTTTATCTAA TAATCGATGCAACAGTTTTGCCGCCTGATAGCCATTTGCCGC GCGCCCTGAGCGACCGAAGAAAGGGCGACACGCGACAGATAG CGGGTCAGTTCTTCGTTATCGATGCCAATCACGCATAATTTTTTC CGGTACGGGAATATGTAGATGTTACATACTTGCAGAATATGC CGCGCTCGGGCGTCAGTAACGGCAATAATCCCGGTTTGCGGT GGTAGCGTTTGTAGCCAGTCTGCCAGCCGATTTTGCGCGTGTT GCCAGTTCTCTGGCGCGGTTTCTAACCCTGATAAACCACTCC GCGATACTTTTCTTCGGCGACAAGCTGACGAAATGCATATTCG CGCTCAGTGGCCCAACGTTTGCCGCTTGATTCCGGAAGACCAT AAAAAGCAAAGCGGTTAACGCCTTCTCTTTTAAATGCAAAAAT GCGCTTTCAACCAGCGCATAGTTATCGGTGGCAATGTAATGAA CGGGTGGGTAACCTTCTGCAAGGTGATACGAGCCGCCAACCC CAACAATGGGGACGTGACATCAGCCAGCGCTTGCTCGATCTG TTTGTCGTCGAAGTCGGCAATGACGCCATCTCCTAACCAAGTCC TTGATTTTATCAATGCGGGCGCGGAAATCTTCTTCAATGAAAAT ATCCCATTCCGATTGTGACGCCTGTAATATTCCCCTACGCCTT CTACTACCTGCCGGTCATAGGCTTTATTGGCATTGAACAGTAAT GTGATGCGGTGACGTTTAGTAAACATGGTTCTTTTCTGCTGAA TCATGCAAAAAGCTAGCACTGTACCTAGGACTGAGCTAGCCGT CAACATTGGACCAAACGAAAAAAGGCCCCCTTTTCGGGAGGC CTCTTTTCTGGAATTTGGTACCGAGGCTTAACGATCGTTGGCTG TGCGAGCGAGCGCACACTTGTGAATTATCTCAATAGCAGTGTG AAATAACATAATTGAGCAACTGAAAGGGAGTGCCCAATATTACG</p>

	ACATCAGAAATAATTTTGTTTAACTTTAAGAAGGAGATATATCCT CCAGGAGACCGTAGCCCTTCCAAGAATCCGTCTAGT
Genes	
<i>pheA</i> G309C	GTTTGCTGCGGTGATGTAAGGATCTAAAGGAGGCCATCCATGA CATCGGAAAACCCGTTACTGGCGCTGCGAGAGAAAATCAGCG CGCTGGATGAAAAATTATTAGCGTTACTGGCAGAACGGCGCGA ACTGGCCGTCGAGGTGGGAAAAGCCAAACTGCTCTCGCATCG CCCGGTACGTGATATTGATCGTGAACGCGATTTGCTGGAAAGA TTAATTACGCTCGGTAAAGCGCACCATCTGGACGCCATTACA TTACTCGCCTGTTCCAGCTCATCATTGAAGATTCCGTATTA CAGCAGGCTTTGCTCCAACAACATCTCAATAAAATTAATCCGCA CTCAGCACGCATCGCTTTTCTCGGCCCCAAAGGTTCTTATTCC CATCTTGCGGCGCGCCAGTATGCTGCCCGTCACTTTGAGCAAT TCATTGAAAGTGGCTGCGCCAAATTTGCCGATATTTTTAATCAG GTGGAAACCGGCCAGGCCGACTATGCCGTCGTACCGATTGAA AATACCAGCTCCGGTGCCATAACGACGTTTACGATCTGCTGC AACATACCAGCTTGTGCGATTGTTGGCGAGATGACGTTAACTATC GACCATTGTTTGTGGTCTCCGGCACTACTGATTTATCCACCAT CAATACGGTCTACAGCCATCCGCAGCCATTCCAGCAATGCAGC AAATTCCTTAATCGTTATCCGCACTGGAAGATTGAATATACCGA AAGTACGTCTGCGGCAATGGAAAAGGTTGCACAGGCCAAAATCA CCGCATGTTGCTGCGTTGGGAAGCGAAGCTGGCGGCCACTTTG TACGGTTTGCAGGTA ACTGGAGCGTATTGAAGCAAATCAGCGAC AAA ACTTACCCGATTTGTGGTGTGGCGCGTAAAGCCATTAA CGTGTCTGATCAGGTTCCGGCGAAAACCACGTTGTTAATGGCG ACCGGGCAACAAGCCTGTGCGCTGGTTGAAGCGTTGCTGGTA CTGCGCAACCACAATCTGATTATGACCCGTCTGGAATCACGCC CGATTCACGGTAATCCATGGGAAGAGATGTTCTATCTGGATATT CAGGCCAATCTTGAATCAGCGGAAATGCAAAAAGCATTGAAAG AGTTAGGGGAAATCACCCGTTCAATGAAGGTATTGGGCTGTTA CCCAAGTGAGAACGTAGTGCCTGTTGATCCAACCTGAGGATCT AAAGGAGGCCATCCATGGCTGGAAACACAATTG

2.2.5 DNA and plasmid extraction

The NEB Monarch Genomic DNA Purification Kit was used for the extraction of genomic DNA (gDNA) following the protocol provided by the manufacturer. The extraction of plasmids was carried out by use of the Monarch Plasmid Miniprep Kit according to the manufacturer instructions.

2.2.6 Gene deletions via homologous recombination

For the deletion *gxpS* an approach based on conjugation and homologous recombination was used⁷⁷. Approximately 700-800 bp long regions flanking the target gene were amplified via PCR. Hereby, overhangs to the other flanking region and to the plasmid pEB17 were introduced. The backbone of pEB17 was amplified with primers (GG8 and GG23, Table 8) and fused to the homologous arms flanking the gene of interest by HotFusion¹²⁶. After transformation of *E. coli* ST18 with the pEB17-deletion plasmid, it was verified and the strain was used as a donor for conjugation with the recipient TT01 strain.

For conjugation overnight cultures of ST18 and TT01 were inoculated in LB (with 50 µg/ml Ala for ST18). On the second day the OD was measured and adjusted to 0.5 in 1 ml for ST18 and 2 for TT01. The cells were harvested and washed twice with LB. Afterwards the cells were pelleted, resuspended in 25 µl and spotted on LB agar supplemented with 50 µg/ml Ala. After overnight incubation at 30°C the cells were scraped off and resuspended in 1 ml LB. 10 µl of the cell suspension was plated onto LB agar plates with 25 µg/ml Km. After two days overnight cultures of the colonies were grown in LB without antibiotics and plated on plates containing 6 % (w/v) sucrose. The colonies were verified via colony PCR and stored at -80°C.

2.2.7 Deletion and promoter exchange via CRISPR/Cas12

In order to generate higher production titers in *Photorhabdus*, TT01 was conjugated with *E. coli* ST18 containing the respective plasmids for deletion of certain genes or plasmids for promoter exchange in front of the biosynthesis genes.

For markerless deletions of target genes (*stlF*, *pliA*, *bkdABC*) two homologous arms (HAs, Table 9) of 500 bps upstream and downstream of the gene of interest were combined with two CRISPR sites (31 bps distal of the PAM motif). The left and right HA which also contained the CRISPR sites (HA-L and HA-R) were and synthesized by Twist Bioscience. For the generation of the deletion plasmid, pAR20 was assembled with HA-L and HA-R via Golden Gate cloning¹²⁷. After verification of the correct assembly via colony PCR with AR533 and AR534 (see Table 8), the ST18 was transformed with the respective deletion plasmid followed by conjugation with the *Photorhabdus* strain.

For markerless promoter exchanges in front of target genes (*stlA*, *stlCDE*, *plu2236*) two HAs (Table 9) of 500 bps upstream (HA-L) at the start of the gene of interest were combined with two CRISPR sites (31 bps distal of the PAM motif) which had to be present between the two HA's. The left and right HA (HA-L and HA-R) containing the respective CRISPR sites were and synthesized by Twist Bioscience. For the generation of the promoter exchange plasmid, pAR20 was assembled with HA-L, HA-R and the respective promoter sequence (Van, *xyl* or *tac*, Table 9) via Golden Gate cloning. The assembled plasmids were used for the transformation of ST18 followed by conjugation with the *Photorhabdus* strain.

After two days a single clone was picked and inoculated. The overnight culture was adjusted to an OD of 0.5 in 10 ml containing 25 µg/ml Km. The culture was cultivated at 30°C for around 1.5 h until an OD of 1 was reached. The recombination genes were induced with anhydrotetracycline (200 ng/ml) and incubated for 1 h at 25°C. Afterwards Cas12 was induced with L-ara (0.4%) and the cultures grown for 3 h at 25°C. 50 µl of the culture were then spotted on LB agar with Km (25 µg/ml) and L-ara (0.4%). After two days the clones were verified via colony PCR and spotted on agar plates containing 6 % (w/v) sucrose. An overnight culture was inoculated and stored at -80°C.

2.2.8 Overproduction of stilbenes

To overproduce stilbene derivatives a few approaches were tested. Genes of pathways using the same substrates as the stilbene biosynthesis and similar retention times in the HPLC were deleted (*antJ* for anthraquinone, *gxpS* for gameXpeptide, *pliA* for phurealipid, *stlF* for stilbene epoxidase, see Table 6 for the respective microorganisms). The titers of substrates and reaction intermediates were increased either by supplementation with 2 mM CA, promoter exchanges (*stlA*, *stlCDE*, s. list of microorganisms in Table 6) or expression of plasmids (pS3, pF3, pACYC_ara-*stlB*, pACYC_ara-*stlF*, s. Table 7 for detailed description). The respective promoters were induced with 1 mM IPTG, 250 µM vanillic acid (VA) and 0.4% xylose. 2% Amberlite® XAD-16 (Sigma-Aldrich) resin was also added to the cultures for purer extracts and to increase the production titers by shifting the equilibrium towards the product.

Another approach to determine optimal production condition was the use of different cultivation media. The TT01 strains were cultivated in LB, XPPM, PP3M, fat media extracted from black soldier flies (*Hermetia illucens*) and media consisting of larvae of the silk moth (*Bombxy mori*) (s. Table 5 for exact composition of different cultivation media).

2.2.9 Production and purification of IPS

P. laumondii TT01 $\Delta antJ \Delta gxpS \Delta sltF$ pex *stlA* (xyl) *stlCDE* (tac) pS3/pF3 was grown in LB medium and 180°rpm at 30°C. Solid media contained also 1.5% (w/v) agar. For selection Km (25 µg/ml final concentration) and Cm (17 µg/ml final concentration) were used.

A 10 ml overnight culture was inoculated and on the next day used to inoculate 1 l of a production culture in LB. The overproduction of IPS was induced with 1 mM IPTG, 250 µM VA and 2% Amberlite® XAD-16 (Sigma-Aldrich) resin. The production culture was incubated for 3 days and 180 rpm at 30°C.

2.2.10 Purification of IPS

The culture was discarded and the XAD resin harvested with a filter. Afterwards the XAD beads were washed three times with each 400 ml ethylacetate (with 0.1% FA) for half an hour. The ethylacetate was combined with C18 silica gel (Sigma Aldrich) and dried in a round bottom flask by rotary evaporation. The dried powder was then applied onto a C18 flash column (PF-15C18AQ-F0120 by Interchim) and purified with an ACN/water gradient ranging from 35 to 70 % ACN and a flow rate of 46 ml/min at the puriFlash 5.050 by Interchim. Fractions with a UV-absorption of 311 nm were collected and dried by rotary evaporation. The purified IPS was verified by HPLC-HR-MS.

2.3 Topic C: Epoxide derivatives and reactions

In the following sections all materials and methods used for the conducted experiments for topic C shown in chapter 2.3 are described.

2.3.1 Microorganisms

All microorganisms, which were used in topic C, their genotype and the references, are listed in Table 10.

Table 10. Overview of used strains, their genotype and their source in topic C.

Strain	Genotype/description	Reference
<i>P. laumondii</i> TT01	wild type, Rif ^r (spontaneous)	124
<i>P. laumondii</i> TT01 $\Delta antJ$ $\Delta gxpS$ $\Delta stlF$ <i>pex stlA</i> (xyl) <i>stlCDE</i> (tac)	wild type, Rif ^r , markerless deletion of <i>plu4185</i> , <i>plu3263</i> , <i>plu2236</i> markerless promoter exchange in front of <i>plu2234</i> with xylose and <i>plu2163</i> with vanillic acid promoter	this work

2.3.2 Plasmids

In the following (Table 11) an overview of the used plasmids for topic B are provided.

Table 11. Overview of the plasmids used in topic C, their description and the source.

Plasmid	Genotype/description	Reference
pACYC_aratacl_ <i>stlF</i>	P15A ori, <i>araC</i> , <i>araBAD</i> , <i>tacl</i> , Cm ^r , containing <i>plu2236</i>	this work
pS3	pBBR1 ori, PLacUV5, Cm ^r	130
pF3	p15A ori, PLacUV5, KN ^r , containing the backbone of pY3-KN and replaced <i>tyrA</i> with <i>pheA</i> G309C	this work

2.3.3 Feeding and inversed feeding experiments

Deuterated cinnamic acid (d₇-CA) or methionin (d₃-methionin) were added in 1 mM concentrations to the respective cultures with 2 % XAD resin.

For the differentiation between leucine- and isoleucine-derived compounds, the respective strains were cultivated in ^{13}C -ISOGRO medium (by Sigma Aldrich). The cultures were supplemented with 1 mM leucine or isoleucine and 2 % XAD.

After 3 days of cultivation at 30 °C the cultures were discarded, the XAD beads harvested and extracted for half an hour with MeOH. Afterwards the extracts centrifugated and were analysed via HPLC-MS as described in chapter 2.1.12.

2.3.4 Purification of EPS

P. laumondii TT01 $\Delta antJ \Delta gxpS \Delta stlF$ pex *stlA* (xyl) *stlCDE* (tac) pACYC_aratacl_ *stlF* was induced and cultivated in 4 l PP3M with 2 % XAD. The culture was discarded and the XAD resin harvested with a filter. Afterwards the XAD beads were washed three times with each 400 ml ethylacetate (with 0.1% FA) for half an hour. The ethylacetate was combined with C18 silica gel (Sigma Aldrich) and dried in a round bottom flask by lyophilization. The dried powder was then applied onto a C18 HPLC column (XBridge Prep C18 5 μm OBD, 19x250 mm by Waters) and purified with an ACN/water gradient ranging from 30 to 70 % ACN and a flow rate of 20 ml/min over 30 min at the preparative Infinity 1260 system by Agilent Technologies. Fractions with a UV-absorption of 311 nm were collected and dried by lyophilization. 17 fractions were analyzed with the amaZon X by Bruker. The fraction eluting between 19.1 and 20.4 min was selected and purified with a phenyl-hexyl column (Luna 5 μm Phenyl-Hexyl 100 Å 250x10 mm by Phenomenex) and a gradient of ACN/water ranging from 30-65 % with a flow of 3 ml/min over 27 min. The purified compound was analyzed by HPLC-HR-MS and NMR.

2.3.5 Solid-phase peptide synthesis

For the solid-phase peptide synthesis (SPPS) the Syro Wave™ was used which has prewritten protocols. The resin which was used was already loaded with alanine (provided by Trinetri Goel). The resin was transferred into a plastic vessel and placed into the reaction chamber of the Syro Wave. Afterwards a script containing the three main steps of the SPPS was written and carried out which consists of coupling, capping and deprotection. The three steps were carried out for every amino acid. The amino acids

were all carrying N-terminal protection groups (Fmoc), serin and tyrosine also *tert*.-butyl (t-Bu) and lysine *tert*.-butoxycarbonyl (boc). All amino acids were solved in dimethylformamide (DMF) and prepared in 0.1 or 0.2 mol/l concentrations. The sequences and structures of the peptides which were synthesized are shown in Figure 15.

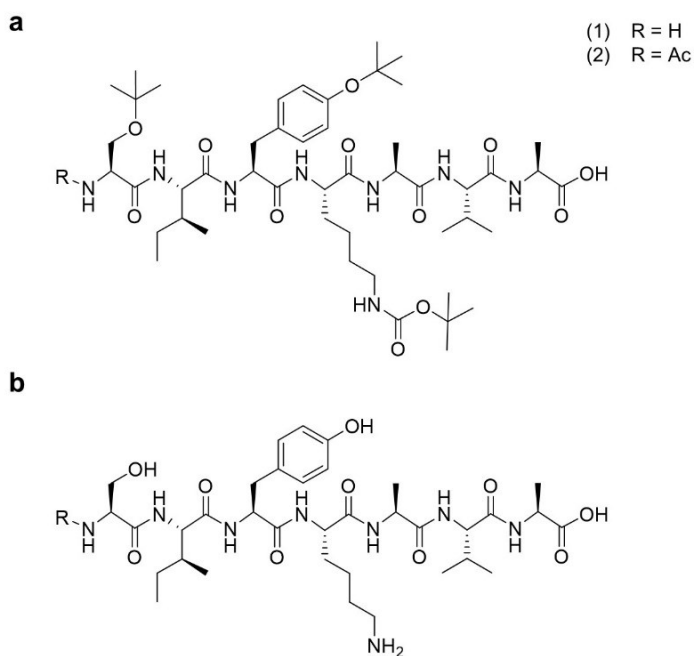


Figure 15. Structure of the synthesized peptides SIYKAVA with unprotected (1) and acetylated (2) N-terminus before (a) and after (b) the cleavage reaction with TFA.

2.3.5.1 Solvents for the SPPS

The following solvents were prepared for the 50 μ mol reaction setup of the SPPS:

40 % Piperidin in NMP (N-Methyl-2-pyrrolidone)

20 % Piperidin in NMP

1 mol/l DIPEA (N,N-Diisopropylethylamine) in NMP

0.27 mol/l HCTU 2-(6-Chloro-1H-benzotriazole-1-yl)-1,1,3,3-tetramethylaminium hexafluorophosphate in DMF

Capping solution: 0.45 ml DIPEA, 0.95 ml Ac₂O, 40 mg HOBT (1-Hydroxybenzotriazole) in 20 ml NMP

2.3.5.2 Coupling

The alanine carrying resin was combined with the protected amino acid (1500 µl of 0.1 mol/l), HCTU in DMF (500µl of 0.27 mol/l for) and DIPEA in NMP (300 µl, 1 mol/l) followed by a 50 min incubation which consists of 15 s of vortexing every 2 min.

2.3.5.3 Capping

1 ml of the capping solution was added to the resin and incubated for 5 min. After removal of the solution, the resin was washed with 800 µl NMP.

2.3.5.4 Fmoc-deprotection

The deprotection reaction of Fmoc followed by addition of 40 % piperidine in NMP (600 µl) and incubation for 3 min. The solution was replaced with 20% piperidine in NMP (600 µl). The solution was removed afterwards and the resin was washed with 800 µl NMP.

In the last step, the resin was washed five times with NMP, DMF and dichlormethan (DCM) respectively. The peptides were cleaved off from the resin by *hexafluoroisopropanol* (HFIP) and DCM mixture. The reaction was carried out in a syringe with 1.5 ml HFIP and incubated for 30 min at room temperature. The mixture was then transferred to a flask and evaporated.

A few grains of resin were put into a 5 ml flask to carry out a test cleavage with trifluoroacetic acid (TFA) and DCM in order to cleave off the t-bu and boc protection groups. The mixture was removed by evaporation and measured at the AmaZon X to verify the efficiency of the cleavage reaction.

2.3.5.5 Purification of peptides

The peptides were dissolved in MeOH and dimethyl sulfoxid (DMSO) were purified at a preparative HPLC-MS by *Agilent*. The purification was carried out with H₂O and ACN (both with 0.1 % FA) as solvents and with an *Eclipse XDB-C18* (21.2 x 250 mm, 7 µm) column by *Agilent* with a flow rate of 20 ml/min and a gradient ranging from 5 to 95 % ACN for 28 minutes. The injection volume was varying between 500 and 800 µl. The

fractions were collected at 7.2 – 7.6 min and at 8.4 – 9.2 min and dried by rotary evaporation and lyophilization. The run was stopped at 11 min.

The purified peptides were verified via HPLC-HR-MS.

2.3.6 Reaction of amino acids, peptides and proteins with epoxides

L-lysine, N ϵ -acetyl lysine, the synthesized peptides and StIE (final concentration of 50 μ M) were used for *in vitro* reactions with styrene oxide and stilbene oxide (100 μ M final concentration, Figure 16). Therefore, the amino acids and the peptide were alkalified with 0.01 mM NaOH while StIE was buffer exchanged and utilized with 200 mM NaCl as buffer. After 2 h incubation at 30°C the samples were measured at the AmaZon X or Impact II on a C18 column (ACQUITY UPLC BEH, 50 mm x 2.1 mm x 1.7 μ m, Waters) using H₂O and ACN containing 0.1% (v/v) formic acid (FA) as mobile phases for the reactions with the lysine derivatives and peptides. HPLC was performed at a flow rate of 0.4 mL/min with 5% ACN equilibration (0-2 min) followed by a gradient from 5-95% ACN (2-14 min, 14-15 min 95% ACN) ending with a re-equilibration step of 5% ACN (15-16 min). The reaction mix with StIE was measured on a C3 column (Zorbax 300SB-C3 300Å, 150 mm x 3.0 mm x 3.5 μ m, Agilent). ACN and H₂O containing 0.1% (v/v) FA were used as mobile phases at a flow rate of 0.6 mL/min. HPLC was performed with 30% ACN equilibration (0-1.5 min), followed by a gradient from 30-65% ACN (1.5-27 min) and a further elution step with 95% ACN (27-30 min).

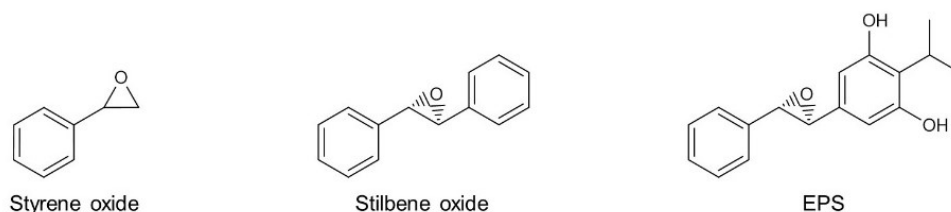


Figure 16. Chemical structures of epoxides utilized in Topic C of this thesis.

3 Results

3.1 Topic A: Biosynthesis characterization of stilbene related pathways

Enzymatic *in vitro* assays are a commonly used method to characterize the biosynthesis of various secondary metabolites. This chapter shows how these assays can be used to elucidate the biosynthesis of IPS, but also other antibacterial compounds as benzylideneacetone from *P. laumondii* TT01 and how those insights were used to produce IPS in a heterologous host.

3.1.1 *In vitro* production of 5-phenyl-2,4-pentadienoyl-StlE

The assays for the *in vitro* reactions were carried out as described in chapter 2.1.9. The proteins for the *in vitro* assays were purified according to chapter 2.1.8.

The PPTase Sfp transfers CoA bound moieties (here malonyl or cinnamoyl) onto the ACP (StlE). The m/z 1120.36, 1115.96 and 1111.55 $[M+H]^{10+}$ represent the StlE loaded CA, malonyl and acetyl (decarboxylated malonyl unit) moieties and their respective specific MS² fragmentations of m/z 391.169, 347.131 and 303.142 $[M+H]^+$ (Figure 17). Addition of 10 μ M of the KS pIFabH (corresponds to the *P. laumondii* derived priming KS of the fatty acid biosynthesis) resulted in a decrease of the starting building blocks and generated a m/z of 1124.56 $[M+H]^{10+}$ and an fragment of 433.182 $[M+H]^+$ which represents the β -ketoacyl moiety. The acetyl-StlE which occurs as a side product did not react anymore. Addition of 10 μ M the KR pIFabG resulted in the reduction of the β -ketoacyl moiety to the β -hydroxyacyl product m/z 1124.77 $[M+H]^{10+}$ and 435.184 $[M+H]^+$. Signals for m/z 1122.96 $[M+H]^{10+}$ and 417.182 $[M+H]^+$ can also be detected and represent the spontaneous dehydrated 5-Phenyl-2,4-pentadienoyl-StlE. With addition of 10 μ M of the dehydratases pIFabA or pIFabZ the signals for the latter product increased.

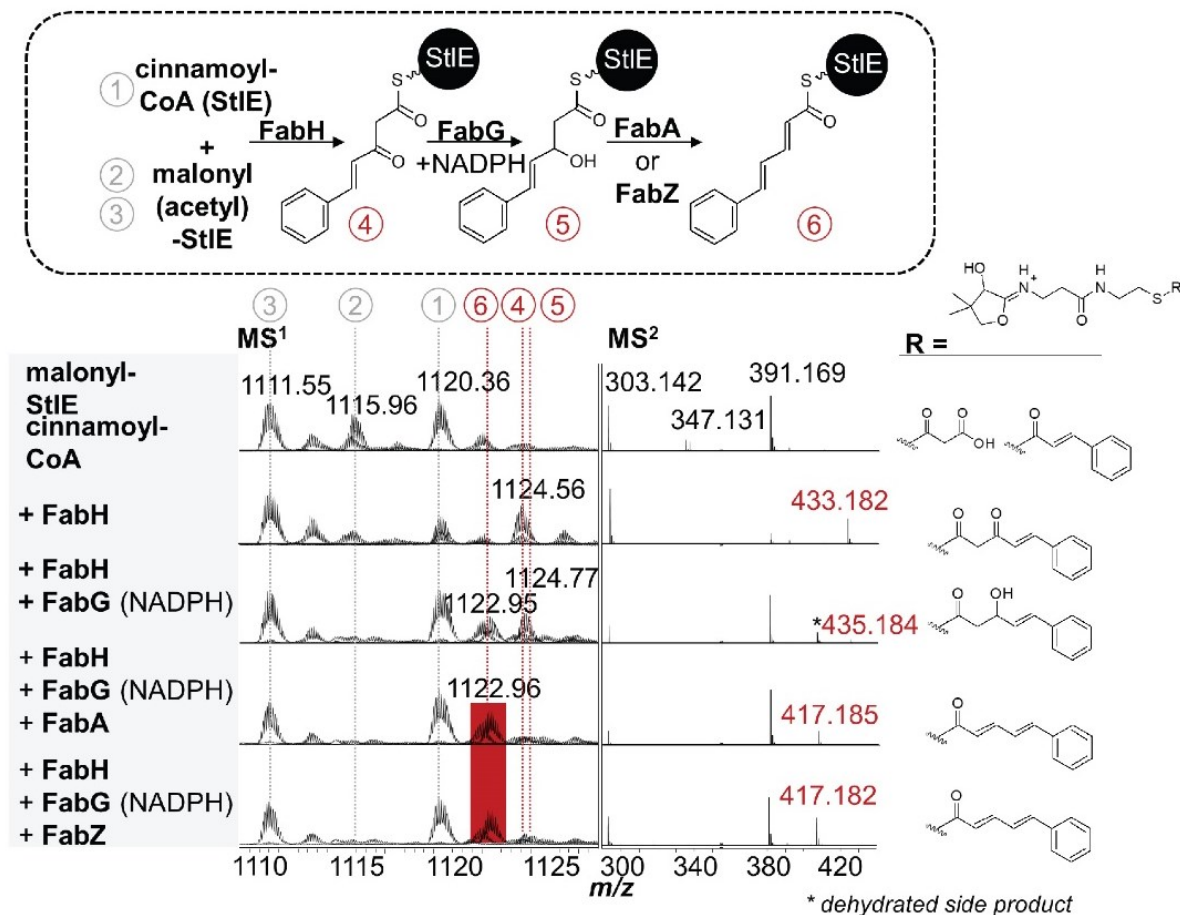


Figure 17. *In vitro* elongation, ketoreduction and dehydration reaction with FAS II enzymes FabH, FabG (+NADPH), FabA, FabZ from *P. laumondii* and cinnamoyl-CoA as starter and malonyl-ACP as elongation unit. Spectra were overlaid for StIE species differing more than 0.4 min in retention time. Adapted and modified from “Biosynthesis of the Multifunctional Isopropylstilbene in *Photorhabdus laumondii* Involves Cross-Talk between Specialized and Primary Metabolism”, see chapter 7¹¹⁶.

3.1.2 Heterologous production of stilbenes

The knowledge attained from the *in vitro* reactions was used for heterologous production of IPS in *E. coli*. Therefore, the plasmids which were utilized for the production of the proteins applied in the *in vitro* assays were used for the transformation of *E. coli* BL21 (DE3). The genes were also cloned with Golden Gate cloning (chapter 2.1.7 in materials and methods) into two plasmids generating artificial operons carrying an arabinose inducible instead of an IPTG inducible T7-promoter (Figure S2) and used for transformation of *E. coli* DH10B. Both setups resulted for the first time in successful heterologous production of IPS (Figure 18a and publication “Biosynthesis of the Multifunctional Isopropylstilbene in *Photorhabdus laumondii* Involves Cross-Talk between

Specialized and Primary Metabolism" in chapter 7) and yielded similar production titers (between 0.6 and 1 mg/l). While the two plasmid approach with the tighter arabinose dependent promoter resulted only in the production of **1**, the strain with the IPTG inducible T7-promoter produced **1** and **2**. Although minor production of **2** was detectable even in the absence of StIB, the addition of StIB increased production of **2** in the heterologous *E. coli* host. Thus, both enzymes, StIB and pIFabH are important to produce the stilbene product, but only pIFabH is essential. The products were verified via MS² fragmentation which were compared to the fragmentation patterns of the TT01 WT (Figure 18b and c) and confirmed the heterologous production.

Results

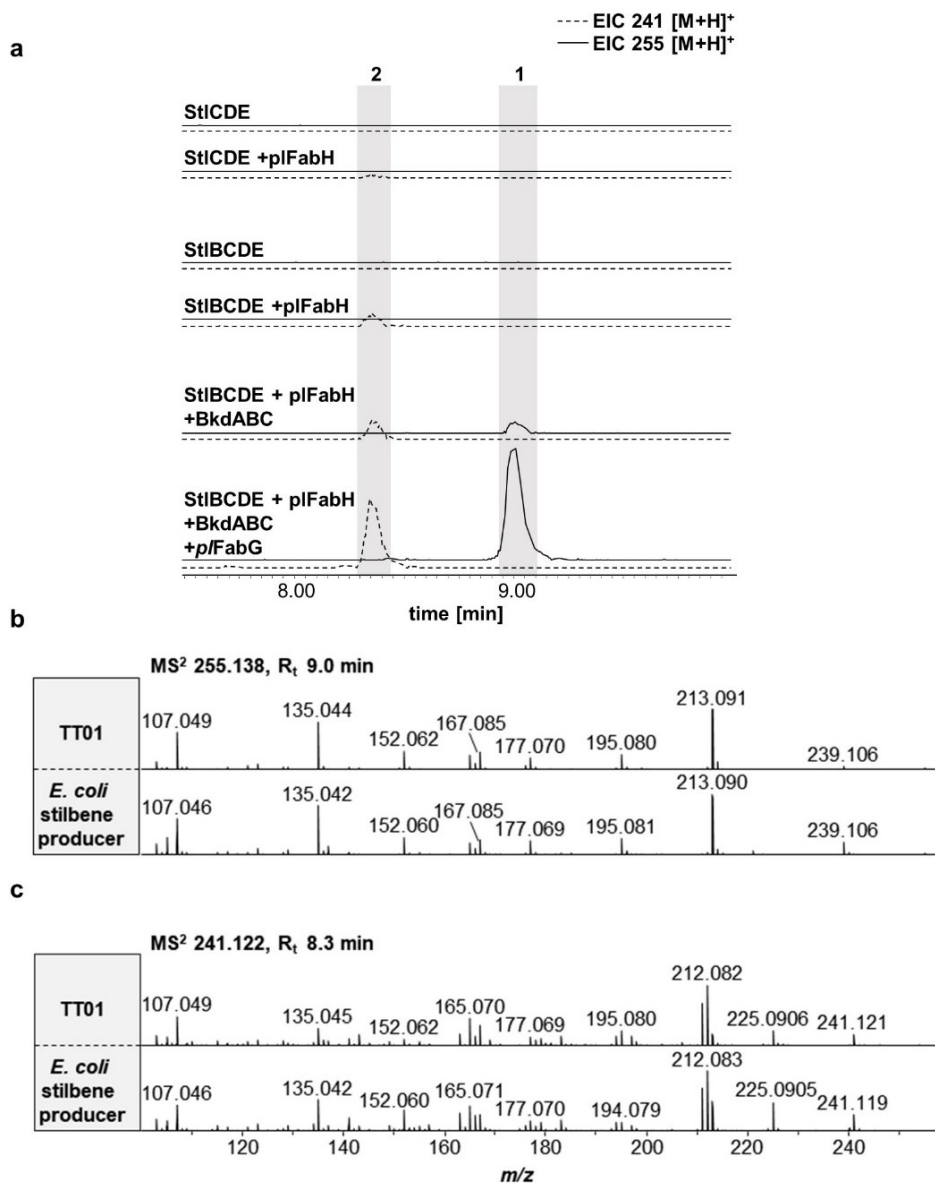


Figure 18. Heterologous stilbene production in *E. coli*. Analysis of IPS production after cultivation of *E. coli* BL21 (DE3) with introduced StICDE ± pIFabH, StIBCDE ± pIFabH, or StIBCDE ± BkdABC and ± pIFabG and supplementation with CA. The crude extracts of the corresponding strains were analyzed by HPLC-UV-MS in positive mode. The EICs of 255 and 241 [M+H]⁺ are shown at retention times between 7 and 11 min (a). The MS²-fragmentations of **1** (b) and **2** (c) produced in *E. coli* are compared to the fragmentations of the corresponding products in TT01.

3.1.3 Quantification of IPS titers

For the quantification of IPS production titers in *E. coli* and *P. laumondii* TT01 a standard curve was plotted. Therefore, 240 mg/l of **1** was purified (chapter 2.2.10 in material and methods) with the interchim PuriFlash 5.050 system and a C18 column and measured in various concentrations at the HPLC-UV-MS. The chromatogram of the HPLC-MS

measurement and the MS¹ spectra (9 min retention time) of the purified compound are depicted in Figure 19a and b. The asterisk indicates an impurity caused by the utilized HPLC vials (m/z 415.21 [M+H]⁺) and can thus be regarded as systematic and be ignored. **1** is UV active and has an absorption maximum at 311 nm. The areas of the UV peaks at 311 nm were integrated and plotted against the applied concentration of **1** (Figure 19c). A linear fit was applied to determine a formula which shows the correlation between signal intensity of **1** with its concentration. The MS spectra of **1** also shows a so far unknown signal with m/z of 296.16 [M+H]⁺ with a sum formula prediction of C₁₉H₂₂NO₂. This shift of 41.026 (corresponds to sum formula of C₂H₃N) is always observed for the measurements of **1** and might be an artefact affiliated with the measurement in ACN.

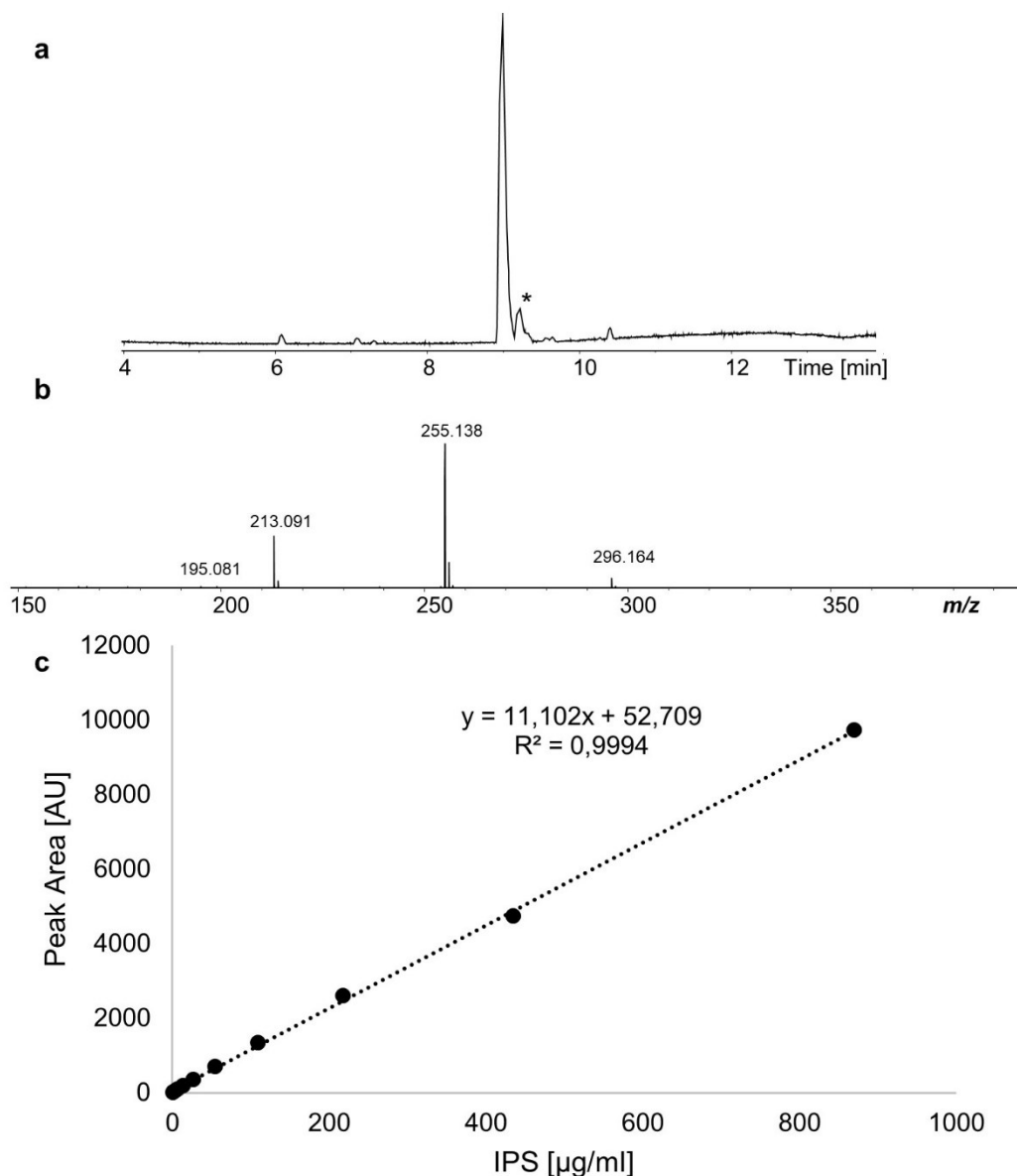


Figure 19. MS chromatogram (a) and spectrum of purified IPS (b). **1** was diluted and measured in different concentrations to obtain a standard curve (c). The peak area of the absorption at 311 nm was quantified and plotted against the adjusted concentrations. A linear fit was carried out in order to calculate the production titers of IPS in TT01 based on the displayed linear equation. The asterisk in (a) indicates a systematic impurity.

3.1.4 Substrate specificity of stilbene related enzymes

In vitro assays with StIB (conducted by Dr. Gina Grammbitter in publication “*Biosynthesis of the Multifunctional Isopropylstilbene in Photorhabdus laumondii Involves Cross-Talk between Specialized and Primary Metabolism*” in chapter 7) and FabH from my masterthesis showed a discrimination of both enzymes towards *para*-substituted CA-

Results

derivatives¹¹⁹. However, StIB was able to catalyze the reaction from 3-Cl-CA to 3-Cl-CA-CoA and hence feeding experiments with *meta*-halogenated CA derivatives were carried out in the TT01 strain ARs77 (deficient to produce kolossin, GameXPptides, phurealipids, rhabdopeptides, glidobactins, odilorhabdins and AQs, provided by Alexander Rill). The spectra were recorded in negative ionization mode since the supplemented acids were not ionizing well in positive mode (Figure 20). It was possible to detect the chloro- and bromo-substituted derivatives of **1** (**1a** and **1b**). The experiments also showed the production of the of 5-(3-chlorophenyl)penta-2,4-dienoic acid (**4a**) and 5-(3-bromophenyl)penta-2,4-dienoic acid (**4b**). The control with supplementation of CA to the ARs77 strain also produced **1** and two further compounds with an absorption at 311 nm. The stilbene derivative at 8.6 min retention time can be assigned to a dihydro-IPS derivative and was labelled as **1c** in Figure 20 while the signal at 7.5 min is proposed to correspond to 5-phenyl-penta-2,4-dienoic acid (**4**).

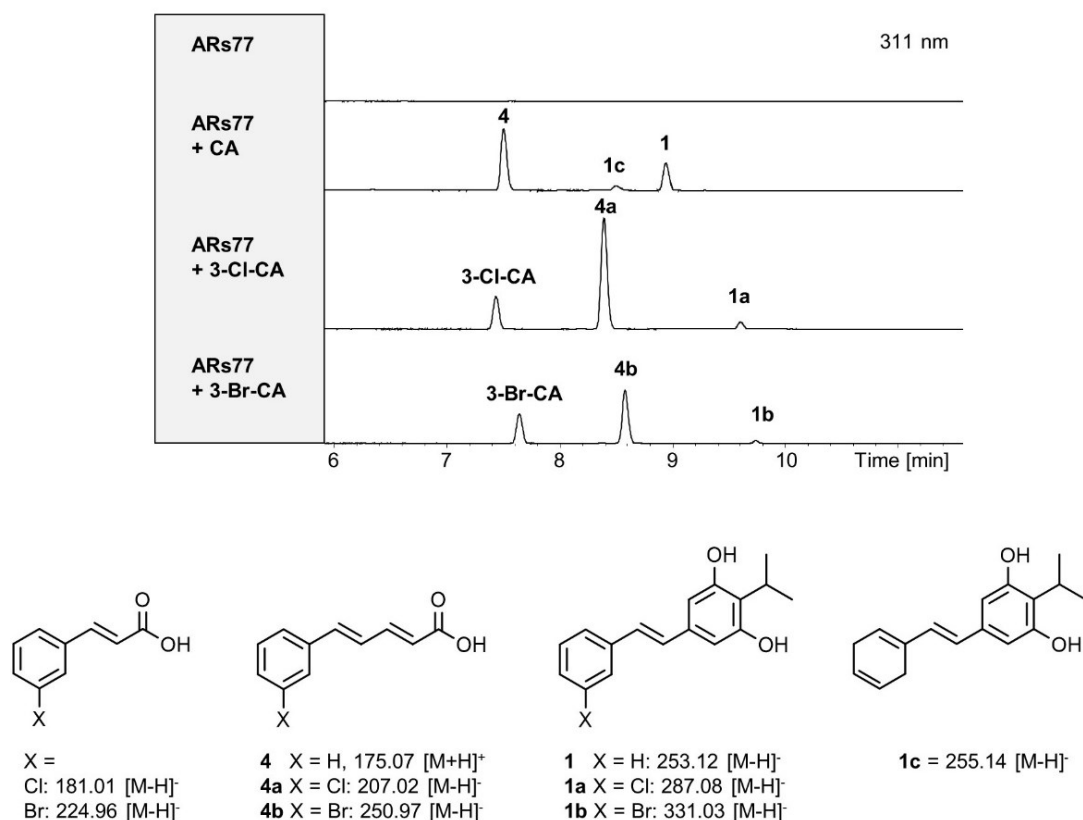


Figure 20. Feeding experiments of ARs77 strain with different CA derivatives (a). Chemical structures and *m/z* of the supplemented *meta*-substituted halogen CA-derivatives and the proposed structures of the resulting compounds (b).

For the verification of the proposed structure of compound **4** and its derivatives, a standard for 5-phenyl-penta-2,4-dienoic acid was purchased and analyzed via HPLC-MS. The resulting MS¹ and MS² spectra were compared to the signals from *P. laumondii* WT (Figure 21a and b) and verified the production of 5-phenyl-penta-2,4-dienoic acid due to the identical fragmentation patterns of 175.08 [M+H]⁺.

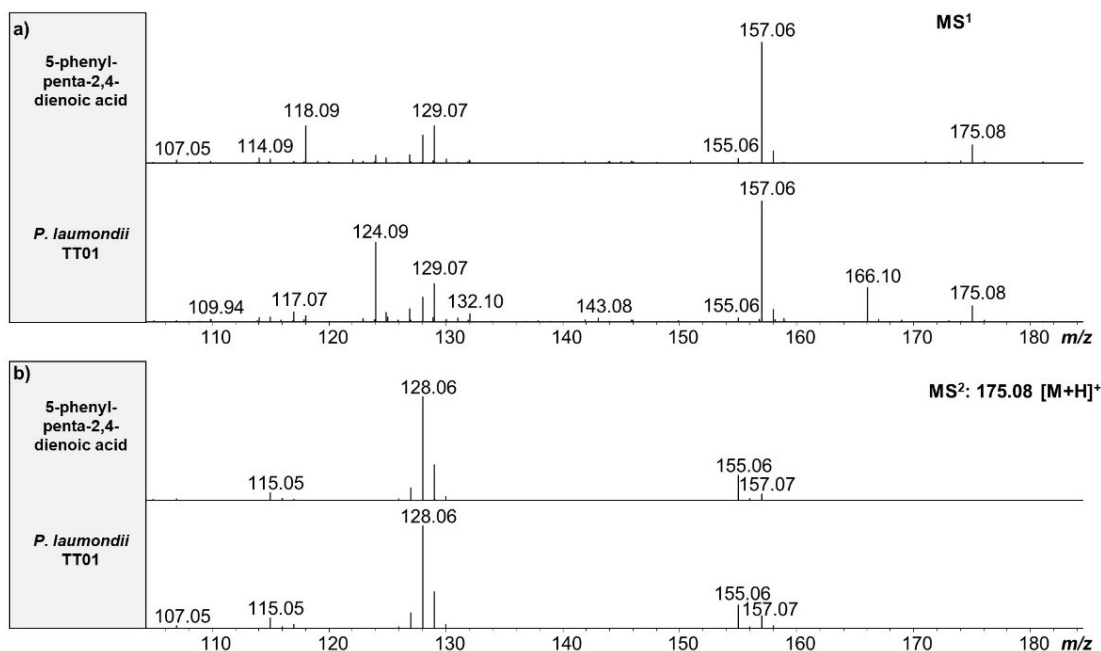


Figure 21. HPLC-MS analysis of 5-phenyl-penta-2,4-dienoic acid from *P. laumondii* with a standard. Compared are the MS¹ (a) and MS² data (b) at retention times of 7.55 min.

3.1.5 SNAC-feeding and formation of hydrazines

Due to the characteristics of StIB being hardly soluble, hence unstable and only producible in low amounts, another approach without utilizing StIB was assessed to elucidate its role in the biosynthesis. Therefore it was tested, if pIFabH would also accept CA-SNAC instead of CA-CoA in order to use a *stIB* deletion strain in the next step and complement the IPS production with CA-SNAC. The comparison of the reactions with SNAC- and CoA-derivatives is illustrated in Figure 22. The elongation reaction with CA-CoA (positive control) as well as the reaction with CA-SNAC resulted in a shift from *m/z* 1120.34 to 1124.54 [M+H]¹⁰⁺ and thus to the production of the β -ketoacyl product.

Results

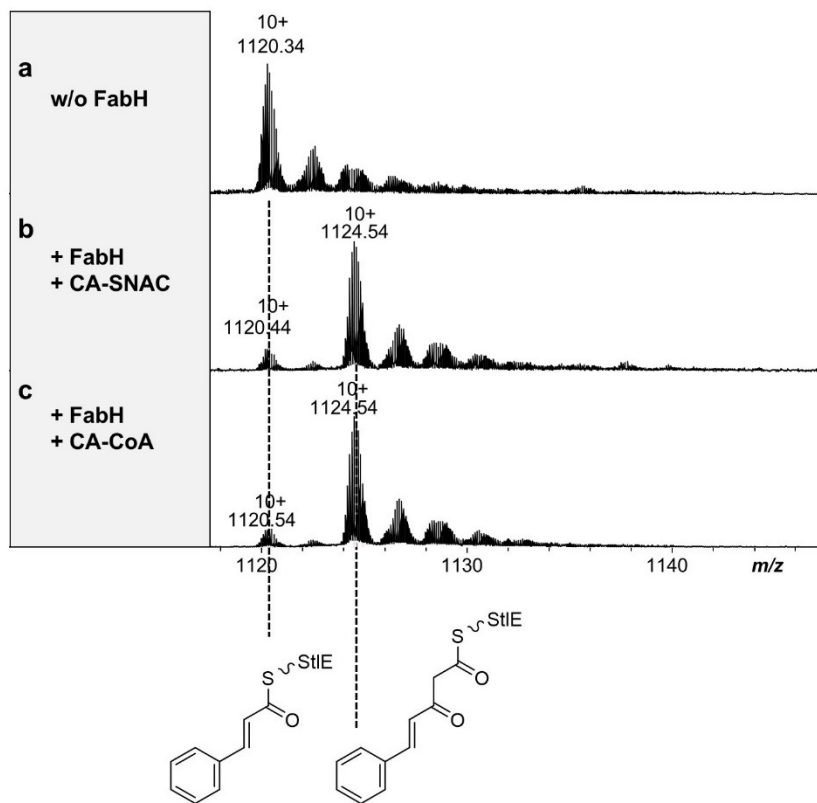


Figure 22. Excerpt of the HPLC-MS chromatogram of the *in vitro* elongation reaction of the CA moiety with MCoA and SttE without FabH (negative control) and in presence of FabH with CA-SNAC or CA-CoA (c, positive control). The shown ACPs were either carrying the cinnamic acid (10^+ corresponds to the m/z of 1120.44) or the β -Ketoacyl moiety (10^+ corresponds to m/z of 1124.54).

Feeding of a stilbene deficient strain (TT01 $\Delta antJ\Delta gxpS\Delta sttA$) with CA-SNAC as shown in Figure 23 did not complement the production of **1**. Instead another signal resulted with a m/z of 413.135 $[M+H]^+$ which could be associated with a hydrazine derivative that was built by deacetylation and dimerization of the supplemented SNAC moiety and is further described as product **5**. The latter fragmented into m/z of 131.049 and 206.063 (Figure 23b).

Results

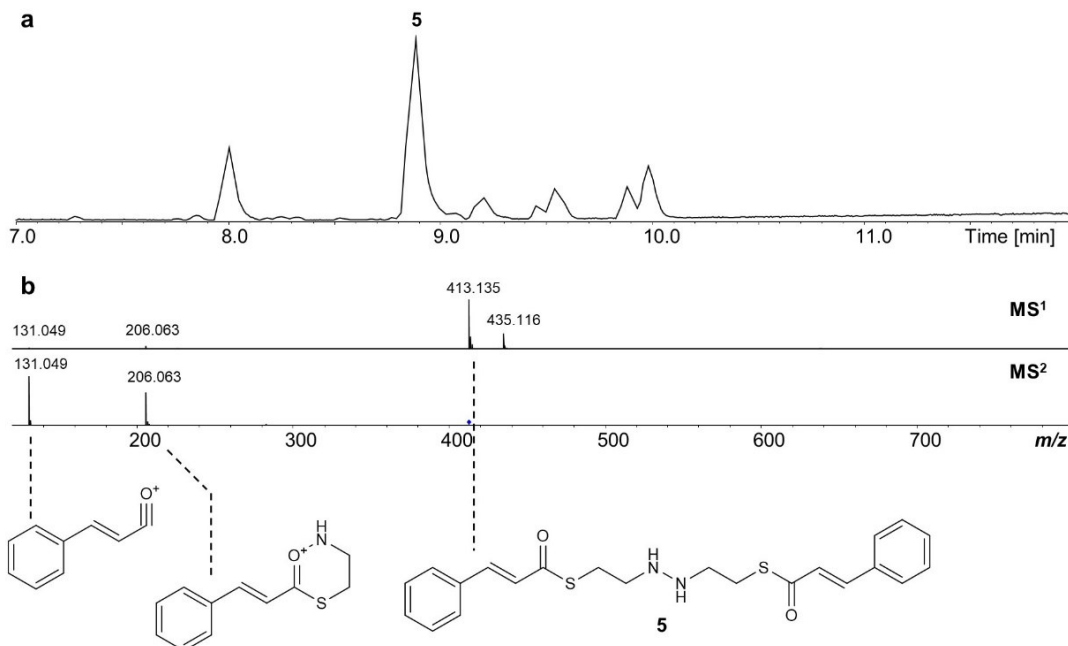


Figure 23. HPLC-HR-MS chromatogram of TT01 $\Delta antJ\Delta gxpS\Delta stlA$ in LB with feeding of 0.5 mM of CA-SNAC (a) with the corresponding MS¹ spectrum at 8.9 min and the fragmentation pattern of the m/z 413.135 [M+H]⁺ and the chemical structures of the parent ion and the fragments (m/z 131.049 and 206.063) (b).

For further assessment regarding the specificity of *P. laumondii* TT01 also towards other SNAC-derivatives, the strain was fed with 4-chloro-cinnamoyl (4-Cl-CA)-SNAC and also C₇- and C₁₁-alkyne analogs. The chromatograms of these feeding experiments were compared in Figure 24a and b. *P. laumondii* TT01 was able to incorporate various different SNAC analogs and could produce the respective hydrazine homodimers which are shown in Figure 24c. Feeding with 4-Cl-CA resulted in the synthesis of **6** (m/z of 481.056 [M+H]⁺). The combination of two different SNAC analogs resulted in the production of the two different homodimers (m/z of 413.135 and 481.056 [M+H]⁺) and of the respective heterodimer **7** (m/z of 447.096 [M+H]⁺). It was also possible to detect various lengths of alkyne bound acyl chains (C₇ and C₁₁) with m/z of 369.166 and 481.291 [M+H]⁺.

Results

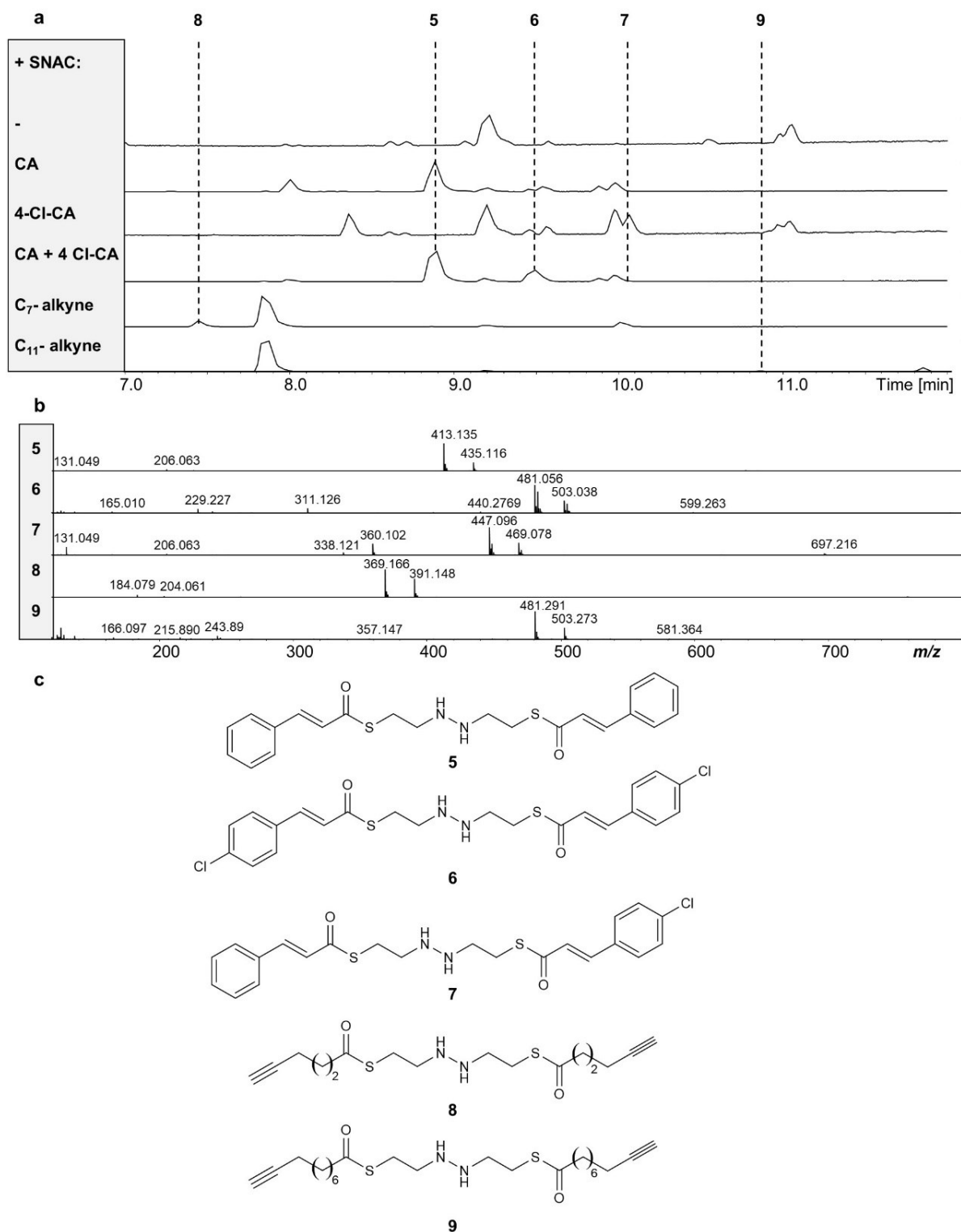


Figure 24. HPLC-MS analysis of TT01 $\Delta antJ \Delta gxpS \Delta stIA$ in LB with feeding of 0.5 mM of different SNAC derivatives (CA, 4-Cl-CA and C7 and C11 alkyne derivatives). Illustrated are the BPCs ranging from a retention time of 7 to 12 min (a) and the corresponding MS1 spectra (b). Chemical structures of the detected products after feeding of SNACS (c).

To rule out any cultivation artefacts it was also tested whether other strains are also able to produce the shown hydrazine analogues. Therefore, the feeding experiments with CA-SNAC were repeated with *E. coli* DH10B and *X. doucetiae* DSM 17909. While *X. doucetiae* was also able to generate **5** the *E. coli* strain was not able to perform this reaction (Figure 25).

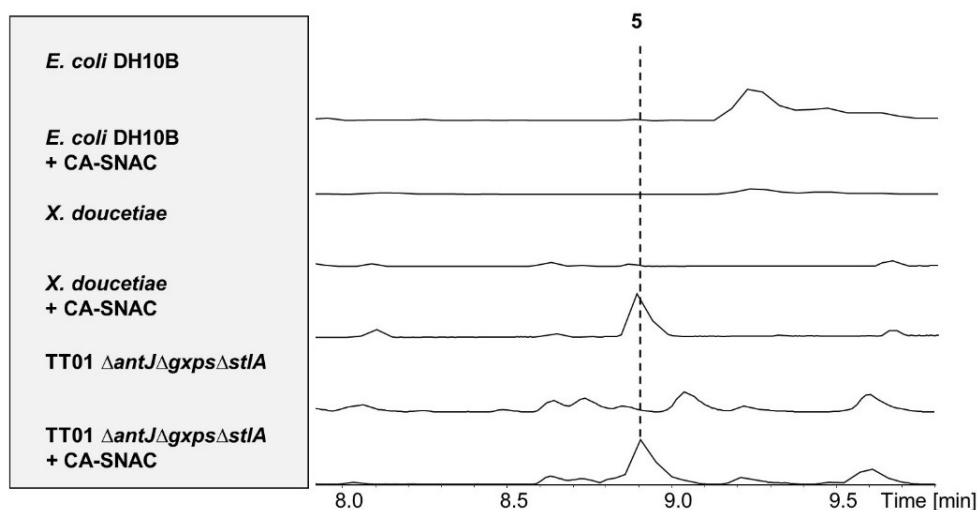


Figure 25. HPLC-MS measurement comparing the BPCs of feeding with 0.5 mM CA-SNAC between *E. Coli* DH10B, *X. doucetiae* and *P. laumondii* TT01 $\Delta antJ\Delta gxpS\Delta stlA$ in LB after 3 days cultivation. Retention time between 7.9 and 9.8 min.

Since the formation of hydrazines is rather unusual in biology, but similar products had been described in the work of Zhao *et al.* where the influence of cupin genes on the formation of N-N bonds was described, five similar cupin genes in the genome of TT01 were deleted via CRISPR/Cas12¹³². The deletion strains were all fed with CA-SNAC and analyzed after three days via HPLC-MS. The EICs of m/z 413.135 $[M+H]^+$ are shown in Figure 26. The data shows that none of the five cupin encoding genes (*plu0952*, *plu0999*, *plu1323*, *plu1886* and *plu2325*) had any influence on the hydrazine formation.

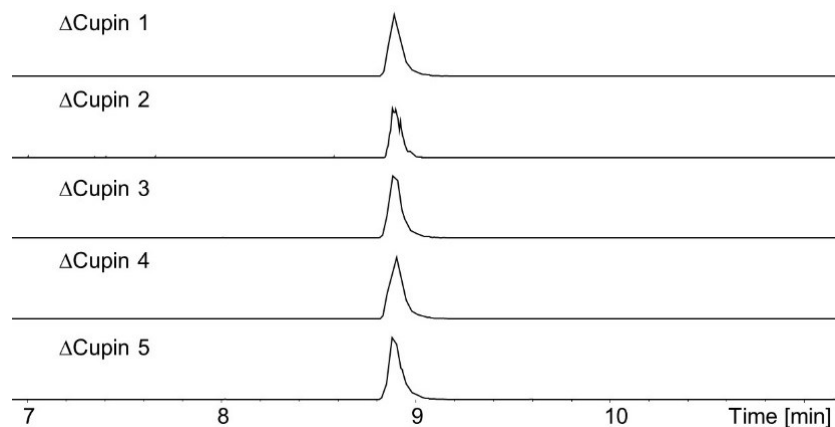


Figure 26. HPLC-MS measurement comparing the feeding of 0.5 mM CA-SNAC between TT01 $\Delta antJ\Delta gxpS\Delta Cupin$ (1-5) in LB after 3 days cultivation. Retention time between 7 and 11 min. (Cupin1 $\triangleq plu0952$, Cupin2 $\triangleq plu0999$, Cupin3 $\triangleq plu1323$, Cupin4 $\triangleq plu1886$, Cupin5 $\triangleq plu2325$). Depicted are the EICS for 413.135 ± 0.05 .

3.1.6 Biosynthesis of benzylideneacetone (BZA)

Another compound with antibiotic activities is benzylideneacetone (BZA). It is common for *Photorhabdus* and *Xenorhabdus* strains, but it was tested *in vitro* and *in vivo* whether it is possible to synthesize that metabolite with enzymes from TT01. Due to its structural similarity to CA, the genes of the stilbene synthesis were used for the assays. For the *in vitro* assay the elongation reaction of CA-CoA and malonyl-StIE with pIFabH which was described previously was performed and terminated with addition of NaOH for the offloading from StIE (Figure 27).

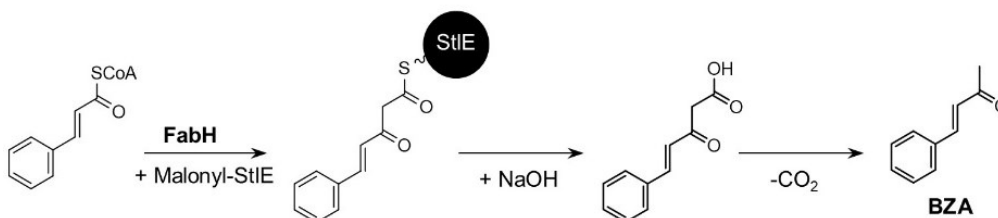


Figure 27. Schematic reaction setup for the *in vitro* synthesis of BZA.

The EIC of the *in vitro* assay and the structure of BZA are shown in Figure 28a. Heterologous expression of plasmids carrying *stlB*, *stlE* and *plfabH* in *E. coli* supplemented with CA resulted in a signal for an m/z of 147.08 $[M+H]^+$ which was associated with BZA (Figure 28b). The signal was compared to purchased standard and verified via MS² fragmentation which generated characteristic patterns for m/z of 129.068,

Results

147.079 and 169.062 $[M+H]^+$ (Figure 28c). After obtaining a standard curve for BZA (Figure 28d), the heterologous production titers of a triplicate measurement in *E. coli* were quantified which amounted in a production titer of 1.84 ± 0.15 mg/l.

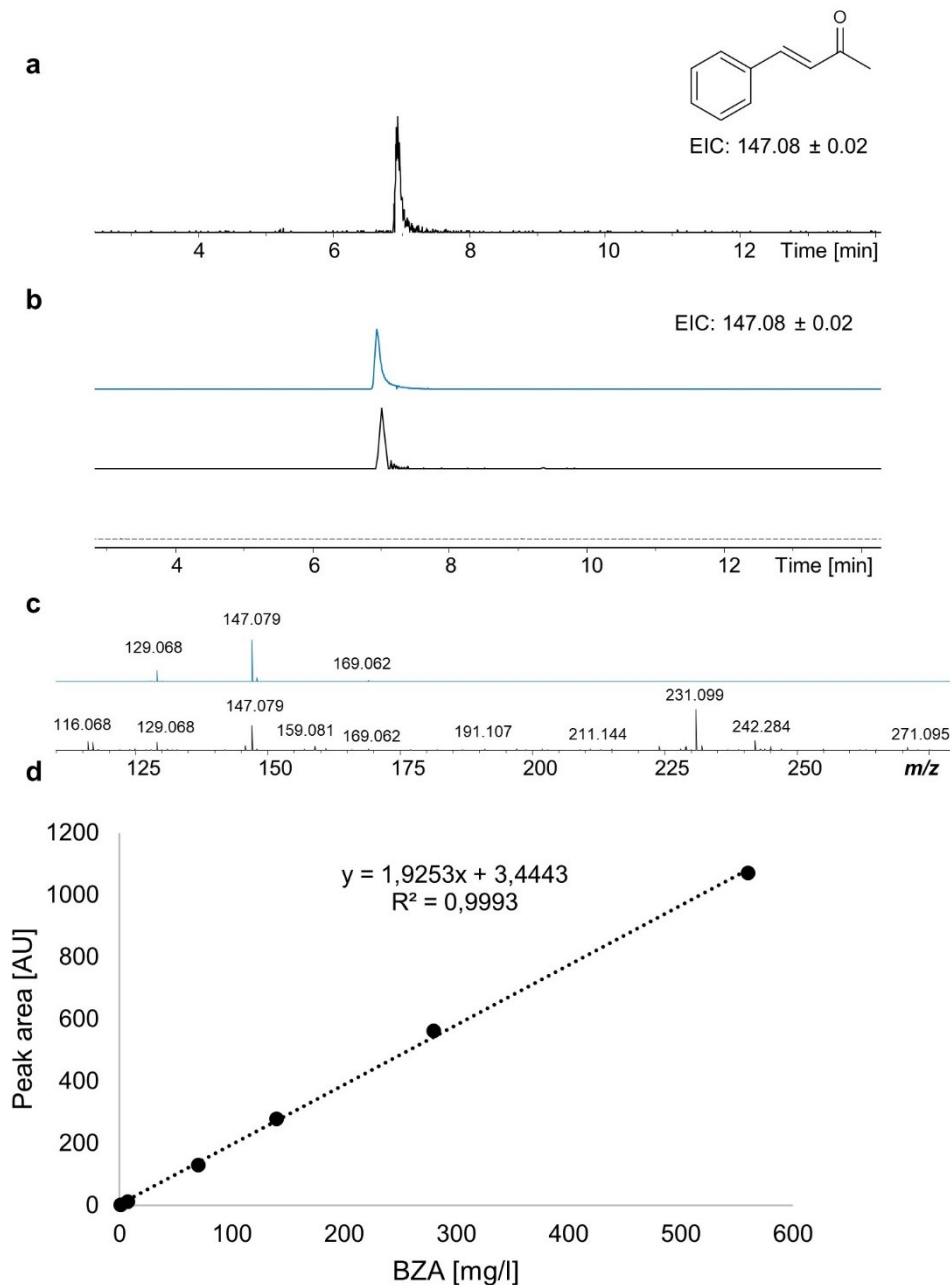


Figure 28. HPLC-HR-MS measurements of *in vitro* assay of benzylideneacetone synthesis. After the elongation reaction of CA-CoA with malonyl-StIE and pIFabH the β -Ketoacyl moiety was hydrolyzed with NaOH (a). Measurements of *E. coli* BL21(DE3) Gold extracts with empty pACYC and pCDF vectors (dashed line), pACYC-pIFabH and pCDF-StIBE (black) fed with 1 mM CA and benzylideneacetone standard (blue) (b) with the respective MS² fragmentation (c). The cultures were cultivated with 2% XAD, induced with 1 mM IPTG, fed with 1 mM CA and cultivated at 180 rpm at 22 °C for 3 days. Standard curve and linear fit of BZA for the quantification of the heterologous production in *E. coli* (d).

3.2 Topic B: Optimization of production titers of stilbene derivatives

In this chapter the production titers of stilbene derivatives were optimized by genetic modification and cultivation in different media. Therefore, deletion of biosynthesis pathways and promoter exchanges were carried out and the production of the starting building blocks were upregulated. An overview of the applied strain modifications is shown in Figure 29.

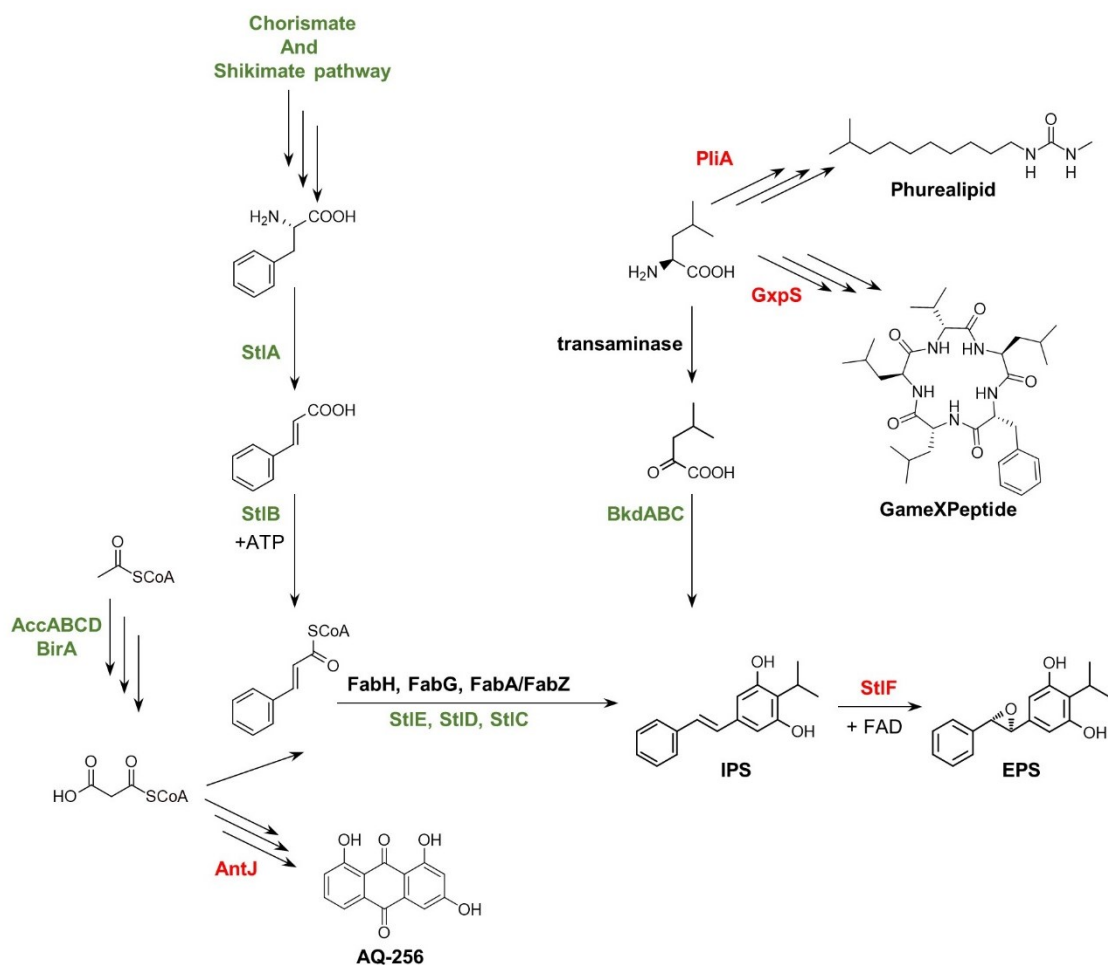


Figure 29. Schematic overview of the IPS pathway and its modifications in order to yield an IPS overproduction strain. The genes associated with the enzymes highlighted in red were deleted, while the green ones were overexpressed. AntJ = Regulator for AQ-biosynthesis, GxpS = GameXPeptide synthetase, PliA = Phurealipid carbamoyl transferase, AccABCD = Acetyl-CoA Carboxylase complex, BirA = Biotin ligase.

3.2.1 Increase of starting building blocks

To enhance the production of **1**, the influence of the building blocks (CA and malonyl-CoA) were assessed. Therefore, TT01 WT was fed with CA and a plasmid encoding the genes (*accA*, *accBC*, *accD*, *birA*) involved in the biosynthesis of malonyl-CoA from TT01. The production titers were quantified based on the data of the IPS standard curve (Figure 19). The titer of **1** in TT01 WT amounts to 23 ± 1 mg/l. Feeding with 2 mM CA increased the titer almost two-fold (40 mg/l, Figure 30). It was not possible to titrate more CA to the culture due to the pH shift of the culture that killed the cells. Expression of the genes from the plasmid encoding the genes for the malonyl-CoA upregulation did not result in an increased titer (Figure 30). The empty vector control and the pACYC-malonyl resulted both in production titers of around 29 mg/l.

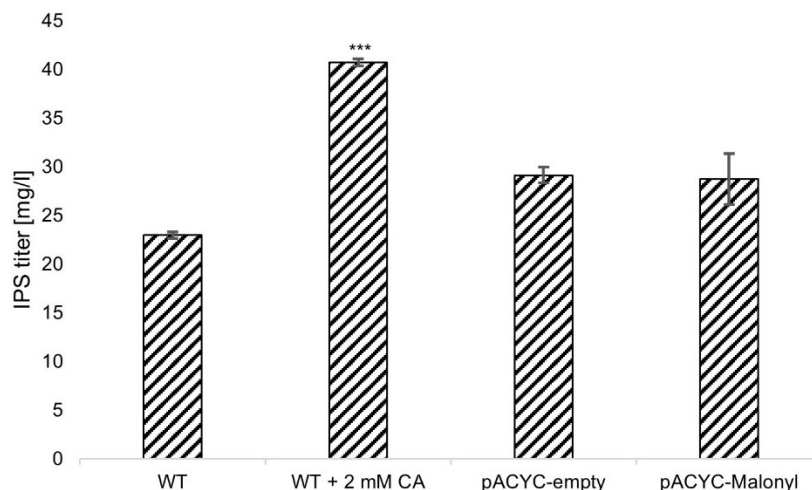


Figure 30. Quantification of HPLC-MS signals of IPS titers dependent on the feeding or overproduction of the starter building blocks CA and malonyl-CoA. The production titers were measured in triplicates after 3 days of cultivation. Error bars represent the standard error of the mean. Asterisks indicate statistical significance (***) $p < 0.0005$ of relative production compared to WT production levels.

3.2.2 Influence of pathway deletions

In the next step two genes encoding for enzymes from biosynthetic pathways utilized for the same building blocks as the IPS production were deleted. Therefore *antJ* involved in anthraquinone production which uses MCoA and *gxpS* involved in GameXPepptide which incorporates leucine, were deleted. The comparison of the WT with the double deletion

strain is shown in Figure 31 after 3 days of cultivation in LB. The deletion of these two genes increased the production of **1** from 23 ± 1 mg/l to 33 ± 3 mg/l. The peak marked with an asterisk next to the signal of **1** represents an impurity caused by the used HPLC vials.

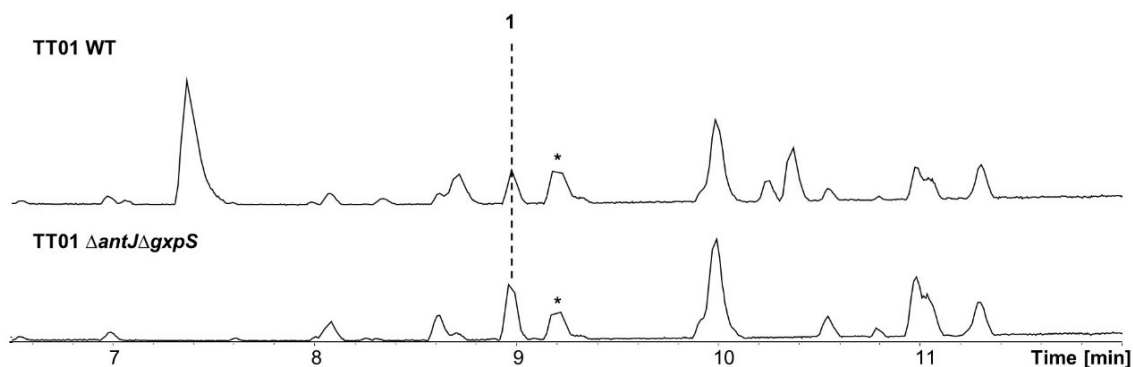


Figure 31. Comparison of HPLC-MS BPCs of TT01 WT and $\Delta antJ\Delta gxpS$ in LB. The asterisk marks the signal of the impurity from the HPLC-vials.

3.2.3 Cultivation in insect media and its influence on epoxide formation

To mimic the natural food source of *Photorhabdus*, cultures with dried and powdered insect larvae of silk worms (*Bombxy mori*) were used to supplement XPP medium (chapter 2.2.1). Figure 32 shows the comparison between the TT01 WT and epoxidase deletion in LB and BM. Regarding stilbene derivatives, cultivation in insect based media led to an increase of **3** indicated by the EIC of m/z 271.138 (Figure 32). Furthermore, it also resulted in different derivatives of **3**, hence the peaks at various retention times between 6 and 8 min. For a better comparison of production titers, the epoxidase StIF which conducts the the reaction from **1** to **3** was deleted. This resulted in a 2.8-fold accumulation of **1** in BM to 75 mg/l, but also increased the titer in LB about 1.65-fold and thus granted 35 mg/l for **1** (Figure 32).

Results

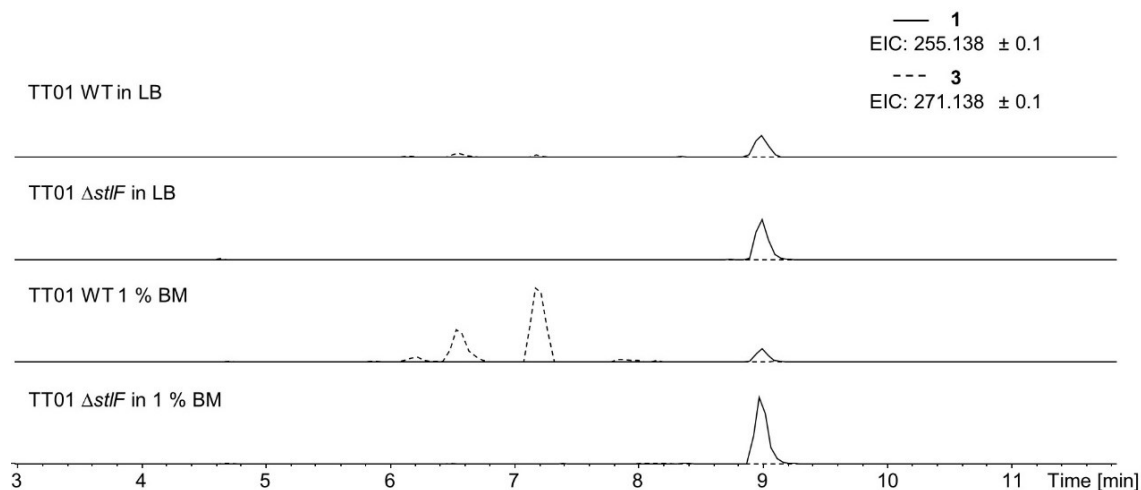


Figure 32. HPLC-MS chromatograms of TT01 WT and Δ epoxidase (Δ stlF) extracts in LB and 1 % BM. Shown are the EICs of compound **1** (m/z 255.138 \pm 0.1 [M+H]⁺) in solid and **3** (m/z 271.138 \pm 0.1 [M+H]⁺) in dashed lines.

The assessment of the optimal amount of BM in the culture was determined with HPLC-MS and compared to cultivation in LB as reference (Figure 33). The production of **1** surged with increasing BM concentrations. The highest amount of production was generated in 5 % BM and started to decrease with further addition of BM. With 1 % BM the production titer doubled from around 35 mg/l to around 75 mg/l. The production levels for 2.5 % and 5 % amounted at around 93 and 158 mg/l and decreased for 10 % BM to 150 mg/l.

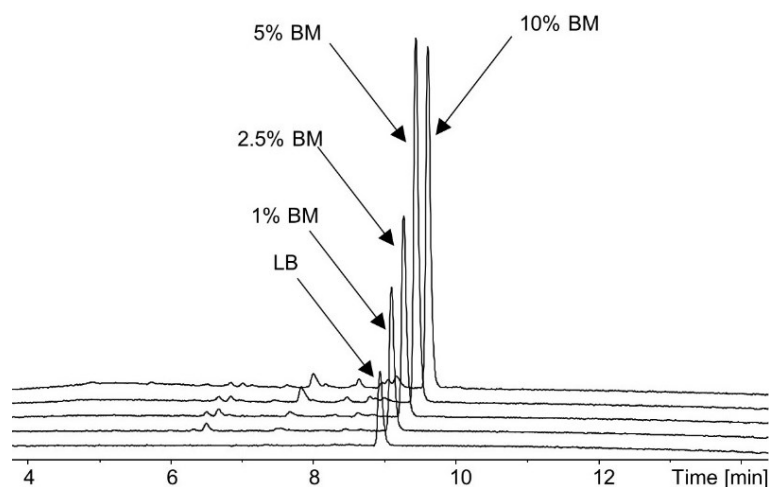


Figure 33. HPLC-UV-MS comparison of IPS production based on varying concentrations of *B. mori* powder with production in LB as reference. Shown is the absorption at 311 nm.

3.2.4 Promoter exchanges in front of stilbene related enzymes and phenylalanine upregulation

To determine the impact of the stilbene genes on the production titers, promoter exchanges in front of *stlA* and *stlCDE* were carried out in the already described double deletion strain ($\Delta antJ\Delta gxpS$). Since *stlA* is encoded next to *stlF* in the TT01 genome, the latter was deleted in parallel while performing the promoter exchange in front of *stlA*. As reference measurements TT01 WT and $\Delta antJ\Delta gxpS$ were also shown in Figure 34 which were described above. The promoter exchange in front of *stlCDE* enhanced the output of **1** around 50 % to 50 ± 5 mg/l starting from $33 \text{ mg/l} \pm 3$ for the $\Delta antJ\Delta gxpS$ strain. The combination of *stlF* deletion and promoter exchange in front of *stlA* in $\Delta antJ\Delta gxpS$ amounted in a titer of 82 ± 3 mg/l. Besides *stlA* and *stlCDE* the promoter in front of the *bkd* operon was also changed. This modification did not result in higher productions (29 ± 2 mg/l) and was therefore not applied for further strain engineering (Figure 34).

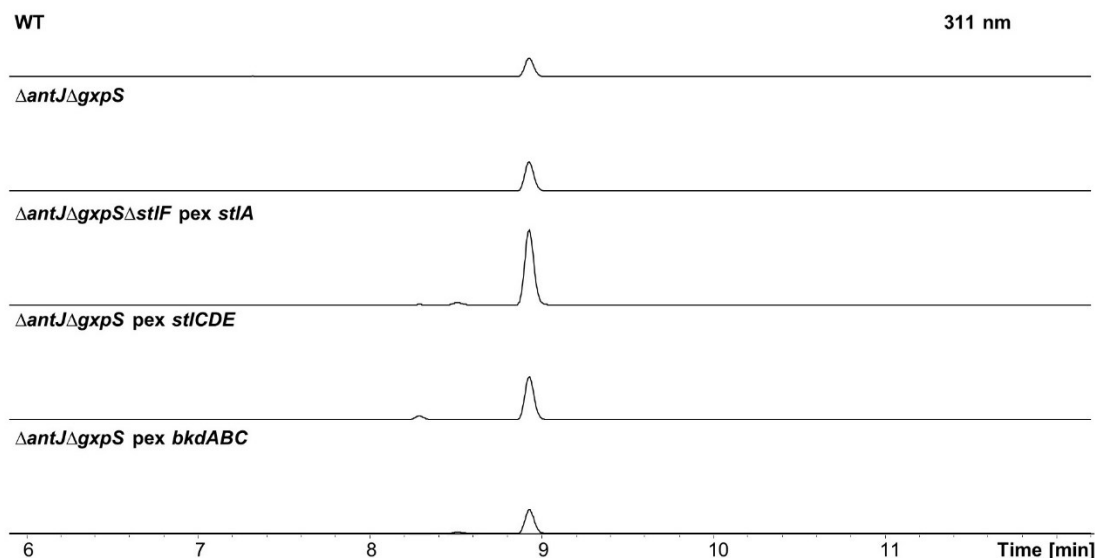


Figure 34. HPLC-UV-MS chromatograms of culture extracts with absorption at 311 nm of genetically modified TT01 strains. The influence of promoter exchanges in front of *stlA* (xylose inducible promoter), *stlCDE* and *bkdABC* (both VA inducible promoter) on the production of **1** were measured and compared after 3 days of cultivation in LB at 30°C. Retention times between 5.9 and 12.2 min.

In the next step two promoter exchanges were generated in front of *stlA* and *stlCDE*. As mentioned above, the exchange in front of *stlA* was again carried out in parallel with the deletion of *stlF*. For the combined approach of promoter exchanges, the IPTG inducible tac promoter was introduced in front of *stlCDE* while *stlA* was induced with either xylose

or VA. Triplicate measurements of $\Delta antJ\Delta gxpS\Delta stlF$ *pex stlA* (VA) *stlCDE* (tac) resulted in a production titer of around 80 mg/l (Figure 35). The same strain with a xylose instead of a VA inducible promoter granted a production of 90 mg/l in LB. Introduction of the plasmids pF3 and pS3 to enhance the conversion of phenylalanine increased the titers of **1** for both strains to 108 ± 1 mg/l (35 % increase) and 152 ± 9 mg/l (70 % increase). Expression of pS3 and pF3 in the WT and the feeding of phenylalanine did not affect the production (Figure S5 in supplementary information). The data showed no difference between the productions of the empty vector control and the strain overexpressing the enzymes of the shikimate and phenylalanine pathways. The production of **1** however increased for both strains about 20 % to around 27.5 mg/l.

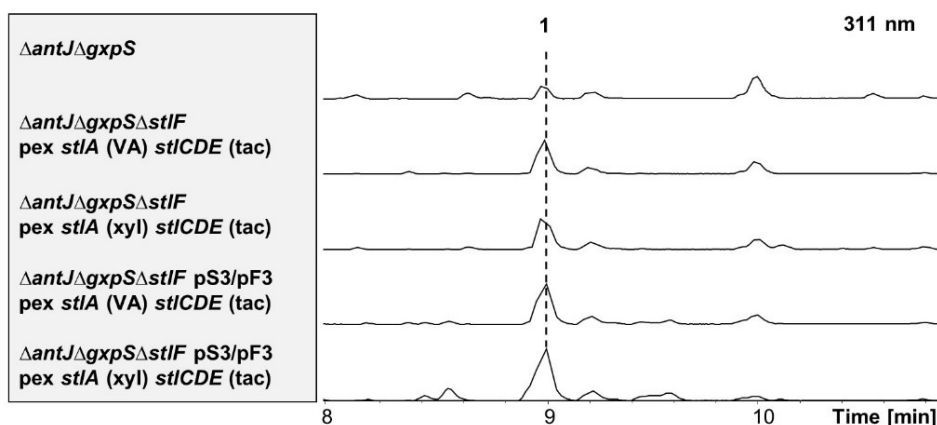


Figure 35. HPLC-MS BPCs of several modified TT01 extracts based on $\Delta antJ\Delta gxpS$ with deletions of *stlF* and two promoter exchanges in front of *stlA* and *stlCDE* in without and with pS3 and pF3. The cultures were cultivated for 3 days in LB at 30 °C and retention times between 8 and 10.9 min.

3.2.5 Cultivation with XAD

Utilization of XAD helps to obtain purer and often higher amounts of certain products since they tend to bind onto the resin of the beads. Therefore, XAD was tested for cultivation of TT01 WT in LB (Figure 36). The production of **1** increased from 23 to 62 mg/l. Therefore, XAD was added to all cultures to maximize the production titer additionally to the genetic strain engineering. Since XAD accumulates IPS, it is thus also easier to purify when applying bigger culture volumes than 10 ml.

Results

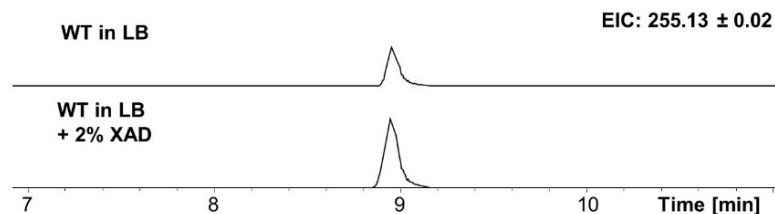


Figure 36. HPLC-MS BPCs of TT01 WT cultivated with 2 % XAD for 3 days at 30 °C. The latter was induced with 1 mM IPTG, 250 μ M VA and 0.4% xylose. Shown are MeOH extracts of the XAD beads.

3.2.6 Dependence of StIB

To elucidate whether the overexpression of *stIB* has a positive influence on the production of **1** TT01 $\Delta antJ \Delta gxpS \Delta stIF$ pex *stIA* (xyl) *stICDE* (VA) was transformed with a *stIB* expressing plasmid. Based on the measurement and the bar diagram in Figure 37a and b the production titers of **1** increased about 30 % from 90 ± 9 to 118 ± 12 mg/l.

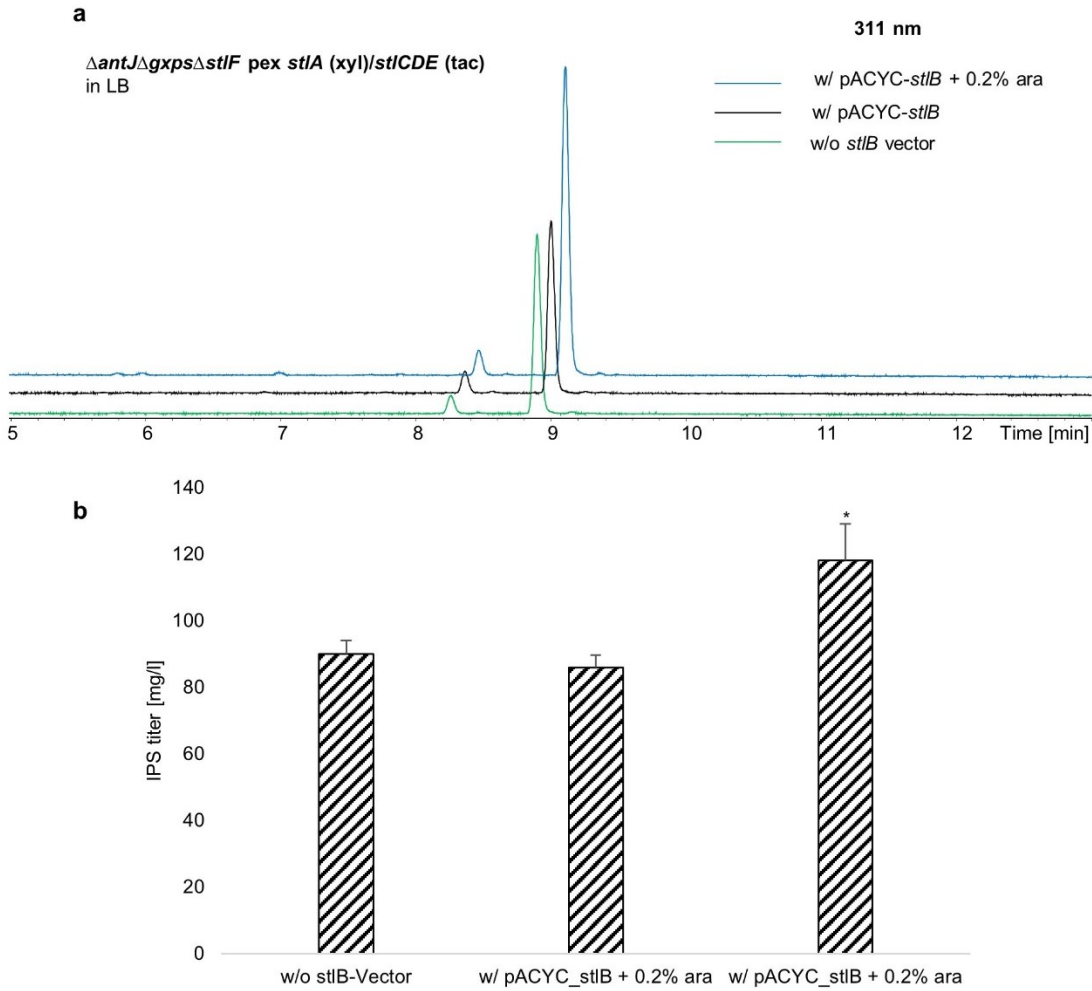


Figure 37. HPLC-UV-MS chromatogram of extracts from TT01 $\Delta antJ \Delta gxpS \Delta stlF$ pex *stlA* (*xyl*) *stlCDE* (*tac*) with induced IPS production. Influence of *stlB* expression on the production levels after 3 days of cultivation at 180 rpm and 30 °C. Depicted is the UV chromatogram at 311 nm (a) and bar diagramm of the integrated peak areas (b). Error bars represent the standard error of the mean. Asterisks indicate statistical significance (* $p < 0.05$) of relative production compared to the production levels of the strain without the vector.

3.2.7 Assessment of different media and combination of all approaches

The so far best producing strain was then used for the deletion of *pliA*. This gene encodes a carbamoyltransferase for the production of phurealipids which elute around 0.5 min later than **1** within the applied standard LC method. The production in XPPM of TT01 $\Delta antJ \Delta gxpS \Delta stlF \Delta pliA$ pex *stlA* (*xyl*) *stlCDE* (*tac*) (named $\Delta 4$ in Figure 38) with induced pS3 and pF3 plasmids yielded a titer of 53 ± 13 mg/l. Cultivation in LB increased the production level three-fold to 158 ± 13 mg/l. In media containing higher concentrations of nitrogen or carbon sources like PP3 media or cultivation in media containing the equal

Results

amount of tryptone as LB and 1 % *Hermetia ilucens* fat granted 288 ± 13 mg/l and 224 ± 40 mg/l of **1**. The highest levels of production in this work were generated in 5 % BM with XAD which yielded 867 ± 33 mg/l. This represents an almost 38-fold increase compared to the standard cultivation of TT01 WT in LB.

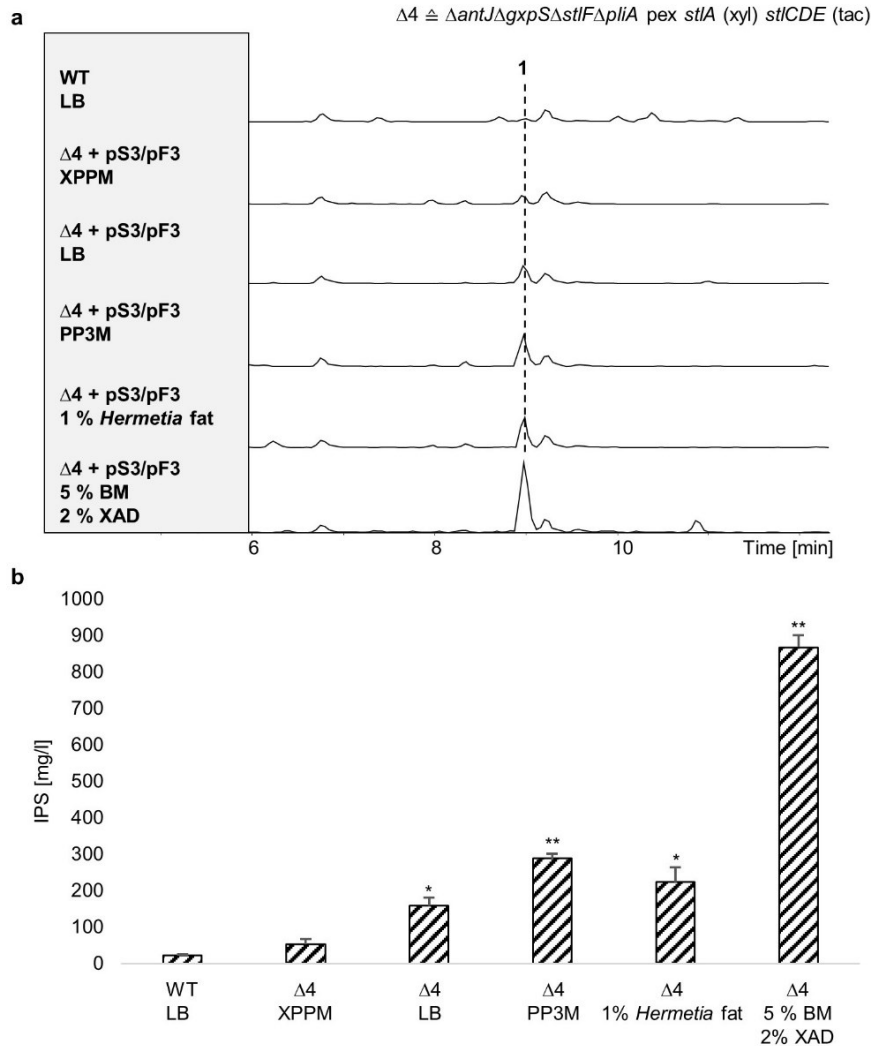


Figure 38. HPLC-UV-MS BPCs of extracts from TT01 $\Delta antJ \Delta gxpS \Delta stlF \Delta pliA$ pex *stlA* (*xyl*) *sltCDE* (*tac*) pS3/pF3 of ethylacetate extracts in various cultivation media with induced production of **1**. TT01 WT cultivated in LB is shown as a reference (a). The production titers in XPPM, LB, PP3M, 1 % *Hermetia* fat (+ 10 g/l tryptone) and 5 % BM were shown in a bar diagram with error bars (b). The culture in BM was cultivated in presence of XAD. Error bars represent the standard error of the mean. Asterisks indicate statistical significance (* $p < 0.05$, ** $p < 0.005$) of relative production compared to WT production levels.

3.2.8 Overproduction of EPS

Although IPS is the pharmaceutically more interesting molecule, it was also tested if it was also possible to utilize the designed production strains and the better cultivation conditions to shift the equilibrium of the production towards the formation of EPS for potential purification attempts as described in topic C. Therefore, the strain $\Delta antJ\Delta gxpS\Delta pliA$ pex *stIA* (xyl) *stICDE* (van) carrying the pACYC-epoxidase plasmid was cultivated in LB and in BM with XAD and compared. HPLC-MS measurements showed an increase of **3** for both cultivation media as indicated by the EIC of m/z 271.13 $[M+H]^+$ (Figure 39). The relative change of production titers between the induced and non-induced epoxidase plasmid was stronger for LB than BM. Nevertheless, it was not possible to accumulate exclusively **3**. Instead, there were also comparable productions of **1** and other derivatives of **3** since the EIC yielded more than one signal for 271.13 $[M+H]^+$.

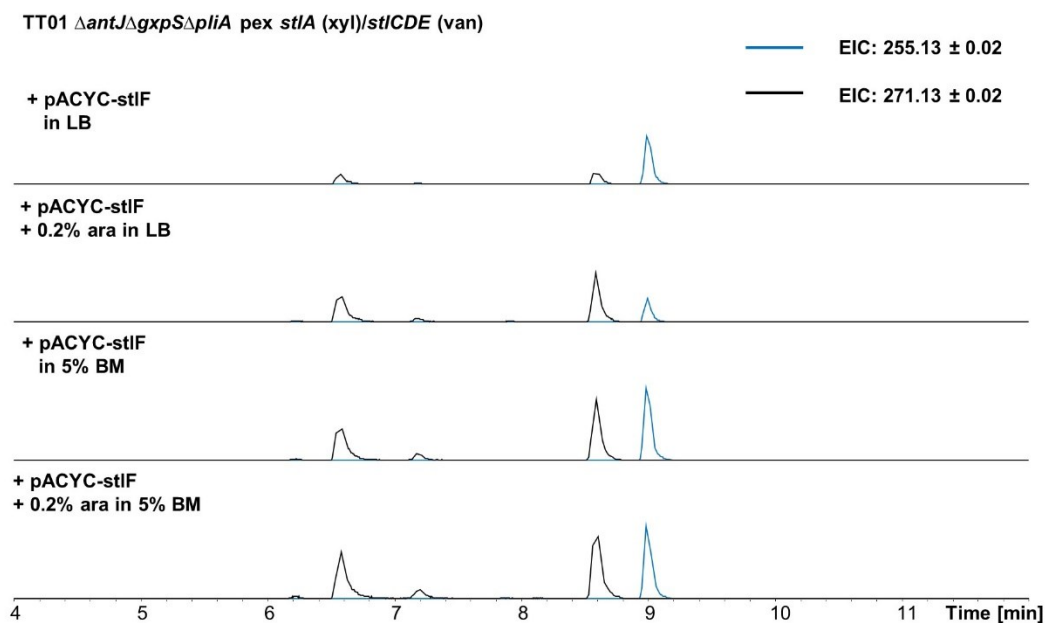


Figure 39. HPLC-MS measurements of extracts from TT01 $\Delta antJ\Delta gxpS\Delta pliA$ pex *stIA* (xyl) *stICDE* (van) overexpressing the monooxygenase *stIF* to produce EPS in LB and BM with XAD. All cultures were induced with 0.4 % xylose and 250 μ M VA and the expression of *stIF* with 0.2 % arabinose. The cultures were cultivated for 3 days and extracted with ethylacetate. Retention times from 4 to 12 min.

In contrast to the IPS-production strains which also showed some production of ethylstilbene, higher productions of EPS did not result in the epoxidized molecule of the

non-branched-derivative. This can also be observed in the measurements shown in Figure 40 where the *bkd*-operon was deleted in the production strain which led to the accumulation of ethylstilbene, but not in the formation of any epoxy-derivatives.

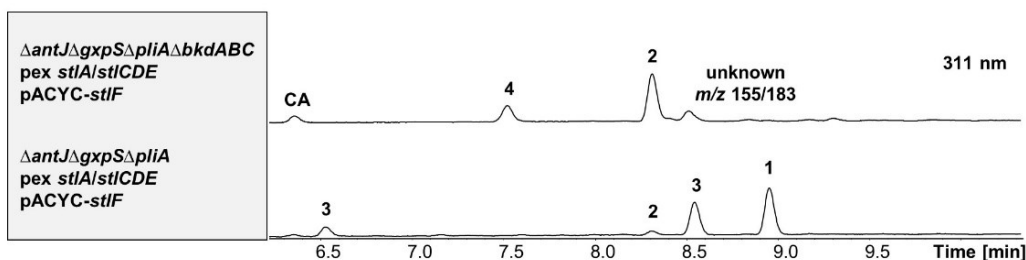


Figure 40. HPLC-UV-MS analysis of XAD extracts from induced TT01 $\Delta antJ\Delta gxpS\Delta pliA$ *pex stlA/stlCDE* *pACYC-stlF* \pm deletion of *bkdABC* cultivated for 3 days in 5 % BM. Shown are the absorption spectra at 311 nm.

3.2.9 Overview of stilbene yields

Table 12. Overview of stilbene yields from engineered strains cultivated in several media. For quantification of ethylstilbene, similar ionization characteristics as for IPS were assumed. When not stated otherwise, the cultivation took place in LB. n.d. = not detectable, n.a. = not applicable since only the other compound was purified.

Strain	IPS [mg/l]	Ethylstilbene [mg/l]	Induction
WT	23 \pm 1 62 \pm 3*	n.d.	-
WT <i>pACYC</i> -empty	29 \pm 1	n.d.	-
$\Delta stlF$	35 \pm 7 159 \pm 32 (BM)	n.d.	-
$\Delta antJ$	33 \pm 2	n.d.	-
$\Delta antJ\Delta gxpS$	33 \pm 3	n.d.	-
$\Delta antJ\Delta gxpS$ <i>pex bkdABC</i>	29 \pm 2	1 \pm 0.1	VA
$\Delta antJ\Delta gxpS\Delta stlF$ <i>pex stlA</i>	82 \pm 3	1 \pm 0.1	VA
$\Delta antJ\Delta gxpS$	50 \pm 5	5 \pm 0.4	VA

Results

<i>pex stlCDE</i>			
$\Delta antJ\Delta gxpS\Delta stlF$ <i>pex stlA/stlCDE</i>	80 ± 3 90 ± 5	- 5 ± 0.3	VA & IPTG L-xylose & IPTG
$\Delta antJ\Delta gxpS\Delta stlF$ <i>pex stlA/stlCDE</i> pACYC- <i>stlB</i>	118 ± 12	14 ± 1	L-ara
$\Delta antJ\Delta gxpS\Delta stlF$ <i>pex stlA/stlCDE</i> pS3/pF3	108 ± 1	7 ± 0.3	VA & IPTG
$\Delta antJ\Delta gxpS\Delta stlF$ <i>pex stlA/stlCDE</i> pS3/pF3	152 ± 9 240 (+ XAD)	5 ± 0.1 n.a.	L-xylose & IPTG L-xylose & IPTG
$\Delta antJ\Delta gxpS\Delta stlF\Delta pliA$ <i>pex stlA/stlCDE</i> pS3/pF3	53 ± 13 (XPPM) 158 ± 23 (LB) 288 ± 13 (PP3M) 224 ± 40 (HF) 867 ± 33 (BM + XAD)	23 ± 6 10 ± 2 38 ± 2 28 ± 7 23 ± 2	L-xylose & IPTG

3.3 Topic C: Stilbene epoxides and epoxidation of peptides and proteins

3.3.1 Analysis of EPS related derivatives

For the production of stilbene derivatives the stilbene epoxidase was cloned onto a plasmid and overexpressed in TT01 WT. The TT01 WT produced almost no EPS (Figure 41, at 8.5 min retention time), while the overexpression of *stlF* resulted in the formation of new and stronger signals at retention times between 4.8 and 8.5 min in the HPLC-MS. At the same time the signal in the EIC of 255.13 corresponding to IPS was decreasing (Figure 41).

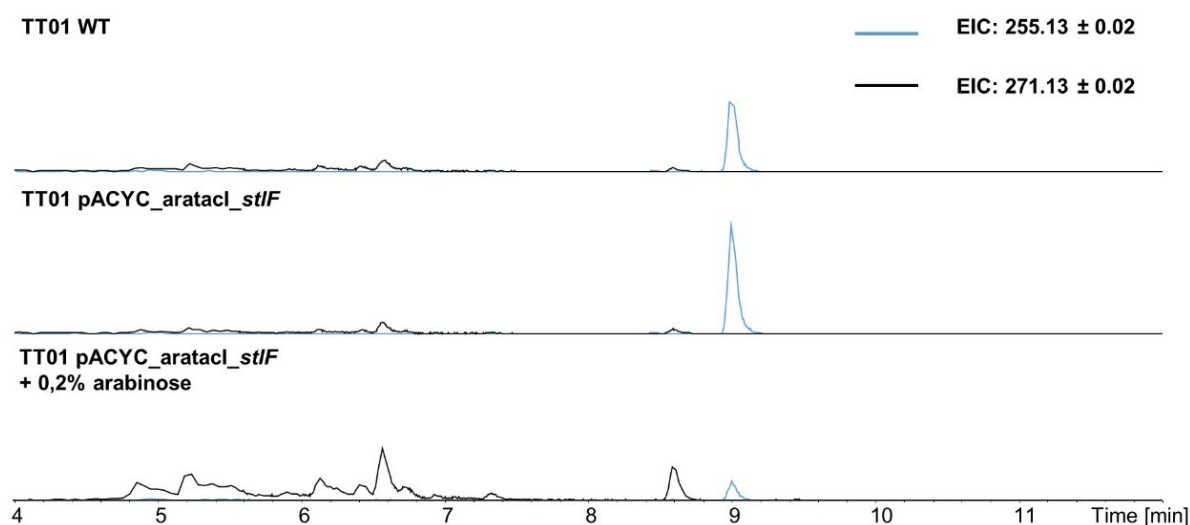


Figure 41. HPLC-MS EICs of **1** (255.13 ± 0.02) and **3** (271.13 ± 0.02) of extracts from TT01 WT and pACYC_aratacl_stlF cultures (non-induced and induced) cultivated over 3 days in LB at 30 °C at retention times from 4 to 12 min.

Since there was not only one distinct peak for the m/z of 271.13 after expression of *stlF* (Figure 41), derivatives yielding the fragment mass of 271.13 were analyzed in order to find potential EPS adducts. One detected derivative based on its m/z fragmentation of 271.132 $[M+H]^+$ yielded an m/z of 402.227 $[M+H]^+$ at a retention time of 6.4 min (Figure 42a). For the verification, the *stlF* expressing strain was additionally cultivated and supplemented with d_7 -CA. Supplementation of the culture led to a m/z shift of 7 from 402.227 to 409.271 $[M+H]^+$ as shown in Figure 42b verifying the incorporation of CA. According to a sum formula prediction of the HR mass which resulted in a prediction of $C_{23}H_{31}NO_5$, a derivative of EPS ($C_{17}H_{18}O_3$) with either leucine or isoleucine was

hypothesized since both amino acids share the same sum formula ($C_6H_{13}NO_2$) and hence the same mass. The structure for an isoleucine-derived molecule with a few proposed MS-fragmentation structures was illustrated in Figure 42c as an example. Thereby, the cyclization accompanied by elimination of H_2O as well as a fragmentation between the stilbene moiety and the amino-group is shown resulting in the formation of the MS signals of m/z 271 and 132 $[M+H]^+$. The EPS moiety indicates potential further fragmentations at the isopropyl-group and at the two hydroxyl-groups resulting in the fragments of 229 and 197 $[M+H]^+$.

Results

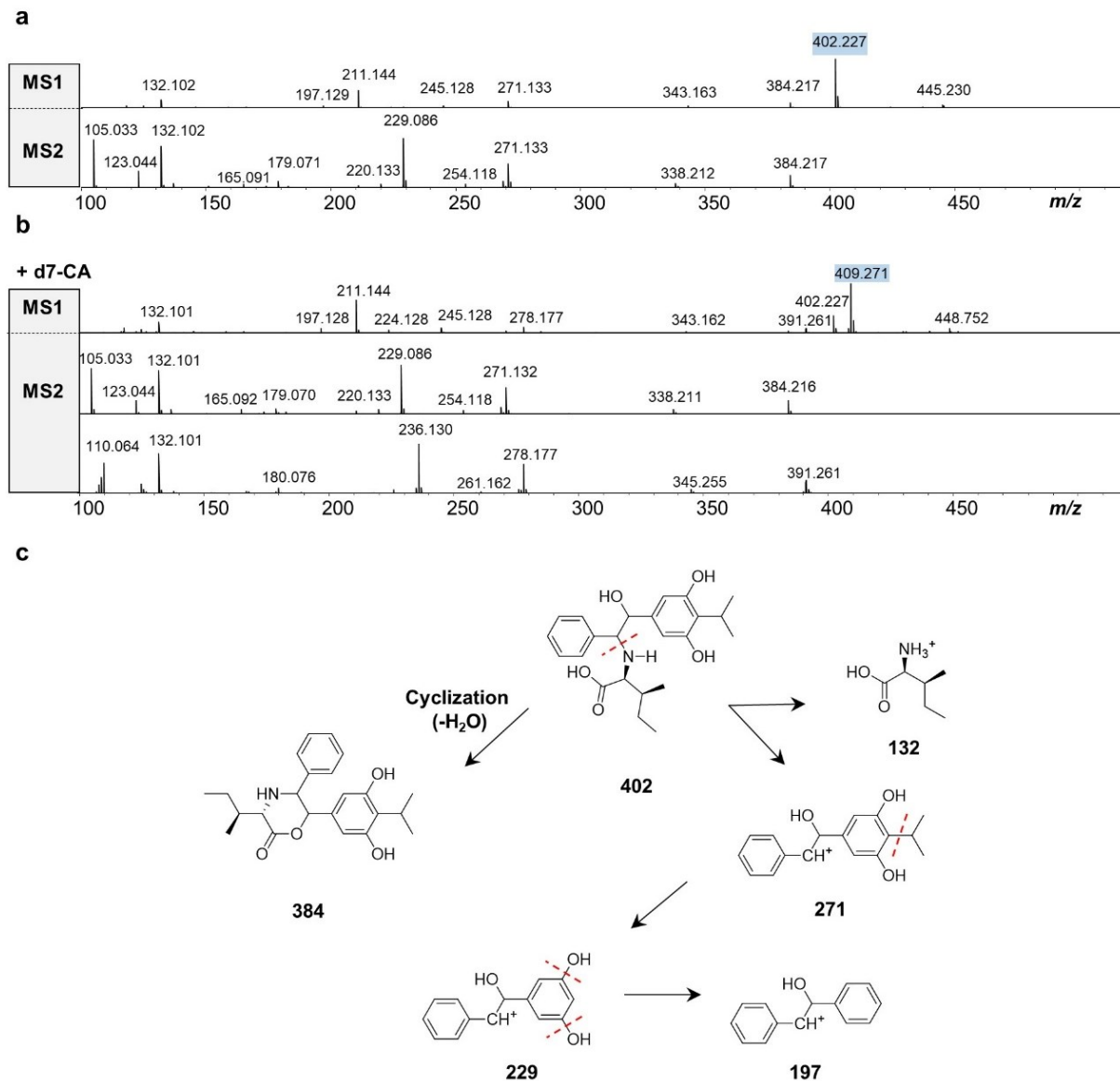


Figure 42. HPLC-MS measurements with MS¹ and MS² fragmentation of MeOH extracts of TT01 pACYC_aratacl_stlF cultures induced with 0.2 % L-ara (a) and with supplementation of d₇-cinnamic acid (b) after 3 days cultivation at retention time of 6.4 min. While **a** shows the fragmentation of 402.227, **b** shows the MS² fragmentation of 402.227 (up) and 409.271 (below). Proposed fragmentation structures indicated with the dashed red line for an isoleucine-derived EPS-derivate as an example (c).

To distinguish between the incorporation of leucine and isoleucine, so called inverse feeding experiments with leucine and isoleucine were carried out (chapter 2.3.3). In the first step it was assessed if the production of the compound corresponding to 402.227 [M+H]⁺ was also accomplished in ¹³C-Isogro medium. Cultivation and extraction in the latter yielded a *m/z* shift of 23 to 425.303 [M+H]⁺ (Figure 43) which was expected due to the 23 C-atoms present in the proposed compound. In the next step the cultures

Results

were supplemented with either 1 mM leucine or isoleucine. For the incorporation of these amino acids, a shift of 6 was expected. In Figure 43 the successful incorporation for both amino acids was shown since both extracts yielded the expected shift to the signal of 419.284 [M+H]⁺.

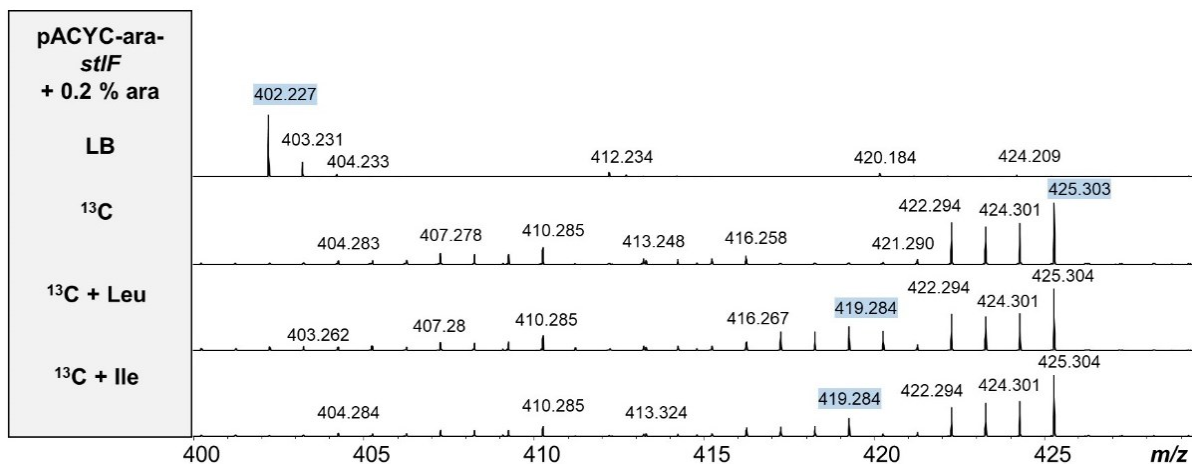


Figure 43. MS1 of induced TT01 pACYC_aratacl_sttF cultures in LB and ¹³C medium. The cultures cultivated in latter were also supplemented with 1 mM Leu and Ile in strain with, pACYC_aratacl_sttF with feeding of 1 mM Leu or 1 mM Ile feeding at retention time of 6 – 6.8. The signals of the leucine and isoleucine associated EPS derivatives are highlighted in blue.

Another signal which was also detected due to its fragmentation of 271.13 [M+H]⁺ was 420.184 [M+H]⁺ at retention times between 5.9 and 6.1 min. Feeding with d₇-CA resulted in a shift of 7 to a m/z of 427.228 [M+H]⁺. Due to the predicted sum formula of C₂₂H₂₉NO₅S the strain was tested on methionine incorporation. Therefore, the strain expressing sttF was cultivated and supplemented with d₃-methionine. A shift from m/z 420.184 to 423.192 [M+H]⁺ confirmed the incorporation of methionine into the stilbene derivative (Figure 44a). Similar to the leucine- and isoleucine-derivatives, the incorporation of methionine leads also to a Δ18 shift (from 420 to 402) indicating the same cyclization reaction (Figure 44b). Moreover, another further Δ14 shift can be observed resulting in an m/z of 388.212 [M+H]⁺ which can be linked to the loss of the methyl-group as a result of a further fragmentation (Figure 44b). This m/z was detected in the d₃-methionine as well as the non-supplemented culture since the cleaved off methyl-group was carrying the deuterated isotopes while the culture with d₇-CA exhibited 388.212 and the Δ7 shift to 395.255 [M+H]⁺.

Results

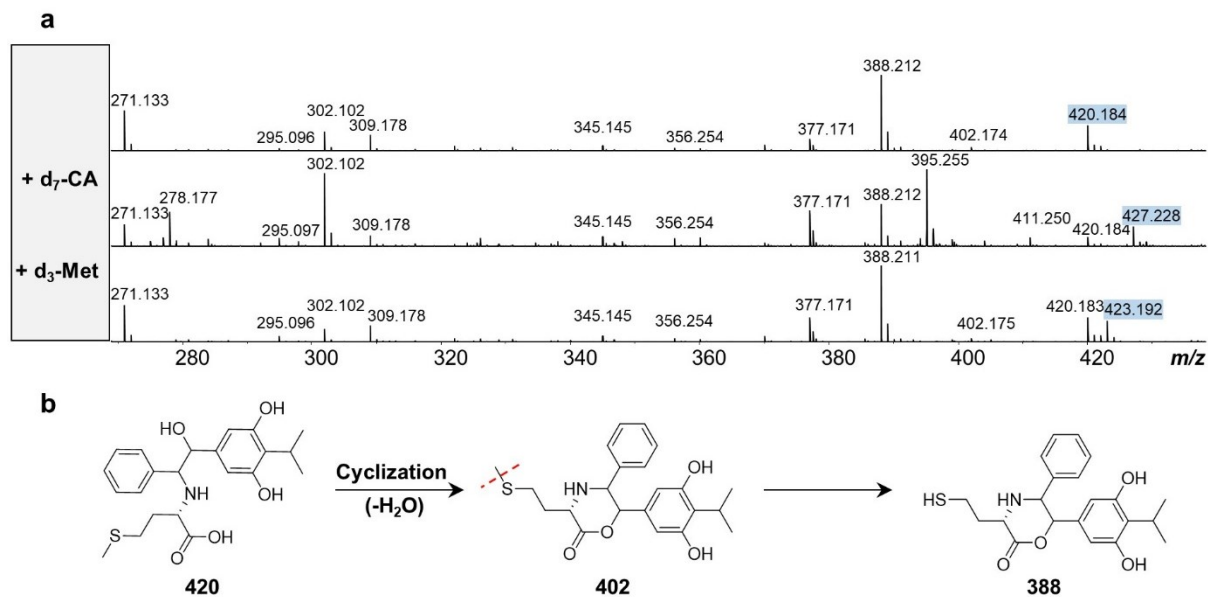


Figure 44. HPLC-MS BPCs of TT01 pACYC-aratacl-*stIF* induced with 0.2 % ara and with supplementation of d_7 -CA and d_3 -Met at a retention time of 5.9 - 6.1 min. The m/z of the shifted main masses are shown in blue (a). Proposed fragmentation structures indicated with the dashed red line (b).

On the basis of the d_7 -CA feeding experiments, it was also possible to detect further and even more complex EPS-derived molecules. Due to their typical MS-fragmentations, it was thus possible to determine the incorporated amino acids and peptides and even the peptide sequence without further feeding experiments.

Figure 45a and b show the MS²-fragmentations of the product derived from EPS moieties with the aromatic amino acids phenylalanine at m/z of 436 [M+H]⁺ and tryptophan at m/z of 475 [M+H]⁺. Both compounds cyclize as already shown for the leucine, isoleucine and methionine adducts (Figure 42 and Figure 44) resulting in 418 and 457 [M+H]⁺. Moreover, it was also possible to detect tetra- and penta-peptides. In Figure 45c the fragmentation of 709 [M+H]⁺ with the associated amino acid pattern is shown. The fragmentation corresponds to a sequence of P-I/L-P-I/L. However, it was not possible to determine whether leucine or isoleucine were incorporated since the measurements in ¹³C media (Figure 43) did not show that derivative. Another detected tetra-peptide-EPS-derivative resulted in an m/z of 758 [M+H]⁺ and exhibited an amino acid sequence of Q-P-P-F (Figure 45d). The last assignable tetra-peptide exhibited an m/z of 793 [M+H]⁺ that was associated with the sequence of P-F-P-Y as shown in Figure 45e. The strain also showed the incorporation of penta-peptides as displayed in Figure 45f where a signal of

874 [M+H]⁺ was observed and assigned to the sequence of P-E-V-P-Y. There were also even more derivatives with *m/z* of 800.42, 823.46 and 938.52 [M+H]⁺ that showed a shift in the d₇-CA supplementation experiments, but did not show any fragmentation and thus could not be analyzed (data not shown).

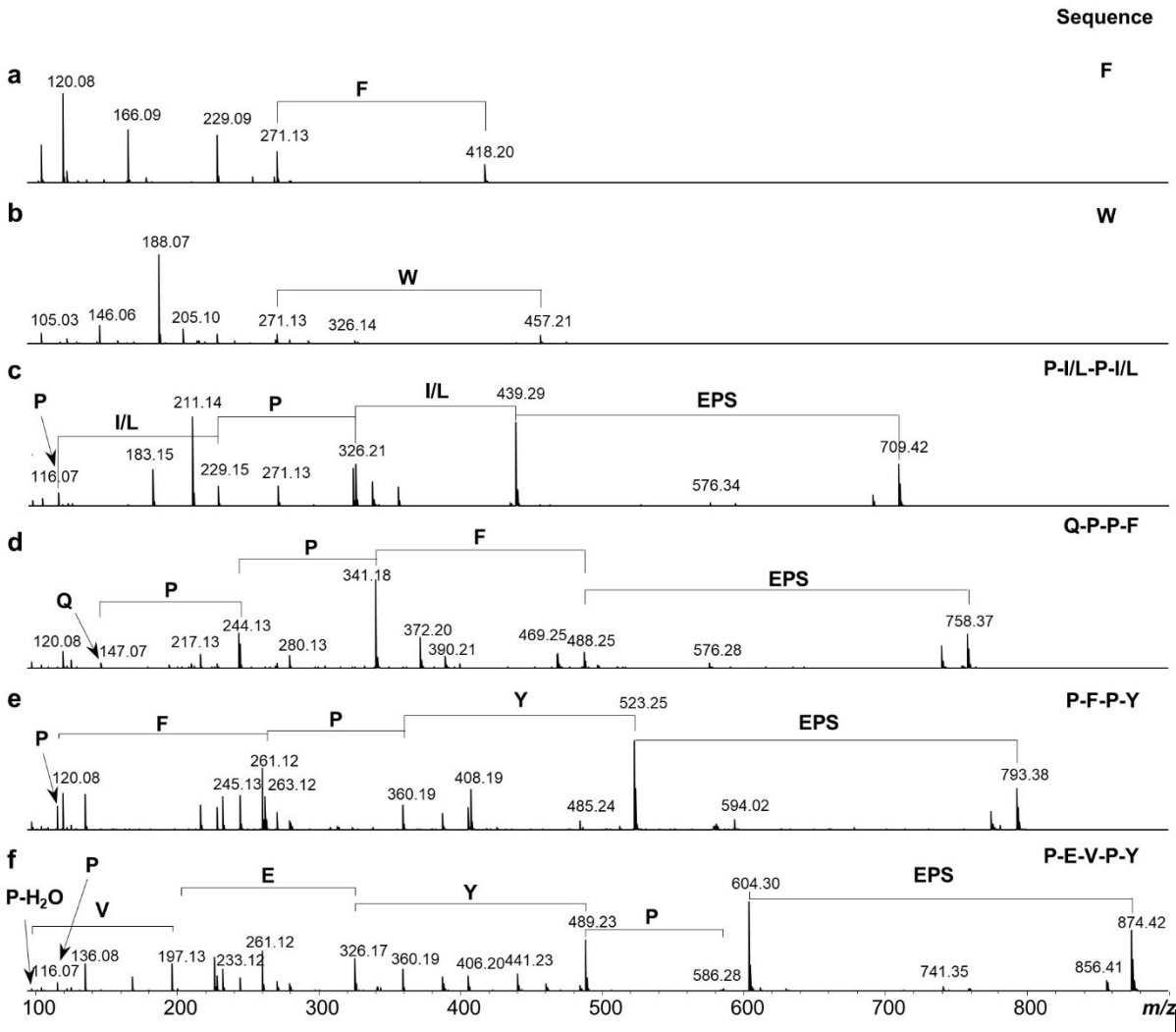


Figure 45. MS² fragmentation patterns of EPS derivatives from TT01 WT pACYC-ara-*stfI*/F MeOH extracts cultivated in LB for 3 days at 30°C. All shown derivatives eluted at retention times between 6.5 and 7.5 min. Fragmentation of 436 [M+H]⁺ corresponds to the phenylalanine derivative (a), 475 [M+H]⁺ to the tryptophan derivative (b). The tetra-peptide derivative of 709 [M+H]⁺ consists of the P-I/L-P-I/L sequence (c), the tetra-peptide sequences of 758 [M+H]⁺ and 793 [M+H]⁺ consisted of Q-P-P-F (d) and P-F-P-Y (e). The sequence of the penta-peptide EPS of 874 [M+H]⁺ derivative is P-E-V-P-Y.

3.3.2 *In vitro* reactions of epoxides with amino acids, peptides and proteins

The formation of EPS derived β -amino alcohol compounds was also investigated with *in vitro* approaches. However, although the purification of EPS yielded a compound with

Results

the expected m/z of 271.13 $[M+H]^+$ (Figure 46), the ^1H - (Figure S8) and ^{13}C -NMR (Figure S9) analysis revealed an already hydrolyzed derivative. The NMR data also ruled out any amino acid or peptide adduct.

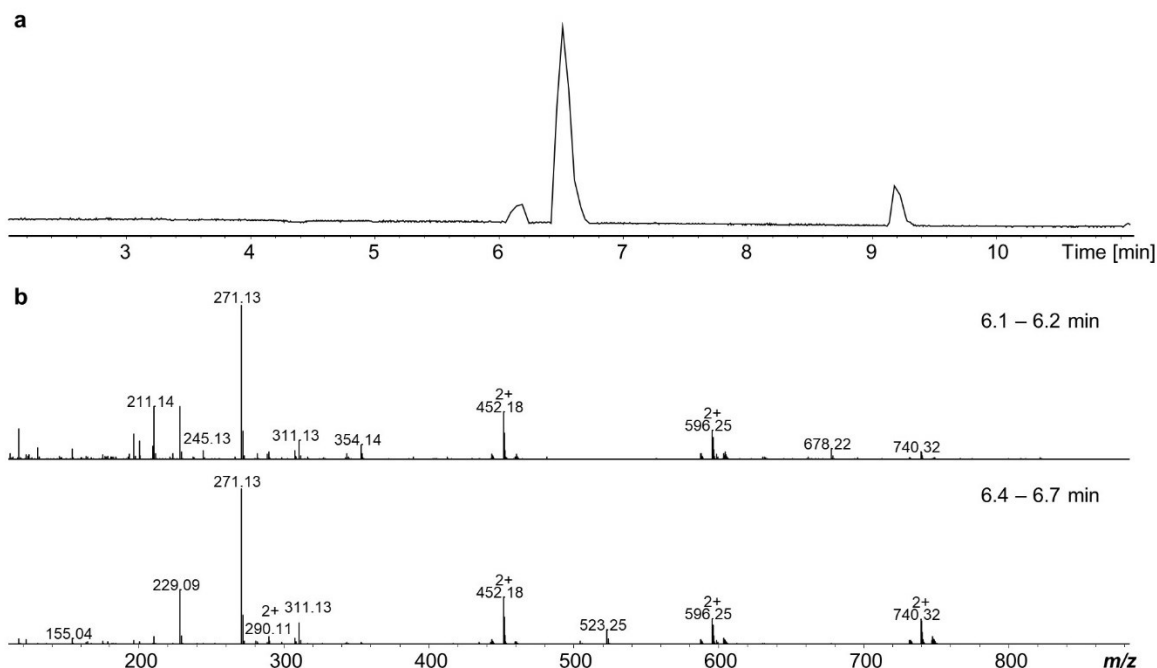


Figure 46. HPLC-MS analysis of a purified EPS-derivative fraction after cultivation of induced TT01 $\Delta antJ\Delta gxpS\Delta pliA$ pex *stlA/stlCDE* pACYC-*stlF* in 4 l PP3M with 2% XAD for 2 days. Purification was carried out in two steps via preparative and semipreparative HPLC-MS. The BPC (a) and the MS-spectra at retention times from 6.1 – 6.2 min and 6.4 – 6.7 min are shown (b). The signal at 9.2 min is an impurity caused by the HPLC-vials.

Since the purification of EPS was not successful, the reactions were carried out with two commercially available epoxides with structural similarities to EPS. In the first step lysine ($\text{C}_6\text{H}_{14}\text{N}_2\text{O}_2$, m/z of 147.11 $[M+H]^+$) was used due to its two potential modification sites with styrene oxide ($\text{C}_8\text{H}_8\text{O}$) and stilbene oxide ($\text{C}_{14}\text{H}_{12}\text{O}$) (Figure 47). For successful modifications, mass shifts of 120.05 for styrene oxide and 196.09 for stilbene oxide were expected. After two hours of incubation in an aqueous solution with 10 mM NaOH at 30 °C, HPLC-MS analysis showed the formation of two lysine derivatives with styrene oxide named compound **10** ($\text{C}_{14}\text{H}_{22}\text{N}_2\text{O}_3$, 267.17 $[M+H]^+$) and **11** ($\text{C}_{22}\text{H}_{30}\text{N}_2\text{O}_4$, 387.23 $[M+H]^+$) in Figure 47. The reaction was repeated with stilbene oxide which led to the modification of one amino-group of lysine that was named compound **12** ($\text{C}_{20}\text{H}_{26}\text{N}_2\text{O}_3$, 343.16 $[M+H]^+$). However, this reaction setup was not suited to give insights on the

position of the modification though. The assays were also performed with N ϵ -acetyl-lysine leading also to successful modifications for each epoxide (Figure S6). For the following reactions, the two peptides with the sequence SIYKAVA and its N-terminal acetylated form were synthesized via solid phase peptide synthesis (Figure S7 for the MS spectra of the acetylated peptide). Since lysine could be modified twice, the reactions with acetylated amino-groups were not further tracked for the next reactions. Therefore, only the SIYKAVA-peptide (compound **13**, C₃₅H₅₈N₈O₁₀) was used for the reaction with styrene and stilbene oxide. In Figure 47, the spectra for the peptide resulted in two signals amounting at 751.43 [M+H]⁺ and 376.22 [M+H]²⁺. Reactions with the respective epoxides yielded compound **14** (C₄₃H₆₆N₈O₁₁, 436.25 [M+H]²⁺) for the reaction with styrene oxide and compound **15** (C₄₉H₇₀N₈O₁₁, 474.27 [M+H]²⁺) for the one with stilbene oxide. Based on the MS²-fragmentation it was possible to assign the lysine-residue as the position of the modifications for each derivative. The fragment of compound **14** with *m/z* of 671.38 [M+H]⁺ corresponds to the loss of the dipeptide with the sequence SI (C₉H₁₈N₂O₃) resulting in a molecule with the sum formula of C₃₄H₅₀N₆O₈. An identical cleavage can be observed for compound **15**, resulting in a signal of 747.41 [M+H]⁺ associated with molecule with a sum formula of C₄₀H₅₄N₆O₈.

Results

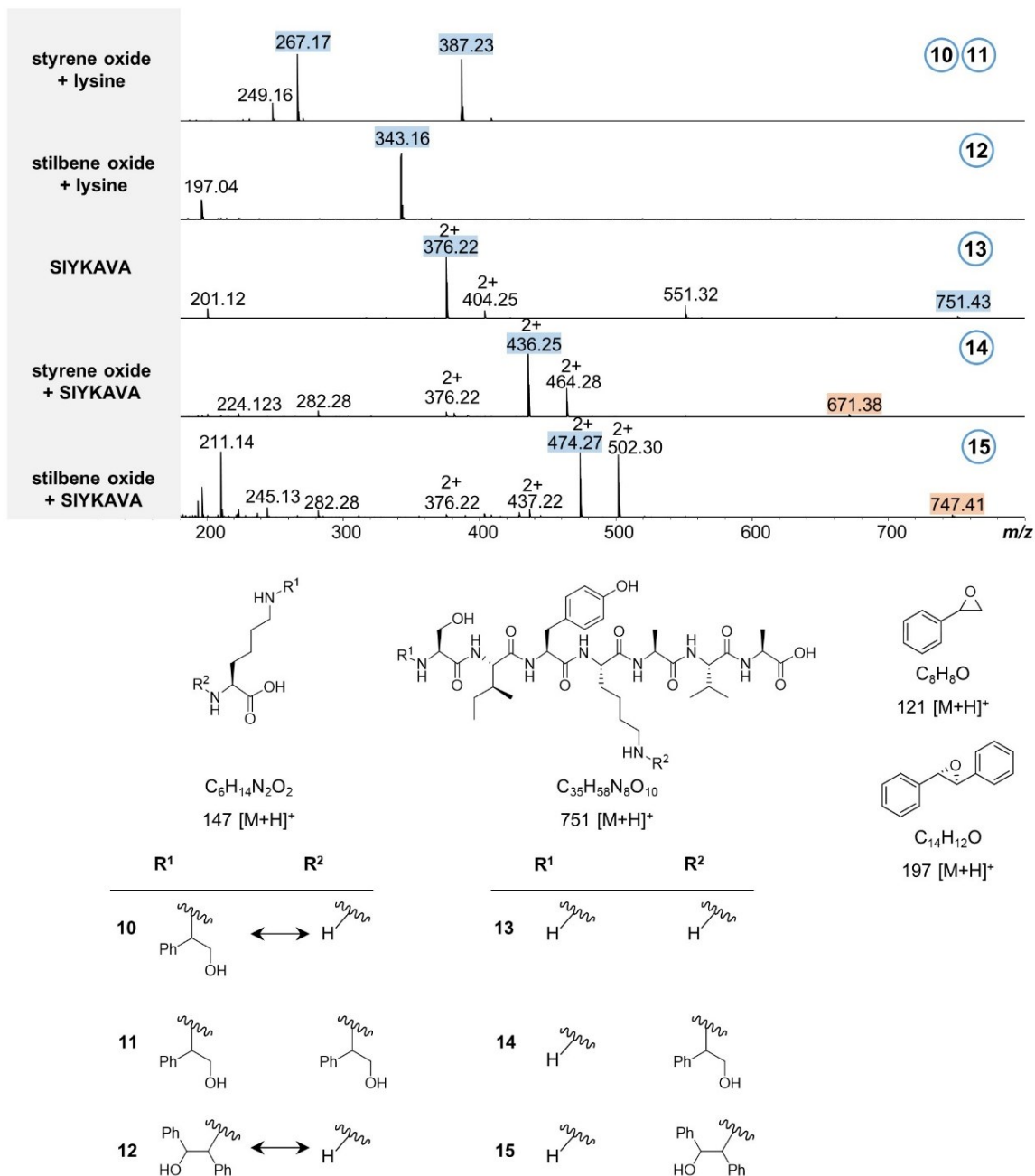


Figure 47. HPLC-MS analysis of the *in vitro* reactions with styrene oxide and stilbene oxide with lysine and the SIYKAVA-peptide. The m/z values of the generated β -amino alcohol containing moieties were highlighted in blue and assigned to the structures **10-15**. The arrows for structure **10**, **12**, **14** and **15** indicate an ambiguity regarding the position of the modification. The aqueous reaction setups containing 10 mM NaOH were incubated for two hours at 30°C. The reaction mixtures were measured on a C_{18} -column with retention times ranging from 4.5 to 4.6 min for the reactions with lysine and 5.5 to 6.2 min for the reactions with the SIYKAVA peptide. The signal for the peptide-epoxide adduct after the fragmentation of the SI-peptide was highlighted in orange.

After successful modification of amino acids and peptides with epoxides, it was evaluated whether it might also be possible to conduct such modification reactions with proteins. Based on the insights of those reactions, it could be assessed whether such reactions might also be likely in *in vivo* approaches. Due to the already established analysis and its small size with few potential modification sites, StIE was selected for the *in vitro* assays with styrene oxide and stilbene oxide. For the analysis, the *m/z*-values for StIE and the potential adducts were determined using *IsotopePattern* (Bruker) (Table 13).

Table 13. Sum formula and theoretical *m/z*-values for the ten-fold charge state of StIE and after the reactions with styrene oxide and stilbene oxide.

Sample	Sum formula	<i>m/z</i> [M+H] ¹⁰⁺
<i>apo</i> -	C ₄₇₀ H ₇₃₆ N ₁₂₀ O ₁₆₀ S ₃	1073.33
<i>holo</i> -	+ C ₁₁ H ₂₁ N ₂ O ₆ PS	1107.34
acetyl-	+ C ₁₃ H ₂₃ N ₂ O ₇ PS	1111.54
styrene adduct	+ C ₈ H ₈ O	1085.34
stilbene oxid adduct	+ C ₁₄ H ₁₂ O	1092.94

The ten-fold state of charge of StIE showed mostly a *m/z* of 1073.33 [M+H]¹⁰⁺ indicating the *apo*-state of StIE (Figure 48a). Besides, also the *holo*- (1107.34 [M+H]¹⁰⁺) and the acetylated-state (1111.54 [M+H]¹⁰⁺) were detected. The reaction with styrene oxide yielded an *m/z* of 1085.34 [M+H]¹⁰⁺ and thus a successful modification (Figure 48b). The reaction mixture also showed a signal for 1092.34 [M+H]¹⁰⁺ which could not be assigned. The reaction setup containing stilbene oxide (Figure 48c) showed an *m/z* of 1092.94 [M+H]¹⁰⁺ confirming a modification of a StIE-moiety with stilbene oxide. Further signals also present in all three measurements were 1074.85 [M+H]¹⁰⁺ and 1081.93 [M+H]¹⁰⁺ indicating other modifications of StIE. Although the *m/z* of 1081.93 [M+H]¹⁰⁺ can be seen only in Figure 48c, it was also present in the other two measurements when visualized with an EIC (not shown).

Results

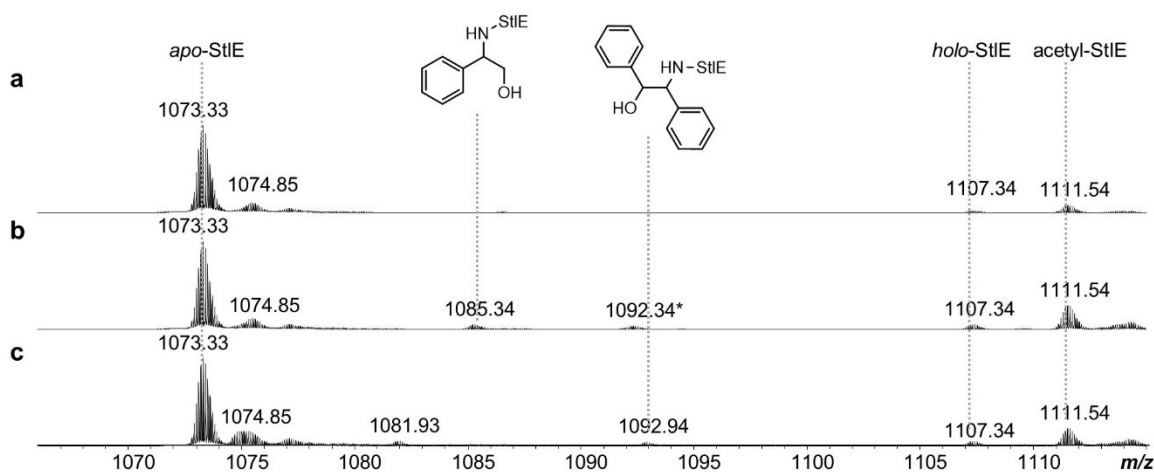


Figure 48. HPLC-MS analysis of StIE after *in vitro* reactions with styrene oxide and stilbene oxide. Purified apo-StIE has a m/z of 1073.33 $[M+H]^{10+}$ while its holo-state amounts at 1107.34 $[M+H]^{10+}$ and acetyl-StIE at 1111.54 $[M+H]^{10+}$ (a). Modifications with styrene oxide (b) and stilbene oxide (c) amounted at 1085.34 $[M+H]^{10+}$ and 1092.94 $[M+H]^{10+}$. The reaction was incubated for two hours at physiological pH and measured on a C₃-column. Shown are the retention times from 9.4 to 11.5 min. Signals with asterisk could not be assigned.

The EIC of 1085.34 visualized in Figure 49a shows two signals at 10 and 11.3 min for the styrene modified StIE indicating two different reaction sites. It was also possible to detect an additional signal between 9.6 and 10 min for the acetylated StIE carrying one styrene moiety which was shown in in Figure 49b for the EIC of 1123.54.

Results

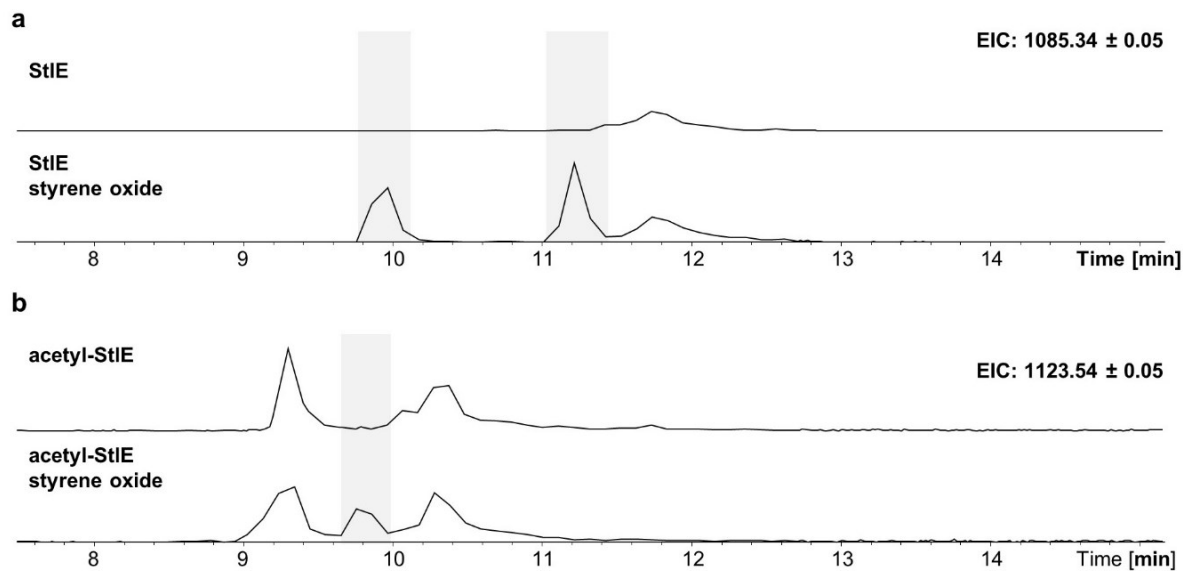


Figure 49. HPLC-MS chromatograms of *in vitro* reactions of StIE with styrene oxide. Shown are the EICS for 1085.34 $[M+H]^{10+}$ and 1123.54 $[M+H]^{10+}$ corresponding to the styrene modified *apo*- and acetyl-StIEs. The reaction was incubated for two hours at physiological pH and measured on a C_3 -column. Shown are the retention times from 7.5 to 15.2 min.

4 Discussion and outlook

4.1 Topic A Biosynthetic characterization of stilbene related pathways

4.1.1 Biosynthesis of stilbenes

Stilbenes are typically produced by plant based PKS III systems which are generated by iterative elongation reactions followed by cyclization and aromatization. Bacterial stilbenes are of special interest for natural product research. IPS which is the best known derivative of this PKS II derived NP class is used as a drug against psoriasis. In contrast to plant derived stilbenes, IPS and its derivatives are formed by two routes in the biosynthetic pathway and exhibit a characteristic iso-branch which is generated by the BKD-pathway. Thereby isovaleryl-CoA is elongated in a Claisen condensation reaction and the subsequent β -ketoacyl product is cyclized with a Michael acceptor derived from the CA-dependent synthesis route. The latter involves the transfer from phenylalanine to CA by the PAL StIA which is then processed by StIB to the corresponding CoA-moiety. The fatty acid synthesis enzymes for the subsequent Claisen condensation, the reduction and dehydration steps for the formation of the Michael acceptor 5-phenyl-2,4-pentadienoyl-StIE were identified in my master thesis, but the heterologous production was not successful and thus the mechanism not verified¹¹⁹.

4.1.1.1 FabH specificity

In a systematic approach all fatty acid related KS domains (FabH, FabF and FabB) of *P. laumondii* and *E. coli* were assessed *in vitro* with CoA and ACP loaded CA-moieties (Figure S1 supplementary information). However, only pIFabH was able to accept and elongate the CA-moiety although alignments of pIFabH with ecFabH showed a 73 % sequence identity. The β -ketoacyl-StIE is then further processed by the KR FabG and the DHs FabA or FabZ to generate 5-phenyl-2,4-pentadienoyl-StIE (Figure 17). While the expression of *stlBCDE* with *bkdABC* supplemented with CA did not result in the production of IPS in *E. coli*, the co-expression with *plfabH* complemented the heterologous IPS production (Figure 18). These insights led to the proposed extension of the IPS biosynthesis pathway illustrated in Figure 50.

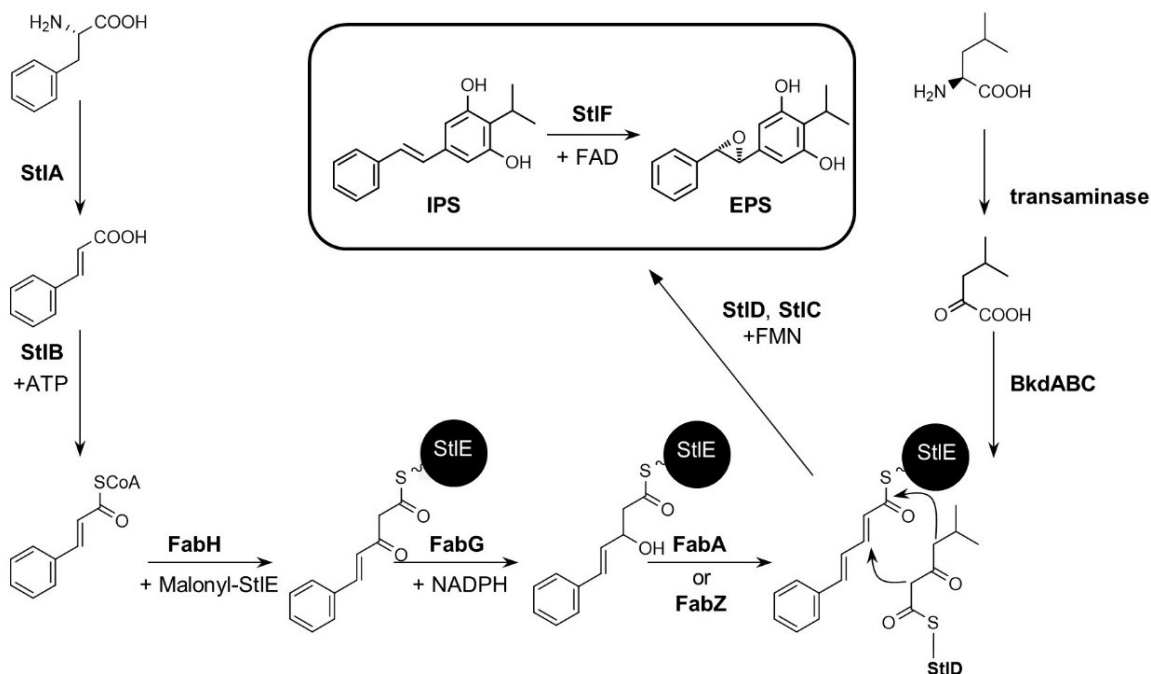


Figure 50. Extended biosynthesis of stilbenes in *Photorhabdus*. BkdABC = branched-chain- α -keto acid dehydrogenase with ketosynthase (*plu1883-1885*), StIB = CoA ligase (*plu2134*), StIC = aromatase (*plu2163*), StID = ketosynthase/cyclase (*plu2164*), StIE = acyl-carrier protein (*plu2165*), StIA = phenylalanine ammonium lyase (*plu2234*), StIF = monooxygenase/epoxidase (*plu2236*), FabH = ketosynthase (*plu2835*), FabG = ketoreductase (*plu2833*), FabA = dehydratase (*plu1772*), FabZ = dehydratase (*plu0683*).

In vitro and *in vivo* data showed a discrimination of substituted precursors in *para*-position for pIFabH. Hence, it was not possible to incorporate substrates like coumaroyl-CoA in order to produce isopropyl-resveratrol. Besides FabH, StIB does also not accept such substrates as has been shown in the data of the publication “*Biosynthesis of the Multifunctional Isopropylstilbene in Photorhabdus laumondii Involves Cross-Talk between Specialized and Primary Metabolism*” (subsequent experiments conducted by Dr. Gina Grammbitter, chapter 7 of this thesis). However, these data also showed an acceptance of 3-substituted CA derivatives for StIB. This led to the hypothesis that pIFabH might also accept such substrates. Therefore, several CA with substitutions in *meta*- and also in *ortho*-position were fed to a CA deficient *P. laumondii* strain (ARs77 strain) which was also deficient to produce various other compounds (kolossin, GameXPeptides, phurealipids, rhabdopeptides, glidobactins, odilorhabdins and AQs) for a SM free background. While supplementation with hydroxyl and nitro groups did not result in any new compounds (not shown), feeding with halogen substituted CA-derivatives in *meta*-

position yielded two new UV-active signals for each substrate (Figure 20). HR-MS analysis led to the prediction of 3-chloro- and 3-bromo-IPS, while the two other compounds with stronger UV-signals did not ionize in the positive polarization mode. Therefore, the measurement was repeated applying negative ionization which is better suited to detect halogens or acids. The measurement led to the ionization of the compounds and to sum formula and structure predictions. The proposed structures are also shown in Figure 51, but need to be purified and verified via NMR since no chemical standard was commercially available for 5-(3-chlorophenyl)penta-2,4-dienoic acid or for 5-(3-bromophenyl)penta-2,4-dienoic acid.

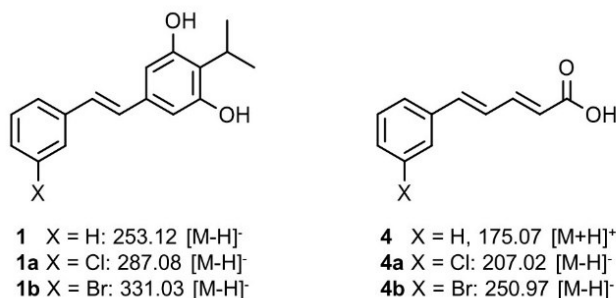


Figure 51. Structure predictions of halogenated IPS- and 5-penta-2,4-dienoic acid derivatives.

Feeding of pure CA also led to the accumulation of 5-phenyl-penta-2,4-dienoic acid, but yielded around four-fold more IPS than the halogen substituted IPS derivatives. The low amount of halogenated IPS derivatives leads to the hypothesis of a lower affinity or kinetic slowdown of the KS/cyclase StID towards the halogen substituted intermediates since the produced acids are similar to the Michael acceptor needed for the cyclization. Since neither of the three detected acids has been described so far, the mechanism can thus only be hypothesized. Since the biological function of 5-phenyl-penta-2,4-dienoic acid is unknown, it can only be speculated whether it is a shunt product of the biosynthesis due to accumulation or is reduced specifically by a TE domain to gain the respective acid. However, aminated derivatives of 5-phenyl-penta-2,4-dienoic and its *meta*-chloro-substituted derivative have been reported regarding their activity as antimalarial agents¹³³.

Halogenation of drugs and drug candidates is a method to enhance its binding affinity as a ligand to receptors, its membrane permeation and to extend its half-life *in vivo*^{134,135}. Especially chloro-substituted organohalogens are most prevalent with 57 % of all launched halogen substituted drugs¹³⁶. It can be hypothesized that also fluoro-substituted CA-derivatives could be incorporated since it has a smaller radius than chlorine or bromine and thus would cover almost 97 % of all approved organohalogene drugs¹³⁶. Therefore, it would be worthwhile to generate and purify these halogen-IPS compounds and assess the impact on the already known biological characteristics of IPS in the symbiont-nematode complex as well as its influence as a drug against psoriasis and as an insect pathogen.

4.1.1.2 CA-catabolism

Although the hydroxyl-group is smaller than the halogens, it was not implemented in the biosynthesis of another IPS derivative. The lack of 3-hydroxy-IPS after supplementation of 3-hydroxy-CA can be explained on the basis of the CA metabolism which was illustrated in Figure 52. CA can be catabolized by enzymes encoded by the *hca* operon (*plu2204-2209* in *P. laumondii*) and by *mhpA-C* (*plu1437*, *plu2208* and *plu2202*) in order to feed the glycolysis and the citrate cycle¹³⁷. MhpA catalyzes, among other reactions, also the conversion from 3-hydroxy-CA to 2,3-hydroxy-CA that can be further processed to fumarate and 2-hydroxypenta-2,4-dienoic acid within two steps by MhpB and MhpC (Figure 52)¹³⁷. While fumarate enters the citrate cycle directly, 2-hydroxypenta-2,4-dienoate is further processed by the 2-keto-4-pentenoate hydratase MhpD (*plu4413*) and the oxaloacetate decarboxylase MhpE (encoded by *plu4081*) to pyruvate and acetaldehyde¹³⁷. While the former is utilized for glycolysis, the latter is used by the acetaldehyde dehydrogenase MhpF (*plu2086*) for the conversion to acetyl-CoA which is also used as a substrate for the citrate cycle¹³⁷. In order to expand the product spectrum, it might be promising to knockout *mhpA* and *mhpB* and supplement the cultures with 3-hydroxy-CA to produce either 3-hydroxy-IPS or 2,3-hydroxy-IPS.

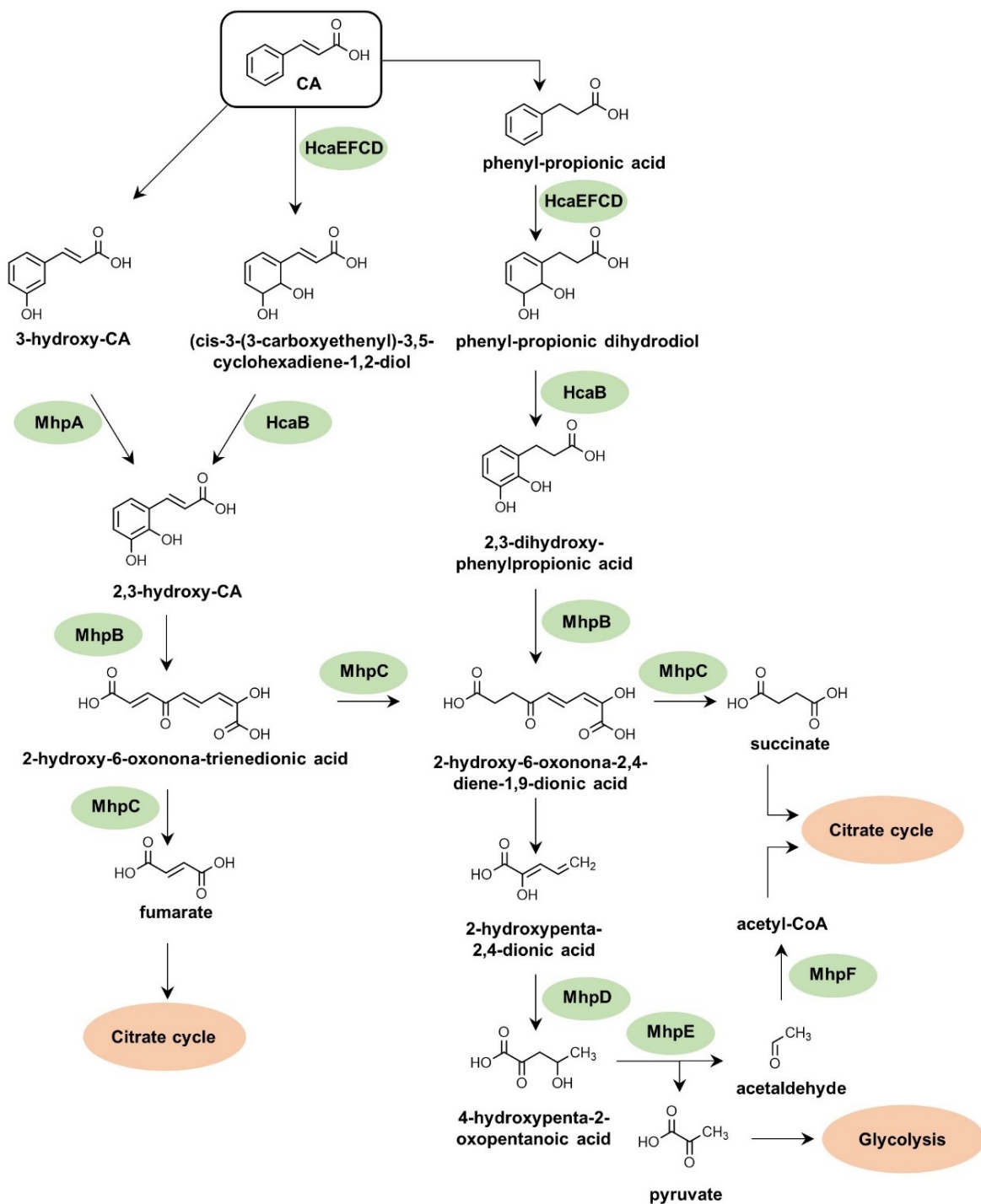


Figure 52. Metabolic pathway of the cinnamic acid catabolism from *P. laumondii* feeding the citrate cycle and the glycolysis. In green caption are the enzymes for the respective reaction while the orange ones show the entry of substrates into another metabolic pathway. Reactions without enzymes as the formation of 3-hydroxy-CA and phenyl-propionic acid are not catalyzed by *Photorhabdus*. Pathway adapted from KEGG (Kyoto Encyclopedia of Genes and Genomes)¹³⁷.

4.1.1.3 Protein-protein interaction of stilbene related genes

Type II carrier proteins from PKS and FAS systems are formed by four alpha helices. The role of helix II is to mediate interactions with other proteins⁵⁸. StIE and AcpP (pIAcpP) from TT01 share a sequence identity of 55 % and of even 80 % in the recognition helix (s. Table S2 for alignments) which might be a reason why both share similar interaction partners like FabH, FabG, FabA, FabZ and StIB which are both able to incorporate fatty acid and stilbene precursor molecules. Alignments with AntF, another ACP from *Photorhabdus* involved in AQ biosynthesis, with the recognition helices of the two mentioned ACPs showed significantly lower identities (27 % to StIE and 33 % to AcpP) with even lower general sequence identities for the whole sequences of 21 % and 23 % (Table S2). The identity between StIE and ecAcpP (*E. coli* derived AcpP, Figure S1) is in the same range as the one to pIAcpP (60 % for the whole protein, 80 % for helix II) which might be the reason for the activation of heterologous produced StIE in *E. coli* by the endogenous PPTases rendering NgrA expendable.

The amino acid sequences of FabHs from *E. coli* and *Photorhabdus* strains were aligned in Table S3. In accordance with the work of the Burkart and Appelt group 4 different FabH isozymes regarding their substrate specificity from *E. coli* (acetyl-, propionyl-CoA), *P. laumondii* (acetyl-, CA-CoA), *Streptomyces* sp. R1128 ((iso)-butyryl-, propionyl-, acetyl-CoA) and *Mycobacterium tuberculosis* (lauroyl-, myristoyl-, palmitoyl-CoA) have been analyzed (Figure 53) to explain the specificity of pIFabH towards CA-CoA¹³⁸⁻¹⁴⁰. Since pIFabH has not been crystallized so far, an AlphaFold structure prediction was utilized. The structures of the used ecFabH and mtFabH were co-crystallized with CoA or lauroyl-CoA^{141,142}.

In the first step, the four FabH isozymes were superposed in order to compare their respective substrate binding sites (Figure 53). The β -chain of the dimeric *E. coli* and *P. laumondii* isozymes exhibits Phe87' while *M. tuberculosis* and *Streptomyces* sp. R1128 showed a Thr-residue in the corresponding position (Thr87' and Thr96') enabling more space in the active site. While the acyl-chain is on one site narrowed by Phe87', the opposite site is constricted by Leu142 in *E. coli* and *M. tuberculosis* and by Met151 in *Streptomyces*. *Photorhabdus* utilizes an Ile142 in this position extending the diameter of

the channel due to the shift of the methyl-group in the side chain. The constriction might explain the discrimination of ortho-substituted phenyl-rings while there are gaps for the incorporation of meta-substituted derivatives.

In the β -chain of pIFabH, Arg196' protrudes into the pocket preventing the binding of longer acyl-chains as lauroyl-CoA, but might also sterically hinder the binding of para-substituted CA-derivatives. EcFabH also carries a rotated Arg196' residue compared to pIFabH, while mtFabH exhibits Ile196', opening a bigger cleft and favoring potential van der Waals interactions with hydrophobic acyl-chains¹⁴³. Leu191 from ecFabH and pIFabH also are in close proximity and hinder long chain acyl-chains to bind, while the corresponding Met-residue from ZhuH grants a slightly bigger gap. In mtFabH Gln191 is used that does not oppose the chain, since it is also rotated away from the lauroyl-chain.

One common aromatic interaction is the π stacking which is expected for the binding of CA-moieties. The only potential aromatic residue in proximity to the binding pocket is Tyr193 only occurring in pIFabH. However, with a distance of around 8 Å to the binding partner, it is not suited for these interactions which usually amount to around 3.5 Å¹⁴⁴.

Another characteristic between the isozymes can be observed at position 205 and 218 (corresponds to ZhuH). While pIFabH has the smallest side chain with Ala205 (pIFabH) the other enzymes exhibit branched amino acids like Leu205 (ecFabH), Val205 (mtFabH), Leu218 (ZhuH). Together with Phe87' and Leu191 as mentioned above, these residues lead to the formation of a narrow tunnel for *E. coli* with a diameter of less than 4 Å. Especially the additional isopropyl-group of the leucine-residue extends towards the direction where the phenyl-ring of CA is to be expected.

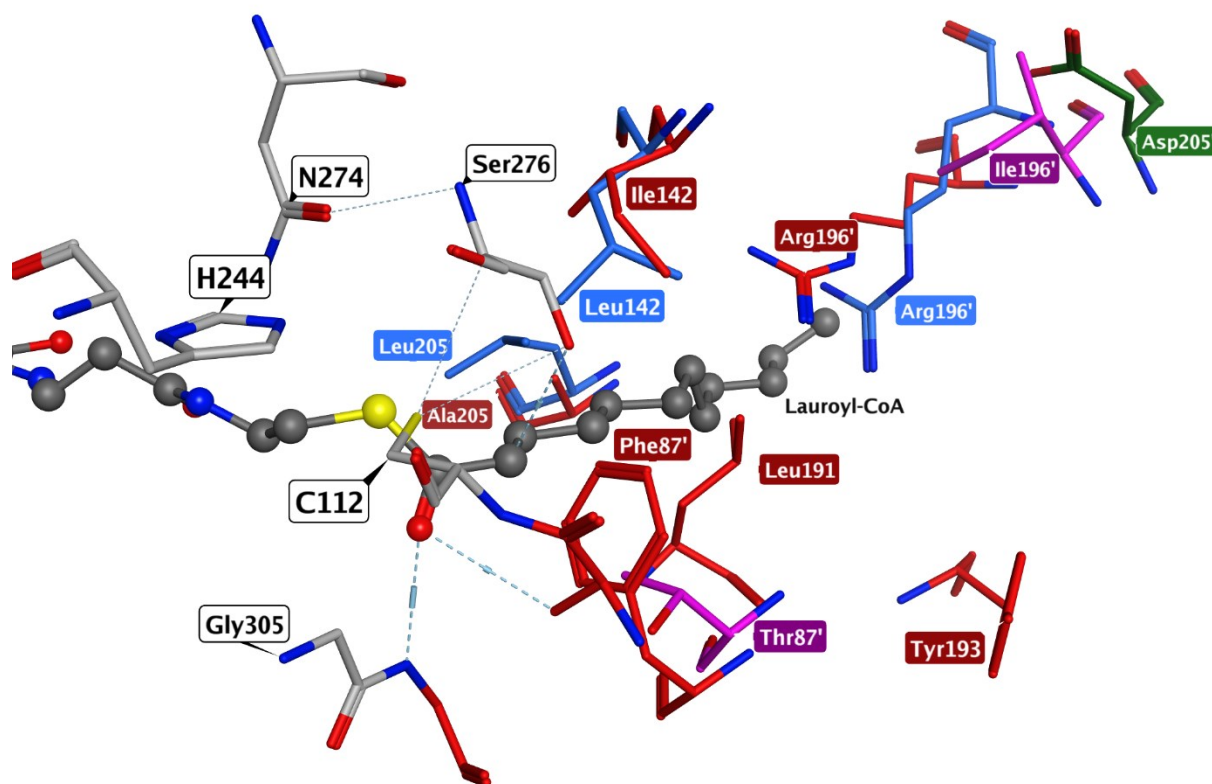


Figure 53. Visualization of the binding pocket of FabH homologs pIFabH (AlphaFold ID: A0A6L9J158), ecFabH (PDB: 1EBL), mtFabH (PDB: 1U6S) and ZhuH (PDB: 1MZJ) with bound Lauroyl-CoA co-crystallized with mtFabH. Conserved residues Ser276, Gly305 and the catalytic triade (shown in one letter code) C112, H244 and N274 are shown in grey. Residues from pIFabH are shown in red, ecFabH in blue, mtFabH in violet and ZhuH in green and influence the substrate specificities. Illustration generated with Molecular Operating Environment 2022.02.

In the next step CA-CoA was docked into the AlphaFold structure of pIFabH which was superposed with ecFabH (Figure 54a and b). The docking was carried out under the assumption of a rigid receptor. The model revealed a sterical hindrance of the phenyl-ring with Leu142 and Leu205 in the *E. coli* derived isozyme which was already predicted based on the model from Figure 53. While superposed, the distance between the leucine side chains and the aromatic ring amounted to distances lower than 0.2 Å. Another difference which could be observed due to the docking model is the orientation of the Phe87' in the β -chain. The rotamer of ecFabH points more towards the aromatic ring of CA in the binding pocket. With a distance of 1.62 Å it is closer to the aromatic ring of CA than the pIFabH derived one with 2.24 Å (Figure 54b). This leads to the hypothesis that the insertion of two point mutations at position 142 and 205 with isoleucine and alanine

might benefit the binding of CA-CoA in *E. coli*, but still retain a lowered efficiency compared to *Photorhabdus*.

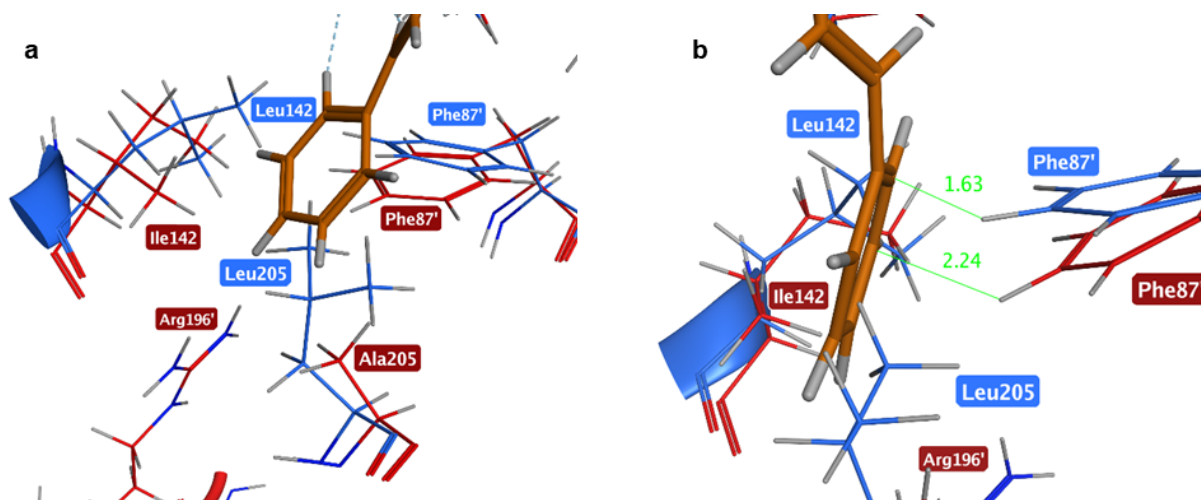


Figure 54. Docking of CA-CoA (shown in orange) to the AlphaFold structure of pIFabH (AlphaFold ID: A0A6L9J158, residues highlighted in red) and superposition with ecFabH (PDB: 1EBL, residues highlighted in blue) from two different angles (a) and (b). The values in (b) highlighted in green correspond to the distances (in Å) between the aromatic ring and the phenylalanine residues from the corresponding β -chains. Docking and illustration generated with Molecular Operating Environment 2022.02.

4.1.2 Hydrazines - N-N bond formation

To assess the role of StIB in the biosynthesis of stilbenes, feeding experiments with CA-SNAC were carried out in stilbene deficient *P. laumondii* strains ($\Delta stIA$, $\Delta stIB$ and $\Delta stIA\Delta stIB$). Previous data on StIB (described in Kavakli *et al.* in chapter 7, conducted by Dr. Gina Grammbitter) showed an ambiguity regarding its role in the biosynthesis since it showed poor turnover rates as a CoA-ligase for the transformation from CA to CA-CoA compared to its ability to generate fatty acid CoA moieties¹¹⁶. On the other hand, StIB exhibited characteristics of an acyl-acyl-carrier protein synthetase (AasS) enzyme as it was loading the CA moiety directly onto the *holo* form of the ACP StIE. However, since the next step of the biosynthesis involves FabH, which uses CoA-moieties as starter building blocks instead of ACP bound ones (opposed to the other KS enzymes FabB or FabF), these data seem contrary. The purpose of CA-SNAC feeding was to circumvent *in vitro* assays with StIB due to its low solubility, low stability and poor purification yields. The similar characteristics of CA-SNAC to CA-CoA and its membrane permeability should be able to mimic and replace the CoA derivative. Depending on the outcome of the feeding experiment regarding the production of **1**, potential new insights in the role of StIB

would have been possible. Although there has been complementation for the production of **1** for the $\Delta stlA$ strain, the $\Delta stlB$ and the $\Delta stlA\Delta stlB$ strains did not produce **1** (Figure S3). The production of **1** for the $\Delta stlA$ strain can be assigned to contaminations or impurities of the CA-SNAC with CA, as the latter was the educt for the chemical synthesis and small amounts still remained despite repeated purification and crystallization (carried out by Dr. Isam Elamri, Figure S3). *In vitro* data (Figure 22) showed the ability of pIFabH to accept CA-SNAC and utilizes it for the elongation to the β -ketoacyl derivative without any difference to the positive control which contained CA-CoA instead.

The failed complementation in the *in vivo* approach might be explained by a kinetically favored transformation of the SNAC moiety over the Claisen condensation step with pIFabH. Another explanation could be the earlier expression of the hydrazine biosynthesis genes regarding the cell density or life cycle of the bacteria than stilbene genes. In Figure 23 the formation of a compound with a m/z of 413.135 $[M+H]^+$ is shown which was assigned to a dimeric deacetylated CA-SNAC-derived compound that is linked with a nitrogen-nitrogen (N-N) bond and resulted in the formation of a hydrazine. Hydrazines and further molecules containing these N-N-bonds are also utilized in various clinical drugs like phenelzine or carbidopa (Figure 55a). N-N bonds can easily be incorporated into structures with organic synthesis, but there are also bacterial derived hydrazine molecules like cremeomycin, streptozocin or actinopyridazinones (Figure 55b)^{132,145}.

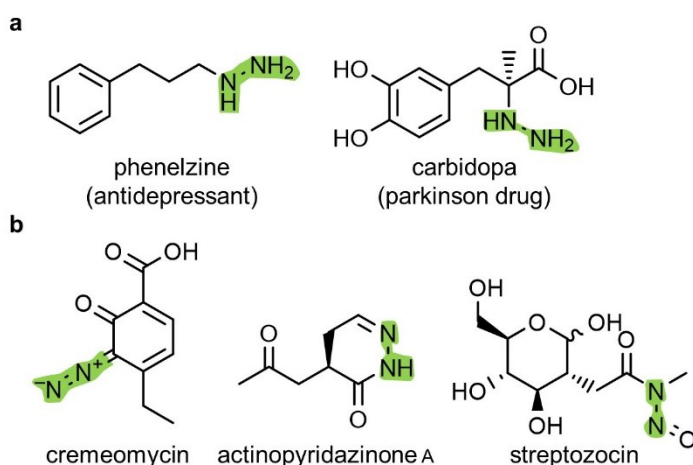


Figure 55. Chemical structures of N-N-bond containing drugs (a) and isolated natural products (b)^{132,145}.

However, the observation of hydrazine derivatives while feeding SNAC moieties which are often supplemented to cultures had not been documented so far, but there are cases when the SNAC was not able to replace the CoA thioester or bound carrier protein^{146,147}. Thus, *Photorhabdus* and *Xenorhabdus* strains are today the only known bacteria to be capable of these kind of SNAC transformation. The reaction also seems to be unspecific regarding the SNAC-substituent since four different SNAC molecules were observed to form those hydrazine structures and even heterodimers were detected for supplementation with two educts (Figure 24, compound 7). Recently a mechanism for the N-N formation dependent on zinc binding cupin enzymes was described by Zhao *et al.* by conducting *in vitro* assays¹³². In this study they showed the impact of a lysine/ornithine N-hydroxylase, a cupin protein and a methionyl-tRNA synthase (MetRS) homolog on the formation of the hydrazine bond. The lysine/ornithine N-hydroxylase derived L-N⁶-OH-lysine was processed with L-glutamate by ATP dependent condensation catalyzed by the MetRS-like domain to an unstable ester intermediate (Figure 56)¹³². In presence of the cupin domain the ester underwent an intramolecular arrangement and formed the N-N containing product by zinc-mediated cleavage of the N-O bond¹³².

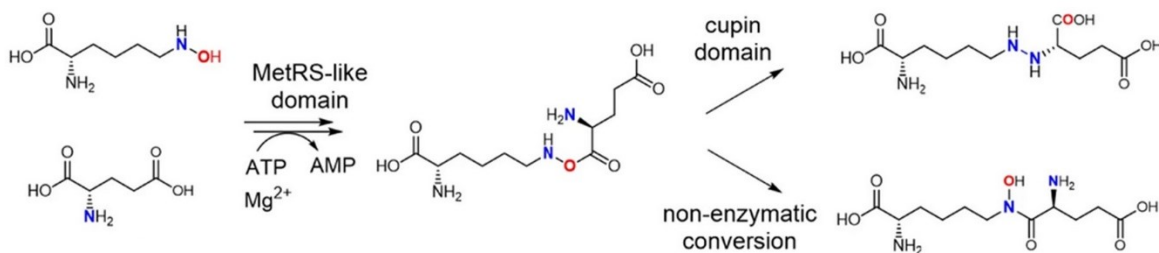


Figure 56. N-N-bond formation catalyzed by a zinc-dependent cupin enzyme after a MetRS-like domain induced condensation reaction between L-glutamate and L-N⁶-OH-lysine. Figure adapted from Zhao *et al.*, 2021¹³².

Therefore, these kind of cupin proteins were blasted against the genome of *P. laumondii* to assess a potential association with the dimeric SNACs although the reaction also probably involves a further deacetylase. The protein blast resulted in five potential cupin proteins. The genes encoding for those proteins were deleted via CRISPR/Cas12 (material and methods chapter 2.2.7). Feeding experiments with the deletion strains did not show any difference regarding the dimer formation though (Figure 26).

Since it was not possible to determine the enzymes related to the formation of the hydrazine derivatives, a systematic approach is needed. A promising procedure is the preparation of a *Photorhabdus* or *Xenorhabdus* gene library which could be cloned into a heterologous host like *E. coli*. Such approaches were often successfully used to clone and express BGCs into heterologous hosts and discover new NPs or confirm biosynthetic pathways for molecules like the *Xenorhabdus* derived ambactin and xenolindicins or the *Streptomyces* derived antibiotics streptothricin and borrelidin¹⁴⁸⁻¹⁵⁰. Therefore, genomic DNA is cleaved with a restriction enzyme and a suitable cloning method (depending on the size of the cleaved fragments) is picked to fuse the DNA with a linearized vector¹⁴⁸. The newly assembled plasmids are then used for transformation of *E. coli* and used for cultivation¹⁴⁸. The cultures can then be supplemented with a SNAC thioester and analyzed through high throughput screening of the strains with UV-MS due to the aromatic character of the used CA-SNAC. If the hydrazine formation is observed, the plasmid is extracted and then sequenced in order to find the involved genes. Another alternative to find the involved genes is transposon mutagenesis. Hereby, genes within the genome of the *Photorhabdus* or *Xenorhabdus* strains would be disrupted via insertion. Therefore a plasmid is needed which encodes a transposase, a machinery for replication in the donor strain and transfer by conjugation and an antibiotic resistance for the screening of the mutated strains^{151,152}. Afterwards the clones need to be screened analogously to the approach with the heterologous library.

Besides determining the involved enzymes in the formation of the N-N-bond, it would also be interesting to understand the chemistry of this reaction. Therefore, the substrate promiscuity shown with the different SNAC-derivatives needs to be assessed. This could be achieved by synthesising and supplementing the cultures with similar molecules which lack the thioester-group like 2-acetamidoethyl acetate or N-(4-oxopentyl)acetamide (Figure 57).

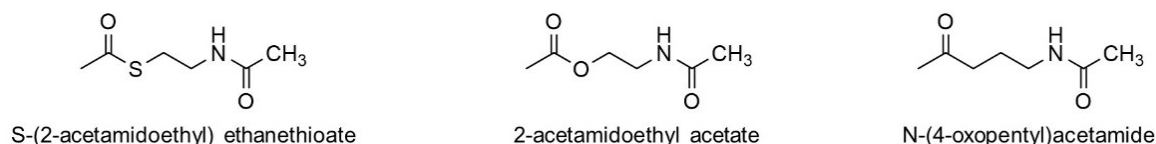


Figure 57. Potential compounds to investigate the substrate promiscuity associated with the hydrazine-formation of SNACs.

4.1.3 Biosynthesis of benzylideneacetone

BZA is the most potent phospholipase A_2 inhibitor from *Photorhabdus* and *Xenorhabdus* strains, but its biosynthesis remained unknown so far⁴⁶. Similar to IPS, it also inhibits the catalytic activity of the PO and thus the immune-required melanization in insects^{110,153}. The core structure of BZA resembles the one of L-3,4-dihydroxyphenylalanine which is the natural substrate of PO and hence acts as a competitive inhibitor¹⁵³. BZA has already been purified from *Xenorhabdus nematophila* and *Photorhabdus temperata* which produced 11.2 and 12.3 $\mu\text{g/l}$ by the Kim lab⁴⁶. Besides those two strains, similar inhibition of the phospholipase A_2 was also observed for *P. laumondii*, *Xenorhabdus bovienni* and *Xenorhabdus poinarii* leading to the hypothesis of BZA production for every *Photorhabdus* and *Xenorhabdus* strain⁴⁵.

In this work the *in vitro* and heterologous production of BZA derived by enzymes from *P. laumondii* have been shown (Figure 28) and thus a pathway for the biosynthesis was elucidated and proposed (Figure 58). Therefore, *stlB*, *stlE* and *plfabH* were expressed in *E. coli* DH10B leading to the production of 1.84 ± 0.15 mg/l BZA. This is a significant increase of production compared to the production titers of *X. nematophila* and *P. temperata*⁴⁶.

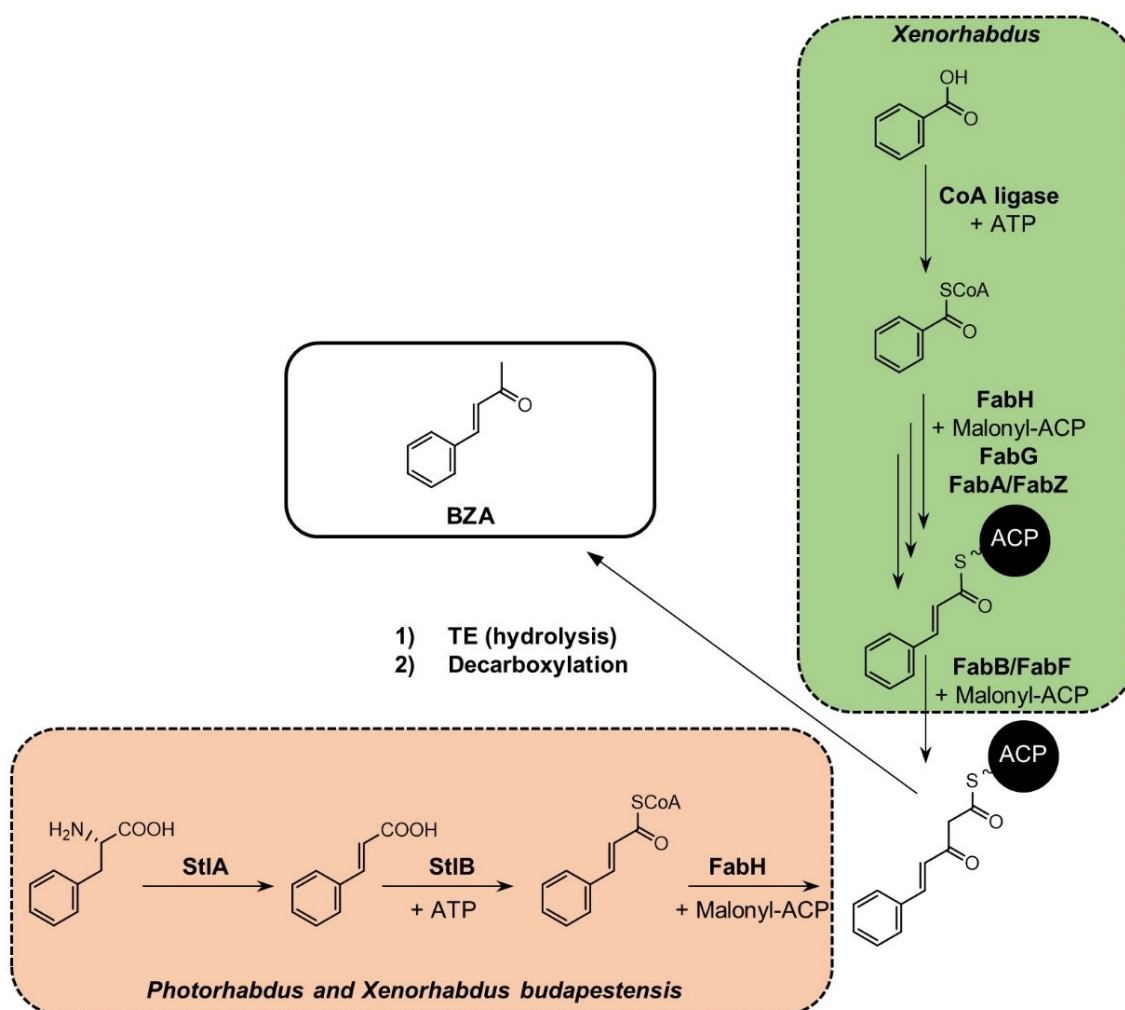


Figure 58. Proposed pathways for the biosynthesis of BZA in *Photorhabdus* (highlighted in orange) and *Xenorhabdus* (highlighted in green) strains. *X. budapestensis* is proposed to share the same mechanism as the *Photorhabdus* strains and hence was included to the pathway of *Photorhabdus* strains.

The biosynthesis pathway was associated with some enzymes responsible for the stilbene biosynthesis. Similar to the synthesis of IPS, CA generated by StIA is needed which is then processed by StIB to CA-CoA. This is then loaded onto an ACP which transports the CA-moiety to FabH for one elongation reaction with MCoA. In contrast to the synthesis of stilbenes, the reaction is then terminated. Although stilbenes are a *Photorhabdus* exclusive biomarker and thus are not produced by *Xenorhabdus* strains the latter encode similar genes which were shown to be involved in the biosynthesis of BZA. BlastP of StIA, StIB and FabH resulted in hits for *Xenorhabdus* strains with around 80 % identity for these genes. While the sequence identities for StIB homologs range from

82 to 84 % for various *Xenorhabdus* strains (Table 14 and alignment Table S6), they expressed around 80 % identities for FabH (Table 14 and alignment in Table S4). *X. budapestensis* is the only *Xenorhabdus* strain exhibiting a high identity (88 %) for the PAL StIA, thus enabling the strain to produce CA. Additionally, *X. budapestensis* exhibits a 31 % sequence identity for a histidine ammonia lyase (HAL) which was also present in the other *Xenorhabdus* strains (alignment in Table S5). Therefore, it can be hypothesized that it shares the identical pathway for the biosynthesis of BZA as *Photorhabdus* strains. However, it must be assessed whether FabH of *X. budapestensis* is able to accept CA-CoA as the isozymes from *Photorhabdus* since all *Xenorhabdus* FabH enzymes exhibit a valine-residue at position 205 instead of alanine (Table S4).

For the other *Xenorhabdus* strains, the precursor might be benzoic acid (BA) derived since these organisms are known for the production of BA derivatives. If BA-CoA is utilized as a precursor for BZA, it has to undergo two Claisen condensations with MCoA (Figure 58). There should not be a potential sterical hindrance regarding position 205 in FabH due to the smaller size of the proposed benzoyl-moiety in comparison to the cinnamoyl-moiety. Regarding the second Claisen condensation, the KS FabB or FabF might be involved in the elongation step, as otherwise the generated CA moiety has to be removed from the ACP and activated again as a CoA thioester. Since *X. budapestensis* is however the only *Xenorhabdus* strain producing CA, such a mechanism can be ruled out. The BlastP (against the NCBI database) of StIE yielded high sequence identity hits for *Photorhabdus*, while for *Xenorhabdus* the best hits were found for AcpP (identity of 57 %) since they do not encode the *stlCDE* operon. Therefore, it is concluded to be the most likely that AcpP, which represents the ACP of the fatty acid biosynthesis, is sufficient for the biosynthesis of BZA in *Xenorhabdus*. Regarding derivatives, at least the *Photorhabdus* and *X. budapestensis* derived pathway offers the opportunity to incorporate halogen substituted benzylideneacetones.

Table 14. Comparison of sequence identities of StIA-, StIB- and FabH-homologs from *P. laumondii* TT01 generated from BlastP (against NCBI-database) of several *Photorhabdus* and *Xenorhabdus* strains.

Organism	StIA [%]	StIB [%]	FabH [%]
<i>P. laumondii</i> TT01	100	100	100
<i>P. bodei</i>	97.9	98.9	98.7

<i>P. temperata</i>	92.3	93.9	93.4
<i>P. thracensis</i>	92.9	93.9	93.1
<i>P. asymbiotica</i>	89.5	92.9	92.4
<i>P. australis</i>	88.7	93.7	93.1
<i>X. budapestensis</i>	87.6 (PAL) 31.3 (HAL)	83	78.5
<i>X. cabanillasii</i>	30.2	84.1	78.6
<i>X. indica</i>	29.1	84.1	77.9
<i>X. nematophila</i>	28.8	83.2	80.4
<i>X. szentirmaii</i>	28.6	82.9	79.2

For the proposed shared pathway between *Photorhabdus* and *X. budapestensis*, the already established heterologous production in *E. coli* (Figure 28) needs to be tested with the isozymes from *X. budapestensis*.

In order to identify the alternative BZA-biosynthesis pathway in *Xenorhabdus* strains a sufficient CoA ligase or AasS has to be determined. Assuming that the biosynthesis requires a benzoyl moiety, the StIB-homologs can be ruled out as CoA ligases since it was not possible to detect the formation of benzoyl-CoA (as shown in chapter 7 of this thesis)¹¹⁶. However, the AasS activity of this enzyme towards benzoic acid was not tested so far. *In vitro* assays in the work of Grammbitter *et al.* showed the AasS ApeH of the arylpolyene BGC from *X. doucetiae* which catalyzed the formation of benzoyl-ACP¹⁵⁴. Nevertheless, in the same work it was shown that this cluster is not present in *X. nematophila* which is the most described *Xenorhabdus* strain regarding the application of BZA^{45,46,155,153}.

To elucidate whether the enzymes of the fatty acid biosynthesis can produce BZA, it would be appropriate to purify FadD (fatty acid CoA ligase) and FabH from *X. nematophila* and carry out *in vitro* assays for the production and elongation of benzoyl-CoA. Depending on the result it might be useful to clone the fatty acid associated genes (*fadD*, *fabH*, *fabF*, *fabB*, *fabG*, *fabA*, *fabZ*) via Golden Gate assembly onto one plasmid and transfer them into *E. coli* for a heterologous production. Another option would be to delete every gene associated with the CoA ligases in the genome of *X. nematophila* (Table 15) and measure

the production. However, in this approach the detection of BZA is more challenging than in the heterologous production, due to the low production titers in the WT and therefore purification steps would be required. Since the CoA ligases from Table 15 seem to be associated with the primary metabolism, it might not be possible to delete them and therefore it might be reasonable to clone these genes also onto a plasmid and combine them with the enzymes of the fatty acid biosynthesis mentioned above. Similar to the in this work used *P. laumondii* ARs77 strain in which most of the BGCs were deleted, it might be necessary to generate a similar strain for *X. nematophila* in the future since these clusters encode also CoA ligases which might accept benzoic acid and hence be involved in the biosynthesis of BZA.

Table 15. CoA ligases not associated with any BGCs and their associated locus tags from the genome of *X. nematophila*.

Enzyme	Locus tag
Fatty acid CoA ligase	XNEMV2_05180
Succinyl-CoA ligase	XNEMV2_06290 + XNEMV2_06295
Fatty acid CoA ligase FadD	XNEMV2_09700
Succinyl-benzoate-CoA ligase MenE	XNEMV2_12555

4.2 Optimization of production titers of stilbenes

4.2.1 Increase of substrate building blocks

One approach to enhance the production levels of IPS and its derivatives comprised the deletion of genes of biosynthetic pathways which compete for the same precursors as the stilbene generating enzymes. The absence of NPs like AQs not only increased the production titers of stilbenes since both NP classes are MCoA derived, but also accompanies easier purification of stilbenes in downstream processes due to a clearer background since AQs form several methylated derivatives leading to a shift in retention times in the HPLC¹⁵⁶. Instead of deleting the whole AQ BGC, it was sufficient to delete *antJ*, a transcriptional regulator for this class of NPs in *P. laumondii*¹⁵⁷. Deletion of *antJ* resulted in a 20% higher production rate yielding 33 ± 2 mg/l for IPS and produced the same amount as the strain with two deletions ($\Delta antJ$ and $\Delta gxpS$) (Table 12 in Topic B results).

In contrast, the increase of amino acid pools (phenylalanine and leucine) related to the production of stilbene were no bottleneck for the production, but were still carried out for the later steps (Figure 31 and Figure S5). Therefore, *gxpS* which encodes the GameXPepetide synthetase was deleted since GameXPepetides incorporate leucine which is the precursor for the isopropyl-group in IPS and EPS^{78,158}. The Keasling lab generated optimized plasmids (obtainable via *addgene*) containing *E. coli* derived genes for the overproduction of shikimate (pS3) that acts as a precursor for the biosynthesis of aromatic amino acids and another plasmid for further procession to tyrosine (pY3)¹³⁰. Since tyrosine and phenylalanine share the same biosynthetic pathway up to the synthesis of prephenate and differ only in the last enzyme of their respective pathway, it was sufficient to replace *tyrA* (encoding for chorismate mutase/prephenate dehydrogenase) with *pheA* (encoding for chorismate mutase/prephenate dehydratase) as illustrated in Figure 59. The incorporated *pheA* encoded for a point mutated PheA (G309C) in order to remove its feedback inhibition and the new plasmid was renamed pF3¹⁵⁹. The increase of phenylalanine was a result of the expression of the plasmids pS3 and pF3 (Figure S4 for the design of the plasmids).

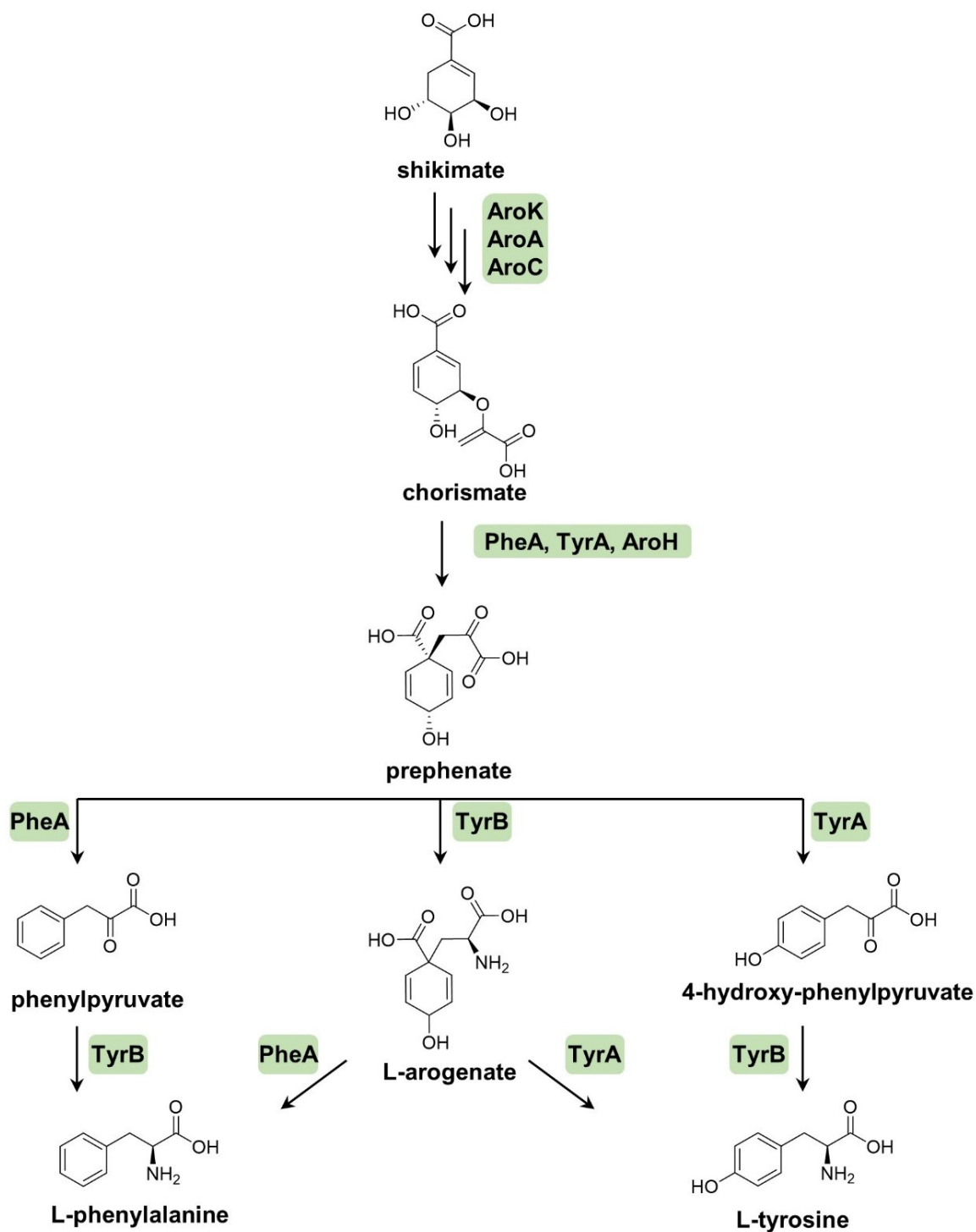


Figure 59. Biosynthesis of shikimate-derived tyrosine and phenylalanine. AroK: shikimate kinase; AroA: 3-phosphoshikimate-1-carboxyvinyltransferase; AroC: chorismate synthase; PheA: chorismate mutase/prephenate dehydratase; TyrA: chorismate mutase/prephenate dehydrogenase; AroH: chorismate mutase; TyrB: aromatic-amino-acid transferase.

Another strategy which is commonly used for the upregulation of MCoA levels is the overproduction of the ACC enzymes which convert acetyl-CoA to MCoA. The heterologous production of the *acc* genes from *Photorhabdus* in *E. coli* have been reported to increase the microbial synthesis of the plant polyphenol pinocembrin seven-fold¹⁶⁰. Therefore, the genes for the corresponding ACC subunits and *birA*, the gene encoding for a biotin ligase were cloned via GoldenGate cloning into a plasmid and expressed in *P. laumondii*. The production of IPS in the strain harboring the pACYC-*acc* plasmid did not increase compared to the one carrying the control plasmid (Figure 30). Nevertheless, the production was 20 % higher than for the WT strain (increase from 23 to 29 mg/l). This can be explained by the comparison of the ODs of both strains. Addition of the antibiotic Cm leads to an increase of the OD from 10 to 12. This indicates a correlation between the OD and the stilbene production. Since the ACC-enzymes did not impact the production of IPS, this indicates an already evolutionary optimized MCoA-pool due to overproduction of these enzymes for the production of PKS-derived compounds. This suggests that also other common approaches to increase the titers of MCoA like the approach to knockdown or silence genes related to enzymes utilizing MCoA as a substrate, via small regulatory RNAs or CRISPRi might not be reasonable in *Photorhabdus*^{161,162}. Furthermore, it is also possible that the *antJ*-deletion related upregulation of IPS is not based on a higher intracellular MCoA-level, but because AQ or one of its derivatives might be regulator for either the IPS or the CA-production. An approach to test this hypothesis would be to delete the other AQ-BGC instead of *antJ*, supplement the strain with AQ-256 and monitor the CA and IPS production. This deletion could also be compared to a strain with an additional *antJ* deletion.

In parallel it was assessed whether another precursor had also an effect on the production levels. Therefore, *P. laumondii* WT cultures were fed with CA. Supplementation with 2 mM CA in LB led to an almost 80 % increase of IPS from 23 ± 1 mg/l to almost 41 mg/l (Figure 30) and thus was determined as a bottleneck. However it was not possible to feed higher concentrations at once, since the cultures died due to a pH shift which might be circumvented with the addition of a phosphate buffer. Instead of titrating CA over the days it was concluded to exchange the promoter in front of *stIA* in order to grant a steadily output of CA. This granted titers of up to 82 ± 3 mg/l for IPS (Figure 34) in the

AQ, GameXPeptide and EPS deficient strain. Due to the close proximity in the genome (7 kb distance) it was possible to combine the promoter exchange in front of *sltA* with the deletion of the epoxidase *stlF* within one cloning/CRISPR step. Deletion of *stlF* in the WT strain resulted in an increase from 23 ± 1 mg/l to 35 mg/l compared in LB (Figure 32). Although this deletion led only to a minor increase of production since the epoxidase activity does not appear to be as active as the other enzymes of the stilbene pathway, the deletion of *stlF* is beneficial for other cultivation media where the ratio between **1** and **3** changes (Figure 32) depending on the desired compound.

4.2.2 Promoter exchanges and impact of XAD

Promoter exchanges were also carried out for the *stlCDE* and *bkdABC* operons. While the exchange in front of *stlCDE* more than doubled the production for the WT strain from 23 ± 1 mg/l to 50 ± 6 mg/l, the influence of the *bkd* promoter was minor and led to 29 ± 2 mg/l. While *StlCDE* is only used for the production of SM like DARs like stilbenes and CHDs and therefore is only activated under certain conditions, the enzymes of the *bkd* operon are needed besides the mentioned SM classes also for photopyrones and also for the production of iso-branched fatty acids for the primary metabolism in *Photorhabdus* strains^{38,88,118}. Therefore, the *bkd* operon was not used for further attempts to optimize the strain. Despite the abundance of the Bkd-enzymes, large scale cultures for the purification of **1** also tend to produce the non-branched derivative **2** while the ratio between these two derivatives shifted regarding of the applied cultivation media (Table 12). Fluorescence microscopic data in strains where the green fluorescence protein gene (*gfp*) is cloned behind the natural promoter of the *bkd* operon show no presence of the Bkd-complex in some peripheral parts of the colonies while the same procedure for *stlCDE* showed fluorescence in the whole cell (unpublished data from Alexander Rill and Christoph Spahn). This suggests that **2** is not a byproduct of **1**, but its biological role remains unknown. Deletion of *bkd* resulted in an accumulation of **2** while it was not possible to detect epoxides with an ethyl group in the 2-position of the resorcinol ring (Figure 40).

The combination of the promoter exchanges in front of *sltA* and *stlCDE* in the $\Delta antJ \Delta gxpS \Delta stlF$ strain increased the production titer of **1** to 90 ± 5 mg/l (Figure 35).

Expression of a plasmid containing *stlB* increased the yield additional 30 % to a titer of 118 ± 12 mg/l (Figure 37). The overproduction of phenylalanine based on the pS3 and pF3 plasmids as described above enhanced the yield from 90 ± 5 mg/l to 152 ± 9 mg/l in LB. An additional exchange of a promoter in front of *stlB* combined with the $\Delta antJ\Delta gxpS\Delta stlF$ pex *stlA/stlCDE* pS3/pF3 strain is due after this work.

Another method to increase the NP production is the utilization of adsorbent XAD resins during cultivation. These resins bind NPs and often increase the production levels due different mechanisms like prevention of the compound degradation or minimization of feedback inhibition and autotoxicity¹⁶³. Usage of these resins also circumvent the necessity to degrease during the extraction from fat rich media. While cultivation with 2 % XAD increased the cultivation in *P. laumondii* WT from 23 ± 1 mg/l to 62 ± 3 mg/l (Figure 36), purification of a 1 l culture of the $\Delta antJ\Delta gxpS\Delta stlF$ pex *stlA/stlCDE* pS3/pF3 strain with 2 % XAD yielded 240 mg/l of **1**.

4.2.3 Assessment of different cultivation media

After further deletion of *pliA* to get a cleaner background for potential large-scale purifications, cultivation in different media were compared as an additional strategy. Therefore, the best producing strain was cultivated in XPPM, LB, PP3M, 1 % *Hermetia* fat and 5 % BM media (Figure 38). The production in XPPM was the lowest and yielded 53 ± 13 mg/l, while cultivation in LB was three-fold higher and amounted at 158 ± 22 mg/l as mentioned above. Richer media containing higher concentrations of amino acids or fatty acids like PP3M and 1 % *Hermetia* fat containing media increased the production titers of **1** to 288 ± 14 mg/l and 224 ± 40 mg/l respectively. The change of media composition also leads to a shift in the ratio within compound **1** to **3**. Although the equilibrium is still in favor of **1**, the relative production of **3** relative increases in richer media like PP3M or BM. While the production of **3** reaches around 25 % relative to **1** for LB, it amounts to around 75 % BM (data not shown).

In silkworm derived BM medium, the strain was co-cultivated with 2 % XAD which led to the so far highest described production of IPS amounting in 867 ± 33 mg/l. The media that contains insects were utilized due to the nature of *P. laumondii* to feed upon insects and especially from the order *lepidoptera* caterpillar (like *Bombxy mori*) and *diptera*

maggots such as *Hermetia illucens*^{164,165}. It was hypothesized that many compounds related to the attack these species might be upregulated. An advantage of such media is the utilization of these insects as animal feed and therefore a cost-efficient alternative for industrial applications. Even though the production levels increase in the insect-based media, there are also disadvantages for these cultivations. The cultures need to be degreased with a mixture of MeOH and heptane and filtered which is especially an issue for larger cultures.

4.2.4 Outlook on further optimization

The optimization of the IPS production in TT01 leads to the opportunity to also produce high amounts of stilbene derivatives. However, the production of halogenated CA or IPS without supplementation of the cultures with CA-derivatives was not successful although genes encoding for enzymes incorporating phenol modifying tailoring enzymes like the halogenases *radH* from the fungus *Chaetomium chiversii* and *dkIH* from the Gram-positive bacterium *Frankia alni* were expressed (data not shown)^{166,167}. One crucial part of the optimization of IPS titers relied on the overproduction of phenylalanine and CA which would not be a sufficient approach, if the production of derivatives like the halogenated IPS are desired since so far no suitable halogenase is known. Better methods to incorporate those derivatives would focus on the promoter exchange in front of *stIB* which is still pending in combination with the already carried out exchange in front of the *st/CDE* operon. Since *stIB* is located next to a gene encoding for a ribonuclease, a promoter exchange might have a negative impact on the cells. An alternative to the promoter exchange would be to incorporate a second copy of *stIB* into the genome. This could be done at the former locus of *gxpS*.

As discussed in topic A, StID is most likely the bottleneck of the production of halogenated stilbenes due to the accumulation of the halogen substituted 5-phenyl-penta-2,4-dienoic acids. With computational protein design strategies like FuncLib it would be possible to incorporate mutations backed by phylogenetic analysis. Hereby, drawbacks regarding lowered stability or enzyme activity are minimized in order to optimize the activity of StID towards halogenated substrates in future studies¹⁶⁸. Alternatively, it might be beneficial to incorporate a second copy of either *st/CDE* or *stID* into the genome via CRISPR/Cas.

This could be tested in a first step by monitoring the IPS titers in the production strains with a plasmid encoding for either *stID* or *st/CDE*. This might overcome the StID bottleneck regarding the production of the byproduct 5-phenyl-penta-2,4-dienoic acid.

Another approach to improve the IPS production even further is the deletion of the *hca* operon. The scheme describing the CA-catabolism (Figure 52) showed additional metabolic pathways besides the procession into IPS which feed CA into the glycolysis and the citrate cycle. Removal of those pathways in the WT and the production strains should thus shift the equilibrium of the reaction even further towards the IPS accumulation.

4.3 Topic C EPS related derivatives and reactions

4.3.1 *In vivo* production of EPS and its derivatives

The biosynthesis of stilbene epoxides like **3** has been described by the group of Jason Crawford in 2017 where they discovered and characterized the FAD-dependent monooxygenase StIF¹²¹. They described similar antimicrobial activities for **1** and **3** while the latter showed less antibacterial host cytotoxicity. Observations from *P. laumondii* expressing *gfp* under the control of the *stIF* promoter showed a stronger fluorescence for colonies on agar plates which were growing closer to another than single clones (Alexander Rill, unpublished). This might indicate that the cell density might influence the expression of the monooxygenase StIF and thus confirm the observations from the Crawford lab regarding the reduced cytotoxicity¹²¹. Switching from LB to XPPM or insect based media also showed a shift in the production ratio from **1** to **3**. While the OD of cultures in insect based media could not be measured due to sediments and fat, the size of the cell pellet showed a higher biomass. However another factor might also be the change of pH from LB (7.5 – 8) to other media since in XPPM (pH 5.8 – 7.4 due to phosphate buffer) *P. laumondii* grows to an OD of 8, while the growth in LB is around 10 or 11. Therefore, **3** might also be a bacterial signaling molecule like reacting not only on the cell density, but also on the pH shift in the environment since also other DARs from *P. laumondii* exhibit signaling characteristics³⁹.

The Crawford group also describes the formation of proline bound epoxide derivative in animal infection models with *Galleria mellonella* where the epoxide ring is opened by the nucleophilic N-group¹²¹. However, they were not able to assign any biological function to these so called probenes and hypothesized that it may be a mechanism of self-defense by the larvae of *G. mellonella* in which they detoxify the effect of **3** onto the phenoloxidase¹²¹. Cultivation of *P. laumondii* in LB expressing *stIF* on a plasmid (Figure 41) showed that the modification with amino acids and peptides can be also achieved without animal infection models disproving this hypothesis although the presence of solely proline in these derivatives could not be observed. With feeding and inverse feeding experiments it was possible to detect leucine, isoleucine and methionine derived EPS derivatives (Figure 43 and Figure 44). Due to their characteristic shifts it was also possible

to detect further derivatives incorporating the aromatic amino acids phenylalanine and tryptophan without specific feeding experiments (Figure 45a and b). By utilization of the fragmentation patterns, it was also possible to assign three tetra-peptides and a penta-peptide to form β -amino-alcohol structures with EPS. All of these peptides integrated two proline units as a crucial building block similar to the probenes in the work of the Crawford group (Figure 45c-e)¹²¹.

The general epoxide ring opening reactions take place under basic or acidic conditions. Hereby, a nucleophile substitution (S_N2 reaction) takes place for both conditions which leads to the formation of a diol¹⁶⁹. Similar reactions can also be enzyme mediated by epoxide hydrolases or oxidoreductases. Epoxide hydrolases catalyze reactions in a non-redox manner, while oxidoreductases are associated with reductions and are dependent on cofactors like FADH₂ or FMNH₂. Recently a non-enzymatic FAD and NADH dependent epoxide ring opening reaction for fluostatin C was described which formed products with either a single hydroxyl group or a diol¹⁷⁰. Several works for the opening of epoxide rings with amines are described in organic chemistry and are used for the synthesis of β -amino alcohols^{171,172}. This class of molecules is utilized for drugs in medical applications such as naftopidil (cardiovascular application), salbutamol (anti-asthma), hydroxychloroquine (antimalarial) or ethambutol (tuberculosis drug) as shown in Figure 60^{173,174}. It might henceforth be useful to purify some of the observed derivatives and analyze them on potential bioactivities.

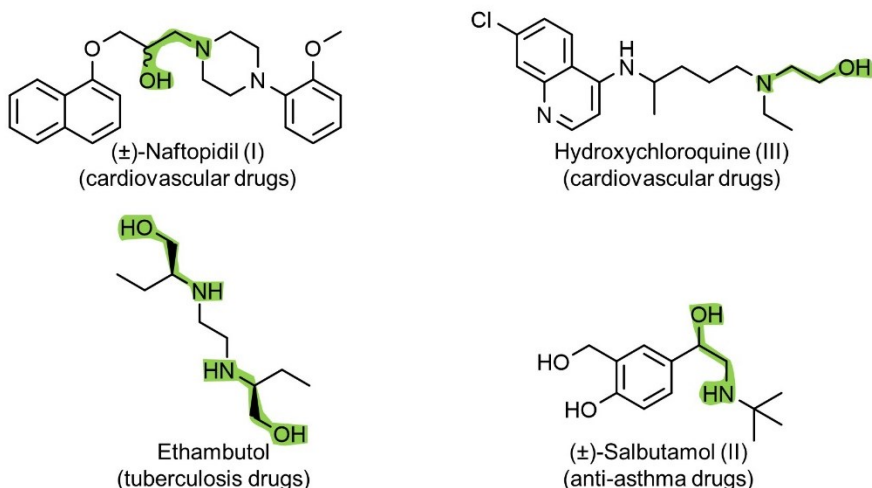


Figure 60. Chemical structures of β -amino alcohol containing drugs (motif highlighted in green)^{173,174}.

4.3.2 Purification of EPS

One hypothesis derived from the observed modifications is the posttranslational modification of proteins in *Photobacterium*. To assess if the observed modifications of peptides with EPS also applied to proteins, it was necessary to obtain EPS. The chemical synthesis of EPS was preferred over the purification from bacterial cultures due to its low stability and high reactivity. Therefore, TT01 $\Delta antJ\Delta gxpS\Delta stlF$ pex *stlA/stlCDE* pS3/pF3 was cultivated in 1 l LB-media with XAD and 240 mg IPS was purified with the Interchim Flash-system. Although the three-step reaction from IPS to EPS containing the protection of the two hydroxyl groups with trichloroacetyl-groups, the epoxidation step with 3-chloroperoxy-benzoic acid and the deprotection step with weak bases was already published and patented, it was not possible to purify the epoxide¹²⁰. Since the synthesis failed, it was tried to purify EPS from cultures of TT01 $\Delta antJ\Delta gxpS\Delta pliA$ pex *stlA/stlCDE* pACYC-*stlF* in 4 l PP3M. Purification with the preparative HPLC yielded 17 UV-absorbing fractions which were mostly β -amino-alcohols derived from EPS. Further purification of one fraction with a semi-preparative-HPLC yielded 80 mg of EPS (Figure 46). However, the alleged EPS did not show any reactivity and ¹H and ¹³C-NMR analysis (Figure S8, Figure S9 and Table S1) confirmed an already hydrolyzed epoxide ring which probably was a result of the acidified solvent (H₂O and ACN contained 0.1 % FA) from the preparative chromatography. Thus two other epoxides, similar in their structure to EPS were purchased and applied for further studies.

It still needs to be assessed if the supplementation of StIF-overproducing *E. coli* or *P. laumondii* strains (e.g. the ARs77 strain which has a diminished background regarding NPs) with IPS would lead to a higher production of EPS. It is also possible to use purified StIF and conduct *in vitro* reactions with IPS as was shown by Park et al., but these reactions were carried out in small scales¹²¹.

4.3.3 *In vitro* reactions of epoxides with amino acids, peptides and proteins

In vitro reactions with styrene oxide and stilbene oxide with lysine, N ϵ -acetyl-lysine, a lysine-containing peptide (SIYKAVA-peptide) and with StIE showed the modification of the nucleophilic amino groups with the epoxide. While the reactions with the amino acids and the peptide were carried out at pH 11 to obtain stronger nucleophiles, the reaction with StIE was carried out at a physiological pH. After two hours of incubation with the epoxide, HPLC-MS analysis showed the addition of up to two styrene oxide molecules to lysine (Figure 47, compound **10** and **11** while it also modified N ϵ -acetyl-lysine (Figure S6) and the SIYKAVA peptide (Figure 47, modification from compound **13** to **14**). The reaction with N ϵ -acetyl-lysine also yielded a lactone after intramolecular cyclization which might be an MS artefact since it is present to the same retention time as the non-cyclized compound. Addition of stilbene oxide to lysine, N ϵ -acetyl-lysine or the mentioned peptide resulted also in the formation of β -amino alcohol moieties (Figure 47, molecule **12** and **15** and Figure S6). The difference regarding the number of modifications with lysine might be due to a higher reactivity of styrene oxide based on a lower steric hindrance.

To study if also proteins might get modified with epoxides, StIE which was already purified for the biosynthesis studies of IPS and BZA was utilized as a proof of concept for potential future proteomics analysis of homogeneously produced proteins from *Photorhabdus*. StIE was selected due to the well-established analysis method, high stability and its small size and therefore limited options of modifiable residues. Analysis of StIE on a C₃-column with an applied 30-65-95 water/ACN gradient (chapter 2.1.12) at retention times from 9.4-11.5 min showed mainly the *apo*-state, but also *holo*- and acetyl-StIE. The *m/z* of 1074.85 [M+H]¹⁰⁺ corresponds to a protein with a mass of 10.740 kDa, thus a 16 Da shift to StIE which has a mass of 10.724 kDa. The shift might be a result of methionine oxidation which is a posttranslational modification (PTM)¹⁷⁵. Another signal which was

detectable in the purified StIE, but is only shown in Figure 48c with an m/z of 1081.93 $[M+H]^{10+}$ might also be a result of PTMs. It represents a protein with a mass of 10.81 kDa (Δ of 86 Da to *apo*-StIE) which might be a result of methionine oxidation (+16 Da) an acetylation of lysine (+ 42 Da) and two methylations (+ 14 Da for each) of lysine or arginine¹⁷⁵.

StIE exhibits five potential modification sites: N-terminus, K in strep tag, K9, K61 and K75, Figure 61). Addition of the epoxides resulted in the formation of one β -amino alcohol for each epoxide. For styrene oxide an m/z of 1085.34 $[M+H]^{10+}$ (shift of 120 Da) and for stilbene oxide 1092.94 $[M+H]^{10+}$ (shift of 196 Da) (Figure 48). However, the EIC for the reaction with styrene oxide showed signals for 1085.34 $[M+H]^{10+}$ at two varying retention times (Figure 49a) indicating two different sites of modification in the protein which could not be determined with the applied experimental setup. Additionally, the same modification was also detected for the protein carrying an acetyl-moiety on its Ppant-arm (Figure 49b) which was visualized via EIC of 1123.54 at 9.6 – 10 min. To assess the position of the modified residues it would be necessary to either carry out NMR experiments, by mutating the lysine residues to unreactive ones like alanine or by enzymatic digestions with trypsin which cuts at the carboxyl site of positively charged amino acids of peptides or proteins. Analysis of the generated fragments via HPLC-HR-MS analog to setups like the *peptide mass fingerprint* (PMF) would give insights on the modification sites. However, the PMF approach suits better in this case, since the whole proteome from *Photorehabdus* could be analyzed on epoxidations, due to the reaction with StIE being only a proof of concept. The described proteome approach might give insights whether a potential new PTM was discovered. Although various epoxide containing NPs have been discovered so far, a systemic epoxide related modification of peptides or proteins has not been described yet¹⁷⁶.

An appropriate approach would be to use the TT01 $\Delta antJ\Delta gxpS\Delta pliA$ pex *stlA/stlCDE* pACYC-*stlF* strain due to its high epoxidase production and inducible promoter in front of *stlA*. Instead of inducing the CA-production, the strain would be supplemented with CA and d_7 -CA in a ratio of 1:1. After cultivation and preparation of the proteomics data, two signals with a $\Delta 7$ mass shift for every EPS-adduct is expected. For other epoxides similar

feeding experiments with the unlabeled and the labeled substrates can be conducted in the TT01 strains provided that the used epoxides have no toxic effect on the cells. Therefore, labeled molecules like d_5 -styrene can be obtained and epoxidized with H_2O_2 ¹⁷⁷. Similar to the already conducted *in vitro* assays, in the first step proteomics approaches could be conducted with the styrene epoxides as a proof of concept for prey insects and also the nematode symbionts of *Photorhabdus*. In a second step, the labeled and unlabeled EPS could be utilized and assessed whether the epoxidation reaction might have effect the symbiont or the prey.

Besides the epoxides, BZA could also be tested for similar protein modifications. BZA is used as Michael acceptor and thus reacts with nucleophiles for example in the synthesis of warfarin¹⁷⁸. Michael additions with proteins and BZA could be investigated in a similar manner as the proposed approach regarding the epoxide adducts. Therefore, deuterated BZA could be produced and purified via heterologous production in *E. coli* in order to get d_7 -BZA. Afterwards BZA and d_7 -BZA could be supplemented in a ratio of 1:1 to *Photorhabdus* or *Xenorhabdus* cultures followed by proteomic analysis as described above. Since BZA acts as an antibiotic against some Gram-negative bacteria, the lethal concentration has to be determined before via titration⁴⁷.

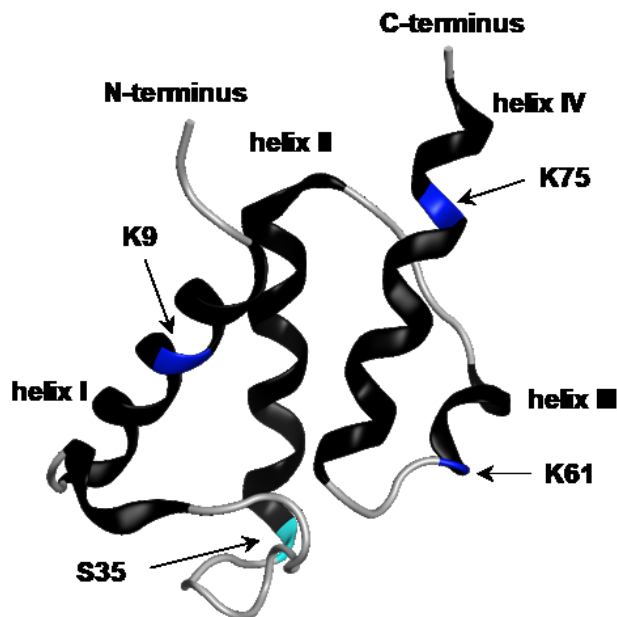


Figure 61. AlphaFold structure of StIE (entry number A0A6L9JI32) from *P. laumondii*. The potential modification sites at the residues K9, K61 and K75 are indicated in blue, the conserved S35 residue in cyan. The structure was visualized with MOE 2022.02.

4.3.4 Observation of further stilbene derivatives

Cultivation of large cultures of *P. laumondii* $\Delta antJ\Delta gxpS$ *pex stlA/stlCDE* *pACYC_ara_stlF* with 2 % XAD in PP3M to purify **3** also led to the production of new, monomeric and dimeric stilbene molecules. Hereby, additionally to the common IPS molecule at a retention time of 9 min, another molecule with the same mass and fragmentation pattern was detected at 7.4 min (Figure S10). The latter might be the *cis*-isomer of IPS which can normally not be detected and should shift on the C_{18} -column due to its smaller size. The signal intensity was around 27-fold lower than the peak area of the signal at 9 min which corresponds to *trans*-IPS. Another observed signal indicated the production of an stilbene derivative with an m/z of 270 $[M+H]^+$ that might be the result of the incorporation of an amino group into the resveratrol ring similar to the formation of lumiquinone A (Figure 62 and Figure S12) which requires α -aminomalonyl-CoA¹⁷⁹. This molecule was already proposed as the precursor of lumiquinone A which undergoes an oxidation to generate the final product, but has not been observed so far¹⁷⁹. However, the titer of that compound was too low or unstable and the signal vanished during the

purification at the semi-preparative HPLC. Therefore the cultivation and purification needs to be repeated in the future for the HR-MS and NMR analysis.

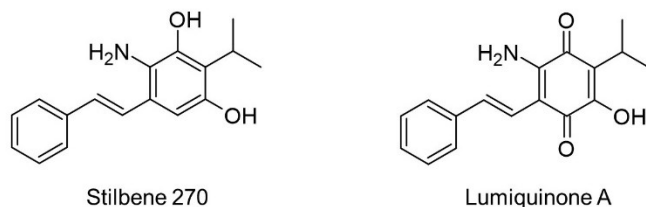


Figure 62. Structure of lumiquinone A and the proposed structure for the stilbene 270 derivative detected in large cultures of *P. laumondii* $\Delta antJ\Delta gxpS$ pex *stlA/stlCDE* pACYC_ara_*stlF* after two days of cultivation in PP3M.

At retention times between nine and ten minutes, derivatives with 511 and 525 $[M+H]^+$ and their dehydrated derivatives 493 and 507 $[M+H]^+$ were observed which might be similar to duotap-520¹²². More likely are structures derived from a nucleophilic attack of one of the hydroxyl groups of IPS or ethylstilbene with the epoxide of an epoxy stilbene monomer (Figure S11). The proposed structures of stilbene-507 and 525 resemble the chemical structure of plant based lignin.

5 Literature

1. Hutchings, M. I.; Truman, A. W.; Wilkinson, B. *Curr Opin Microbiol* **2019**, *51*, 72-80.
2. Newman, D. J.; Cragg, G. M. *J Nat Prod* **2020**, *83*, 770-803.
3. Sparks, T. C.; Hahn, D. R.; Garizi, N. V. *Pest Manag Sci* **2017**, *73*, 700-715.
4. González-Manzano, S.; Dueñas, M. *Foods* **2021**, *10*.
5. Haslam, E. *Natural Product Reports* **1986**, *3*, 217-249.
6. Williams, D. H.; Stone, M. J.; Hauck, P. R.; Rahman, S. K. *J Nat Prod* **1989**, *52*, 1189-208.
7. Shi, Y. M.; Bode, H. B. *Nat Prod Rep* **2018**, *35*, 309-335.
8. Fleming, A. *British Journal of Experimental Pathology* **1929**, *10*, 226-236.
9. Prescott, J. F. *Vet Microbiol* **2014**, *171*, 273-8.
10. O'Neill, J. *Tackling drug-resistant infections globally: final report and recommendations*; Government of the United Kingdom, 2016.
11. Harring, N.; Krockow, E. M. *Humanities and Social Sciences Communications* **2021**, *8*, 125.
12. Burnham, J. P. *Therapeutic Advances in Infectious Disease* **2021**, *8*, 2049936121991374.
13. Rodríguez-Verdugo, A.; Lozano-Huntelman, N.; Cruz-Loya, M.; Savage, V.; Yeh, P. *iScience* **2020**, *23*, 101024.
14. Mann, J. *Natural Product Reports* **2001**, *18*, 417-430.
15. Bérdy, J. *J Antibiot (Tokyo)* **2005**, *58*, 1-26.
16. Scott, T. A.; Piel, J. *Nat Rev Chem* **2019**, *3*, 404-425.
17. Albarano, L.; Esposito, R.; Ruocco, N.; Costantini, M. *Mar Drugs* **2020**, *18*.
18. Abo-Kadoum, M. A.; Abouelela, M. E.; Al Mousa, A. A.; Abo-Dahab, N. F.; Mosa, M. A.; Helmy, Y. A.; Hassane, A. M. A. *Frontiers in Microbiology* **2022**, *13*.
19. Zhang, L.; Chen, F.; Zeng, Z.; Xu, M.; Sun, F.; Yang, L.; Bi, X.; Lin, Y.; Gao, Y.; Hao, H.; Yi, W.; Li, M.; Xie, Y. *Front Microbiol* **2021**, *12*, 766364.
20. Cunha, B. A.; Sibley, C. M.; Ristuccia, A. M. *Ther Drug Monit* **1982**, *4*, 115-35.
21. Hauptman, J. B.; Jeunet, F. S.; Hartmann, D. *Am J Clin Nutr* **1992**, *55*, 309s-313s.
22. Mir, L. M.; Tounekti, O.; Orłowski, S. *Gen Pharmacol* **1996**, *27*, 745-8.
23. Hamill, R. J. *Drugs* **2013**, *73*, 919-34.
24. Park, S. R.; Tripathi, A.; Wu, J.; Schultz, P. J.; Yim, I.; McQuade, T. J.; Yu, F.; Arevang, C.-J.; Mensah, A. Y.; Tamayo-Castillo, G.; Xi, C.; Sherman, D. H. *Nature Communications* **2016**, *7*, 10710.
25. Thomas, G. M.; Poinar, G. O. *International Journal of Systematic Bacteriology* **1979**, *29*, 352-360.
26. Waterfield, N. R.; Ciche, T.; Clarke, D. *Annu Rev Microbiol* **2009**, *63*, 557-74.
27. Fischer-Le Saux, M.; Mauléon, H.; Constant, P.; Brunel, B.; Boemare, N. *Appl Environ Microbiol* **1998**, *64*, 4246-54.
28. Akhurst, R. J. *Journal of General Microbiology* **1980**, *121*, 303-309.
29. Akhurst, R. J.; Boemare, N. E. *Journal of General Microbiology* **1988**, *134*, 1835-1845.
30. Georgis, R.; Koppenhofer, A. M.; Lacey, L. A.; Belair, G.; Duncan, L. W.; Grewal, P. S.; Samish, M.; Tan, L.; Torr, P.; van Tol, R. W. H. M. *Biological Control* **2006**, *38*, 103-123.
31. Forst, S.; Nealson, K. *Microbiol Rev* **1996**, *60*, 21-43.
32. Zamora-Lagos, M. A.; Eckstein, S.; Langer, A.; Gazanis, A.; Pfeiffer, F.; Habermann, B.; Heermann, R. *BMC Genomics* **2018**, *19*, 854.
33. Imai, Y.; Meyer, K. J.; Iinishi, A.; Favre-Godal, Q.; Green, R.; Manuse, S.; Caboni, M.; Mori, M.; Niles, S.; Ghiglieri, M.; Honrao, C.; Ma, X.; Guo, J. J.; Makriyannis, A.; Linares-Otoya, L.; Bohringer, N.; Wuisan, Z. G.; Kaur, H.; Wu, R.; Mateus, A.; Typas, A.; Savitski, M. M.; Espinoza, J. L.; O'Rourke, A.; Nelson, K. E.; Hiller, S.; Noinaj, N.; Schaberle, T. F.; D'Onofrio, A.; Lewis, K. *Nature* **2019**, *576*, 459-464.

34. Pantel, L.; Florin, T.; Dobosz-Bartoszek, M.; Racine, E.; Sarciaux, M.; Serri, M.; Houard, J.; Campagne, J. M.; de Figueiredo, R. M.; Midrier, C.; Gaudriault, S.; Givaudan, A.; Lanois, A.; Forst, S.; Aumelas, A.; Cotteaux-Lautard, C.; Bolla, J. M.; Vingsbo Lundberg, C.; Huseby, D. L.; Hughes, D.; Villain-Guillot, P.; Mankin, A. S.; Polikanov, Y. S.; Gualtieri, M. *Mol Cell* **2018**, *70*, 83-94 e7.
35. Kanda, N.; Ishizaki, N.; Inoue, N.; Oshima, M.; Handa, A. *J Antibiot (Tokyo)* **1975**, *28*, 935-42.
36. Hu, K.; Li, J.; Webster, J. M. *Nematology* **1999**, *1*, 457-469.
37. Tobias, N. J.; Wolff, H.; Djahanschiri, B.; Grundmann, F.; Kronenwerth, M.; Shi, Y. M.; Simonyi, S.; Grün, P.; Shapiro-Ilan, D.; Pidot, S. J.; Stinear, T. P.; Ebersberger, I.; Bode, H. B. *Nat Microbiol* **2017**, *2*, 1676-1685.
38. Brachmann, A. O.; Brameyer, S.; Kresovic, D.; Hitkova, I.; Kopp, Y.; Manske, C.; Schubert, K.; Bode, H. B.; Heermann, R. *Nat Chem Biol* **2013**, *9*, 573-8.
39. Brameyer, S.; Kresovic, D.; Bode, H. B.; Heermann, R. *Proc Natl Acad Sci U S A* **2015**, *112*, 572-7.
40. Parsek, M. R.; Val, D. L.; Hanzelka, B. L.; Cronan, J. E., Jr.; Greenberg, E. P. *Proc Natl Acad Sci U S A* **1999**, *96*, 4360-5.
41. González-Santoyo, I.; Córdoba-Aguilar, A. *Entomologia Experimentalis et Applicata* **2012**, *142*, 1-16.
42. Crawford, J. M.; Portmann, C.; Zhang, X.; Roeffaers, M. B.; Clardy, J. *Proc Natl Acad Sci U S A* **2012**, *109*, 10821-6.
43. Cai, X.; Nowak, S.; Wesche, F.; Bischoff, I.; Kaiser, M.; Furst, R.; Bode, H. B. *Nat Chem* **2017**, *9*, 379-386.
44. Reimer, D.; Cowles, K. N.; Proschak, A.; Nollmann, F. I.; Dowling, A. J.; Kaiser, M.; French-Constant, R.; Goodrich-Blair, H.; Bode, H. B. *Chembiochem* **2013**, *14*, 1991-7.
45. Kim, Y.; Ji, D.; Cho, S.; Park, Y. *J Invertebr Pathol* **2005**, *89*, 258-64.
46. Seo, S.; Lee, S.; Hong, Y.; Kim, Y. *Appl Environ Microbiol* **2012**, *78*, 3816-23.
47. Ji, D.; Yi, Y.; Kang, G. H.; Choi, Y. H.; Kim, P.; Baek, N. I.; Kim, Y. *FEMS Microbiol Lett* **2004**, *239*, 241-8.
48. Satyavathi, V. V.; Minz, A.; Nagaraju, J. *Cell Signal* **2014**, *26*, 1753-63.
49. Zhao, L.; Le Chapelain, C.; Brachmann, A. O.; Kaiser, M.; Groll, M.; Bode, H. B. *Chembiochem* **2021**, *22*, 1582-1588.
50. Stein, M. L.; Beck, P.; Kaiser, M.; Dudler, R.; Becker, C. F.; Groll, M. *Proc Natl Acad Sci U S A* **2012**, *109*, 18367-71.
51. Hertweck, C. *Angew Chem Int Ed Engl* **2009**, *48*, 4688-716.
52. Cronan, J. E.; Thomas, J. In *Complex Enzymes in Microbial Natural Product Biosynthesis, Part B: Polyketides, Aminocoumarins and Carbohydrates*, 2009; pp. 395-433.
53. Mootz, H. D.; Finking, R.; Marahiel, M. A. *J Biol Chem* **2001**, *276*, 37289-98.
54. Tsai, S. C.; Miercke, L. J.; Krucinski, J.; Gokhale, R.; Chen, J. C.; Foster, P. G.; Cane, D. E.; Khosla, C.; Stroud, R. M. *Proc Natl Acad Sci U S A* **2001**, *98*, 14808-13.
55. Dunn, B. J.; Khosla, C. *J R Soc Interface* **2013**, *10*, 20130297.
56. Shen, J. J.; Chen, F.; Wang, X. X.; Liu, X. F.; Chen, X. A.; Mao, X. M.; Li, Y. Q. *Front Microbiol* **2018**, *9*, 1840.
57. Beld, J.; Sonnenschein, E. C.; Vickery, C. R.; Noel, J. P.; Burkart, M. D. *Nat Prod Rep* **2014**, *31*, 61-108.
58. Yadav, U.; Arya, R.; Kundu, S.; Sundd, M. *Biochemistry* **2018**, *57*, 3690-3701.
59. Mercer, A. C.; Burkart, M. D. *Nat Prod Rep* **2007**, *24*, 750-73.
60. Beld, J.; Cang, H.; Burkart, M. D. *Angew Chem Int Ed Engl* **2014**, *53*, 14456-61.
61. Haapalainen, A. M.; Meriläinen, G.; Wierenga, R. K. *Trends Biochem Sci* **2006**, *31*, 64-71.
62. Heil, C. S.; Wehrheim, S. S.; Paithankar, K. S.; Gringer, M. *Chembiochem* **2019**, *20*, 2298-2321.

63. Mindrebo, J. T.; Chen, A.; Kim, W. E.; Re, R. N.; Davis, T. D.; Noel, J. P.; Burkart, M. D. *ACS Catalysis* **2021**, *11*, 6787-6799.
64. Heath, R. J.; Rock, C. O. *Nat Prod Rep* **2002**, *19*, 581-96.
65. Keatinge-Clay, A. T.; Stroud, R. M. *Structure* **2006**, *14*, 737-48.
66. Keatinge-Clay, A. T. *Chem Biol* **2007**, *14*, 898-908.
67. Dillon, S. C.; Bateman, A. *BMC Bioinformatics* **2004**, *5*, 109.
68. Hopf, F. S. M.; Roth, C. D.; de Souza, E. V.; Galina, L.; Czczot, A. M.; Machado, P.; Basso, L. A.; Bizarro, C. V. *Front Microbiol* **2022**, *13*, 891610.
69. Du, L.; Lou, L. *Nat Prod Rep* **2010**, *27*, 255-78.
70. Yu, F.; Zaleta-Rivera, K.; Zhu, X.; Huffman, J.; Millet, J. C.; Harris, S. D.; Yuen, G.; Li, X. C.; Du, L. *Antimicrob Agents Chemother* **2007**, *51*, 64-72.
71. Xie, X.; Meehan, M. J.; Xu, W.; Dorrestein, P. C.; Tang, Y. *J Am Chem Soc* **2009**, *131*, 8388-9.
72. Smith, S.; Tsai, S. C. *Nat Prod Rep* **2007**, *24*, 1041-72.
73. Khosla, C.; Tang, Y.; Chen, A. Y.; Schnarr, N. A.; Cane, D. E. *Annual Review of Biochemistry* **2007**, *76*, 195-221.
74. Hertweck, C.; Luzhetskyy, A.; Rebets, Y.; Bechthold, A. *Nat Prod Rep* **2007**, *24*, 162-90.
75. Du, D.; Katsuyama, Y.; Shin-Ya, K.; Ohnishi, Y. *Angew Chem Int Ed Engl* **2018**, *57*, 1954-1957.
76. Bilyk, O.; Brötz, E.; Tokovenko, B.; Bechthold, A.; Paululat, T.; Luzhetskyy, A. *ACS Chem Biol* **2016**, *11*, 241-50.
77. Brachmann, A. O.; Joyce, S. A.; Jenke-Kodama, H.; Schwär, G.; Clarke, D. J.; Bode, H. B. *Chembiochem* **2007**, *8*, 1721-8.
78. Joyce, S. A.; Brachmann, A. O.; Glazer, I.; Lango, L.; Schwär, G.; Clarke, D. J.; Bode, H. B. *Angew Chem Int Ed Engl* **2008**, *47*, 1942-5.
79. Okamoto, S.; Taguchi, T.; Ochi, K.; Ichinose, K. *Chemistry & Biology* **2009**, *16*, 226-236.
80. Hutchinson, C. R. *Chem Rev* **1997**, *97*, 2525-2536.
81. Napan, K.; Zhang, S.; Morgan, W.; Anderson, T.; Takemoto, J. Y.; Zhan, J. *Chembiochem* **2014**, *15*, 2289-96.
82. Yu, D.; Xu, F.; Zeng, J.; Zhan, J. *IUBMB Life* **2012**, *64*, 285-95.
83. Choi, K. H.; Heath, R. J.; Rock, C. O. *J Bacteriol* **2000**, *182*, 365-70.
84. Edwards, P.; Nelsen, J. S.; Metz, J. G.; Dehesh, K. *FEBS Lett* **1997**, *402*, 62-6.
85. Morgan-Kiss, R. M.; Cronan, J. E. *Arch Microbiol* **2008**, *190*, 427-37.
86. Price, A. C.; Zhang, Y. M.; Rock, C. O.; White, S. W. *Biochemistry* **2001**, *40*, 12772-81.
87. Heath, R. J.; Rock, C. O. *J Biol Chem* **1996**, *271*, 27795-801.
88. Brachmann, A. O.; Reimer, D.; Lorenzen, W.; Augusto Alonso, E.; Kopp, Y.; Piel, J.; Bode, H. B. *Angew Chem Int Ed Engl* **2012**, *51*, 12086-9.
89. Hafner, E. W.; Holley, B. W.; Holdom, K. S.; Lee, S. E.; Wax, R. G.; Beck, D.; McArthur, H. A.; Wernau, W. C. *J Antibiot (Tokyo)* **1991**, *44*, 349-56.
90. Franke, J.; Hertweck, C. *Cell Chem Biol* **2016**, *23*, 1179-1192.
91. Bode, H. B.; Bethe, B.; Höfs, R.; Zeeck, A. *Chembiochem* **2002**, *3*, 619-27.
92. Singh, V.; Haque, S.; Niwas, R.; Srivastava, A.; Pasupuleti, M.; Tripathi, C. K. *Front Microbiol* **2016**, *7*, 2087.
93. Huis, A.; Van Itterbeeck, J.; Klunder, H.; Mertens, E.; Halloran, A.; Muir, G.; Vantomme, P. *EDIBLE INSECTS future prospects fo food and feed security*, 2013; Vol. 171.
94. Marmann, A.; Aly, A. H.; Lin, W.; Wang, B.; Proksch, P. *Mar Drugs* **2014**, *12*, 1043-65.
95. Medema, M. H.; Kottmann, R.; Yilmaz, P.; Cummings, M.; Biggins, J. B.; Blin, K.; de Bruijn, I.; Chooi, Y. H.; Claesen, J.; Coates, R. C.; Cruz-Morales, P.; Duddela, S.; Düsterhus, S.; Edwards, D. J.; Fewer, D. P.; Garg, N.; Geiger, C.; Gomez-Escribano, J. P.; Greule, A.; Hadjithomas, M.; Haines, A. S.; Helfrich, E. J.; Hillwig, M. L.; Ishida, K.; Jones, A. C.; Jones, C. S.; Jungmann, K.; Kegler, C.; Kim, H. U.; Kötter, P.; Krug, D.; Masschelein, J.;

- Melnik, A. V.; Mantovani, S. M.; Monroe, E. A.; Moore, M.; Moss, N.; Nützmann, H. W.; Pan, G.; Pati, A.; Petras, D.; Reen, F. J.; Rosconi, F.; Rui, Z.; Tian, Z.; Tobias, N. J.; Tsunematsu, Y.; Wiemann, P.; Wyckoff, E.; Yan, X.; Yim, G.; Yu, F.; Xie, Y.; Aigle, B.; Apel, A. K.; Balibar, C. J.; Balskus, E. P.; Barona-Gómez, F.; Bechthold, A.; Bode, H. B.; Borriss, R.; Brady, S. F.; Brakhage, A. A.; Caffrey, P.; Cheng, Y. Q.; Clardy, J.; Cox, R. J.; De Mot, R.; Donadio, S.; Donia, M. S.; van der Donk, W. A.; Dorrestein, P. C.; Doyle, S.; Driessen, A. J.; Ehling-Schulz, M.; Entian, K. D.; Fischbach, M. A.; Gerwick, L.; Gerwick, W. H.; Gross, H.; Gust, B.; Hertweck, C.; Höfte, M.; Jensen, S. E.; Ju, J.; Katz, L.; Kaysser, L.; Klassen, J. L.; Keller, N. P.; Kormanec, J.; Kuipers, O. P.; Kuzuyama, T.; Kyrpides, N. C.; Kwon, H. J.; Lautru, S.; Lavigne, R.; Lee, C. Y.; Linqun, B.; Liu, X.; Liu, W.; Luzhetskyy, A.; Mahmud, T.; Mast, Y.; Méndez, C.; Metsä-Ketelä, M.; Micklefield, J.; Mitchell, D. A.; Moore, B. S.; Moreira, L. M.; Müller, R.; Neilan, B. A.; Nett, M.; Nielsen, J.; O'Gara, F.; Oikawa, H.; Osbourn, A.; Osburne, M. S.; Ostash, B.; Payne, S. M.; Pernodet, J. L.; Petricek, M.; Piel, J.; Ploux, O.; Raaijmakers, J. M.; Salas, J. A.; Schmitt, E. K.; Scott, B.; Seipke, R. F.; Shen, B.; Sherman, D. H.; Sivonen, K.; Smanski, M. J.; Sosio, M.; Stegmann, E.; Süssmuth, R. D.; Tahlan, K.; Thomas, C. M.; Tang, Y.; Truman, A. W.; Viaud, M.; Walton, J. D.; Walsh, C. T.; Weber, T.; van Wezel, G. P.; Wilkinson, B.; Willey, J. M.; Wohlleben, W.; Wright, G. D.; Ziemert, N.; Zhang, C.; Zotchev, S. B.; Breitling, R.; Takano, E.; Glöckner, F. O. *Nat Chem Biol* **2015**, *11*, 625-31.
96. Blin, K.; Kim, H. U.; Medema, M. H.; Weber, T. *Brief Bioinform* **2019**, *20*, 1103-1113.
97. Rutledge, P. J.; Challis, G. L. *Nat Rev Microbiol* **2015**, *13*, 509-23.
98. Brachmann, A. O.; Kirchner, F.; Kegler, C.; Kinski, S. C.; Schmitt, I.; Bode, H. B. *J Biotechnol* **2012**, *157*, 96-9.
99. Bode, E.; Heinrich, A. K.; Hirschmann, M.; Abebew, D.; Shi, Y. N.; Vo, T. D.; Wesche, F.; Shi, Y. M.; Grün, P.; Simonyi, S.; Keller, N.; Engel, Y.; Wenski, S.; Bennet, R.; Beyer, S.; Bischoff, I.; Buaya, A.; Brandt, S.; Cakmak, I.; Çimen, H.; Eckstein, S.; Frank, D.; Fürst, R.; Gand, M.; Geisslinger, G.; Hazir, S.; Henke, M.; Heermann, R.; Lecaudey, V.; Schäfer, W.; Schiffmann, S.; Schöffler, A.; Schwenk, R.; Skaljac, M.; Thines, E.; Thines, M.; Ulshöfer, T.; Vilcinskis, A.; Wichelhaus, T. A.; Bode, H. B. *Angew Chem Int Ed Engl* **2019**, *58*, 18957-18963.
100. Jinek, M.; Chylinski, K.; Fonfara, I.; Hauer, M.; Doudna, J. A.; Charpentier, E. *Science* **2012**, *337*, 816-821.
101. Zhang, Q.-W.; Lin, L.-G.; Ye, W.-C. *Chinese Medicine* **2018**, *13*, 20.
102. Xiao, J. F.; Zhou, B.; Ressom, H. W. *Trends Analyt Chem* **2012**, *32*, 1-14.
103. Rinkel, J.; Dickschat, J. S. *Beilstein J Org Chem* **2015**, *11*, 2493-508.
104. Schoenheimer, R.; Rittenberg, D. *Science* **1935**, *82*, 156-7.
105. Bode, H. B.; Reimer, D.; Fuchs, S. W.; Kirchner, F.; Dauth, C.; Kegler, C.; Lorenzen, W.; Brachmann, A. O.; Grün, P. *Chemistry* **2012**, *18*, 2342-8.
106. Reimer, D.; Nollmann, F. I.; Schultz, K.; Kaiser, M.; Bode, H. B. *J Nat Prod* **2014**, *77*, 1976-80.
107. Hagen, A.; Poust, S.; Rond, T.; Fortman, J. L.; Katz, L.; Petzold, C. J.; Keasling, J. D. *ACS Synth Biol* **2016**, *5*, 21-7.
108. Li, J.; Chen, G.; Wu, H.; Webster, J. M. *Appl Environ Microbiol* **1995**, *61*, 4329-33.
109. Buscato, E.; Buttner, D.; Bruggerhoff, A.; Klingler, F. M.; Weber, J.; Scholz, B.; Zivkovic, A.; Marschalek, R.; Stark, H.; Steinhilber, D.; Bode, H. B.; Proschak, E. *ChemMedChem* **2013**, *8*, 919-23.
110. Eleftherianos, I.; Boundy, S.; Joyce, S. A.; Aslam, S.; Marshall, J. W.; Cox, R. J.; Simpson, T. J.; Clarke, D. J.; French-Constant, R. H.; Reynolds, S. E. *Proc Natl Acad Sci U S A* **2007**, *104*, 2419-24.
111. Watson, R. J.; Joyce, S. A.; Spencer, G. V.; Clarke, D. J. *Mol Microbiol* **2005**, *56*, 763-73.

112. Kronenwerth, M.; Brachmann, A. O.; Kaiser, M.; Bode, H. B. *Chembiochem* **2014**, *15*, 2689-91.
113. Lebwohl, M. G.; Stein Gold, L.; Strober, B.; Papp, K. A.; Armstrong, A. W.; Bagel, J.; Kircik, L.; Ehst, B.; Hong, H. C.; Soung, J.; Fromowitz, J.; Guenther, S.; Piscitelli, S. C.; Rubenstein, D. S.; Brown, P. M.; Tallman, A. M.; Bissonnette, R. *N Engl J Med* **2021**, *385*, 2219-2229.
114. Peppers, J.; Paller, A. S.; Maeda-Chubachi, T.; Wu, S.; Robbins, K.; Gallagher, K.; Kraus, J. E. *J Am Acad Dermatol* **2019**, *80*, 89-98 e3.
115. Zhao, L.; Chen, X.; Cai, L.; Zhang, C.; Wang, Q.; Jing, S.; Chen, G.; Li, J.; Zhang, J.; Fang, Y. *J Clin Pharm Ther* **2014**, *39*, 418-23.
116. Kavakli, S.; Grammbitter, G. L. C.; Bode, H. B. *Tetrahedron* **2022**.
117. Mori, T.; Awakawa, T.; Shimomura, K.; Saito, Y.; Yang, D.; Morita, H.; Abe, I. *Cell Chem Biol* **2016**, *23*, 1468-1479.
118. Fuchs, S. W.; Bozhüyük, K. A.; Kresovic, D.; Grundmann, F.; Dill, V.; Brachmann, A. O.; Waterfield, N. R.; Bode, H. B. *Angew Chem Int Ed Engl* **2013**, *52*, 4108-12.
119. Kavakli, S. *Goethe University Frankfurt/Main (Germany)* **2019**.
120. Hu, K.; Li, J.; Li, B.; Webster, J. M.; Chen, G. *Bioorg Med Chem* **2006**, *14*, 4677-81.
121. Park, H. B.; Sampathkumar, P.; Perez, C. E.; Lee, J. H.; Tran, J.; Bonanno, J. B.; Hallem, E. A.; Almo, S. C.; Crawford, J. M. *J Biol Chem* **2017**, *292*, 6680-6694.
122. Park, H. B.; Goddard, T. N.; Oh, J.; Patel, J.; Wei, Z.; Perez, C. E.; Mercado, B. Q.; Wang, R.; Wyche, T. P.; Piizzi, G.; Flavell, R. A.; Crawford, J. M. *Angew Chem Int Ed Engl* **2020**, *59*, 7871-7880.
123. Goddard, T. N.; Patel, J.; Park, H. B.; Crawford, J. M. *Biochemistry* **2020**, *59*, 1966-1971.
124. Fischer-Le Saux, M.; Viallard, V.; Brunel, B.; Normand, P.; Boemare, N. E. *International Journal of Systematic and Evolutionary Microbiology* **1999**.
125. Martinez-Garcia, E.; Goni-Moreno, A.; Bartley, B.; McLaughlin, J.; Sanchez-Sampedro, L.; Pascual Del Pozo, H.; Prieto Hernandez, C.; Marletta, A. S.; De Lucrezia, D.; Sanchez-Fernandez, G.; Fraile, S.; de Lorenzo, V. *Nucleic Acids Res* **2020**, *48*, D1164-D1170.
126. Fu, C.; Donovan, W. P.; Shikapwashya-Hasser, O.; Ye, X.; Cole, R. H. *PLoS One* **2014**, *9*, e115318.
127. Engler, C.; Marillonnet, S. *Methods Mol Biol* **2014**, *1116*, 119-31.
128. Thoma, S.; Schobert, M. *FEMS Microbiol Lett* **2009**, *294*, 127-32.
129. Fischer-Le Saux, M.; Viallard, V.; Brunel, B.; Normand, P.; Boemare, N. E. *Int J Syst Bacteriol* **1999**, *49 Pt 4*, 1645-56.
130. Juminaga, D.; Baidoo, E. E.; Redding-Johanson, A. M.; Batth, T. S.; Burd, H.; Mukhopadhyay, A.; Petzold, C. J.; Keasling, J. D. *Appl Environ Microbiol* **2012**, *78*, 89-98.
131. Lorenzen, W.; Ahrendt, T.; Bozhüyük, K. A.; Bode, H. B. *Nat Chem Biol* **2014**, *10*, 425-7.
132. Zhao, G.; Peng, W.; Song, K.; Shi, J.; Lu, X.; Wang, B.; Du, Y. L. *Nat Commun* **2021**, *12*, 7205.
133. Werbel, L. M.; Headen, N.; Elslager, E. F. *J Med Chem* **1968**, *11*, 1073-4.
134. Gerebtzoff, G.; Li-Blatter, X.; Fischer, H.; Frentzel, A.; Seelig, A. *Chembiochem* **2004**, *5*, 676-84.
135. Gunaydin, H.; Altman, M. D.; Ellis, J. M.; Fuller, P.; Johnson, S. A.; Lahue, B.; Lapointe, B. *ACS Med Chem Lett* **2018**, *9*, 528-533.
136. Xu, Z.; Yang, Z.; Liu, Y.; Lu, Y.; Chen, K.; Zhu, W. *J Chem Inf Model* **2014**, *54*, 69-78.
137. Kanehisa, M.; Goto, S. *Nucleic Acids Res* **2000**, *28*, 27-30.
138. Chen, A.; Re, R. N.; Burkart, M. D. *Nat Prod Rep* **2018**, *35*, 1029-1045.
139. Gajiwala, K. S.; Margosiak, S.; Lu, J.; Cortez, J.; Su, Y.; Nie, Z.; Appelt, K. *FEBS Lett* **2009**, *583*, 2939-46.
140. Pan, H.; Tsai, S.; Meadows, E. S.; Miercke, L. J.; Keatinge-Clay, A. T.; O'Connell, J.; Khosla, C.; Stroud, R. M. *Structure* **2002**, *10*, 1559-68.

141. Davies, C.; Heath, R. J.; White, S. W.; Rock, C. O. *Structure* **2000**, *8*, 185-95.
142. Musayev, F.; Sachdeva, S.; Scarsdale, J. N.; Reynolds, K. A.; Wright, H. T. *J Mol Biol* **2005**, *346*, 1313-21.
143. Alvarez, S. *Dalton Transactions* **2013**, *42*, 8617-8636.
144. Janiak, C. *Journal of the Chemical Society, Dalton Transactions* **2000**, 3885-3896.
145. Matsuda, K.; Arima, K.; Akiyama, S.; Yamada, Y.; Abe, Y.; Suenaga, H.; Hashimoto, J.; Shin-Ya, K.; Nishiyama, M.; Wakimoto, T. *J Am Chem Soc* **2022**, *144*, 12954-12960.
146. Foulke-Abel, J.; Townsend, C. A. *Chembiochem* **2012**, *13*, 1880-4.
147. Hiratsuka, T.; Suzuki, H.; Kariya, R.; Seo, T.; Minami, A.; Oikawa, H. *Angew Chem Int Ed Engl* **2014**, *53*, 5423-6.
148. Huo, L.; Hug, J. J.; Fu, C.; Bian, X.; Zhang, Y.; Muller, R. *Nat Prod Rep* **2019**, *36*, 1412-1436.
149. Schimming, O.; Fleischhacker, F.; Nollmann, F. I.; Bode, H. B. *Chembiochem* **2014**, *15*, 1290-4.
150. Xu, M.; Wang, Y.; Zhao, Z.; Gao, G.; Huang, S. X.; Kang, Q.; He, X.; Lin, S.; Pang, X.; Deng, Z.; Tao, M. *Appl Environ Microbiol* **2016**, *82*, 5795-805.
151. Goodman, A. L.; McNulty, N. P.; Zhao, Y.; Leip, D.; Mitra, R. D.; Lozupone, C. A.; Knight, R.; Gordon, J. I. *Cell Host Microbe* **2009**, *6*, 279-89.
152. Neubacher, N.; Tobias, N. J.; Huber, M.; Cai, X.; Glatzer, T.; Pidot, S. J.; Stinear, T. P.; Lütticke, A. L.; Papenfort, K.; Bode, H. B. *Nat Microbiol* **2020**, *5*, 1481-1489.
153. Song, C. J.; Seo, S.; Shrestha, S.; Kim, Y. *Journal of Microbiology and Biotechnology* **2011**, *21*, 317-322.
154. Grammbitter, G. L. C.; Schmalhofer, M.; Karimi, K.; Shi, Y. M.; Schoner, T. A.; Tobias, N. J.; Morgner, N.; Groll, M.; Bode, H. B. *J Am Chem Soc* **2019**, *141*, 16615-16623.
155. Shrestha, S.; Kim, Y. *J Invertebr Pathol* **2007**, *96*, 64-70.
156. Zhou, Q.; Bräuer, A.; Adihou, H.; Schmalhofer, M.; Saura, P.; Grammbitter, G. L. C.; Kaila, V. R. I.; Groll, M.; Bode, H. B. *Chem Sci* **2019**, *10*, 6341-6349.
157. Heinrich, A. K.; Glaeser, A.; Tobias, N. J.; Heermann, R.; Bode, H. B. *Heliyon* **2016**, *2*, e00197.
158. Nollmann, F. I.; Dauth, C.; Mulley, G.; Kegler, C.; Kaiser, M.; Waterfield, N. R.; Bode, H. B. *Chembiochem* **2015**, *16*, 205-8.
159. Nelms, J.; Edwards, R. M.; Warwick, J.; Fotheringham, I. *Appl Environ Microbiol* **1992**, *58*, 2592-8.
160. Leonard, E.; Lim, K. H.; Saw, P. N.; Koffas, M. A. *Appl Environ Microbiol* **2007**, *73*, 3877-86.
161. Yang, D.; Kim, W. J.; Yoo, S. M.; Choi, J. H.; Ha, S. H.; Lee, M. H.; Lee, S. Y. *Proc Natl Acad Sci U S A* **2018**, *115*, 9835-9844.
162. Zhang, R.; Xu, W.; Shao, S.; Wang, Q. *Front Microbiol* **2021**, *12*, 635227.
163. Phillips, T.; Chase, M.; Wagner, S.; Renzi, C.; Powell, M.; DeAngelo, J.; Michels, P. *Journal of Industrial Microbiology and Biotechnology* **2013**, *40*, 411-425.
164. Abd-Elgawad, M. M. M. *Plants (Basel)* **2021**, *10*.
165. da Silva, W. J.; Pilz-Júnior, H. L.; Heermann, R.; da Silva, O. S. *Parasit Vectors* **2020**, *13*, 376.
166. Menon, B. R. K.; Brandenburger, E.; Sharif, H. H.; Klemstein, U.; Shepherd, S. A.; Greaney, M. F.; Micklefield, J. *Angew Chem Int Ed Engl* **2017**, *56*, 11841-11845.
167. Kolling, D.; Stierhof, M.; Lasch, C.; Myronovskiy, M.; Luzhetskyy, A. *Molecules* **2021**, *26*.
168. Khersonsky, O.; Lipsh, R.; Avizemer, Z.; Ashani, Y.; Goldsmith, M.; Leader, H.; Dym, O.; Rogotner, S.; Trudeau, D. L.; Prilusky, J.; Amengual-Rigo, P.; Guallar, V.; Tawfik, D. S.; Fleishman, S. J. *Mol Cell* **2018**, *72*, 178-186 e5.
169. Hansen, T.; Vermeeren, P.; Haim, A.; van Dorp, M. J. H.; Codée, J. D. C.; Bickelhaupt, F. M.; Hamlin, T. A. *European Journal of Organic Chemistry* **2020**, *2020*, 3822-3828.

-
170. De, B. C.; Zhang, W.; Yang, C.; Mandi, A.; Huang, C.; Zhang, L.; Liu, W.; Ruszczycky, M. W.; Zhu, Y.; Ma, M.; Bashiri, G.; Kurtan, T.; Liu, H. W.; Zhang, C. *Nat Commun* **2022**, *13*, 4896.
 171. Li, D.; Wang, J.; Yu, S.; Ye, S.; Zou, W.; Zhang, H.; Chen, J. *Chemical Communications* **2020**, *56*, 2256-2259.
 172. Babic, A.; Sova, M.; Gobec, S.; Pecar, S. *Tetrahedron Letters* **2006**, *47*, 1733-1735.
 173. Du, L.-H.; Xue, M.; Yang, M.-J.; Pan, Y.; Zheng, L.-Y.; Ou, Z.-M.; Luo, X.-P. *Catalysts* **2020**, *10*.
 174. Mahendran, P.; Jeya Rajendran, A.; Balachandran, C.; Stalin, A.; Rangan, S.; Kothandapani, L.; Chennakesava Rao, K.; Awale, S.; Hiteshkumar, B. N. *Research on Chemical Intermediates* **2017**, *44*, 535-552.
 175. Larsen, M. R.; Trelle, M. B.; Thingholm, T. E.; Jensen, O. N. *Biotechniques* **2006**, *40*, 790-8.
 176. Thibodeaux, C. J.; Chang, W. C.; Liu, H. W. *Chem Rev* **2012**, *112*, 1681-709.
 177. Yadav, G. D.; Pujari, A. A. *Organic Process Research & Development* **2000**, *4*, 88-93.
 178. Halland, N.; Hansen, T.; Jørgensen, K. A. *Angew Chem Int Ed Engl* **2003**, *42*, 4955-7.
 179. Park, H. B.; Crawford, J. M. *J Nat Prod* **2015**, *78*, 1437-41.

6 Supplementary information

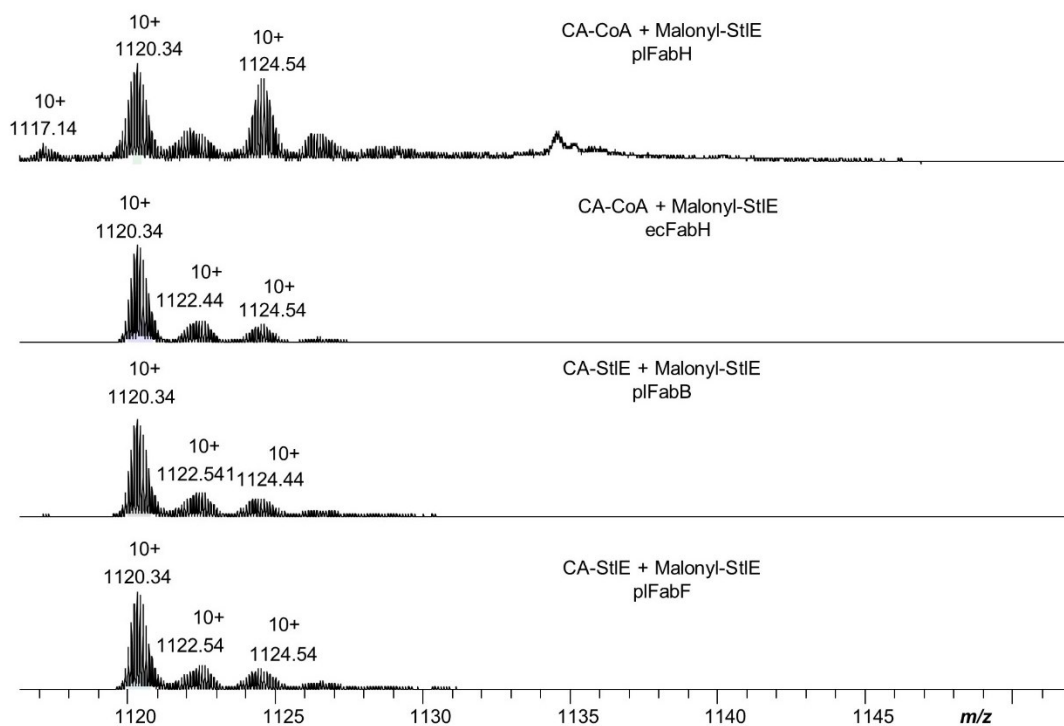


Figure S1. Excerpt of HPLC-MS measurements of *in vitro* condensation reactions with CA-moieties, Malonyl-StIE and different KS domains from *P. laumondii* (pIFabH, pIFabB, pIFabF) and *E. coli* (ecFab) at retention times between 11.3 and 13.3 min and *m/z* range of 1117 – 1150.

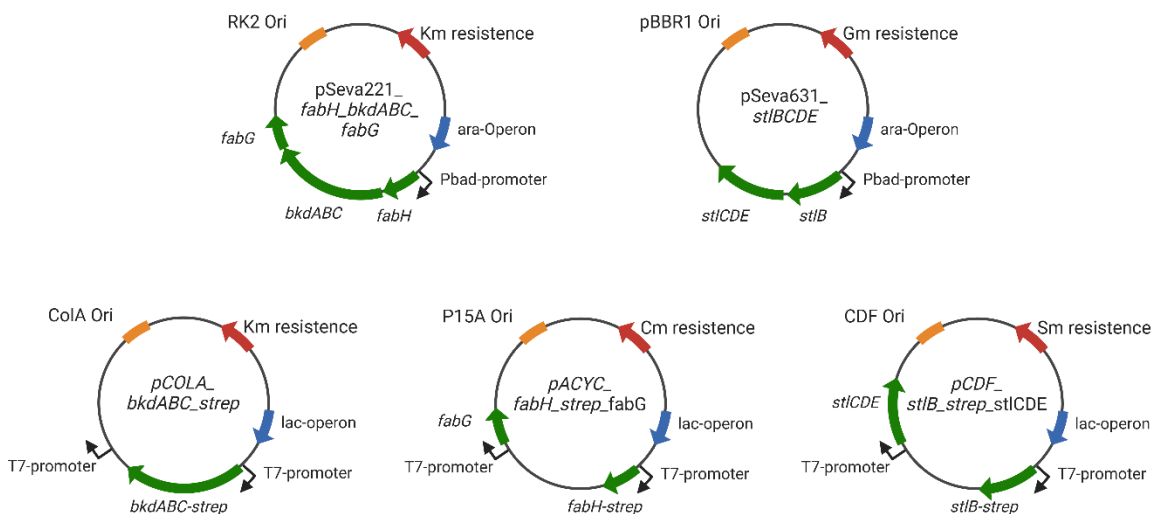


Figure S2. Plasmids for the heterologous production of IPS. The two plasmid approach (a) was cloned via Golden Gate assembly into the pSEVA vectors while the three plasmid approach (b) was cloned via Hofusion into the pDuet vectors.

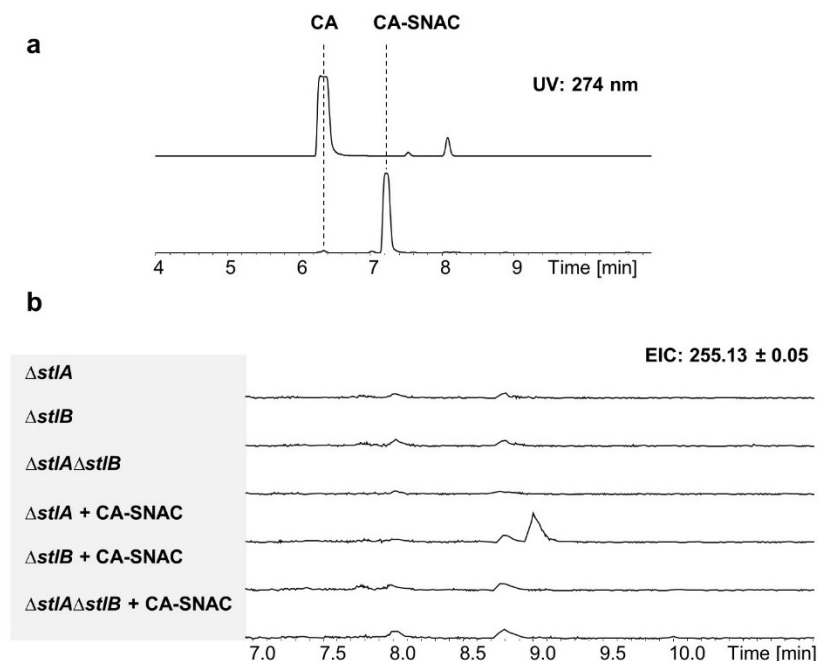


Figure S3. HPLC-UV chromatograms of the in this thesis used CA and CA-SNAC at 274 nm wavelength at retention times between 4 and 10 min (a). Complementation experiments for the biosynthesis of IPS (b). EICs of 255.13 corresponding to **1** for *P. laumondii* $\Delta stIA$, $\Delta stIB$ and $\Delta stIA\Delta stIB$ \pm CA-SNAC at retention times 7-11 min (b).

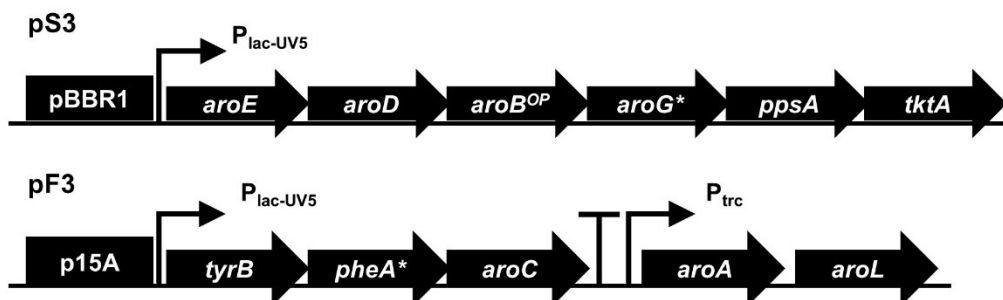


Figure S4. Excerpts from the pS3 and pF3 plasmids showing the pBBR1 and p15A oris, IPTG inducible promoters ($P_{lac-UV5}$ and P_{trc}) with the shikimate and phenylalanine relevant genes. The asterisk indicates genes encoding for feedback inhibition resistant enzymes while the in superscript written “OP” stands for the codon optimized gene. Adapted from Juminaga *et al*, 2012.¹³⁰

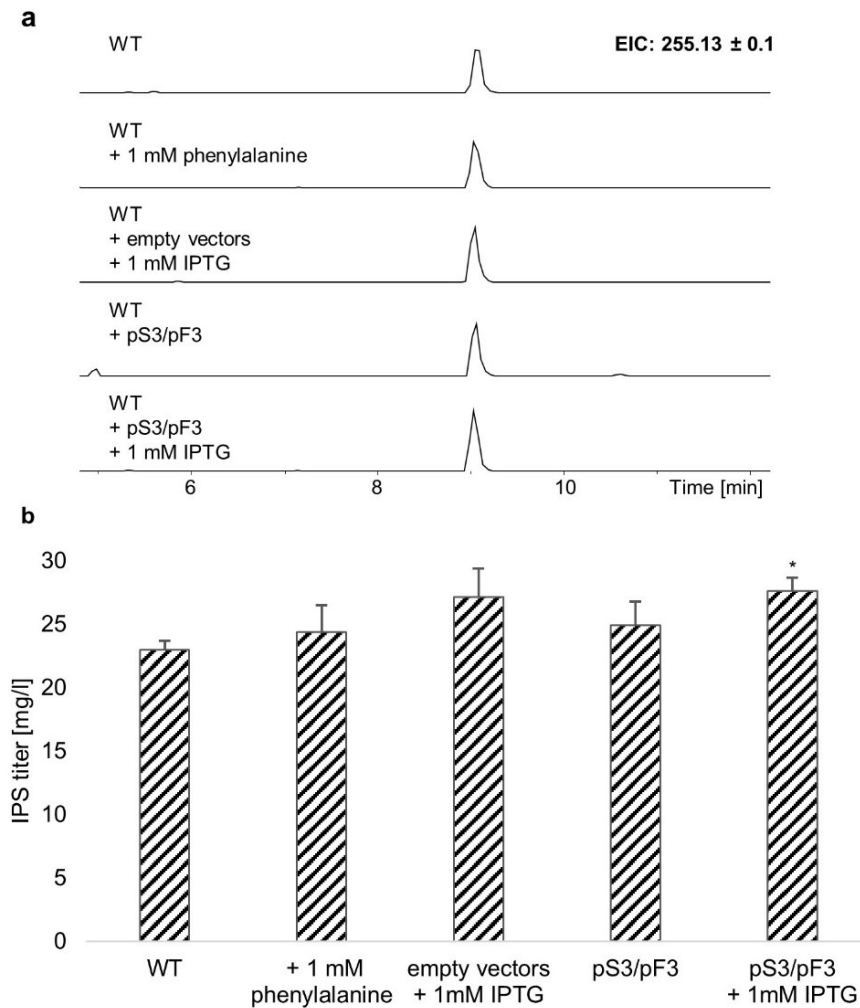


Figure S5. Dependence of IPS production on phenylalanine levels. The EICs of 255.13 ± 0.1 [M+H]⁺ are shown for *P. laumondii* WT (control), supplemented with 1 mM phenylalanine or expressing the shikimate and phenylalanine pathway plasmids pS3 and pF3 (uninduced and induced with 1 mM IPTG) in comparison to the empty vector control (a) and bar diagrams from triplicates with standard deviations for quantification of 1(b). Error bars represent the standard error of the mean. Asterisks indicate statistical significance (* $p < 0.05$) of relative production compared to WT production levels.

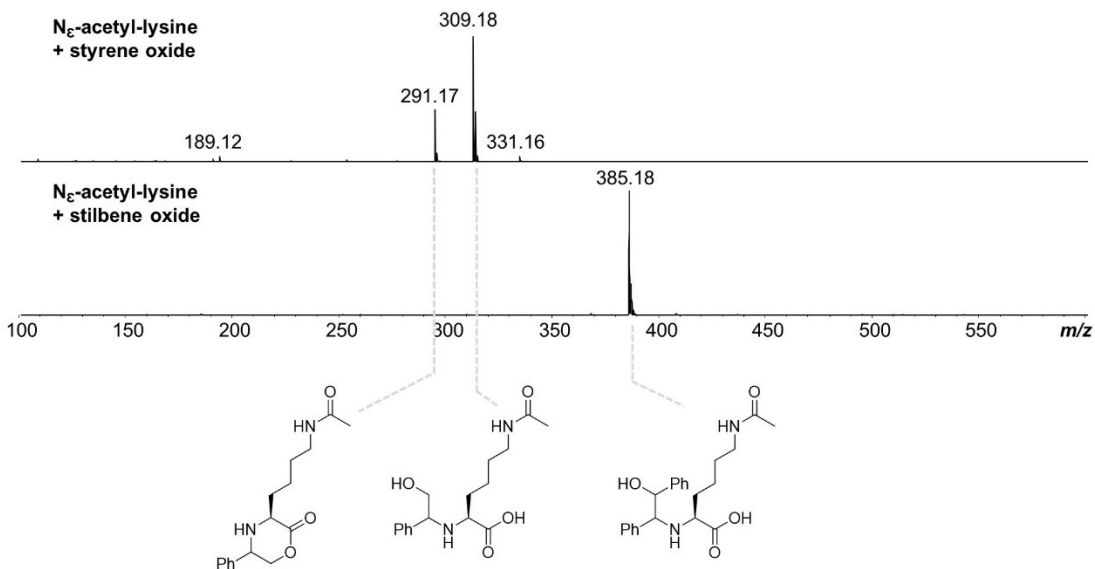


Figure S6. HPLC-MS analysis of the *in vitro* reactions with N_ε-acetyl-lysine with styrene oxide and stilbene oxide and the structures of the formed compounds. The aqueous reaction setups containing 10 mM NaOH were incubated for two hours at 30°C. The reaction mixtures were measured on a C₁₈-column with retention times at 4 and 5.5 min.

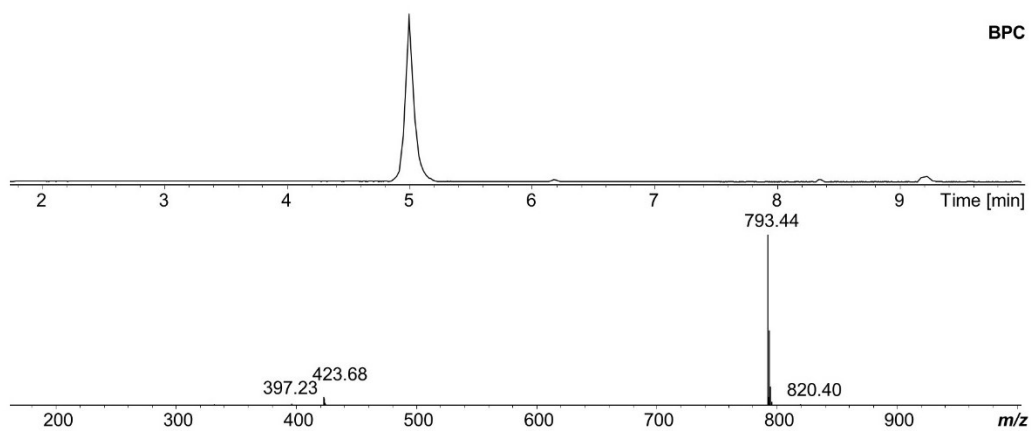


Figure S7. HPLC-MS analysis of the synthesized and purified N-acetyl-SIYKAVA peptide. The *m/z* of 793.44 [M+H]⁺ corresponds to the peptide while 397.23 [M+H]²⁺ correspond to the double charged peptide.

Supplementary information

Table S1. Chemical shifts of ^1H - and ^{13}C -NMR data of the purified compound from Figure S9 in $\text{DMSO-}d_6$ (δ_{H} 2.54, δ_{C} 40.45). The data for the ^1H -NMR was obtained via 600 MHz NMR and for ^{13}C -NMR at 125 MHz NMR. The structure of the compound is shown in Figure S10 and S11.

Position	δ_{H} mult (J, Hz)	δ_{C}	
1	7.19, m	128.29	CH
2	7.19, m	127.96	CH
3	7.19, m	128.29	CH
4	7.23, m	127.55	CH
5		141.33	C
6	7.23, m	127.55	CH
7	4.31, dd (6.0, 4.1)	78.22	CH
8	4.52, dd (6.0, 4.08)	78.39	CH
9		143.70	C
10	6.14, s	106.82	CH
11		156.27	C
12		119.04	C
13		156.27	C
14	6.14, s	106.82	CH
15-OH	5.11, d (4.1)		
16-OH	5.19, d (4.5)		
17	3.39, m	24.37	CH
18/19	1.22, d (2.58)	21.64	CH_3
18/19	1.21, d (2.74)	21.60	CH_3
20-OH	8.73, s		
21-OH	8.73, s		

Supplementary information

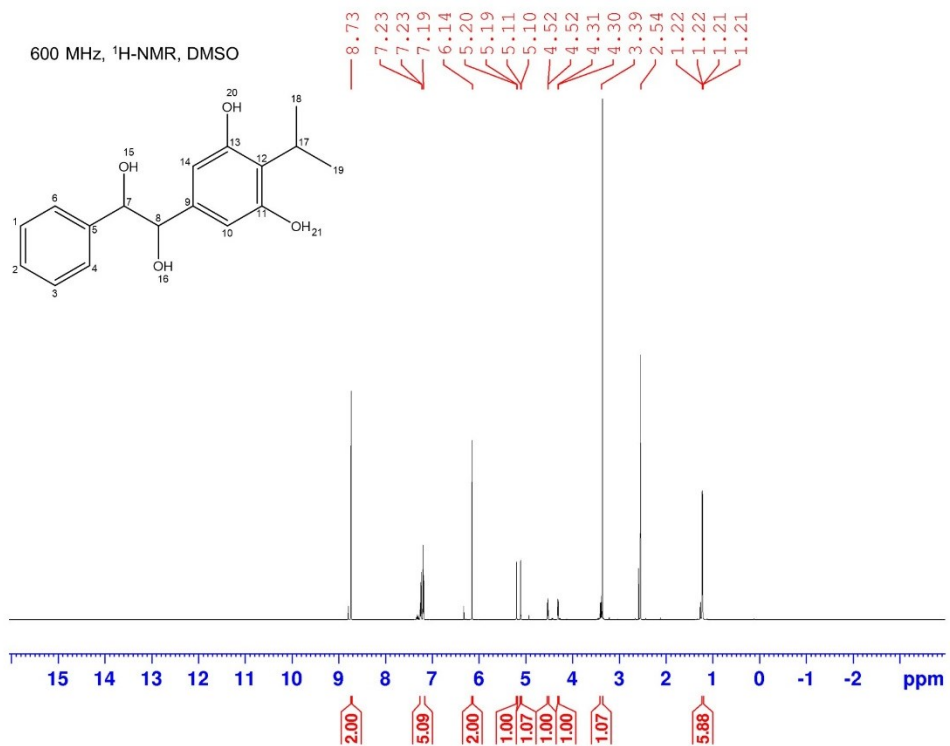


Figure S8. ¹H-NMR spectrum (600 MHz) of 5-(1,2-dihydroxy-2-phenylethyl)-2-isopropylbenzene-1,3-diol measured in DMSO-*d*₆. The chemical shifts are shown in red above the spectra in ppm and the integrals below the x-axis.

Supplementary information

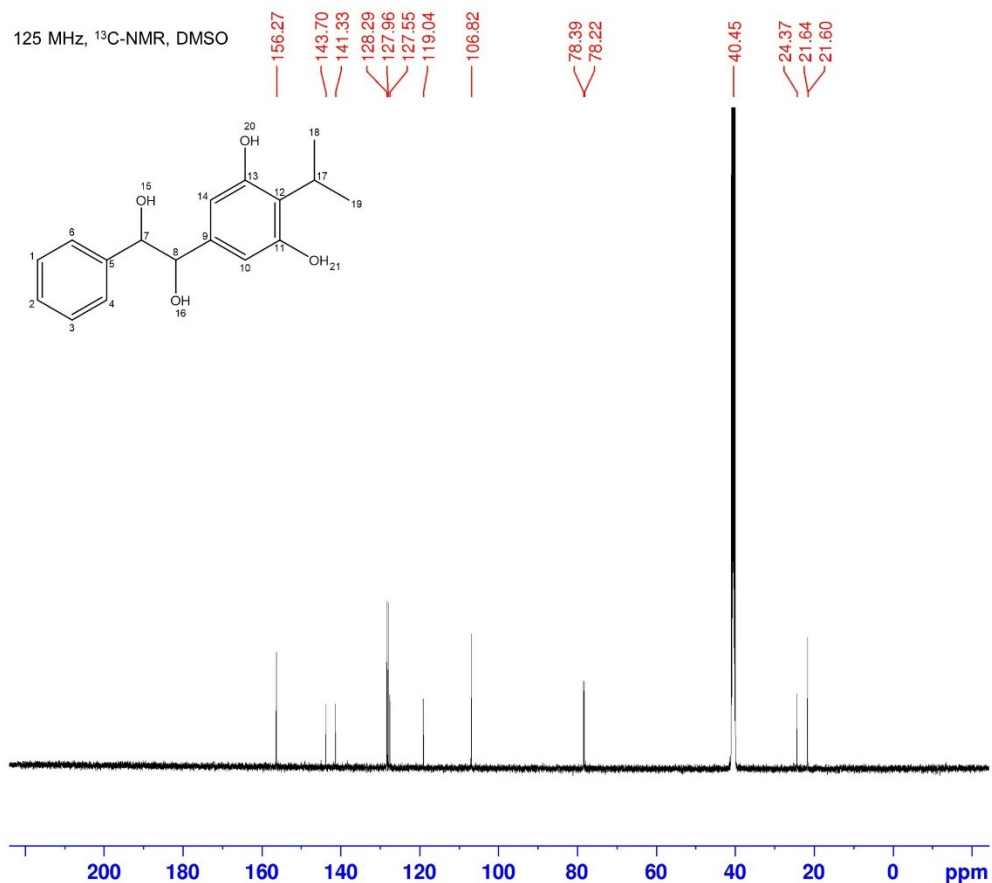


Figure S9. ^{13}C -NMR spectrum (125 MHz) of 5-(1,2-dihydroxy-2-phenylethyl)-2-isopropylbenzene-1,3-diol measured in $\text{DMSO-}d_6$. The chemical shifts are shown in red above the spectra in ppm.

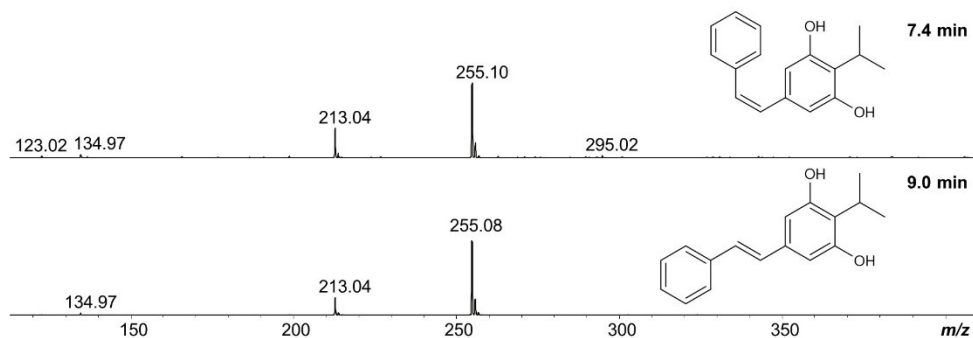


Figure S10. HPLC-MS analysis of IPS-isomers at retention times of 7.4 and 9.0 min after cultivation of induced TT01 $\Delta antJ \Delta gxpS \Delta pliA$ pex *stlA/stlCDE* pACYC-*stlF* in 4 l PP3M with 2% XAD for 2 days and separation via preparative HPLC-MS.

Supplementary information

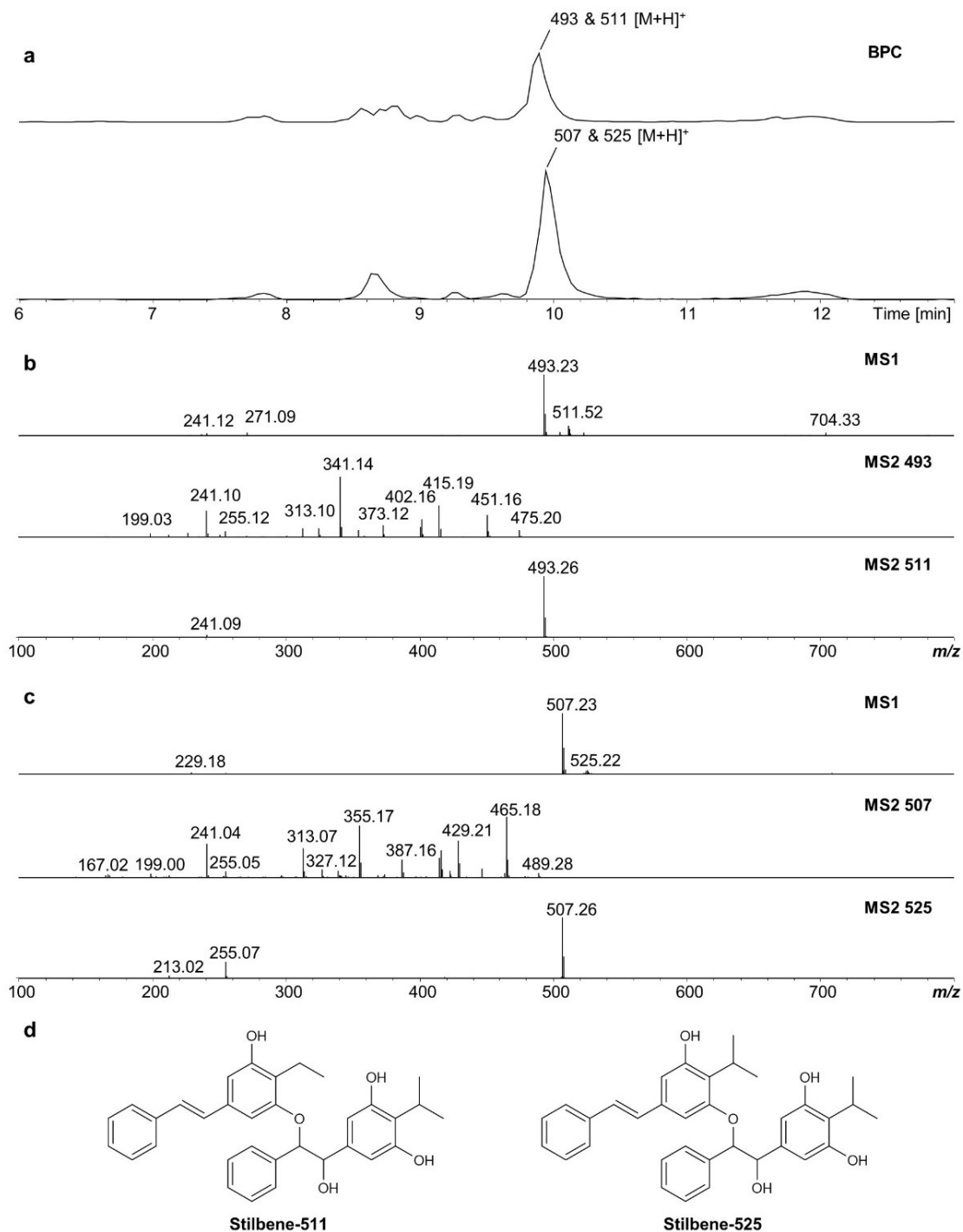


Figure S11. HPLC-MS analysis of stilbene dimers after cultivation of induced TT01 $\Delta antJ \Delta gxpS \Delta pliA$ pex *stiA/stiCDE* pACYC-*stiF* in 4 l PP3M with 2% XAD for 2 days and separation via preparative HPLC-MS. Shown are BPC (a), MS¹ and MS² fragmentations at retention times of 9.9 min (b) and 10 min (c) of two different fractions with chemical structures of proposed stilbene dimers with *m/z* of 511 and 525 (d).

Supplementary information

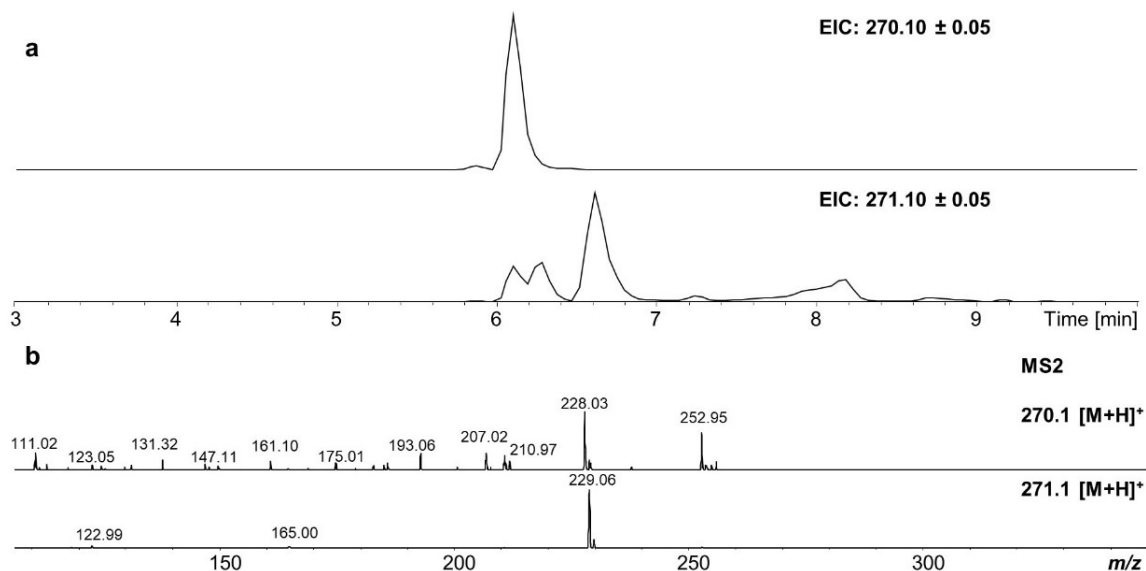


Figure S12. HPLC-MS chromatograms (a) and MS² Fragmentation patterns (b) of EPS (271.1 [M+H]⁺) and the proposed amino-stilbene derivative (270.1 [M+H]⁺) from induced TT01 $\Delta antJ \Delta gxpS \Delta pliA$ pex *stI/stICDE* pACYC-*stIF* extracts cultivated in 4 l PP3M with XAD for 2 days. The shown chromatograms were generated after the first purification step at the preparative HPLC.

Table S2. Clustal Omega alignment of ACP sequences (StIE, AntF and AcpP) from *E. coli* and *Photobacterium* strains. The consensus residues are shown as dots while the disagreements are shown. The residues highlighted in cyan build the recognition helix II.

	10	20	30	40	50	60
Consensus	MMSTIEERVKKIIXEQLGKKEEVXNXASFVXDLGAD	SLDTVELVMALEEEF			XIEIPDEE	60
StIE	- .ENL .N . . .SVVA . . .IP.TQIL .TQT .-EEN . . .IH.G.T.D . .					58
AntF	.NNHP.VKI.T.LSLF.NINIDDFNMD.NLADAYDM . .TELAD.AKEI.K . .G.SVTKSQ					60
pIAcpP	-VVV.SDD					59
ecAcpP	-GV.QT.NEDT					59
Consensus	70	80				
StIE	AEKITTVQAAIDYXXSXLEXN					82
AntFV.I.NCIG.K . . .SA.					80
pIAcpP	FSHWE.GR.VL.FVS.S.NDK.					82
ecAcpPVQNQS					78
INGHQA					78

Table S3. Clustal Omega alignment of FabH sequences from *E. coli* and *Photobacterium* strains. The consensus residues are shown as dots while the disagreements are shown.

	10	20	30	40	50	60
Consensus	MYTKIJGTGSYLPXQVVRTNADLEKMDVTSDEWIVTRTGXRERXIAXXBETVXTMGFEAAT					60
<i>E. coli</i> BL21(DE3)IEIHAPNS					60
<i>E. coli</i> DH10BIEIHAPNS					60
<i>E. coli</i> K12IEIHAPNS					60
<i>E. coli</i> P12bIEIHAPNS					60
<i>E. coli</i> K12 MG1655IEIHAQNS					60
<i>P. laumondii</i> TT01LAVRL.TDDAVRK					60
<i>P. laumondii</i> subsp <i>clarkei</i>LAVRTNDAIRE					60
<i>P. asymbiotica</i>LAVRL.TDDAVRK					60

Supplementary information

P. bodeiL.....A.....I...V...R..TDD...AV...R..K	60
P. temperataL.....A.....V...R..TDD...AM..LW..E	60
Consensus	RAIEMXGIXKQDQIGLIXVATXSXTHAFPSXACQIQSMLGKXXXAFDXXAACXGFTYALS	120
E. coli BL21(DE3)A..E.....V...T.A.....A.....I.GCP...VA...A.....	120
E. coli DH10BA..E.....V...T.A.....A.....I.GCP...VA...A.....	120
E. coli K12A..E.....V...T.A.....A.....I.GCP...VA...A.....	120
E. coli P12bA..E.....V...T.A.....A.....I.GCP...VA...A.....	120
E. coli K12 MG1655A..E.....V...T.A.....A.....I.GCP...VA...A.....	120
P. laumondii TT01	K....S..D.E..D..I..A.S.....S.....H...TQNSA...IS...S.V....	120
P. laumondii subsp clarkeiS..D...D..I..A.SS.....S.....Y...TQNSA...IS...S.A...G	120
P. asymbiotica	K....S..D.E..D..I..A.S.....S.....H...TQNSA...IS...S.V....	120
P. bodei	K....S..D.E..D..I..A.S.....S.....H...TQNSA...IS...S.V....	120
P. temperata	K....S..D...I...A.SS.....S.....H...T.NSA...IS...S.A....	120
Consensus	XADXXXKXGAXKYALVXGSDXJXRTXDPXDRGTJJJFGDGAGAXVXXASEEPIJSTHLH	180
E. coli BL21(DE3)	V..QYV.S..V...V...VLA..C..T...I.I.....A.LA.....I.....	180
E. coli DH10B	V..QYV.S..V...V...VLA..C..T...I.I.....A.LA.....I.....	180
E. coli K12	V..QYV.S..V...V...VLA..C..T...I.I.....A.LA.....I.....	180
E. coli P12b	V..QYV.S..V...V...VLA..C..T...I.I.....A.LA.....I.....	180
E. coli K12 MG1655	V..QYV.S..V...V...VLA..C..T...I.I.....A.LA.....I.....	180
P. laumondii TT01	I..KFI.T.VA.H...I...SIT..L..E...LVL.....M.VG..D...L....	180
P. laumondii subsp clarkei	I..KFI.T..A...I...SIT..L..E...LVL.....MIVG..D...L....	180
P. asymbiotica	I..KFI.T.VA.H...I...SIT..L..E...LVL.....M.VG..D...L....	180
P. bodei	I..KFI.T..A.H...I...SIT..L..E...LVL.....M.VG..N...L....	180
P. temperata	I..KFI.T..A.H...I...SIT..LN.E...L.L.....M.VG..D...L....	180
Consensus	ABGSYGELLXLPNXDRXNPEXXXXXXMXGNEVFKXAVXELAXIVDETLAANNLDRSQLDW	240
E. coli BL21(DE3)	.D.....T...A..V...NSIHLT.A.....V..T...H.....	240
E. coli DH10B	.D.....T...A..V...NSIHLT.A.....V..T...H.....	240
E. coli K12	.D.....T...A..V...NSIHLT.A.....V..T...H.....	240
E. coli P12b	.D.....T...A..V...NSIHLT.A.....V..T...H.....	240
E. coli K12 MG1655	.D.....T...A..V...NSIHLT.A.....V..T...H.....	240
P. laumondii TT01	.N.....V..YQE.Q.LKEPAYAS.I.....I..R...N...E...PY.E... 240	
P. laumondii subsp clarkei	.N.G....V..HQ..Q.R.EPAYAS.I.....I..R...NL...E...SH.A... 240	
P. asymbiotica	.N.....V..YQE.Q.LKEPAYAS.I.....I..R...N...E...PY.E... 240	
P. bodei	.N.....V..YQE.Q.LKEPAYAS.I.....I..R...N...E...PY.E... 240	
P. temperata	.N.....V..YQ..Q.RKEPAYAS.I.....I..R...NL...D...SH.E... 240	
Consensus	LVPHQANLRIIXATAKLLGMXMDXVVVTLDRHGNTSAASVPXAXDEAVRDGRKXGQLXL	300
E. coli BL21(DE3)S.....S..N.....C.L.....P..V.. 300	
E. coli DH10BS.....S..N.....C.L.....P..V.. 300	
E. coli K12S.....S..N.....C.L.....P..V.. 300	
E. coli P12bS.....S..N.....C.L.....P..V.. 300	
E. coli K12 MG1655S.....S..N.....C.L.....P..V.. 300	
P. laumondii TT01A.....N.T..K.....Y.....T.F.....R...I.. 300	
P. laumondii subsp clarkeiA.....H.T..K.....T.F.....R...I.. 300	
P. asymbioticaA.....N.T..K.....Y.....T.F.....R...I.. 300	
P. bodeiA.....N.T..K.....Y.....T.F.....R...I.. 300	
P. temperataA.....H.T..K.....T.F.....R...I.. 300	
Consensus	JEAFGGGXTWGSALXRF	317
E. coli BL21(DE3)	L.....F.....V.. 317	
E. coli DH10B	L.....F.....V.. 317	
E. coli K12	L.....F.....V.. 317	
E. coli P12b	L.....F.....V.. 317	
E. coli K12 MG1655	L.....F.....V.. 317	
P. laumondii TT01	I.....L.....I.. 317	
P. laumondii subsp clarkei	I.....L.....I.. 317	
P. asymbiotica	I.....L.....I.. 317	
P. bodei	I.....L.....I.. 317	
P. temperata	I.....L.....I.. 317	
Consensus	MYTKILGTGSYLPQAVRTNADLEKMDVTSDEWIVTRTGXRERRIAXEDETVAVMGFRAAE	60
P. laumondii TT01V...L.TD.....K 60	
P. asymbioticaV.....TN....I..... 60	
P. bodeiI...V.....TD.....K 60	

Table S4. Clustal Omega alignment of FabH sequences from *Photorhabdus* and *Xenorhabdus* strains. The consensus residues are shown as dots while the disagreements are shown.

Consensus	MYTKILGTGSYLPQAVRTNADLEKMDVTSDEWIVTRTGXRERRIAXEDETVAVMGFRAAE	60
P. laumondii TT01V...L.TD.....K	60
P. asymbioticaV.....TN....I.....	60
P. bodeiI...V.....TD.....K	60

Supplementary information

P. laumondii subsp clarkeiV....L.TD.....K	60
P. namnaonensisV.....TD.....K	60
P. temperataV.....TD.....M..LW...	60
X. beddingiiI.....A..N..L..K...	60
X. budapestensisS.....T.....I.....A..G...I.....	60
X. hominickiiI.....A...D.STL..K..A	60
X. miraniensisI.....A..N..L..K...	60
X. szentirmaiI.....A..N..TL..K...	60
X. vietnamensisI.....I.....A..N..IL..K...	60

	70	80	90	100	110	120	
Consensus	KAIEMXGIDKTQIDLIXVATXSSTHAFSSACQIQHXLGXQNSAAFDISAACXGFTYALS						120
P. laumondii TT01S....E....I...A.....M..T.....S..V....						120
P. asymbiotica	R.....S....D....I...A..S.....YM..T.....S..A...G						120
P. bodeiS....E....I...A.....M..T.....S..V....						120
P. laumondii subsp clarkeiS....E....I...A.....M..T.....S..V....						120
P. namnaonensisS....D....I...A.....M..T.....S..V....						120
P. temperataS....D....G...I...A..S.....M..TK.....S..A...						120
X. beddingiiA.....V...T.....A..V..QL..I..GVP...VA...A.....						120
X. budapestensisA..N.....V...TTGS.....KL..INSIP...A...A...A.....						120
X. hominickiiA.....V...T.....A.....L..I..GV...V...A.....						120
X. miraniensisA.....V...T.....A.....QL..I..GV...VA...A.....						120
X. szentirmaiA.....V...T.....A.....QL..IPGV...VT...A.....						120
X. vietnamensisA...A.....V...T.....A.....QL..I..GI...VA...A.....						120

	130	140	150	160	170	180	
Consensus	IXDKFIKTGAAKHALVIGSDXIXRTLDPEDRGTLLILFGDXAGAMVVGASEEPPGILSTHLH						180
P. laumondii TT01	.A.....V.....S..T.....V...G.....D.....						180
P. asymbiotica	.A.....Y.....S..T.....V...G...I...D.....						180
P. bodei	.A.....V.....S..T.....V...G.....N.....						180
P. laumondii subsp clarkei	.A.....V.....S..T.....V...G.....D.....						180
P. namnaonensis	.A...R..V.....S..T.....V...G.....N.....						180
P. temperata	.A.....V.....S..T...N.....G.....D.....						180
X. beddingii	VV.....I..S.VV..Q..S..I...A.....						180
X. budapestensis	.V.Q.....IVSKIVN...S.V...A.....A..V.....						180
X. hominickii	.V.....I..S.VV...S..I..I...A.....						180
X. miraniensis	VV.....I..S.V...S..I...A.....						180
X. szentirmai	VV.....I..S.V...I...A...L.....						180
X. vietnamensis	VV.....I..S.VV...S.V...A.....V.....						180

	190	200	210	220	230	240	
Consensus	ABGSYGELLXLPHQERQNLKEPAYXSMIGNEVFKXAVRELANIVDETLEANNLXHSQLDW						240
P. laumondii TT01	.N.....V..Y.....A.....I.....PY.E...						240
P. asymbiotica	.N.G....V...D...RE...A.....I.....L.....S..A...						240
P. bodei	.N.....V..Y.....A.....I.....PY.E...						240
P. laumondii subsp clarkei	.N.....V..Y.....A.....I.....PY.E...						240
P. namnaonensis	.N.....V..Y.....A.....I.....PY.E...						240
P. temperata	.N.....V..Y.D...R...A.....I.....L...D...S..E...						240
X. beddingii	.D.R..D..S...S.VQ.DT.E.VT.A...V.....A.....						240
X. budapestensis	.D.H...SV...D..K.GS..VT.V...V.....K...D.....						240
X. hominickii	.D.R..D..S...S.VKCDT.E.VK.A...V.....A.....						240
X. miraniensis	.D.R..D..S...RQMKGDT..VT.V...V.....A.T...						240
X. szentirmai	.D.R..D..S.A..K.TKEAS.E.VT.A...V...S...E...D.S...						240
X. vietnamensis	.D.Q..D..S.S..S.VKRDT.E.VT.A...V.....A.....						240

	250	260	270	280	290	300	
Consensus	LVPHQANLRIIXATAKLDMTMDKVVVTLDRHGNTSAASVPTAFDEAVRDGRIXRQGLIL						300
P. laumondii TT01A.....N.....Y.....K.....						300
P. asymbioticaA.....H.....K.....						300
P. bodeiA.....N.....Y.....K.....						300
P. laumondii subsp clarkeiA.....N.....Y.....K.....						300
P. namnaonensisA.....N.....Y.....K.....						300
P. temperataA.....H.....K.....						300
X. beddingiiS.....I.....Q...V...						300
X. budapestensisS.....N.....Q...V...						300
X. hominickiiS.....Q...V...						300
X. miraniensisS.....I.....Q...V...						300
X. szentirmaiS.....Q...V...						300
X. vietnamensisS.....Q...V...						300

	310	
Consensus	JEAFGGGXTWGSALXRF	317
P. laumondii TT01	I.....L.....I..	317
P. asymbiotica	I.....L.....I..	317
P. bodei	I.....L.....I..	317
P. laumondii subsp clarkei	I.....L.....I..	317
P. namnaonensis	I.....L.....I..	317
P. temperata	I.....L.....I..	317
X. beddingii	L.....F.....V..	317
X. budapestensis	L.....F.....V..	317
X. hominickii	L.....F.....V..	317

Supplementary information

X. miraniensis	L.....F.....V..	317
X. szentirmai	L.....F.....V..	317
X. vietnamensis	L.....F.....V..	317

Table S5. Clustal Omega alignment of StIA homolog sequences from *Photorhabdus* and *Xenorhabdus* strains. The consensus residues are shown as dots while the disagreements are shown.

	10	20	30	40	50	60	
Consensus	MKAKDVQPTIIIIHNGXISLEXIYHIAIKQKQKVEISTQXXXXLARGREKLEEKLSNGEVI	60					60
P. laumondii TT01NK..L...D..D.....EITEL.TH.....	60					60
P. asymbiotica	.N...I.....NE..F...D..Q..TN.....GVIDI.N.....L...	60					60
P. bodeiNK..L...D..D.....EITEL.TH.....	60					60
P. temperata-N.NV...D..N.....KDIIEL.S.....	59					59
P. thracensisN.NV...D..N.....K..KDIIEL.S.....	60					60
X. budapestensis	.NT..I.....NE..F...E..Q..T.....KGVINI.N..K...D.....	60					60
X. cabanillasii	-----MKH...P.KMT..ELR.VYQHPVQITLD..CFPAI.SSV.CVNCIISENRTA	53					53
X. indica	-----MKHMT..P.KMT..ELR.VYQHPVQITLDA.CFPAI.SSV.CVNRIISENRTA	53					53
X. nematophila	-----MKN.T.YP.QMT..ELR.VYLHPVQIKLDE.CFPAI.SSVACVNRIISENRTA	53					53
X. szentirmai	-----MKNLT..P.NMT..ELR..YQHPVQIRLDE.CFPAIANSVACVNRIISENRTA	53					53
	70	80	90	100	110	120	
Consensus	YGINTGFGGNANLVVPFZKISEHQXNLLTFLSAGTGDXMSKTCIRASQFTXLLSVCKGWS	120					120
P. laumondii TT01E..A...Q.....Y...P..K...M.....	120					120
P. asymbioticaE.....K.....Y.....V...I.....	120					120
P. bodeiE.....Q.....Y...P..K...M.....	120					120
P. temperataD.....K.....EF.....K...M.....	119					119
P. thracensisD.....K.....F...S.K...M.....	120					120
X. budapestensisE.....K.....V...Y.....V.....	120					120
X. cabanillasiiLL..TRIAEQDLE.L.RSIVMSHA..V.EPL.DEIV.LIMVLKIN.LAR.Y.	113					113
X. indicaLL..TRIAEQDLE.L.RAIVMSHA..V.EPL.DEIV.LIMVLKIN.LAR.Y.	113					113
X. nematophilaLL..TRIAEQDLE.L.RSIVMSHA..V.KPLPDDIV.LIMVLKIN.LAR.Y.	113					113
X. szentirmaiLL..TRIAEQDLE.L.RSIVMSHA..V.EPL.DDIV.LIMVLKIN.LAR.Y.	113					113
	130	140	150	160	170	180	
Consensus	ATRPIVAQTIVDHNHNDIVPLVPRYGSVGSGLXPLSYIARALCGIGKXYMGEEIPAA	180					180
P. laumondii TT01A...I.....I.....Y...A..D..	180					180
P. asymbioticaL.....I.....N.....N..	180					180
P. bodeiI.....I.....L...Y...A..D..	180					180
P. temperataA..I.....V.....Y.....S..	179					179
P. thracensisA..I.....V.....Y.....S..	180					180
X. budapestensisAN.L.....I.....Q.N.....S..	180					180
X. cabanillasii	GI.LE.I.AL.TLV.AEVY.CI.SK.....A..AHMSLL.L.E..AR.R..WL..K	173					173
X. indica	GI.LE.I.AL.TLV.AEVY.CI.SK.....A..AHMSLL.L.E..AR.R..WL..K	173					173
X. nematophila	GI.LD.I.GL.ALV.AGVY.CI.GK.....A..AHMSLL.L.E..AR.R..WL..K	173					173
X. szentirmai	GI.LD.I.ALITLV.AEVY.CI.SK.....A..AHMSLL.L.E..AR.R..WL..K	173					173
	190	200	210	220	230	240	
Consensus	EAIKXAGLTPLSLXAKEGLALINGTRVMSGISXKXVIKLEKLXKAXISXIALAVEALLAS	240					240
P. laumondii TT01	...R.....K.....AIT.....F..S..A.....	240					240
P. asymbiotica	...R.....Q.....SVT.....L..T..S.....	240					240
P. bodei	...R.....K.....AIT.....F..S..A.....	240					240
P. temperata	...H.....Q.....AVA.....F..S..A.....	239					239
P. thracensis	...H.....Q.....AVA.....F..S..A.....	240					240
X. budapestensis	...R.....Q.....GSLTI.....L..T..V.....F..	240					240
X. cabanillasii	..LAK...K.IQ.V.....L...QTSTAFAL.GLFAA.E.FASA.VCG..S...A.G.	233					233
X. indica	..LAK...KSIQ.V.....L...QTSTAFAL.GLFAA.E.LASA.VCG..S...A.G.	233					233
X. nematophila	..LEK...K.IT.V.....L...QTSTAFAL.GLFAA.D.LASA.ICG..S...A.G.	233					233
X. szentirmai	..LEK...K.IT.V.....L...QTSTAFAL.GLFAA.D.LASA.VCGSMS..S...A.G.	233					233
	250	260	270	280	290	300	
Consensus	HEHYDARIQQVKNHPGQKAVASXLRLNLEGSTQISLLXGXKEQANKACRHQEXTQLNDTL	300					300
P. laumondii TT01N...A...A...VN..S.V.....I.....	300					300
P. asymbioticaV.....T.....T...E.I.....V.R.....	300					300
P. bodeiA..D..A...VN..S.V.....V.....	300					300
P. temperataA...A...VD..S.I.....V.....	299					299
P. thracensisA...A...VD..S.I.....V.....	300					300
X. budapestensisT.....N..A.I.....I.R.....	300					300
X. cabanillasii	RKPF...HE.RGQQ..ID..ALY.FV..EQSD..AF-----HENCKTV	277					277
X. indica	RKPF...HE.RGQQ..ID..ALY.FV..EQSN..AS-----HENCCKV	277					277
X. nematophila	RKPF...HEARGQK..MD..TLY.LV..EQSG..ES-----HKNCCKV	277					277
X. szentirmai	RKPF...HEARGQK..ID..TLY.FV..EQSG..ES-----HKNCCKV	277					277
	310	320	330	340	350	360	
Consensus	QEVYSIRCAPOXLGIVPESLATARKILEREVISXNDNPLXDPENGDVHLHGNGFMGQYVAR	360					360
P. laumondii TT01V.....A...I.....	360					360
P. asymbioticaI.....A...I.....	360					360
P. bodeiI.....E.....A...I.....	360					360
P. temperataI.....S.....A...V.....	359					359

Supplementary information

P. thracensisI.....A.....I.....	360
X. budapestensisI.....V.....I.....	360
X. cabanillasii	.DT..L..Q..VM.ACLTQIRH.ADVIMV.ANAVS...VFT.QDE.IS...HAEP..M	337
X. indica	.DP..L..Q..VM.ACLTQIRY.ADVIMV.ANAVS...VFT.QDE.IS...HAEP..M	337
X. nematophila	.DP..L..Q..VM.ACLTQIRH.ADVIMV.ANAVS...VFS.EDE.IS...HAEP..M	337
X. szentirmai	.DP..L..Q..VM.ACLTQIRH.ADVIMV.ANAVS...VFA.EDE.IS...HAEP..M	337
	370 380 390 400 410 420	
Consensus	TMDALKLDIALIANHLHAIVALMMDSRFSRGLPNSLSPTPGMYQGFKGVQLSQTALVAAI	420
P. laumondii TT01N.....	420
P. asymbioticaL.....	420
P. bodeiN.....	420
P. temperataV.....N.....	419
P. thracensisV.....N.....	420
X. budapestensisI.....	420
X. cabanillasii	AS.N.AIAL.E.GALSERRI..L..NM.Q-.PF.VKNS.VNS..MIA.VTAA..ASEN	396
X. indica	AS.N.AIAL.E.GALSERRI..L..NM.Q-.PF.VKNS.VNS..MIA.VTAA..ASEN	396
X. nematophila	AS.N.AIAL.E.GALSERRI..L..NM.Q-.PF.VENS.VNS..MIA.VTAA..ASEN	396
X. szentirmai	AS.N.AIAL.E.GALSERRI..L..NM.Q-.PF.VENS.VNS..MIA.VTAA..ASEN	396
	430 440 450 460 470 480	
Consensus	RHDCXASXIHTLATEQYNQDIVSLGLHAAQDVLEMEQKLRNIVAMTILVVCQAIXLRGNI	480
P. laumondii TT01A..G.....S.....H.....	480
P. asymbioticaS..G.....Y.....	480
P. bodeiS..G.....S.....H.....	480
P. temperataA..G.....S.....I.....Y..D..	479
P. thracensisA..G.....S.....Y.....	480
X. budapestensisA..S.....Y..D..	480
X. cabanillasii	KALAH.P.SVDS.P.SANQE.H..MAPA.GRRLW..ADNV.G.L.IEW.TA..GMDF.EGL	456
X. indica	KALAH.P.SVDS.P.SANQE.H..MAPA.GRRLW..TDNV.G.L.IEW.TA..GVDF.AGL	456
X. nematophila	KALSHP.SVDS.P.SANQE.H..MAPA.GRRLW..ADNV.G.L.IEW.TA..GMDF.HGL	456
X. szentirmai	KALSHP.SVDS.P.SANQE.H..MAPA.GRRLW..ADNV.G.L.IEW.TA..GMDF.HGL	456
	490 500 510 520 530 540	
Consensus	SSXAPETAKFYHAVREISPLDXDRALDXDIIR----IADAIINDQLPLPEILLEEXLK	536
P. laumondii TT01	.EI.....S..IT.....E.....M.....	536
P. asymbiotica	.KL.....EA.....Q.....N.....I.....	536
P. bodei	.EI.....IT.....E.....I.....	536
P. temperata	.QI.....I.....VT.....E.....	535
P. thracensis	.QI.....VT.....E.....N.....I.....	536
X. budapestensis	.KL.....Q.....EI.....N.....I..D.....	536
X. cabanillasii	T.-S.ILE.AR.IL..KVTTY.K..FFSP..EMAIQLL.EQQLSAL..SGT..SNGSV..	515
X. indica	T.-S.ILE.AR.IL..KVTHY.K..FFSP..ETAIQLL.EQQLSAL..TGT..SNNNI..	515
X. nematophila	K.-S.ILE.AR.IL.NKVAHY.K..FFAP..DEAIQLL.EQQLSAL..TGK..EN.....	515
X. szentirmai	QG-S.ILE.AR.IL.NEVAHY.K..FFAP..DKAIQLL.EQQLSAL..AGK..AS.....	515
Consensus	NHIN	540
P. laumondii TT01	----	532
P. asymbiotica	----	532
P. bodei	----	532
P. temperata	----	531
P. thracensis	----	532
X. budapestensis	----	532
X. cabanillasii	519
X. indica	519
X. nematophila	----	510
X. szentirmai	----	510

Table S6. Clustal Omega alignment of StIB homolog sequences from *Photorhabdus* and *Xenorhabdus* strains. The consensus residues are shown as dots while the disagreements are shown.

	10	20	30	40	50	60	
Consensus	MEKVWLKHPADVPAEIDPDRYASLXEMFENAVAHYADQPAFINMGEVMTFRKLEERSRA						60
P. laumondii TT01V.....I.....						60
P. asymbioticaI.V.....V.....Y.....						60
P. namnaonensisV.....I.....						60
P. temperataV.....Y.....						60
P. thracensisV.....Y.....						60
X. budapestensisS..I.....RV.....V.....						60
X. doucetiaeT..I.....R..S.....						60
X. hominickiiS..I.....R..V.....						60
X. szentirmaiS..I.....R..V.....						60
X. vietnamensisV.....S..I.....C..V.....						60

Supplementary information

	70	80	90	100	110	120	
Consensus	FAAYLQNLGLXKGDVALMMPNLLQYPVALFGVLRAGMIVVNVNPLYTPRELEHQLNDS						120
P. laumondii TT01S.....						120
P. asymbioticaS...I.....S...LV.....						120
P. namnaonensisS.....						120
P. temperataS.....V...M.....						120
P. thracensisS.....V...M.....						120
X. budapestensisK.....I.....V.....T..						120
X. doucetiaeK..A.....I.....						120
X. hominickii	.S.....K.....I.....A.....						120
X. szentirmaiiK.....I.....						120
X. vietnamensisK.....I.....A.....						120
	130	140	150	160	170	180	
Consensus	GTSIAIVIVSNFAHTLEKIVFNTQVKHVILTRMGDQLSRPKGTLVDFXVKYXKRLVPKYHL						180
P. laumondii TT01K.....A...I.....N..						180
P. asymbiotica	.A.....R.....A...I.....						180
P. namnaonensisK.....A...I.....N..						180
P. temperataE.....V.....A...I.....N..						180
P. thracensisE.....L.....A...I.....N..						180
X. budapestensisP.....L.....V...V.....						180
X. doucetiae	D.....P.....F.....V...V.....						180
X. hominickiiA.....V...V.....						180
X. szentirmaiiV.....V...V.....						180
X. vietnamensisV...V.....						180
	190	200	210	220	230	240	
Consensus	PDAISFRSAIHKGYRMQYVKPDINGEDLAFMQYGGTTGVAKGAMLTNRNMLANLEQAKA						240
P. laumondii TT01C..Q.....E...N.....I.....						240
P. asymbioticaC.....D.....S.....						240
P. namnaonensisC..Q.....E...N.....I.....						240
P. temperataA.....P.....I.....S..						240
P. thracensisA.....I.....S..						240
X. budapestensisV.....N.....T..						240
X. doucetiaeM.....VQS.....						240
X. hominickiiM.....VK.....I.....						240
X. szentirmaiiM.....V.....						240
X. vietnamensisMQ.....VK.....						240
	250	260	270	280	290	300	
Consensus	VYSPLLRVGGQELIVTALPLYHIFALTXNCLLXIXLGGCNLLITNPRDIXGTXKELSRYXF						300
P. laumondii TT01MV...L.Y.....T..A...G..P..						300
P. asymbioticaMV...L.YV.....T..A...Q..						300
P. namnaonensisA.....MV...L.Y.....T..A...G..P..						300
P. temperataHS.....LV...L.Y.....A..A...P..						300
P. thracensisHS.....LV...L.Y.....V..A...P..						300
X. budapestensis	N.A...PS...VI.....I...F.E...Q.....VN...V...K..						300
X. doucetiae	C...KP...VV.....I...FF.EM..Q.....H..V...A..RV						300
X. hominickii	S.A...K..E..VI.....I...FF.E...Q.....VN...V...R..						300
X. szentirmaii	S.A...KI...I.....I...FF.E...Q.....VH...V...R..						300
X. vietnamensis	S.....Q...V.....I...FF.E...K.....VN...V...R..						300
	310	320	330	340	350	360	
Consensus	TXXXGVNTLFNAWLNNEEFQKLDLDFSSRLRVGGGMXVQKAVAQKAKXTGCHLLEGYGLT						360
P. laumondii TT01	.SVT.....K...T.....P.....V..TN.....						360
P. asymbiotica	.SVT.....K...A.....P...T.....V..RT.....						360
P. namnaonensis	.SVT.....K...T.....P.....V..TN.....						360
P. temperata	.SVT.....R.....P.....DR..EV..RP.....						360
P. thracensis	.SVT.....R.....P.....R..VEV..RP.....						360
X. budapestensis	.ALS.....P...I...A..MA...A..S...D..E..L.....						360
X. doucetiae	.ALS.....A.....S...A..RV...QNL.....						360
X. hominickii	.ALS.....SP...N...S...A..RS...QNL.....						360
X. szentirmaii	.ALS.....V..A.....N..S...A...ENL.....						360
X. vietnamensis	.ALS.....P...N...S...A..RV...QSL.....						360
	370	380	390	400	410	420	
Consensus	ECSPLVSCNPYNLKHXYGSGIFPVSSSTEIKLVDDDGNEVPIGZQGXWVRGQVMKGYWN						420
P. laumondii TT01S...T.....EM.Q...L.I.....A...A...A...						420
P. asymbioticaV.N.T.....D...T.....Q...L...V...V...						420
P. namnaonensisS...T.....EM.Q...L.I.....V...V...						420
P. temperataV...T.....Q...L...V...V...						420
P. thracensisV...T.....Q...L...V...V...						420
X. budapestensis	..A.V.AG...T..S.....P.....E.E..LQ.ES..M.....						420
X. doucetiaeA..H..T..S.....A.....GN.....SPDEV..M.....						420
X. hominickiiA..H..TY.S.....A.....GEN.....E.EA..M.....						420
X. szentirmaiiAA...D.A..S...L..A...L..IG...LP.EA..M.....						420
X. vietnamensisAA..HS.SY.S.....A.....IGN.N...L.EA..M.....						420
	430	440	450	460	470	480	
Consensus	RPDATXEVLLKDGWATGDIANXBEQGFIHIVDRKKDMILVSGFNVPNEVEDVVSXHPKV						480

Supplementary information

P. laumondii TT01E.....V.....VN...S.....A....	480
P. asymbioticaD.....V.....IN.....A....	480
P. namnaonensisE.....V.....VN...S.....A....	480
P. temperata	.H...E.....V.....VN...Y.....A....	480
P. thracensis	.H...E.....V.....VN.....A....	480
X. budapestensisD.....L.....ID.K..L.....I..S....	480
X. doucetiaeD.....L.....VD.K..F.....E...S....	480
X. hominickiiA.....L.....RID.KC.FN.....I..S....	480
X. szentirmaiiD.....E..L.....ID.N..F.....I.A.S....	480
X. vietnamensisK.....L.....ID.K..F.....S....	480

	490	500	510	520	530	540	
Consensus	LESAAIGVXSEXSGETVKVFVVRKDP	SLTEDELKTHCRRYL	TGYKVPKII	EFDELPKSN			540
P. laumondii TT01S..S.....I..G.....						540
P. asymbioticaP..S.....I..S.....						540
P. namnaonensisS..S.....I.....R.....						540
P. temperataS..S.....R.....						540
P. thracensisS..S.....R.....						540
X. budapestensisLN.N..S.....S.....A.....						540
X. doucetiaeV..P..N.....H.....L..N.....						540
X. hominickiiL.KN...I.....R.....L...E.....						540
X. szentirmaiiV..P..N.....I.....T.....A.....L.....T.....						540
X. vietnamensisV..P..N.....S.....M.....L...N.....						540

	550	560	
Consensus	VGKILRREL	RDEEXKXRN	XAXANH
P. laumondii TT01E..V..V.---		560
P. asymbioticaG..E..V..AVV.--		562
P. namnaonensisE..V..V..I.--		562
P. temperataE..V..A..I.--		562
P. thracensisE..V..A..I.--		562
X. budapestensisK.....LRKASN.K--		561
X. doucetiaeK...N..LVKDDDA.T.		564
X. hominickiiK...N..LAKADNVAKS-		563
X. szentirmaiiK...N..LEKA.K.VV.-		563
X. vietnamensisN..LAKV.N.AI.-		563

7 Attachment

Tetrahedron 128 (2022) 133116



Contents lists available at ScienceDirect

Tetrahedron

journal homepage: www.elsevier.com/locate/tet

Biosynthesis of the multifunctional isopropylstilbene in *Photorhabdus laumondii* involves cross-talk between specialized and primary metabolism

Siyar Kavakli ^{a, 1}, Gina L.C. Grammbitter ^{a, 1}, Helge B. Bode ^{a, b, c, d, *}^a Molekulare Biotechnologie, Fachbereich Biowissenschaften, Goethe Universität Frankfurt, 60438 Frankfurt am Main, Germany^b Department of Natural Products in Organismic Interactions, Max Planck Institute for Terrestrial Microbiology, 35043 Marburg, Germany^c Chemische Biologie, Fachbereich Chemie, Philipps Universität Marburg, 35043 Marburg, Germany^d Senckenberg Gesellschaft für Naturforschung, 60325 Frankfurt, Germany

ARTICLE INFO

Article history:

Received 14 August 2022

Received in revised form

20 October 2022

Accepted 22 October 2022

Available online 29 October 2022

Keywords:

In vitro biosynthesis

Michael addition

Polyketide biosynthesis

Fatty acid biosynthesis

Stilbene

Tapinarof

ABSTRACT

Isopropylstilbene (IPS) derived from the entomopathogenic bacterium *Photorhabdus* represents the only known stilbene which is not produced by a plant stilbene synthase but a bacterial PKS II synthase. While the exclusive cyclization reaction, responsible for the formation of the characteristic iso-branched side-chain of the molecule, was studied in the past, some parts of the biosynthetic route remained elusive. In this study, we revealed the role of StIB that is able to produce CoA-derivatives and demonstrated the elongation of cinnamoyl-CoA with enzymes from the bacterial fatty acid biosynthesis pathway. Thus, we deciphered cross-talk between the enzymes from primary and specialized metabolism. These insights led, for the first time, to the production of IPS in a heterologous host.

© 2022 Elsevier Ltd. All rights reserved.

1. Introduction

Stilbenes are well-known natural products usually produced by type III PKS systems (or stilbene synthases, STS) in plants. The biosynthetic mechanism is well-described and involves elongation of cinnamoyl- or coumaroyl-CoA thioesters with three malonyl-extender units [1–3]. Subsequent cyclization and aromatization leads to the formation of stilbenes, giving rise to resveratrol, pterostilbene and pinosylvin as some examples for this compound class, which is widespread in plants (Fig. 1) [4].

The only non-plant stilbene is isopropylstilbene (IPS, Fig. 1, 1) and derivatives thereof produced in *Photorhabdus* strains (Fig. 1) [5–11]. IPS is found in all *Photorhabdus* strains analyzed so far and can be regarded as a species-specific biomarker [12]. *Photorhabdus* lives in mutualistic symbiosis with *Heterorhabditis* nematodes,

acting together as an insect pathogen complex [13–15]. It has been proven that IPS is required for nematode development, is important for the mutualistic symbiosis between bacterium and nematode, might act as live cycle signal for *Photorhabdus* itself and shows developmental and behavioral effects on other nematodes as well [5,16,17]. Due to its antimicrobial activity, IPS might furthermore serve as a protection against microbial competitors during insect infection. Additionally, IPS inhibits protozoa and even the mammalian soluble epoxide hydrolase, which is involved in the arachidonic acid cascade and thus in several inflammatory processes [5]. IPS is also known as tapinarof or benvitimid selectively modulating the cytokine cascade deep under the skin when applied as atopic cream [18]. Within the last years it was developed as treatment against psoriasis, recently approved by the FDA and marketed as Vtama® [5,18–20].

Interestingly, *Photorhabdus laumondii* utilizes a non-plant-like mechanism to produce IPS that relies on the condensation of two intermediates derived from different biosynthetic routes (Fig. 2b) which is crucial for obtaining the iso-branch [5,6,21]. The corresponding genes are distributed within the genome and are encoded as stand-alone genes or short operons (*stiA* and *stiB*, *stiCDE* and

* Corresponding author. Department of Natural Products in Organismic Interactions, Max Planck Institute for Terrestrial Microbiology, 35043 Marburg, Germany.

E-mail address: helge.bode@mpi-marburg.mpg.de (H.B. Bode).

¹ authors contributed equally.

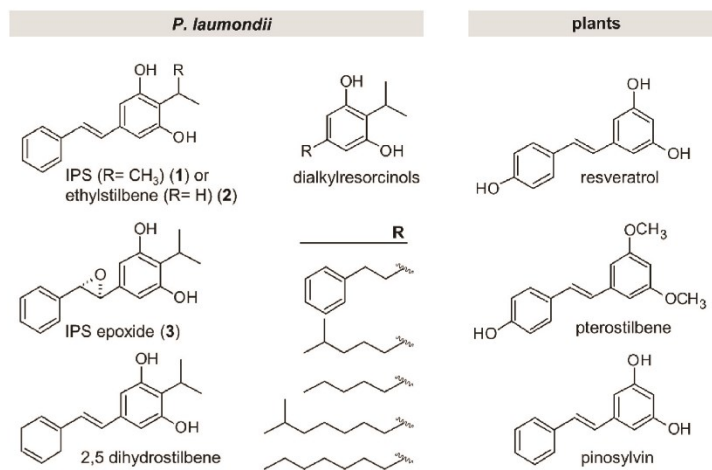


Fig. 1. Selected stilbene and dialkylresorcinol (DAR) compounds produced by *P. laumondii* and stilbene representatives from plants.

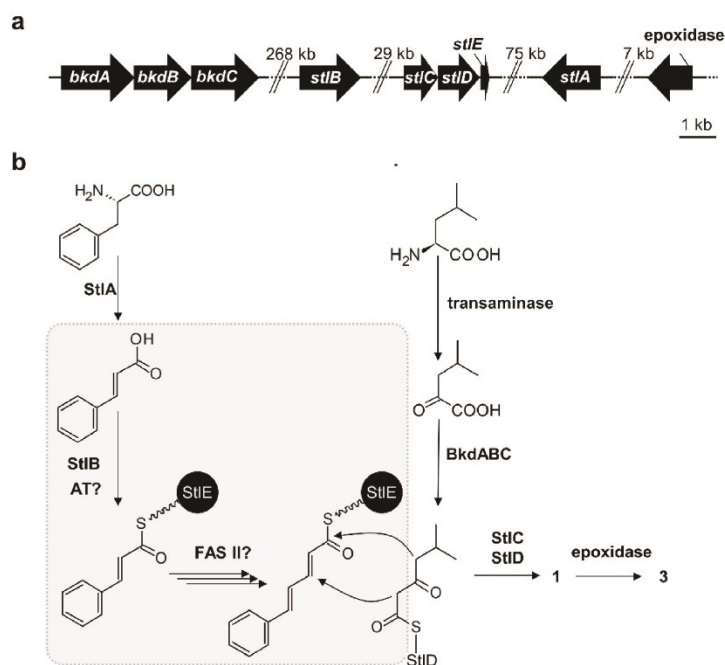


Fig. 2. Genes involved in IPS production (a) and suggested IPS biosynthesis (b) in *P. laumondii*. *BkdABC* = branched-chain- α -keto acid dehydrogenase with ketosynthase (*plu1883-1885*), *StlB* = CoA ligase (*plu2134*), *StlC* = aromatase (*plu2163*), *StlD* = ketosynthase/cyclase (*plu2164*), *StlE* = acyl-carrier protein (*plu2165*), *StlA* = phenylalanine ammonium lyase (*plu2234*), epoxidase = *plu2236*, *AT* = acyltransferase, *FAS II?* = fatty acid synthase type II. Highlighted in grey are steps, which were investigated by *in vitro*-studies.

bkdABC) (Fig. 2a). IPS-biosynthesis starts with the generation of cinnamic acid from phenylalanine catalyzed by a phenylalanine ammonia lyase (PAL, *StlA*). *StlB* is proposed to act as a CoA-ligase,

activating cinnamic acid to cinnamoyl-CoA. The acyl moiety of cinnamoyl-CoA is suggested to be transferred on an acyl-carrier protein (ACP) followed by elongation, reduction and dehydration

steps to obtain 5-phenyl-2,4-pentadienoyl-ACP. Since there are no ketosynthase, ketoreductase or dehydratase encoded in the *Photobacterium* genomes in proximity with the already known genes, these reactions might be performed by enzymes from the fatty acid biosynthesis. To date, there is no proof for this hypothesis and furthermore, no acyltransferase transferring the acyl-moiety of cinnamoyl-CoA to the ACP (StIE) was identified so far. The dependence of these reactions on StIE was shown from analysis of a *ngrA* deletion [5]. *NgrA* is an Sfp-type PPTase that is required for the biosynthesis of most PKS and non-ribosomal peptide synthetase derived peptides in *P. laumondii* TT01 [22]. The Michael acceptor 5-phenyl-2,4-pentadienoyl-StIE is further cyclized and aromatized with a β -ketoacyl isovalerate moiety derived from the branched-chain- α -keto acid dehydrogenase (BKD) complex (BkdABC), leading to IPS formation with the characteristic iso-branched side chain of stilbenes produced from *P. laumondii* (Fig. 2b) [5,6]. While the exclusive cyclization reaction was studied in the past with an *in vitro*-approach of the condensation (StID) and subsequent aromatization (StIC) and with X-ray crystallography of the cyclase/ketosynthase (CYC/KS) StID, the formation of the native substrate 5-phenyl-2,4-pentadienoyl-StIE remained elusive [21].

Here, we report the *in vitro* substrate characterization of StIB and furthermore the conversion of cinnamoyl-CoA to 5-phenyl-2,4-pentadienoyl-StIE by the orchestration of enzymes from the fatty acid biosynthesis pathway. Furthermore, we focused on IPS production in a heterologous *E. coli* host.

2. Results and discussion

We started our investigations by characterizing StIB for its postulated function as a CoA ligase. Although cinnamic acid is the proposed natural substrate, cinnamoyl-CoA was hardly detectable during *in vitro* analysis with purified StIB via MALDI-MS when compared to CoA derivatives generated from fatty acid substrates including chain length from C₆ to C₁₆ (Fig. S1, Table S5).

To rule out any ionization problems of cinnamoyl-CoA compared to the fatty acid acyl-CoA thioesters, we analyzed reactions with cinnamic, caproic, heptanoic and palmitic acid with HPLC-UV-MS and were able to detect all formed CoA-esters by UV (260 nm, Fig. S2) and MS (Fig. S1) except cinnamoyl-CoA.

We further observed that StIB accepts some cinnamic acid derivatives but discriminates substituents in the *para*-position (Table S5). These findings are in accordance with previously conducted mutasynthesis experiments, where *para*-substituted cinnamic acid derivatives did not lead to novel IPS derivatives in *P. laumondii*, while meta-substituted substrates were incorporated by the producer [23].

Since *stlB* is annotated as a FadD homolog, a fatty acyl-CoA synthetase, converting fatty acids to acyl-CoAs for further fatty acid degradation [24], its influence on the fatty acid degradation profile was studied. Supplementation of TT01 cultures with azido-labelled palmitic acid (C₁₆-fatty acid) and application of click-chemistry showed no difference between WT and *stlB* mutant since both showed similar degradation profiles in the HPLC-MS analysis (Figs. S3 and S4). Thus, we could not verify the characteristics of StIB as a FadD enzyme.

The importance of *stlB* for IPS production was further assessed by introduction of an insertion mutation which resulted in the loss of the production (Fig. S5).

Since StIB produces less cinnamoyl-CoA than fatty acyl-CoA *in vitro*, we tested StIB for its activity as an adenylating enzyme, thus being capable of direct-loading of adenylated cinnamoyl-

precursor to *holo*-StIE. Such enzymes are known as acyl-acyl carrier protein synthetases (AasS) or AMP-ligases [25–28]. Hence, we purified the ACP StIE and transferred it into its *holo*-form with the PPTase Sfp [29]. When we tested StIB for AasS activity in the presence of cinnamic acid and *holo*-StIE, we were indeed able to show the transferase reaction (Fig. 3a). Hence, we suggested StIB to substitute the “missing” acyltransferase responsible for cinnamic acid activation and StIE acylation to result in cinnamoyl-StIE. Furthermore, analysis of StIB with fatty acid substrates demonstrated acyl transfer of the fatty acid substrates and also acylation of AcpP from *E. coli* (Fig. S6). StIE and the *E. coli* derived AcpP share around 60% sequence identity and around 80% in the region of the helix II which is essential for the recognition and interaction with other proteins leading to similar interaction partners between those two ACPs [30].

IPS biosynthesis requires the formation of 5-phenyl-2,4-pentadienoyl-StIE as substrate for the cyclization reaction catalyzed by the ketosynthase/cyclase StID (see Fig. 2b) [5,6,21]. StID only accepts unsaturated intermediates [6,21]. Hence, the elongation of cinnamoyl-StIE and its subsequent reduction and dehydration is crucial for cyclization. Since none of the required enzymes, namely a ketosynthase, ketoreductase and a dehydratase, are encoded next to the known IPS biosynthesis enzymes, we tested enzymes from the fatty acid biosynthesis of *P. laumondii* as possible candidates for these reactions. For elongation reaction, we selected FabH, FabB and FabF as plausible ketosynthase candidates, as the special ketosynthase StID is not able to fulfill this task. FabH is usually responsible for the initial elongation of acetyl-CoA starter with malonate as elongation units in FA biosynthesis, while FabB and FabF are responsible for elongation of longer acyl-ACP supported by distinct protein-protein interactions [31,32]. In our *in vitro* analysis with purified enzymes (Fig. S7), only FabH was able to elongate the cinnamoyl-moiety with malonyl-ACP to its β -ketoacyl product, while FabB or FabF were not (Fig. S8). These findings contradict with the usual role of FabH as a priming ketosynthase involved in the initiation of the biosynthesis with a short chain acyl-CoA in the fatty acid metabolism. It is also in contrast to the ability of StIB to act as an AasS enzyme within the pathway that would not require an extra FabH for the procession of a CoA-bound moiety. However, we showed that in the *in vitro* approach cinnamoyl-CoA was sufficient for the procession into 5-phenyl-2,4-pentadienoyl-StIE since the cinnamoyl-moiety is loaded onto StIE (Fig. 3b, m/z 1120.36 [M+H]⁺) in that reaction setup and that further ketoreduction was performed by FabG and dehydration by FabA or FabZ (Fig. 3b).

Although the dehydrated product was formed even without the addition of either FabA nor FabZ, the amount of dehydrated product was increased upon the addition of a dehydratase (Fig. 3b). Furthermore, in the absence of the dehydratases, the amount of the dehydrated side product remained stable upon 2 h incubation time, which is equivalent to the incubation time used for the assay (Fig. S9).

With the gained knowledge from our *in vitro*-assays, we focused on the production of stilbene compounds in a heterologous host. So far, only dialkylresorcinol (DAR) compounds, lacking the cinnamoyl side chain, were detected in heterologous expression experiments with StCDE-homologs [33]. Having now identified all key players for stilbene biosynthesis, for the first time, we successfully produced IPS (**1**) in 0.61 ± 0.09 mg/L in a heterologous *E. coli* host (Fig. 4). The quantification was achieved by preparation of a standard curve of purified IPS from *P. laumondii* via HPLC-MS and cultivation of triplicates from the *E. coli* production strain. The

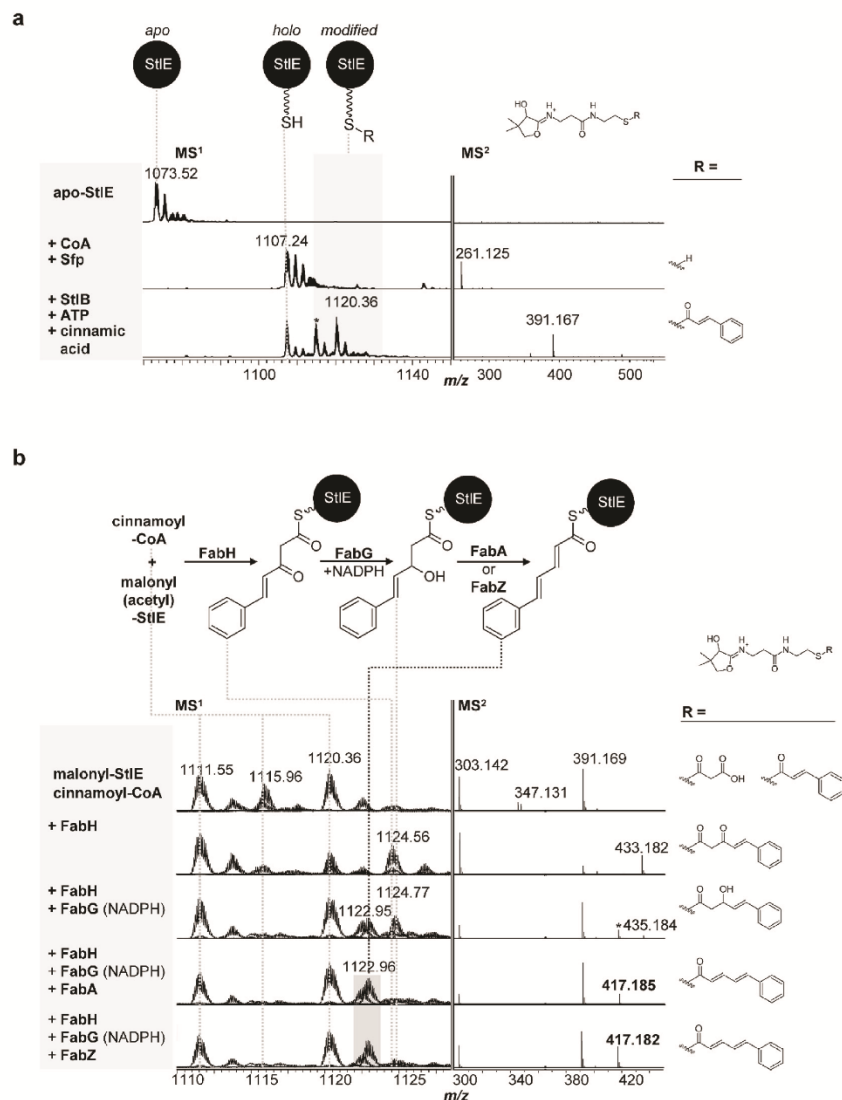


Fig. 3. AaS loading of StIE catalyzed by StIB. apo-StIE was transferred to holo StIE with Sfp. holo-StIE was transferred to cinnamoyl-StIE by the AaS activity of StIB. Reaction marked with an asterisk indicates an unknown side product arising during overnight incubation (a). *In vitro* elongation, ketoreduction and dehydration reaction with FAS II enzymes FabH, FabG (+NADPH), FabA, FabZ from *P. laumondii* and cinnamoyl-CoA as starter and malonyl-ACP as elongation unit. Spectra were overlaid as described in the experimental section. Signal marked with an asterisk represents the dehydrated product without the addition of FabA/FabZ (b).

production of **1** was achieved by co-expression of *stCDE*, *stIB*, *plFabH*, *plFabG* and *plBkdABC* and cinnamic acid supplementation. It was not necessary to express *ngrA* since the *E. coli* PPTases were able to catalyze the modification of StIE from apo- to holo-form.

3. Conclusion

We revealed the missing parts of the IPS biosynthesis from *P. laumondii* to generate 5-phenyl-2,4-pentadienyl-StIE, the

required precursor for cyclization reaction by the KS/CYC StID (Fig. 5). We demonstrated that StIB is able to acylate the cognate ACP StIE to form cinnamoyl-StIE and cinnamoyl-CoA. Cinnamoyl-CoA is further used by enzymes from FAS II biosynthesis for elongation, reduction and dehydration reaction, mediated by FabH, FabG and FabA or FabZ, respectively. While especially the role of FabH in the biosynthesis requires further investigations including structural biology data, our data shows that the IPS biosynthesis is another example of cross-talk between FAS II enzymes from

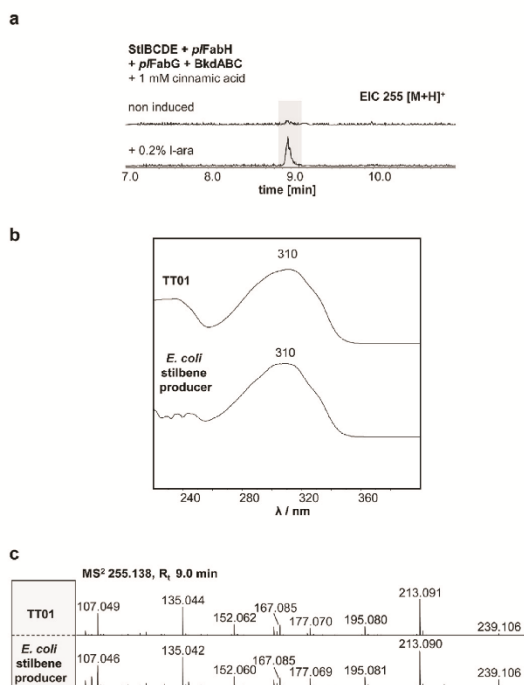


Fig. 4. Heterologous stilbene production in *E. coli*. Analysis of IPS production after cultivation of *E. coli* DH10B with introduced *stIBCDE*, *pIFabHbkdABC* and *pIFabG*. The cultures were supplemented with 1 mM cinnamic acid. The crude extracts of the corresponding strains were analyzed by HPLC-UV-MS in positive mode. The EIC of IPS (255.138 ± 0.005 [M+H]⁺) is depicted (a) and compared to the UV and MS-MS data from IPS isolated from *P. laumondii* TT01 (b and c).

primary metabolism and proteins from specialized metabolism. Similar cross-talk between specialized and primary metabolism and metabolites was described in the formation of the rhabdoplans formed via an 'Ugi-like' reaction, including building blocks from primary metabolism and the specialized metabolite rhabduscin [34]. Our results helped us to further select the minimal gene set needed for the production of isopropylstilbenes in a heterologous host. These efforts might be the starting point for further engineering strategies in order to produce additional stilbene derivatives in the future.

4. Experimental section

4.1. Cloning

For isolation of genomic DNA from *P. laumondii*, Genra Pure-gene Yeast/Bact Kit (Qiagen) was used. Polymerase chain reaction (PCR) was performed with Phire Hot Start II DNA polymerase (Thermo Scientific), Phusion High-Fidelity DNA Polymerase, or Q5 polymerase (New England Biolabs) according to manufacturers' instructions. Oligonucleotides were purchased from Eurofins Genomics. The Invisorb Spin DNA Extraction Kit (Stratagene) was used for DNA purification from agarose gels. Plasmid isolation was performed with the Invisorb Spin Plasmid Mini Two Kit (Stratagene). Plasmid-backbone PCRs were restriction digested with *DpnI* (New England Biolabs) following the manufacturers' protocol. All used

primers and templates and final plasmids are listed in Tables S2 and S3. If not stated otherwise, all plasmids were cloned via Hot Fusion [35] reaction with corresponding primers listed in Table S2. *plu2134* gene region was amplified using TS120 and TS121, generating a PCR product of 649 bp, which was digested (*SacI* and *SphI*) and ligated (T4 DNA ligase, Sigma) into the linearized vector (*SacI* and *SphI*) pDS132. *E. coli* S17λpir (pDS132_*plu2134*) and *E. coli* DH10B (remaining plasmids) were used as cloning strains and electro-transformed with desalted ligation/Hot Fusion reaction (MF-Millipore membrane, VSWP, 0.025 μm).

4.2. Generation of TT01 mutant

The *plu2134* (*stlB*)-insertion mutant of *P. laumondii* TT01 was created by conjugation with the *E. coli* S17λpir strain harboring pDS132_*plu2134*, which carries the first 578 bp of *plu2134*, as described earlier for creating insertion-mutants [36]. As a result, in a homologous recombination event, the plasmid backbone is inserted within the gene of interest in the case of *plu2134*, resulting in a non-functional gene (*plu2134*-insertion, *P. laumondii* TT01::pDS132_*plu2134*).

Therefore, both strains, *P. laumondii* TT01 and *E. coli* S17λpir with pDS132_*plu2134*, were grown in 10 mL LB-medium (10 g/L tryptone, 5 g/L yeast extract and 5 g/L NaCl at pH 7.5) (*E. coli* S17λpir was supplemented with 35 μg/mL chloramphenicol) to an OD₆₀₀ of 0.6–0.8. Cells of 1 mL culture were harvested, washed and resuspended in 400 μL LB and mixed in a ratio of 3:1 (75 μL TT01:25 μL *E. coli*) prior to pipetting them in one drop on an LB agar plate. After 1 d at 30 °C, cells were resuspended in 1 mL LB. Insertion mutants were selected by streaking several dilutions of cell suspension on LB-Cm^R-Rif^R (35 μg/mL and 100 μg/mL, respectively) agar plates. Positive insertion mutants were PCR-verified with primer TS122 and pDS132_rev leading to an 1147 bp product.

4.3. Click reaction and XAD-extraction of TT01 wildtype and mutants

The fatty acid degradation profile of *P. laumondii* was analyzed via feeding of azido palmitic acid followed by a click reaction with bicyclononyne (BCN) [37]. Therefore, pre-cultures of TT01 and mutants were grown overnight in LB-medium. The following day appropriate cell material was used for inoculation of the main cultures to an OD₆₀₀ of 0.1, supplemented with 0.1 mM azido palmitic acid and incubated for 24 h at 30 °C and 200 rpm. After 2 h, 4 h, 6 h, 10 h, 20 h and 24 h, 1 mL cell culture of each strain was harvested and stored at –20 °C. The click reaction of (the degraded) azido palmitic acid was performed as previously described [37]. Briefly, the cell pellet was resuspended in 500 μL 1 M NaOH and incubated for 1–2 h at 85 °C and 750 rpm on a thermocycler. The solution was acidified with 100 μL 6 M HCl prior to extraction with 800 μL hexane. 600 μL of the organic layer was evaporated under reduced pressure. The click reaction was performed with 150 μL of 0.2 mM BCN (in ACN) and incubated overnight at RT. A 1:10 dilution of each click reaction was analyzed via HR-HPLC-MS. The expected masses of the click products are listed in Fig. S3.

To obtain a comparable growth rate of wildtype and mutant strains, the cultivation was carried out without the addition of antibiotics. After 72 h, the plasmid insertion of *P. laumondii* TT01::pDS132_*plu2134* was proven (no production of 1) by HPLC-MS (Fig. S5). Therefore, the strain was cultivated in 10 mL LB as described above, with further supplementation of 2% Amberlite® XAD-16 (Sigma-Aldrich) beads. After 48 h, the XAD-beads were extracted with 10 mL MeOH, filtrated and dried under reduced pressure. Samples were further analyzed by HPLC-UV/MS.

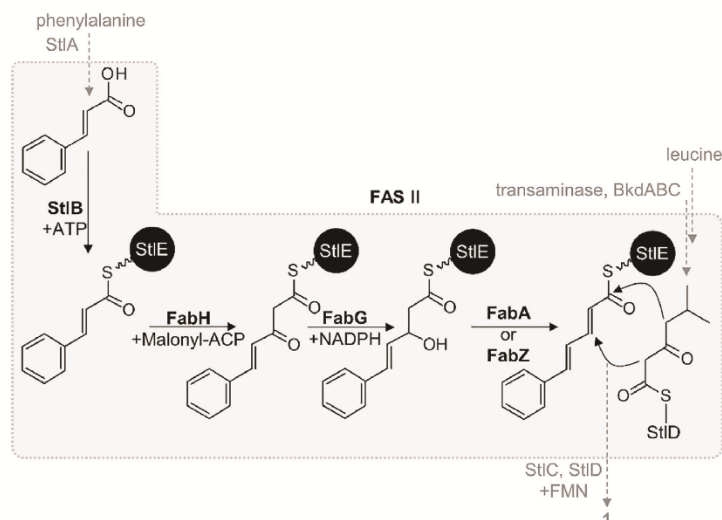


Fig. 5. Extended IPS-biosynthesis. The cinnamoyl moiety of the adenylated precursor is loaded to StIE by the acyl-acyl-carrier protein synthetase (AasS) activity of StIB before being elongated with one malonate unit by FabH. The resulting β -ketoacyl product is further reduced and dehydrated by FabG and FabZ/FabA. StIB = AasS, FabH = ketosynthase; FabG = ketoreductase; FabA/FabZ = dehydratase; FAS II = fatty acid synthase type II, StIC = aromatase, StID = ketosynthase/cyclase; BkdABC = branched-chain- α -keto acid dehydrogenase with ketosynthase (for further details see Fig. 2).

4.4. Heterologous stilbene production

DH10B was transformed with the production plasmids listed in Table S4, respectively.

For detection of IPS (1), extracts from 10 mL LB-culture of each strain were prepared upon XAD-bead addition. Therefore, the corresponding overnight pre-culture was used for inoculation of 10 mL LB-medium to an OD_{600} of 0.2 and supplemented with 0.2% L-arabinose, with and without 1 mM cinnamic acid (Sigma-Aldrich) (from 100 mM cinnamic acid stock solution in ethanol) and 2% Amberlite® XAD-16 (Sigma-Aldrich) resin. After 48 h, XAD-beads of each culture were extracted with 10 mL MeOH, filtered and dried under reduced pressure. For HR-HPLC-MS measurement, the samples were dissolved in 1 mL MeOH.

4.5. Protein production and purification

E. coli BL21 (DE3) was transformed with protein production plasmids (Table S3). Protein production was achieved using an auto-induction protocol [5]. Therefore 1 L LB-medium was supplemented with 20 mL 50 \times 5052 (25% glycerol, 2.5% glucose, and 10% α -lactose monohydrate), 50 mL 20 \times NPS (1 M Na_2HPO_4 , 1 M KH_2PO_4 , and 0.5 M $(NH_4)_2SO_4$), 1 mL 1 M $MgSO_4 \cdot 7H_2O$ and the respective antibiotics (35 μ g/mL chloramphenicol, 50 μ g/mL kanamycin, 50 μ g/mL Spectinomycin, 20 μ g/mL Gentamicin). This auto-induction medium was inoculated with the appropriate pre-culture and incubated at 37 $^\circ$ C and 180 rpm to an OD_{600} = 0.4–0.8, cooled down for 15–45 min at 4 $^\circ$ C and incubated overnight at 25 $^\circ$ C and 180 rpm.

Purification of Strep-tagged StIB, StIE, FabB, pIFabF, pIFabH, pIFabG, pIFabA, pIFabZ. Cells were harvested and resuspended in Strep-tag binding buffer (400 mM NaCl, 50 mM Tris, pH 8, pH 8.5 StIB, pH 7.4 StIC) and with the addition of one tablet cOmplete Protease Inhibitor Cocktail (Roche) and lysozyme incubated for 20–50 min

at 4 $^\circ$ C. After cell lysis by sonication, cell debris was removed by centrifugation (35 min, 20,000 rpm, 4 $^\circ$ C) and the supernatant was passed over a 5 mL StrepTrap HP column (GE Healthcare) by an ÄKTApurifier system (GE Healthcare). Proteins were eluted with Strep-tag elution buffer (400 mM NaCl, 50 mM Tris, 2.5 mM d-thiobiotin, pH 8, pH 8.5 StIB, pH 7.4 StIC). All proteins were buffer exchanged in storage buffer (20 mM HEPES, 1 mM DTT, 25% (v/v) glycerol, pH 8), concentrated to 2–10 mg/mL using Amicon concentration devices (Merck, 3000 or 10,000 Da cut-off filter) and stored in aliquots at -80 $^\circ$ C until needed. StIB was directly used after purification.

Purification of His₆-tagged Sfp-SUMO. Cells were harvested and resuspended in His-tag binding buffer (300 mM NaCl, 20 mM Tris, 20 mM imidazole, pH 8.5) and with addition of one tablet cOmplete Protease Inhibitor Cocktail (Roche) and lysozyme incubated for 20–50 min at 4 $^\circ$ C. After cell lysis by sonication, cell debris was removed by centrifugation (35 min, 20,000 rpm, 4 $^\circ$ C) and the supernatant was passed over a 5 mL HisTrap FF column (GE Healthcare) by an ÄKTApurifier system (GE Healthcare). Proteins were eluted with His-tag elution buffer (300 mM NaCl, 20 mM Tris, 500 mM imidazole, pH 8.5) and buffer exchanged in storage buffer (20 mM HEPES, 1 mM DTT, 25% (v/v) glycerol, pH 8.5) using a PD-10 desalting column (Amersham Biosciences). Proteins were further concentrated to 2–10 mg/mL using Amicon concentration devices (Merck, 3000 Da, 10,000 Da, or 30,000 Da cut-off filter, respectively) and stored in aliquots at -80 $^\circ$ C until needed.

Proteins were separated on 10–15% SDS-polyacrylamide gels and visualized with Coomassie Brilliant Blue G250.

4.6. In vitro reactions

4.6.1. CoA ligase activity assay

Reaction was performed in reaction buffer (10 mM Tris, 1 mM DTT, pH 8.5) with 1 mM CoA, 2 mM ATP, 5 mM $MgCl_2$, 1 mM acid-

substrate (Table S5) (solubilized as 10 mM stock in ethanol), 25 μ M StIB (in Strep-elution buffer) and incubated for 1 h at 37 °C. Reactions were analyzed by HR-HPLC-MS.

4.6.2. AasS activity of StIB

StIE (ACP) or ecACP (AcpP) was buffer exchanged in reaction buffer (10 mM Tris, 1 mM DTT, pH 8.5) with PD SpinTrap G-25 columns (Amersham Biosciences) and reactions were performed using 50 μ M ACP, 1 mM CoA, 0.5 μ M Sfp-SUMO (in storage buffer), 2 mM ATP, 5 mM MgCl₂, 1 mM acid-substrate (Table S5) (solubilized as 10 mM stock in ethanol), 5–15 μ M StIB (in storage buffer) and incubated over night at 30 °C. Reactions were analyzed by HR-HPLC-MS.

4.6.3. Preparation of malonyl-StIE (elongation-ACP)

ACP StIE was buffer exchanged in reaction buffer (10 mM Tris, 1 mM DTT, pH 8.5) with PD SpinTrap G-25 columns (Amersham Biosciences). Reactions were performed using 50 μ M StIE, 1 mM malonyl-CoA, 0.5 μ M Sfp-SUMO (in storage buffer) and incubated for 1 h at 30 °C. The reaction was analyzed by HR-HPLC-MS.

4.6.4. Chain elongation, ketoreduction and dehydration with FAS II enzymes

Starter-CoA and elongation-ACP assay were mixed 1:2 and chain elongation reaction was performed by adding 10 μ M FabH or FabB or FabF and further incubated for 1 h at 30 °C, prior to adding 10 μ M FabG and 1 mM NADPH for ketoreduction reaction and 10 μ M FabA or FabZ for dehydration reaction.

All ACP-bound *in vitro* reactions were analyzed using HR-HPLC-MS. MS and MS-MS BPC and TIC spectra were summarized according to the retention time of modified ACP. If the retention time of two ACP species differed more than 0.4 min, the separately summarized spectra were overlaid. Theoretical average masses of modified ACPs were predicted using IsotopePattern (Bruker).

4.7. HR-HPLC-UV/MS

Click-reactions and XAD extracts of TT01 and TT01 mutants as well as *in vitro*-assays of CoA ligase and ACP-bound reactions were analyzed via high resolution (HR)-HPLC-ESI-UV-MS using a Dionex Ultimate 3000 LC system (Thermo Fisher) equipped with a DAD (Impact II) or MWD (micrOTOF II)-3000 RS UV-detector (Thermo Fisher) and coupled to an Impact II or micrOTOF II electrospray ionization mass spectrometer (Bruker).

Click-reactions and XAD extracts. Separation of Click-reaction and XAD extracts was achieved on a C18 column (ACQUITY UPLC BEH, 50 mm \times 2.1 mm \times 1.7 μ m, Waters) using H₂O and ACN containing 0.1% (v/v) formic acid as mobile phases. HPLC was performed at a flow rate of 0.4 mL/min with 5% ACN equilibration (0–2 min) followed by a gradient from 5 to 95% ACN (2–14 min, 14–15 min 95% ACN) ending with a re-equilibration step of 5% ACN (15–16 min). For internal mass calibration, 10 mM sodium formate was injected. The HPLC-MS analysis was set to negative mode with a mass range of *m/z* 100–1200 with and an UV at 190–800 nm.

CoA ligase-reaction (Impact II). Analysis of CoA-esters was performed on a C18 column (ACQUITY UPLC BEH, 50 mm \times 2.1 mm \times 1.7 μ m, Waters) using MeOH and 50 mM ammonium acetate as mobile phases. HPLC was performed at a flow rate of 0.3 mL/min with 5% ACN equilibration (0–2 min), followed by a gradient from 5 to 95% ACN (2–14 min, 14–15 min 95% ACN) ending with a re-equilibration step of 5% ACN (15–16 min). For internal mass calibration, 10 mM sodium formate was injected.

ACP-bound reactions (micrOTOF II). Analysis of ACP derivatives was performed with a C3 column (Zorbax 300SB-C3 300 Å, 150 mm \times 3.0 mm \times 3.5 μ m, Agilent). ACN and H₂O containing 0.1%

(v/v) formic acid were used as mobile phases at a flow rate of 0.6 mL/min. HPLC was performed with 30% ACN equilibration (0–1.5 min), followed by a gradient from 30 to 65% ACN (1.5–27 min) and a further elution step with 95% ACN (27–30 min). For internal mass calibration, an ESI-L Mix (Agilent) was injected.

For data analysis of UV-MS-chromatograms, Compass Data-Analysis 4.3 (Bruker) was used. The theoretical average masses of StIE and ecACP were calculated using Compass IsotopePattern 3.0 (Bruker).

4.8. MALDI-MS

In vitro CoA ligase reactions were analyzed via MALDI-MS on an LTQ Orbitrap XL instrument (Thermo Fisher Scientific, Inc.) equipped with a nitrogen laser at 337 nm. The samples were mixed with the matrix (3 mg/mL in 75% ACN with 0.1% TFA) while spotting them onto a polished stainless steel MALDI target in a 1:3 ratio (0.5 μ L sample/1.5 μ L matrix) with addition of 0.25 μ L ProteoMass Normal Mass Calibration Mix (1:10 dilution, ProteoMass™ MALDI Calibration Kit, Sigma-Aldrich) for acquisition of high resolution spectra. Mass spectra were acquired in positive ion mode (FTMS) over a range of 700–1200 *m/z*. MS² experiments were performed in ITMS mode with \pm 0.1 Da mass accuracy window, wideband activation and 23 eV collision energy. Data analysis was performed using Xcalibur 2.0.7 (Thermo Fisher Scientific, Inc.) by averaging 30–100 consecutive laser shots.

Declaration of competing interest

The authors declare the following financial interests/personal relationships which may be considered as potential competing interests: Helge Bode reports financial support was provided by BMBF Rhabdoform (031B0856A). Helge Bode reports financial support was provided by ERC Advanced Grant SYNPEP. Helge Bode reports equipment provided by the German Research Foundation. Helge Bode reports a relationship with Myria Biosciences AG that includes: equity or stocks.

Data availability

Data will be made available on request.

Acknowledgements

Work in the Bode laboratory was supported by the BMBF project RhabdoFerm (031B0856A) and in part by the ERC advanced grant SYNPEP (835108) and the LOEWE Schwerpunkt MegaSyn, funded by the State of Hesse. We acknowledge the Deutsche Forschungsgemeinschaft for funding of the Impact II qTOF mass spectrometer (Grant INST 161/810-1). We thank Alexander Perez for providing the azido-C₁₆ fatty acid, Alexander Rill for providing the plasmid backbones for the heterologous production, Carsten Kegler and Charles O. Rock for providing the plasmids for Sfp- and AcpP-production, respectively. We further thank Michael Karas for MALDI access.

Appendix A. Supplementary data

Supplementary data to this article can be found online at <https://doi.org/10.1016/j.tet.2022.133116>.

References

- [1] T.P. Martins, C. Rouger, N.R. Glasser, S. Freitas, N.B. de Fraissinette, E.P. Balskus, D. Tasdemir, P.N. Leao, Nat. Prod. Rep. 36 (2019) 1437–1461.

- [2] M.B. Austin, J.P. Noel, *Nat. Prod. Rep.* 20 (2003) 79–110.
- [3] J. Schröder, G.Z. Schröder, *C. Naturforsch., J. Biosci.* (1990).
- [4] J. Chong, A. Poutaraud, P. Huguency, *Plant Sci.* 177 (2009) 143–155.
- [5] S.A. Joyce, A.O. Brachmann, I. Glazer, L. Lango, G. Schwär, D.J. Clarke, H.B. Bode, *Angew Chem. Int. Ed. Engl.* 47 (2008) 1942–1945.
- [6] S.W. Fuchs, K.A. Bozhdyuk, D. Kresovic, F. Grundmann, V. Dill, A.O. Brachmann, N.R. Waterfield, H.B. Bode, *Angew Chem. Int. Ed. Engl.* 52 (2013) 4108–4112.
- [7] H.B. Park, P. Sampathkumar, C.E. Perez, J.H. Lee, J. Tran, J.B. Bonanno, E.A. Hallem, S.C. Almo, J.M. Crawford, *J. Biol. Chem.* 292 (2017) 6680–6694.
- [8] J.M. Crawford, R. Kontnik, J. Clardy, *Curr. Biol.* 20 (2010) 69–74.
- [9] J.M. Crawford, S.A. Mahlstedt, S.J. Malcolmsen, J. Clardy, C.T. Walsh, *Chem. Biol.* 18 (2011) 1102–1112.
- [10] R. Kontnik, J.M. Crawford, J. Clardy, *ACS Chem. Biol.* 5 (2010) 659–665.
- [11] H.B. Park, J.M. Crawford, *J. Nat. Prod.* 78 (2015) 1437–1441.
- [12] N.J. Tobias, H. Wolff, B. Djahanschiri, F. Grundmann, M. Kronenwerth, Y.M. Shi, S. Simonyi, P. Grün, D. Shapiro-Ilan, S.J. Pidot, T.P. Stinear, I. Ebersberger, H.B. Bode, *Nat. Microbiol.* 2 (2017) 1676–1685.
- [13] E.E. Herbert, H. Goodrich-Blair, *Nat. Rev. Microbiol.* 5 (2007) 634–646.
- [14] Y.M. Shi, H.B. Bode, *Nat. Prod. Rep.* 35 (2018) 309–335.
- [15] N.J. Tobias, Y.M. Shi, H.B. Bode, *Trends Microbiol.* 26 (2018) 833–840.
- [16] A. Hapeshi, J.M. Benarroch, D.J. Clarke, N.R. Waterfield, *Microbiology (Read.)* 165 (2019) 516–526.
- [17] J. Wang, L. Cao, Z. Huang, X. Gu, Y. Cui, J. Li, Y. Li, C. Xu, R. Han, *J. Invertebr. Pathol.* 188 (2022), 107717.
- [18] J. Peppers, A.S. Paller, T. Maeda-Chubachi, S. Wu, K. Robbins, K. Gallagher, J.E. Kraus, *J. Am. Acad. Dermatol.* 80 (2019) 89–98 e3.
- [19] L. Zhao, X. Chen, L. Cai, C. Zhang, Q. Wang, S. Jing, G. Chen, J. Li, J. Zhang, Y. Fang, *J. Clin. Pharm. Therapeut.* 39 (2014) 418–423.
- [20] M.G. Lebwahl, L. Stein Gold, B. Strober, K.A. Papp, A.W. Armstrong, J. Bagel, L. Kircik, B. Ehst, H.C. Hong, J. Soung, J. Fromowitz, S. Guenther, S.C. Piscitelli, D.S. Rubenstein, P.M. Brown, A.M. Tallman, R. Bissonnette, *N. Engl. J. Med.* 385 (2021) 2219–2229.
- [21] T. Mori, T. Awakawa, K. Shimomura, Y. Saito, D. Yang, H. Morita, I. Abe, *Cell Chem Biol* 23 (2016) 1468–1479.
- [22] J. Beld, E.C. Sonnenschein, C.R. Vickery, J.P. Noel, M.D. Burkart, *Nat. Prod. Rep.* 31 (2014) 61–108.
- [23] M. Kronenwerth, A.O. Brachmann, M. Kaiser, H.B. Bode, *Chembiochem* 15 (2014) 2689–2691.
- [24] L. Jimenez-Diaz, A. Caballero, A. Segura, in: F. Rojo (Ed.), *Aerobic Utilization of Hydrocarbons, Oils, and Lipids*, Springer, 2018, pp. 1–23.
- [25] D. Campopiano, *J. Chem Biol* 21 (2014) 1257–1259.
- [26] T.K. Ray, J.E. Cronan Jr., *Proc. Natl. Acad. Sci. U. S. A.* 73 (1976) 4374–4378.
- [27] C.O. Rock, J.E. Cronan, *J. Biol. Chem.* 254 (1979) 7116–7122.
- [28] J. Beld, K. Finzel, M.D. Burkart, *Chem. Biol.* 21 (2014) 1293–1299.
- [29] L.E. Quadri, P.H. Weinreb, M. Lei, M.M. Nakano, P. Zuber, C.T. Walsh, *Biochemistry* 37 (1998) 1585–1595.
- [30] Y.M. Zhang, H. Marrakchi, S.W. White, C.O. Rock, *J. Lipid Res.* 44 (2003) 1–10.
- [31] J. Beld, D.J. Lee, M.D. Burkart, *Mol. Biosyst.* 11 (2015) 38–59.
- [32] A. Chen, R.N. Re, M.D. Burkart, *Nat. Prod. Rep.* 35 (2018) 1029–1045.
- [33] T.A. Schöner, S.W. Fuchs, B. Reinhold-Hurek, H.B. Bode, *PLoS One* 9 (2014), e90922.
- [34] J. Oh, N.Y. Kim, H. Chen, N.W. Palm, J.M. Crawford, *J. Am. Chem. Soc.* 141 (2019) 16271–16278.
- [35] C. Fu, W.P. Donovan, O. Shikapwashya-Hasser, X. Ye, R.H. Cole, *PLoS One* 9 (2014) e115318.
- [36] A.O. Brachmann, S.A. Joyce, H. Jenke-Kodama, G. Schwär, D.J. Clarke, H.B. Bode, *Chembiochem* 8 (2007) 1721–1728.
- [37] A.J. Perez, H.B. Bode, *Chembiochem* 16 (2015) 1588–1591.

SUPPORTING INFORMATION

Supporting Tables

Table S1. Strains used in this study.

Strain	Genotype	Reference
<i>E. coli</i> DH10B	F ⁻ <i>araDJ39</i> Δ (<i>ara</i> , <i>leu</i>)7697 Δ <i>lacX74 galU galK rpsL deoR</i> ϕ 8O <i>dlacZ</i> Δ M15 <i>endAI nupG recAI mcrA</i> Δ (<i>mrr hsdRMS mcrBC</i>)	Invitrogen
<i>E. coli</i> BL21 (DE3) Star	F ⁻ , <i>ompT</i> , <i>gal</i> , <i>dcm</i> , <i>hsdSB</i> (<i>rB</i> ⁻ <i>mB</i> ⁻), <i>lon</i> , λ (DE3 [<i>lacI</i> , <i>lacUV5-T7</i> , <i>gene1</i> , <i>ind1</i> , <i>sam7</i> , <i>nin5</i>])	Invitrogen
S17-1 λ <i>pir</i>	Tp ^f Sm ^r <i>recA thi hsdRM</i> ⁺ , RP4-2-Tc::Mu-Km::Tn7, λ <i>pir</i> phage lysogen	¹
<i>P. laumondii</i> TT01	wild type, Rif ^R (spontaneous)	²
<i>P. laumondii</i> TT01::pDS132_ <i>plu2134</i>	wild type with a P _{DS132} insertion in <i>plu2134</i> , Cm ^R	this work

Table S2. Oligonucleotides used for plasmid construction and verification. Overhangs are underlined.

Plasmid	Oligonucleotide 5' to 3'		Template
pDS132_plu2134	TS120	<u>AAAGTGAGTCCTGGCTAAAACATTATCCGG</u>	<i>P. laumondii</i> TT01
	TS121	<u>TGCCACCAAGTATATTGCAGA</u>	
pACYC_plu2134_strep (<i>stfB</i>)	GG185	<u>TTCGAAAAAGAGAACCTATACTTCCAGGGAGAGAAAATC</u> <u>TGGCTAAAACATTATC</u>	<i>P. laumondii</i> TT01
	GG186	<u>AGCGGTGGCAGCAGCCTAGGTTAACTATGCTACATTCCT</u> <u>GACCTTTTC</u>	
	GG68	<u>TCCCTGGAAGTATAGGTTCTCTTTTTCGAACTGCGGGTG</u> <u>GCTCCACATGGTATATCTCCTTATTAAGTTAAAC</u>	pACYC Duet-1
	SW1	<u>TTAACCTAGGCTGCTG</u>	
pCOLA_plu2134_strep (<i>stfB</i>)	GG185	<u>TTCGAAAAAGAGAACCTATACTTCCAGGGAGAGAAAATC</u> <u>TGGCTAAAACATTATC</u>	<i>P. laumondii</i> TT01
	GG186	<u>AGCGGTGGCAGCAGCCTAGGTTAACTATGCTACATTCCT</u> <u>GACCTTTTC</u>	
	GG68	<u>TCCCTGGAAGTATAGGTTCTCTTTTTCGAACTGCGGGTG</u> <u>GCTCCACATGGTATATCTCCTTATTAAGTTAAAC</u>	pCOLA Duet-1
	SW1	<u>TTAACCTAGGCTGCTG</u>	
pACYC_fabH_Strep	SK18	<u>GAGAACCTATACTTCCAGGGATATACAAAAATTTAGGTA</u> <u>CAGGTAGTTATC</u>	<i>P. laumondii</i> TT01
	SK22	<u>GATTACTTTCTGTTCCGACTTAAGCATTATTA</u> <u>AAAAACGTCATCAGTGCCG</u>	
	GG68	<u>TCCCTGGAAGTATAGGTTCTCTTTTTCGAACTGCGGGTG</u> <u>GCTCCACATGGTATATCTCCTTATTAAGTTAAAC</u>	pACYC Duet-1
	SW1	<u>TTAACCTAGGCTGCTG</u>	
pCOLA_bkdABC_Strep	SK23	<u>GAGAACCTATACTTCCAGGGAATAGACGTACAGATCAAT</u> <u>GAAGTACC</u>	<i>P. laumondii</i> TT01
	SK24	<u>GATTACTTTCTGTTCCGACTTAAGCATTAT</u> <u>TACTGTTTTGC AACCACG</u>	
	GG68	<u>TCCCTGGAAGTATAGGTTCTCTTTTTCGAACTGCGGGTG</u> <u>GCTCCACATGGTATATCTCCTTATTAAGTTAAAC</u>	pCOLA Duet-1
	SW1	<u>TTAACCTAGGCTGCTG</u>	
pCDF_stfB_Strep	SK25	<u>GAGAACCTATACTTCCAGGGAGAGAAAATCTGGCTAAAA</u> <u>CATTATC</u>	<i>P. laumondii</i> TT01
	SK26	<u>GATTACTTTCTGTTCCGACTTAAGCATTACTATGCTACATT</u> <u>CCTGACCTTTTC</u>	
	GG68	<u>TCCCTGGAAGTATAGGTTCTCTTTTTCGAACTGCGGGTG</u> <u>GCTCCACATGGTATATCTCCTTATTAAGTTAAAC</u>	pCDF Duet-1
	SW1	<u>TTAACCTAGGCTGCTG</u>	
pCDF_stfB_Strep_ StfCDE	SK27	<u>GTTAAGTATAAGAAGGAGATATACATATGAAACGTGTTCT</u> <u>TGTAGTGTCG</u>	<i>P. laumondii</i> TT01
	SK28	<u>GTGGCAGCAGCCTAGGTTAATTAGTTAGCGGATTCCAAC</u> <u>TTTG</u>	
	GG108	<u>CATATGTATATCTCCTTCTTATACTTAAC</u>	pCDF_stfB_Strep
	GG109	<u>TAATTAACCTAGGCTGCTGCCAC</u>	
pACYC_fabH_Strep_ fabG	SK29	<u>GTTAAGTATAAGAAGGAGATATACATATGAGATTAGATG</u> <u>GAAAGATTGCATTAG</u>	<i>P. laumondii</i> TT01
	SK30	<u>GTGGCAGCAGCCTAGGTTAATTAGTTATACATACATGCCG</u> <u>CC</u>	
	GG108	<u>CATATGTATATCTCCTTCTTATACTTAAC</u>	pACYC_fabH_ Strep
	GG109	<u>TAATTAACCTAGGCTGCTGCCAC</u>	
pACYC_darABC (<i>stfCDE</i>)	GG1	<u>TATAAGAAGGAGATATACATATGAAACGTGTTCTTGTAGT</u> <u>G</u>	<i>P. laumondii</i> TT01
	GG8	<u>GTTTCTTTACCAGACTCGAGTTAGTTAGCGGATTCCAAC</u>	
	GG3	<u>CTCGAGTCTGGTAAAGAAAC</u>	pACYC Duet-1
	GG4	<u>CATATGTATATCTCCTTCTTATACTTAAC</u>	
pCDF_fabH_Strep	SK18	<u>GAGAACCTATACTTCCAGGGATATACAAAAATTTAGGTA</u> <u>CAGGTAGTTATC</u>	<i>P. laumondii</i> TT01
	SK19	<u>AGCGGTGGCAGCAGCCTAGGTTAATTA</u> <u>AAAAACGTCATCAGTGCCG</u>	
	GG68	<u>TCCCTGGAAGTATAGGTTCTCTTTTTCGAACTGCGGGTG</u> <u>GCTCCACATGGTATATCTCCTTATTAAGTTAAAC</u>	pCDF Duet-1
	SW1	<u>TTAACCTAGGCTGCTG</u>	
pCDF_fabB_Strep	SK1	<u>GAGAACCTATACTTCCAGGGAAGGTATTTAATGAAGCGC</u> <u>GTAG</u>	<i>P. laumondii</i> TT01
	SK2	<u>AGCGGTGGCAGCAGCCTAGGTTAA</u> <u>TAAAGCTGAATACTTGCTCATCAC</u>	
	GG68	<u>TCCCTGGAAGTATAGGTTCTCTTTTTCGAACTGCGGGTG</u> <u>GCTCCACATGGTATATCTCCTTATTAAGTTAAAC</u>	pCDF Duet-1
	SW1	<u>TTAACCTAGGCTGCTG</u>	

Attachment

pCDF_fabF_Strep	SK3	<u>GAGAACCCTATACTTCCAGGGATCTAAGCGTCGAGTAGTTG</u>	<i>P. laumondii</i> TT01
	Sk4	<u>AGCGGTGGCAGCAGCCTAGGTTAA</u> TTAATCAGGTTTAATCTTACGG	
	GG68	<u>TCCCTGGAAGTATAGGTTCTCTTTTTTCGAACTGCGGGTG</u> <u>GCTCCACATGGTATATCTCCTTATTAAGTTAAAC</u>	pCDF Duet-1
pACYC_fabG_Strep	SW1	TTAACCTAGGCTGCTG	
	SK5	<u>GAGAACCCTATACTTCCAGGGAAGATTAGATGGAAAGATTGCATTAG</u>	<i>P. laumondii</i> TT01
	SK6	<u>AGCGGTGGCAGCAGCCTAGGTTAA</u> TTAGTTTCATATACATGCCGC	
pACYC Duet-1	GG68	<u>TCCCTGGAAGTATAGGTTCTCTTTTTTCGAACTGCGGGTG</u> <u>GCTCCACATGGTATATCTCCTTATTAAGTTAAAC</u>	
	SW1	TTAACCTAGGCTGCTG	
	SK7	<u>GAGAACCCTATACTTCCAGGGAGTTGATAAACTTAAATCCTACACAAAAG</u>	<i>P. laumondii</i> TT01
pCOLA_fabA_Strep	SK8	<u>AGCGGTGGCAGCAGCCTAGGTTAA</u> TTAGAAAAGCGCTGGTATCTTTAAAC	
	GG68	<u>TCCCTGGAAGTATAGGTTCTCTTTTTTCGAACTGCGGGTG</u> <u>GCTCCACATGGTATATCTCCTTATTAAGTTAAAC</u>	pCOLA Duet-1
	SW1	TTAACCTAGGCTGCTG	
pCOLA_fabZ_Strep	SK9	<u>GAGAACCCTATACTTCCAGGGAAGTGATAATCATACTCTGCACATTG</u>	<i>P. laumondii</i> TT01
	SK10	<u>AGCGGTGGCAGCAGCCTAGGTTAACTAAACCTCACGACGGC</u>	
	GG68	<u>TCCCTGGAAGTATAGGTTCTCTTTTTTCGAACTGCGGGTG</u> <u>GCTCCACATGGTATATCTCCTTATTAAGTTAAAC</u>	pCOLA Duet-1
pSEVA221-ara	SW1	TTAACCTAGGCTGCTG	
	AR585	<u>GTCGTGACTGGGAAAACC</u>	pSEVA221 + araC Pbad fragment
pSEVA631-ara	AR586	<u>TCCTGTGTGAAATTGTTATCC</u>	pSEVA631 + araC Pbad fragment
	AR585	<u>GTCGTGACTGGGAAAACC</u>	
pSEVA221-fabH-bkdABC-fabG	AR586	<u>TCCTGTGTGAAATTGTTATCC</u>	
	SK188	<u>AGAAAGAGGGGAAATACTAGATGTATACAAAAATTTTAGGTACAG</u>	
	SK189	TTAATGCTTGTAAAAACGTATCAGTGCC	
	SK190	ACGTTTTTAAACAAGCATTAAAGCGCAATAAC	
	SK192	<u>AAGCTGTGCTTACTGTTTTGCAACCAC</u>	pSEVA221-ara
	SK193	<u>AAAACAGTAAGCACACAGCTTCACTAATAAC</u>	
	SK194	<u>AGGGTTTTCCCAAGTCACGACTTAGTTTCATATACATGCCG</u>	
	AR585	<u>GTCGTGACTGGGAAAACC</u>	
pSEVA631-stlBCDE	AR587	CTAGTATTTCCCTCTTTCTC	
	SK184	<u>AGAAAGAGGGGAAATACTAGTTGGAGAAAGTCTGGCTAAAC</u>	
	SK185	<u>ATCGGCACCTCTATGCTACATTCTGACC</u>	
	SK186	<u>TGTAGCATAGAGGTGCCGATGAATGGCTC</u>	
	SK187	<u>AGGGTTTTCCCAAGTCACGACTTAGTTAGCGGATTCACACTTTGAAC</u>	pSEVA631-ara
araC-Pbad	AR585	<u>GTCGTGACTGGGAAAACC</u>	
	AR587	CTAGTATTTCCCTCTTTCTC	
		AAGCGGATAACAATTTACACAGGATCATGACAACCTGACGCTACATCATTCACTTTTTCTTCCAAACCGGCACGGA ACTCGCTCGGGCTGGCCCCGGTGCATTTTTTAAATACCC GCGAGAAATAGAGTTGATCGTCAAAACCAACATTGCGAC CGACGGTGGCGATAGGCATCCGGGTGGTGTCAAAGC AGCTTCGCCTGGCTGATACGTTGGTCTCGGCCAGCT TAAGACGCTAATCCCTAAGCTGCTGGCGGAAAAGATGGA CAGACGCGACGGCGACAAGCAACATGCTGTGCGACGC TGGCGATATCAAAATTGCTGTCTGCCAGGTGATCGCTGA TGACTGACAAGCCTCGCGTACCCGATTATCCATCGGTG GATGGAGCGATCCGTTAATCGCTAGCATGCCCGCAGT ACAATTGCTCAAGCAGATTTATCGCCAGCAGCTCCGAA TAGCGCCCTTCCCTTGCCTGGCGTTAATGATTTGCCA AAAAAGTCGCTGAAATGCGGCTGGTGGCTTCATCCGG GCGAAAGAACCCCGTATTGGCAATATTGACGGCCAGTT AAGCCATTGATGCCAGTAGGCGCGGACGAAAGTAAA CCCCTGGTATACATTCCGCGAGCCTCCGGATGACGA CCGTAGTGATGAATCTCTCTGGCGGAAACAGCAAATA TCACCCGGTCGGCAACAAATTCGTCCTGATTTTTTC ACCACCCCTGACCGCAATGGTGAGATTGAGAAATAAA CCTTTCAATCCAGCGGTGGTGCATAAAAAATCGAGA TAACCGTTGGCCTCAATCGCGTTAAACCCGCCACCAGA TGGCATTAAACGAGTATCCCGCAGCAGGGGATCATTT TGCGCTTACGCCATATTCACCACCCTGAATTGACTCTCTT	Purchased from Twist Bioscience

Attachment

		<p> CCGGGCGCTATCATGCCATACCGCGAAAGGTTTGCAC CATTGATGGCGCGCCGCAATTGGACAAAACGAAAA AGGCCCCCTTTCGGGAGGCCTCTTTCTGGAATTTGGT ACCGAGGCTTAACGATCGTTGGCTGAGAAACCAATTGTC CATATTGCATCAGACATTGCCGCACTGCGTCTTTTACTG GCTCTTCTCGCTAACCAAAACCGGTAACCCCGCTTATTAA AAGCATTCTGTAAACAAGCGGGACCAAGCCATGACAAA AACGCGTAACAAAAGTGTCTATAATCACGGCAGAAAAGT CCACATTGATTATTTGCACGGCGTCACACTTTGCTATGC CATAGCATTTTTATCCATAAGATTAGCGGATCCTACCTGA CGCTTTTATCGCAACTCTACTGTTTCTCCATACCCGA GCTGTCACCGGATGTGCTTTCGGTCTGATGAGTCCGT GAGGACGAAACAGCCTCTACAATAATTTTGTAAACT AGAGAAAGAGGGGAAACTAG </p>	
Verification of <i>P. laumondii</i> TT01 <i>plu2134</i> - insertion mutant			
Oligonucleotide 5' to 3'			
TS121	TCTCAGTAGCAGCATCAAT		
pDS132_rev	GATCGATCCTCTAGAGTCGACCT		

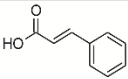
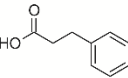
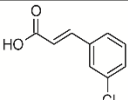
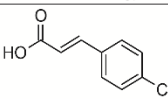
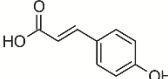
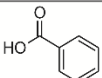
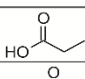
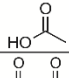
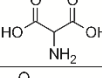
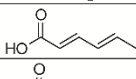
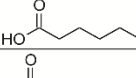
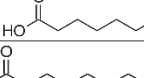
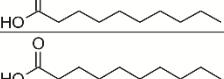
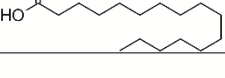
Table S3. Plasmids used in this study.

Plasmid	Genotype	Reference
pACYC Duet-1	P15A ori, T7lac promoter, Cm ^r	Novagen
pCDF Duet-1	CDF ori, T7lac promoter, Sm ^r	Novagen
pCOLA Duet-1	ColA ori, T7lac promoter, Km ^r	Novagen
pCAT14	ColA ori, T7lac promoter, <i>cherry</i> , Km ^r	³
pDS132	R6Ky ori, <i>oriT</i> , <i>sacB</i> , <i>traJ</i> , <i>mob RP4</i> , Cm ^r	⁴
pSUMO_sfp	ColE1 ori, T7lac promoter, <i>sumo</i> , <i>sfp</i> , Km ^r	⁵
pET15b-AcpP	pBR322 ori, T7lac promoter, <i>acpP</i> , Amp ^r	Charles. O. Rock
pDS132_plu2134	Insertion plasmid based on pDS132 with 578 bp of <i>plu2134</i> , Cm ^r	this work
pACYC_plu2134_strep	P15A ori, T7lac promoter, <i>plu2134 (stlB)</i> , Cm ^r	this work
pCOLA_plu2134_strep	ColA ori, T7lac promoter, <i>plu2134 (stlB)</i> , Km ^r	this work
pCOLA_darC_strep	ColA ori, T7lac promoter, <i>plu2165 (stlE)</i> , Km ^r	this work
pCDF_darA_Strep_BC (<i>stlCDE</i>)	CDF ori, T7lac promoter, <i>plu2163-2165 (stlCDE)</i> Sm ^r	this work
pACYC_darA_Strep_B (<i>stlCD</i>)	P15A ori, T7lac promoter, <i>plu2163, plu2164 (stlCD)</i> , Cm ^r	this work
pACYC_darA_Strep (<i>stlC</i>)	P15A ori, T7lac promoter, <i>plu2163 (stlC)</i> , Cm ^r	this work
pCDF_darC_Strep (<i>stlE</i>)	CDF ori, T7lac promoter, <i>plu2165 (stlE)</i> , Sm ^r	this work
pCDF_darC_Strep_darB (<i>stlDE</i>)	CDF ori, T7lac promoter, <i>plu2164 (stlD) plu2165 (stlE)</i> , Sm ^r	this work
pACYC_darABC (<i>stlCDE</i>)	P15A ori, T7lac promoter, <i>plu2163-2165 (stlC)</i> , Cm ^r	this work
pCDF_fabH_Strep	CDF ori, T7lac promoter, <i>plu2835</i> , Sm ^r	this work
pCDF_fabB_Strep	CDF ori, T7lac promoter, <i>plu3184</i> , Sm ^r	this work
pCDF_fabF_Strep	CDF ori, T7lac promoter, <i>plu2831</i> , Sm ^r	this work
pACYC_fabG_Strep	P15A ori, T7lac promoter, <i>plu2833</i> , Cm ^r	this work
pCOLA_fabA_Strep	ColA ori, T7lac promoter, <i>plu1772</i> , Km ^r	this work
pCOLA_fabZ_Strep	ColA ori, T7lac promoter, <i>plu0683</i> , Km ^r	this work
pACYC_fabH_Strep	P15A ori, T7lac promoter, <i>plu2835</i> , Cm ^r	this work
pCOLA_bkdABC_Strep	ColA ori, T7lac promoter, <i>plu1883-1885</i> , Km ^r	this work
pSEVA221	RK2 ori, Km ^r	⁶
pSEVA631	pBBR1 ori, Gm ^r	⁶
pSEVA221_ara	RK2 ori, ara promoter, Km ^r	Alexander Rill
pSEVA631_ara	pBBR1 ori, ara promoter, Gm ^r	Alexander Rill
pSEVA221-fabH-bkdABC-fabG	RK2 ori, ara promoter, <i>plu2835 (fabH)</i> , <i>plu1883-1885 (bkdABC)</i> , <i>plu2833 (fabG)</i> , Km ^r	this work
pSEVA631-stlBCDE	pBBR1 ori, ara promoter, <i>plu2134 (stlB)</i> , <i>plu2163-2165 (stlCDE)</i> , Gm ^r	this work

Table S4. *E. coli* DH10B strain used for heterologous stilbene production.

Name	Introduced plasmids
StlBCDE+ <i>p</i> /FabH+BkdABC+ <i>p</i> /FabG	pSEVA221-fabH-bkdABC-fabG pSEVA631-stlBCDE

Table S5. Substrate specificity of StIB from *P. laumondii* TT01 by its CoA ligase reaction with substrates **1-14**. CoA ester formation was analyzed via MALDI-MS (Fig. S1).

substrate	Compound name	structure	accepted
1	Cinnamic acid		+
2	Phenylpropanoic acid		+
3	3-Chlorocinnamic acid		+
4	4-Chlorocinnamic acid		-
5	Coumaric acid		-
6	Benzoic acid		-
7	Propionic acid		-
8	Acetic acid		-
9	Aminomalonic acid		-
10	Hexa-2,4-dienoic acid		+
11	Caproic acid		+
12	Heptanoic acid		+
13	Decanoic acid		+
14	Palmitic acid		+

Supporting Figures

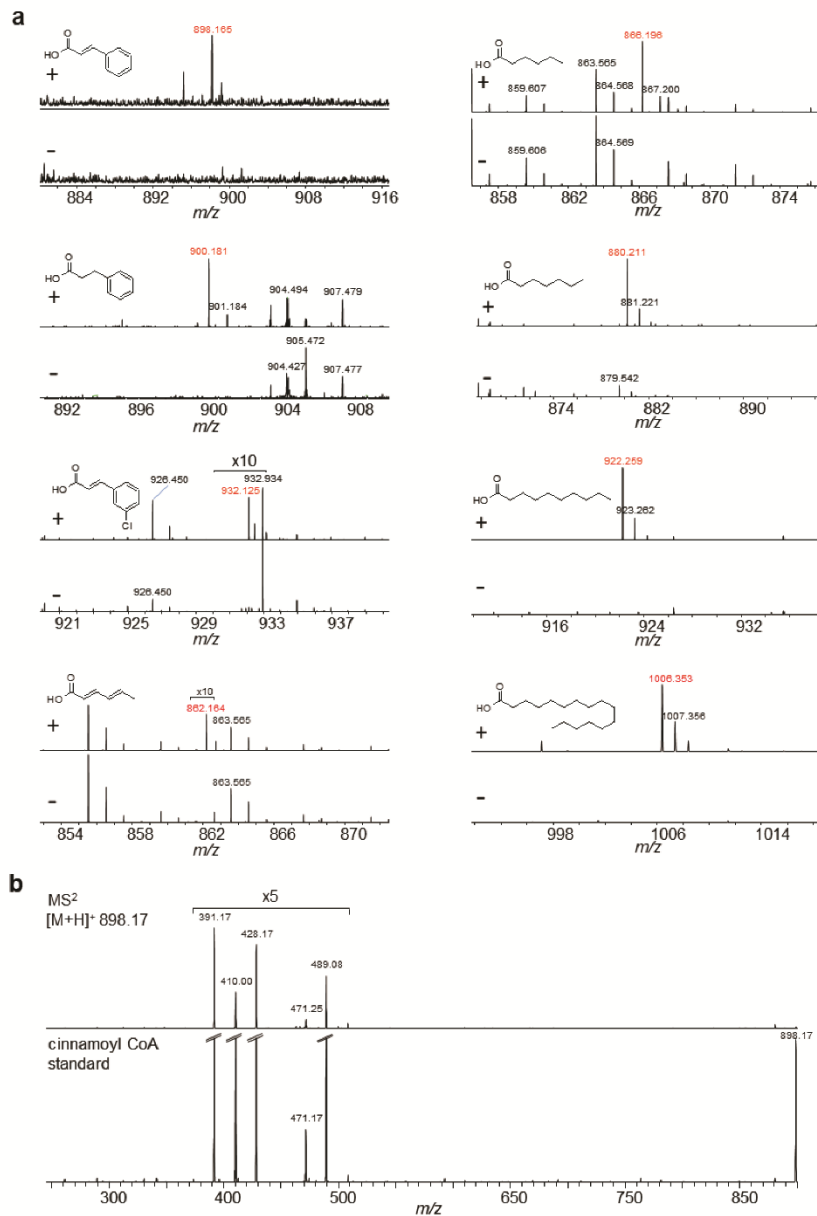


Figure S1. Detection of CoA-derivatives built upon the CoA-ligase activity of StIB. CoA ligase reaction was tested for substrates **1-14** (Table 1), CoA-esters were detected by *high resolution* MALDI-MS (**a**). Due to the weak signal of cinnamoyl-CoA in MS¹, a further MS²-experiment was performed in comparison with a cinnamoyl-CoA standard (**b**).

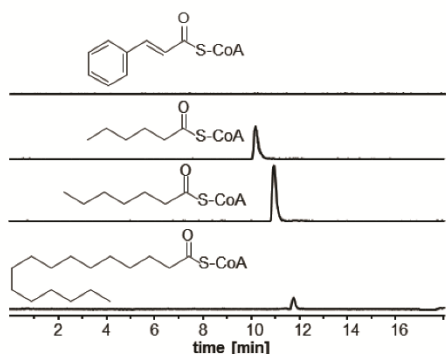


Figure S2. CoA-ligase reaction of StIB. Caproic (C₆)-, heptanoic (C₇)- and palmitic (C₁₆) acid were converted to their corresponding CoA ester by the CoA ligase activity of StIB. The conversion of cinnamic acid to cinnamoyl CoA was not detectable in this setup.

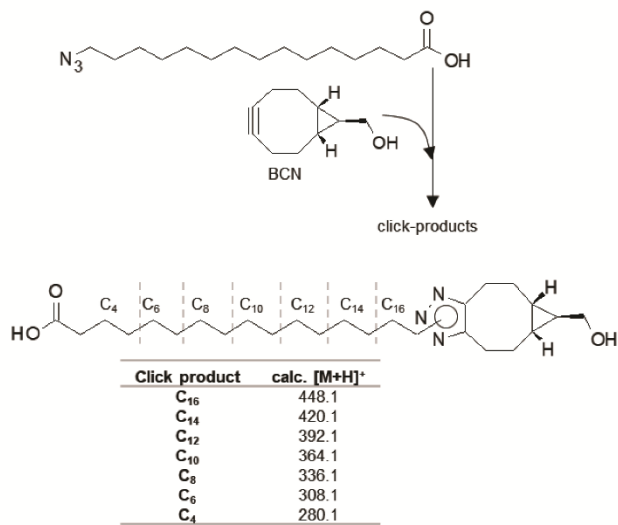


Figure S3. Expected click-products (table) after click-reaction with azido-palmitic acid and BCN.^[3] HPLC-data, see Fig. S4

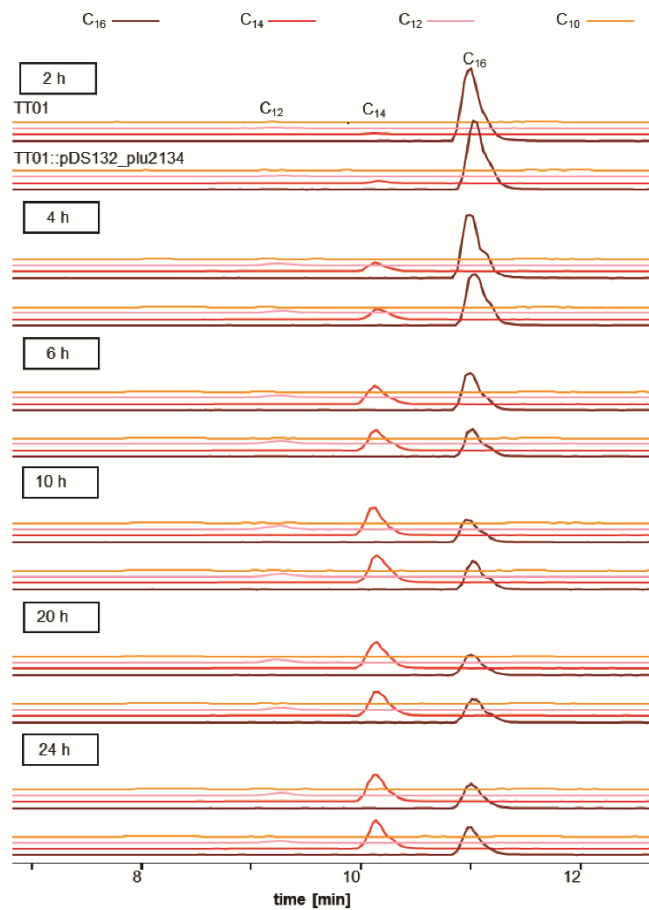


Figure S4. Fatty acid degradation profile of *P. laumondii* TT01 *stlB* (*plu2134*) plasmid insertion mutant compared to the wildtype. TT01 was fed with azido-labelled C₁₆-fatty acid and a click-reaction with BCN was performed to detect the degradation products (C₁₄, C₁₂, C₁₀, C₈) after 2 h, 4 h, 6 h, 10 h, 20 h and 24 h.

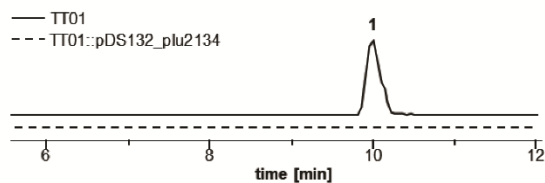


Figure S5. Growth of *P. laumondii* TT01 and insertion mutant TT01::pDS132_plu2134 (*stlB*) without antibiotic. Plasmid insertion of TT01::pDS132_plu2134 was verified by the loss of **1** production. **1** in TT01 was detected via HPLC-UV-MS at 9.9 min with a mass of 255.1 [M+H]⁺ and its characteristic UV.

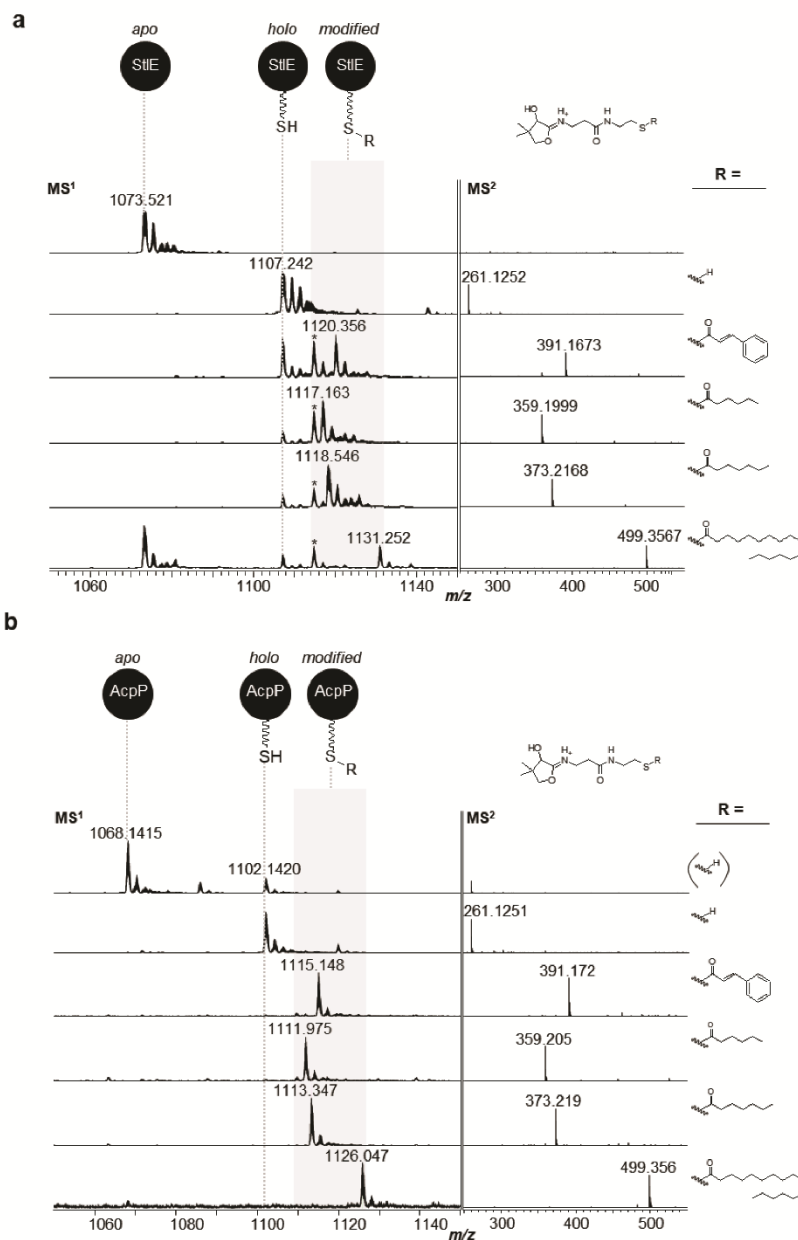


Figure S6. Loading of StIE (a) and AcpP (b) by AasS reaction of StIB with cinnamic, caproic, heptanoic and palmitic acid. The ACPs StIE and AcpP were transferred to their *holo*-forms by means of Sfp. In MS¹, the 10⁺ charge state of the ACPs is shown and in MS², the corresponding Ppant ejection ions are displayed. In the case of StIE loading reactions, a side product was detected during overnight reaction (corresponding signals are marked with an asterisk).

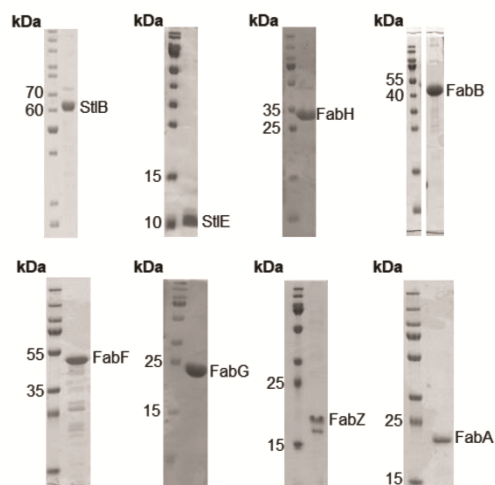


Figure S7. SDS-PAGE of strep-tagged StIB, StIE and FabH, FabB, FabF, FabG, FabZ, FabA.

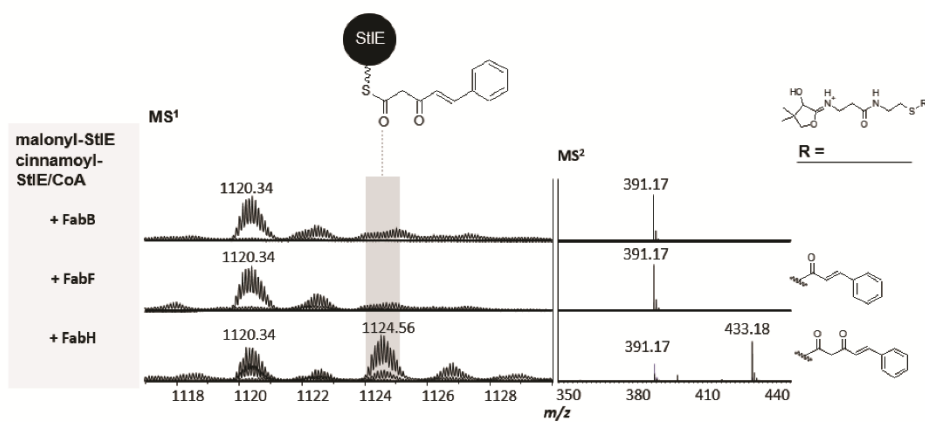


Figure S8. *In vitro* elongation with FAS II enzymes FabH, FabB and FabF and cinnamoyl-ACP as starter and malonyl-ACP as elongation unit. Spectra were overlaid as described in the experimental section.

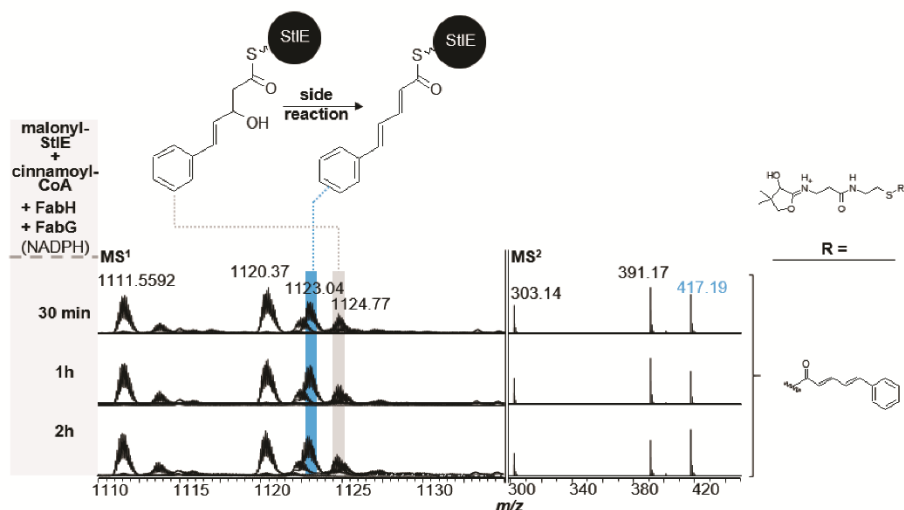


Figure S9. Time dependent *in vitro* analysis of side reaction with cinnamoyl-CoA as starter and malonyl-ACP as elongation unit being elongated and reduced by FabH and FabG (+NADPH), respectively. Spectra were overlaid as described in the experimental section. The dehydrated side product did not increase with increased reaction time.

References

1. Simon, R.; Priefer, U.; Pühler, A. *Nat Biotechnol* **1983**, *1*, 784–791
2. Fischer-Le Saux, M.; Viillard, V.; Brunel, B.; Normand, P.; Boemare, N. E. *Int J Syst Evol Microbiol* **1999**.
3. Schöner, T. A.; Fuchs, S. W.; Reinhold-Hurek, B.; Bode, H. B. *PLoS One* **2014**, *9*, e90922.
4. Philippe, N.; Alcaraz, J. P.; Coursange, E.; Geiselmann, J.; Schneider, D. *Plasmid* **2004**, *51*, 246–55.
5. Lorenzen, W.; Ahrendt, T.; Bozhüyük, K. A.; Bode, H. B. *Nat Chem Biol* **2014**, *10*, 425–7.
6. Martinez-Garcia, E.; Goni-Moreno, A.; Bartley, B.; McLaughlin, J.; Sanchez-Sampedro, L.; Pascual Del Pozo, H.; Prieto Hernandez, C.; Marletta, A. S.; De Lucrezia, D.; Sanchez-Fernandez, G.; Fraile, S.; de Lorenzo, V. *Nucleic Acids Res* **2020**, *48*, D1164–D1170.

8 Erklärung

Ich erkläre hiermit, dass ich mich bisher keiner Doktorprüfung im Mathematisch-Naturwissenschaftlichen Bereich unterzogen habe.

Frankfurt am Main, den

.....

Siyar Kavakli

9 Versicherung

Ich erkläre hiermit, dass ich die vorgelegte Dissertation mit dem Titel

“Investigation and optimization of biosynthetic pathways from entomopathogenic bacteria”

selbständig angefertigt und mich anderer Hilfsmittel als der in ihr angegebenen nicht bedient habe, insbesondere, dass alle Entlehnungen aus anderen Schriften mit Angabe der betreffenden Schrift gekennzeichnet sind.

Ich versichere, die Grundsätze der guten wissenschaftlichen Praxis beachtet, und nicht die Hilfe einer kommerziellen Promotionsvermittlung in Anspruch genommen zu haben.

Frankfurt am Main, den

.....

Siyar Kavakli